UAB

Universitat Autònoma de Barcelona

DEVELOPMENT AND CHARACTERIZATION OF PROTEIN NANOFORMULATIONS AS ALTERNATIVE THERAPEUTICS TO REDUCE ANTIBIOTIC USAGE

Jose Vicente Carratalá Tomás

PhD Thesis 2021

Doctorat en Biotecnologia

Development and characterization of protein nanoformulations as alternative therapeutics to reduce antibiotic usage

Tesi doctoral 2021

Departament de Genètica i de Microbiologia

Facultat de Biociències

UAB
Universitat Autònoma
de Barcelona

ibb
Institut de Biotecnologia
i de Biomedicina

Memòria presentada per el Jose Vicente Carratalá Tomás per optar al grau de Doctor en Biotecnologia per la Universitat Autònoma de Barcelona

Jose Vicente Carratalá Tomás

Vist i plau dels directors de la tesi:

Neus Ferrer Miralles   **Elena Garcia Fruitós**

A todos los que estuvieron ahí durante esta etapa,

CONTENTS

CONTENTS

ABBREVIATIONS

AMPs: Antimicrobial peptides

AMR: Antimicrobial resistance

APPs: Aggregation-prone peptides

BDCT: Blanket antibiotic dry cow therapy

BFP: Blue fluorescent protein

CM: Clinical mastitis

DLS: Dynamic light scattering

FDA: Food and drug administration

FESEM: Field emission scanning electron microscopy

FRET: Fluorescence resonance energy transfer

G-CSF: Granulocyte colony-stimulating factor

GFP: Green fluorescent protein

GRAS: Generally recognized as safe

GST: Glutathione S-transferase

HDPs: Host defense peptides

IBs: Inclusion bodies

IFN-γ: Interferon gamma

IL: Interleukin

IMAC: Immobilized metal affinity chromatography

IMI: Intramammary infection

IPTG: Isopropyl ß-D-1-thiogalactopyranoside

iRFP: Near-infrared fluorescent protein

LAB: Lactic acid bacteria

LPS: Lipopolysaccharide

MBP: Maltose-binding protein

MMP-9: Matrix metalloproteinase-9

MOI: Multiplicity of infection

MRSA: Methicillin-resistant *Staphylococcus aureus*

M-SAA3: Mammary serum amyloid A3

NICE: Nisin-inducible controlled gene expression

NusA: N-utilization substance protein A

PEG: Polyethylene glycol

PI: Polydispersity index

rBoIFN-γ: Recombinant bovine interferon gamma

SCM: Subclinical mastitis

SDCT: Selective dry cow therapy

SUMO: Small ubiquitin-like modifier

TEM: Transmission electron microscopy

TNFα: Tumor necrosis factor alpha

Trx: Thioredoxin

VLPs: Virus-like particles

WHO: World health organization

5-FdU: 2′-deoxy-5-fluorouridine pentamer

INTRODUCTION
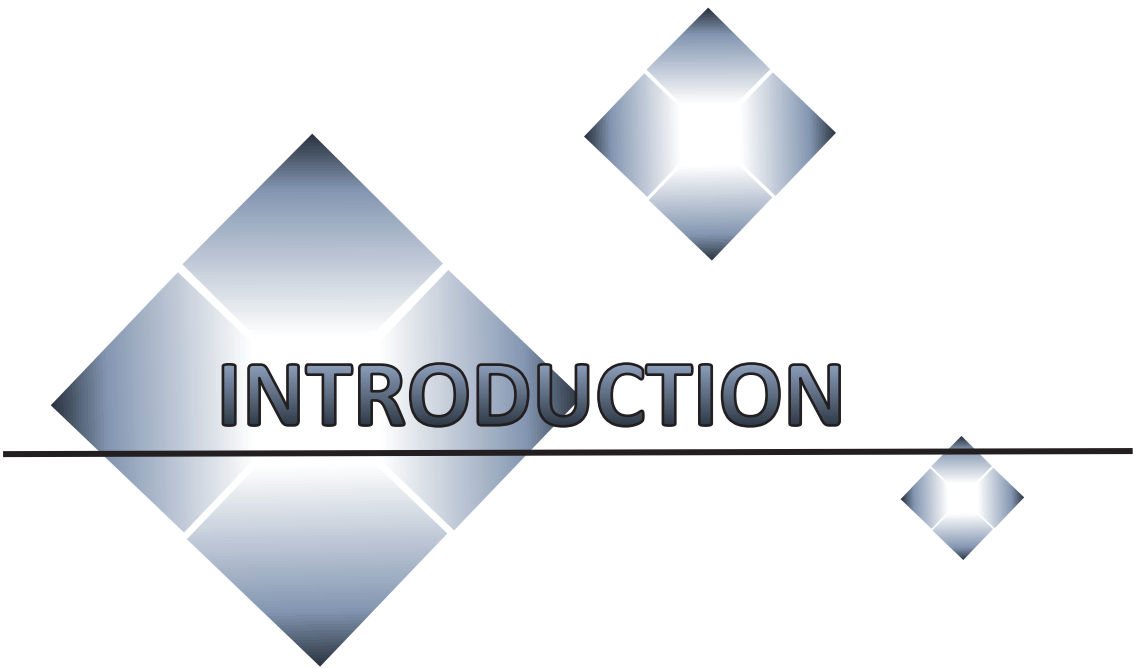
1. ANTIMICROBIAL RESISTANCES

Historically, infectious diseases have been one of the major causes of mortality. At the beginning of the 20th century, infectious diseases were responsible of one-third of all deaths [1]. However, the discovery of penicillin in 1928 by Alexander Fleming and the implementation of improved sanitation measures relegated infectious diseases to the background. During the "golden era" of antibiotic discovery, where many new antibiotics were developed and introduced, it was typically thought that infectious diseases were completely defeated. However, with the emergence of multidrug-resistant bacteria, humanity is faced with the challenge of a post-antibiotic era. Thus, although in the current century, other non-communicable diseases such as cancers and cardiovascular illness are the leading cause of mortality [2], it is estimated that in 2050 untreatable bacterial infections will lead this list [3].

Antimicrobial resistance (AMR) has existed for millions of years, and is an inevitable evolutionary consequence of microbial competition in the environment [4]. Bacteria, just like any other living being, are able to evolve and adapt to unfavorable conditions. Therefore, as an answer to antibiotic usage, these prokaryotic organisms have developed mechanisms to resist the action of the currently-prescribed and newly-developed antibiotics. AMR occurs when microbes stop responding to the antagonistic effects of antibiotics, being able to survive even when they have been exposed to standard doses of clinically relevant antimicrobial drugs [5]. When an antibiotic drug is used in humans or animals, whether appropriately or not, there is a little chance for the exposed microorganism to develop resistance. This possibility increases with the continuous exposure and the use of suboptimal concentrations [6], therefore, antimicrobial usage is the main driving force for the stabilization and persistence of AMR.

Bacteria can develop resistance against antibiotics by two different mechanisms: i) vertical gene transfer, which consist on the accumulation of multiple mutations on existing genes which, after generations, may result in the creation of new resistance genes [7,8]; or ii) horizontal gene transfer, where bacteria is able to acquire new resistance genes from environment, other species, or strains [9,10]. Both molecular mechanisms endow bacteria with resistance genes that overpass the deleterious effect of antibiotics through different strategies including antibiotic modification or its inactivation, modifying the metabolic pathways to overcome the antimicrobial effect, alteration of the target site of the antibiotic, or reduction of antibiotic entry and/ or increase of the efflux of the antibiotic [11].

This AMR issue has been known for a long time. Already in 1945, Alexander Fleming, during his Nobel Prize speech, stated that microbes could develop resistance against antibiotics [5,12]. In fact, there are reports describing the emergence of resistance for every new antibiotic that has been discovered to date [5]. Additionally, as the world becomes more interconnected and global networks becomes smaller, the risks associated with transmission and spread of antibiotic resistant bacteria increases and so does the global concern about antimicrobial usage. Nowadays, approximately 700,000 people die every year due to complications associated to antibiotic resistant bacteria, and if urgent actions are not taken, it is estimated that, by 2050, more than 10 million people will die each year from diseases involving antibiotic resistant bacteria with an associated economic loss of US$ 100 trillion [13]. In this context, AMR has become an urgent public health concern which could trigger a global catastrophe if no action is taken decisively to remedy the current situation.

1.1. Causes of the antibiotic resistance crisis

There are different factors which play a role to the rise in the prevalence of antibiotic resistance. Among them we can find clinical misuse, ease of availability, significant lack of research on new antibiotics, and the overuse and misuse of antibiotics in animal production.

Sometimes, when treating infections, the lack of a proper diagnosis method leads to an inadequate prescription of antibiotics. Especially on developing countries, many clinicians only rely on clinical signs and symptoms instead of using the recommended microbiological bacterial cultures and drug sensitivity tests. It has previously been reported that between 30 % to 50 % of cases where antibiotics have been prescribed, the choice of drug or treatment time were incorrect [14]. Furthermore, in many countries, antibiotics are unregulated and can be easily accessible without a medical prescription. This contributes to self-medication, where drugs are frequently used to treat common colds that are mainly caused by viruses [15], or when the patient experiences a cough or sore throat. Even in countries where antibiotics are tightly regulated and are only accessible under prescription, the use of "left-over" antibiotics from previous prescriptions is also a contributing factor to the overconsumption of antibiotics. In this context, the lack of information and diagnosis criteria leads to self-medication and inappropriate prescription, respectively. In those cases, there is an increased and unnecessary use of antibiotics that may select resistant microorganisms, favoring the spread of resistance genes.

Besides, during the last 50 years, research intended to discover new antibiotic drugs has slowed down [16]. Between 1980 and 1984, 19 new antibiotics were approved, however, during the same period of time, between 2010 and 2014, only 6 new products reached the market [1]. This observation is more evident when looking at companies that have left the antibiotic field. Of the 18 largest pharmaceutical companies, only 3 of them are still investing on the development of new antibiotics [14]. This lack of interest on the development of new antimicrobial drugs has two primary reasons, economic and regulatory. From the economic point of view, antibiotic research and development is no longer considered to be an economically favorable investment for these pharmaceutical companies [17]. In contrast to medications for chronic diseases, antibiotics are used for relatively short periods of time, and in most cases are curative, and this makes them less profitable, being the economic returns for the pharmaceutical companies relatively low [1,14]. Often, when a new antibiotic is marketed, physicians tend to reserve it as a last resort in case older agents do not work, therefore, these new antibiotics are considered as "last-line" drugs to combat serious illnesses due to the threat of promoting drug resistance. This practice results in a diminished return on investment because of the reduced use [14,18]. As a further complication, new antibiotics have to compete in the market with other existing antibiotics that are currently off-patent and can be supplied by manufacturers as generic drugs, being a cheaper option for the public [1,14]. Finally, it is a matter of time before bacteria develop resistance to new antibiotics, a process that may occur during the clinical trials themselves, prematurely curtailing the profits [14]. With regard to regulatory aspects, bureaucracy, differences in clinical trial requirements among countries, and changes in regulatory and licensing rules are some of the reasons that keep pharmaceutical companies away from this area of research [14].

Another area that has contributed to the appearance and spread of antibiotic-resistant bacteria is the excessive use of antibiotics in food-producing animals. In these animals, antibiotics are not only used to treat bacterial infections, but also as a prophylactic measure to avoid the appearance of infections and in some countries as a non-therapeutical strategy to increase animal growth [19]. Just in the United States it is estimated that around 70 % of antibiotics are sold to prevent infections or as growth promoters in food animals [20]. During 2018, China employed 29,774.09 tons of antibiotics for its animal husbandry, being half of this amount (53.2 %) used to promote animal growth [21]. On the other hand, some European countries show a clear commitment to promote a responsible use of antibiotics in animals. During the period from 2011 to 2017, the overall sales of veterinary antibiotics across Europe has dropped by more than 32% [22]. However, although these are the first steps, there is still much to be done.

In food-producing-animals, the ingestion of large amounts of antibiotics in a sustained manner, creates a selective pressure where only those bacteria, pathogenic or not, carrying resistance genes will thrive, while susceptible bacteria will perish. This worsens when low (sub-therapeutic) doses are used, creating the perfect environment for emergence of AMR [20]. The transfer of resistant bacteria originated in animals can be transmitted to humans through a complex web on interactions including direct contact, the environment or food products **(Figure 1)** [23].
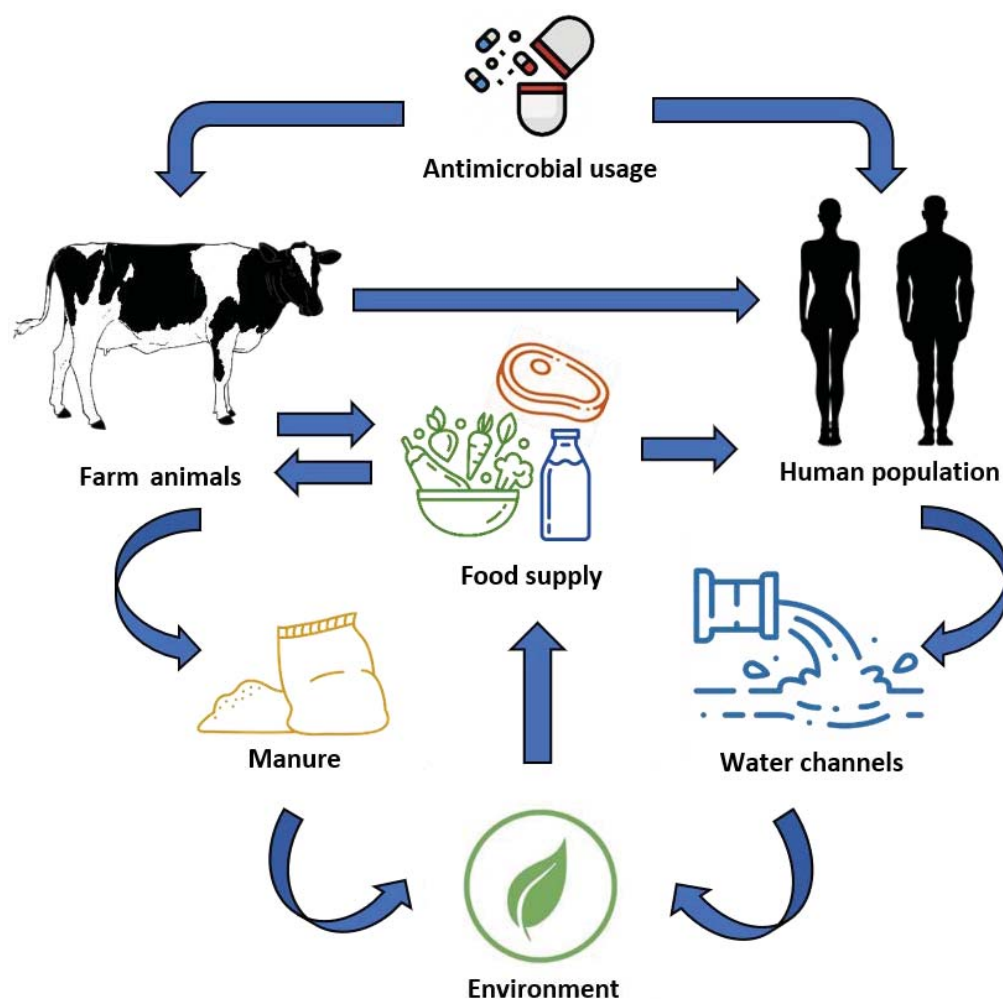
Figure 1. Diagrammatic representation of the possible routes of transmission of AMR. Drug-resistant strains of animal origin can spread to humans either through direct animal contact, food supply chain, or environmental routes. Adapted from [5].

There are many studies done globally that confirm this association between antibiotic use in animal production, the emergence of antibiotic-resistant bacterial species and their presence on human infections. For example, a study performed in two large swine production farms demonstrated that 45 % of the workers were colonized with a methicillin-resistant *Staphylococcus aureus* (MRSA) strain which was different from strains normally found in humans, but similar to that found in swine [24]. In a different study, it was demonstrated that a

proportion of human extraintestinal expanded-spectrum cephalosporin-resistant *E. coli* infections originate from food-producing animals [25]. One of the most compelling studies to date is Hummel's 1986 report, that tracked the spread of nourseothricin resistance. After 2 years using the antibiotic nourseothricin for growth promotion in pigs, a resistant *E. coli* plasmid was found not only in treated pigs, but also in the employees, their family members and in the infected urinary tract of an individual that lived in the same territory where nourseothricin was applied to pigs, but who had no direct contact to pig farms [26]. These facts emphasize the leading role of antibiotic use in food-producing animals as a major force behind the increasing prevalence of antibiotic resistance.

1.2. Critically important antimicrobials for human medicine

Different public organizations have classified antimicrobial drugs according to their importance in human medicine. The World Health Organization (WHO), classify antimicrobial drugs into three categories, "critically important", "highly important" and "important" [27,28]. Antimicrobials drugs included in this list are essential for human medicine and its use as therapeutics in food animals should be properly justified by the corresponding bacteriological culture and susceptibility tests. A fourth group, "highest-priority critically antimicrobials", which include quinolones, third and fourth-generation cephalosporins, macrolides, ketolides, and glycopeptides should be avoided in food animal, due to its highest prioritization for human health [27]. These lists are frequently revised and updated and depending on the different criteria, classification of certain antimicrobial drugs may change. For example, lincosamides, a group of antimicrobial drugs that has gained relevance for treating *S. aureus* (including MRSA from animals), has been moved to "highly important" from "important" [27]. In summary, reducing and even severely limiting antimicrobial usage in food-producing animals is closely related to lower resistance rates, as described in many examples from the agriculture sector [29–31].

1.3. Antimicrobial usage in food-producing animals: the bovine mastitis case

As we already pointed out above, antibiotics are used extensively in food-producing animals to prevent or combat disease and to improve animal productivity. On dairy farms, antibiotics are used for treatment and prevention of diseases affecting dairy cows, particularly mastitis, and are often administered routinely to entire herds to prevent mastitis during the non-lactating period. A typical lactation cycle, that commonly lasts 12 months, comprises four different stages;

early, mid and late lactation, and a non-lactating state, known as the dry period or dry off. This last period is extremely important, as it allows the involution and complete regeneration of the mammary gland tissue and guarantee an optimal production in the subsequent lactation cycle [32]. Immediately after the cessation of milking, during the early stage of the dry period, the mammary gland continues synthesizing and accumulating milk, which causes a high internal pressure and results in milk leakage. While milk leakage provides an entry for bacteria inside the udder through the teat channel, the stagnant milk provides an environment in which bacteria can grow, increasing the risk for the acquisition of new environmental intramammary infections (IMIs). It is estimated that over 60 % of new IMIs occur at this time [33].

Mastitis is defined as the persistent inflammation of the mammary gland, which in most cases is caused by an IMI. This is one of the costliest diseases for the dairy industry worldwide [34], and depending on the symptoms, mastitis can be classified as clinical or subclinical [35]. Clinical mastitis (CM) is characterized by visible signs of an udder inflammation. On the other hand, subclinical mastitis (SCM) is defined as an apparently unaffected mammary gland without visible and palpable signs of inflammation and an unaltered milk secretion, with normal appearance, but reduced yield.

Bacteria are the major cause of mastitis, however, its distribution vary depending on the country, region, and farm, and no specific bacteria can be identified as the primary cause of mastitis **(Figure 2)** [34,36].
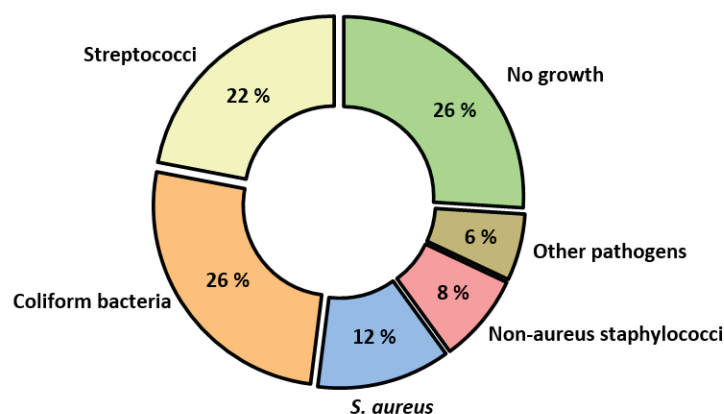
Figure 2. Bacterial distribution in milk samples collected from cows with CM. The cases where no growth was detected may indicate the presence of SCM, where the number of microorganisms is low, and therefore, bellow the detection limit. The provided data are an average result from different studies conducted in many countries. Adapted from [36].

Additionally, the causative pathogen determines the severity and symptomatology of mastitis, being some bacteria more prone to develop a CM than SCM and *vice versa*. For example, coliform bacteria, and especially *Escherichia coli*, are often associated with the most severe progression of CM in dairy cows, while gram-positive bacteria such as *S. aureus, Streptococcus agalactiae* and the coagulase-negative *Staphylococci* are frequently the major agents causing mild CM or SCM with no obvious clinical symptoms [37].

Traditionally, the main option for treatment when mastitis cases are detected is the use of antibiotics. The use of these antimicrobial agents in dairy cows occurs at two specific times of the lactation cycle. During the lactation period, when a mastitis case occurs, the intramammary infusion of antibiotics (local treatment) is the selected method for its treatment [38,39]. As previously mentioned, the other time point when the use of antimicrobials is recommended is at the beginning of the dry off, namely on the day of drying off, which is a routine practice to prevent bacterial IMI during this non-lactating period. This strategy is typically referred as blanket antibiotic dry cow therapy (**BDCT**). The problem with the use of this non-selective strategy as a prophylactic measure to control the occurrence of mastitis is that exposes large numbers of healthy cows to antimicrobials, creating a selective pressure on both mastitis-causing pathogens as well as commensal bacteria in animals' body and farms environment. Previous studies have demonstrated that nearly 80 % of all antimicrobial drugs used in dairy animals were administered for control and prevention of mastitis worldwide [40–42].

There has been a growing concern with the extensive use of antimicrobials in production animals, especially non-therapeutic usage such as dry cow therapy in the case of dairy production. For that reason, different organizations and countries have begun to implant restrictions to the use of antimicrobial drugs. The majority of these actions are based on the rational use of a specific antibiotic in the adequate situation. For example, in contrast to **BDCT**, the selective dry cow therapy (**SDCT**) makes a more judicious use of antimicrobial drugs, where administration is only recommended in those cases that will benefit from treatment. For that purpose, IMI at drying off need to be identified in order to correctly select cows for antimicrobial treatment. Switching from **BDCT** to **SCDT** highly reduce antimicrobial usage and represent an appropriate alternative to address the emergence of AMR. For example, some countries such as the Netherlands have completely adopted this alternative, while **BDCT** has become obsolete [43].

2. ALTERNATIVE THERAPEUTIC APPROACHES IN ANIMAL HEALTH

The increasing concern about the emergence of resistant bacteria, mainly due to antimicrobial drug misuse, has increased interest in the development of new alternative solutions which could reduce dependence on antibiotics in both humans and animals. Although the measures intended to promote a "rational use" adopted so far have significantly reduced antimicrobial usage, and consequently slowed down the spread and appearance of antimicrobial resistant pathogens, in the specific case of bovine mammary gland infections, the incidence of mastitis has remained the same or even increased in recent years [43]. For that reason, the development of novel strategies to tackle with antibiotic resistant pathogens including those causing mastitis are needed. Some of these alternatives are described below.

2.1. Vaccines

Vaccination is a prophylactic measure that prevents the escalation of new infections thanks to acquired immunity. In this sense, vaccines work by training the immune system to recognize and respond to pathogenic agents by the rapid establishment of an effective immune defense. This strategy is indicated as a preventive treatment, and one of the main advantages of vaccines is that targets multiple immunogenic epitopes, hence the development of bacterial resistance is more complex [44]. Furthermore, the use of vaccines prevents the proliferation of bacteria, which do not reach the necessary numbers for the appearance of resistant mutations [45]. In this context, disease prevention by vaccination lowers antibiotic use and consequently reduces AMR [46]. Depending on the immunizing agent, vaccines can be divided into three categories; inactivated vaccines, attenuated vaccines, and recombinant vaccines. This last group includes, DNA or RNA vaccines, subunit antigens, and vectored vaccines [5].

In the specific case of the prevention of mammary gland infections, most of the bacterial vaccines used are designed to target *S. aureus*, *S. agalactiae*, and *E. coli*. For example, the efficacy of an experimental inactivated polyvalent vaccine containing the three strains was generated and evaluated in 20 pregnant cows two months prior to calving. The results showed that immune response was significantly higher in the vaccinated group than that of controls [47]. Most of the commercially available vaccines against coliform bacteria consist on the *E. coli* J5 strain, which has a relatively exposed J5 core antigen, present in many kinds of gram-negative bacteria. J5 bacterin immunization proved to be able to reduce the number of coliform mastitis

by 70-80 % [48]. Startvac (Hipra S.A., Girona, Spain) is another available commercial vaccine that specifically targets *S. aureus*, however, different studies have reported contradictory results regarding its efficacy [49,50]. The multi-etiological nature of bovine mastitis may be responsible of the inefficacy observed in some cases during vaccine treatments, for that reason, the limited range of protection is a problem that needs to be addressed in future developments. Nowadays, vaccination alone is not effective preventing mastitis in dairy herds with high mastitis rates, and should be combined with other infection control measures (excellent milking hygiene, treatment of clinical cases, segregation, and the slaughter of infected cows diagnosed with the disease) [51].

2.2. Probiotics

Probiotics are live microorganisms that are intended to have health benefits when consumed or applied to the body in adequate amounts. Candidate probiotics typically used in humans and livestock include; *Lactobacillus* sp., *Bacillus* sp., *Enterococcus* sp., *Bifidobacterium* sp., *Lactococcus* sp., *Pediococcus* sp., *Streptococcus* sp., *Propionibacterium* sp., *Saccharomyces* sp., and *Aspergillus* sp. [5]. The basis of its efficacy relies on the establishment of a microbial population that hinders the invasion or overproduction of pathogens that lead to a diseased condition of the host organism [52]. Probiotic microorganisms mainly inhibit the growth of other pathogenic bacteria by competing for nutrients or adhesion space (competitive exclusion), releasing antimicrobial compounds (short chain fatty acids, hydrogen peroxide, nitric oxide, and bacteriocins) and stimulating the host immune system [53]. All these properties enhance the ability of probiotics to avoid or eradicate the establishment of pathogenic microorganism at the mucosal site. For example, an engineered probiotic strain of *E. coli* able to release a specific bacteriocin that selectively target *P. aeruginosa* showed a remarkable prophylactic and therapeutic activity against this pathogenic bacterium in two gut-infected animal models [54].

The infusion of probiotics into the mammary gland has raised as a potential alternative in the prevention and treatment of bovine mastitis, especially during the dry off period [55]. Pellegrino et al. evaluated the immunoglobulin isotype levels in blood and milk of animals inoculated at drying off with two lactic acid bacteria (LAB) *Lactobacillus lactis subsp. lactis* CRL1655 and *Lactobacillus perolens* CRL1724. The amount of IgG increased in blood and milk, and these antibodies were able to recognize *S. aureus* epitopes [56]. In a later study, the *in vitro* bactericidal activity of bovine blood and milk of cows inoculated intramammarily with two LAB was

evaluated against different mastitis pathogens (*E. coli*, *S. uberis, S. aureus*, and *S. haemolyticus*). The results indicated that milk serum inhibited the growth of all tested pathogens, while blood serum only affected *E. coli* and *S. uberis* [57]. The establishment of biofilms during IMIs is a trait that has been related to chronic and recurring cases of mastitis. In a recent study, the ability of different LAB to remove and to replace pathogenic biofilms *in vitro* was evaluated. Among all of them, only *Lactobacillus (L.) rhamnosus* ATCC 7469 and *L. plantarum* 2/37 formed biofilms of their own to replace the pathogenic ones [58].

In contrast to antibiotic therapy, probiotic treatment does not develop drug resistance and do not destroy the normal microbiota, diminishing the chances or reinfection [53]. However, microbes used as probiotics are not exempted from the natural processes governing antibiotic resistance, and in some cases, the presence of mobile genetic element carrying antibiotic resistance genes have been reported [59,60]. These studies highlight the threat of probiotics for the spread of antibiotic resistance genes. Thus, this strategy seems more suitable for preventive or complementary use than for the exclusive treatment of infectious animal diseases.

2.3. Phytocompounds

Plant-derived substances include a wide variety of structurally different compounds (alkaloids, terpenoids, essential oils, lectins, tannins, steroids, coumarins and flavonoids) that have the potential to be used as an alternative or complement to antibiotics. The mechanisms by which these metabolites interfere with bacteria are diverse and include: alterations in bacterial cell wall and cell membrane, increase in cell permeability and leakage of cell constituents, inhibition of protein and DNA synthesis, intracytoplasmic damage, DNA damage and inhibition of quorum sensing [61]. These natural compounds have been considered as an alternative to antibiotics in controlling mastitis causing pathogens due to their low toxicity and the advantage of not inducing resistance after prolonged exposure [55,62]. There are several studies in the literature describing the *in vitro* effect of this plant derivatives. Santana et al. evaluated the efficacy of ethanolic extracts of propolis against *S. aureus* cultivated in complex media or milk. Propolis extracts showed bactericidal effects against *S. aureus* in complex media, however, milk constituents decreased the inhibitory activity [63]. In a similar study, the antibacterial activity of ethyl acetate extract of plant *Terminalia chebula* was evaluated against four different isolates from milk samples of cows with subclinical mastitis. Ethyl acetate extract showed antimicrobial activity with varying magnitudes against all identified isolates, being the 500 µg/mL

concentration as effective as amoxicillin treatment (100 μg/mL) [64]. Similar results are obtained when it comes to essential oils, for example, citrus-derived oil completely eliminated *S. aureus* in a dose- and time-dependent manner and significantly inhibited its invasion in bovine mammary cells *in vitro* [65]. *Cinnamon cassia* oil also showed inhibitory activity against different pathogens isolated from bovine mastitis *in vitro* [66]. In the light of the above, there is growing interest in adopting plant-based compounds as therapeutics. However, most of the results are based on *in vitro* studies and further investigation involving *in vivo* experiments is required for further validation of these results. One example of application of plant derivatives *in vivo* was presented by Abboud et al. where the intramammary application of 10 % solution of *Thymus vulgaris* and *Lavandula angustifolia* essential oils caused a drastic decrease in the bacterial colony counts in the different milk samples after four consecutive days of treatment [67].

2.4. Bacteriophages

Bacteriophages are viruses that specifically infect and kill bacteria through cell lysis and are harmless to humans, animals, and plants. For that reason, bacteriophage therapy has been considered as a valuable antimicrobial alternative with the potential to reduce antibiotic usage. The phage life-cycle can be lytic or lysogenic. In the lytic cycle, after infection, the phage replicates and lyses the host cell, while in the lysogenic cycle, phage DNA is incorporated into the host genome (quiescent mode). Due to the mode of action, lytic phages are preferred for therapeutic application, because temperate phages doing a lysogenic cycle increase the possibility of transfer of virulence or antibiotic resistance traits to the host bacterium [5].

These bactericidal entities have been employed for 90 years in the treatment of bacterial infections in humans and livestock [68]. Bacteriophages were used as a means of treating bacterial infections in livestock before antibiotics were employed for the same purpose [69]. In fact, some Eastern European countries, such us Poland, have continued to investigate and use phage therapy to treat infectious diseases, generating valuable practical experience [70]. Nowadays, phage therapy has received again research attention due to the debilitated state of the antibiotic arsenal. In this context, different studies have reported promising results in the field of control and treatment of bovine mastitis. Hamza et al. demonstrated the lytic activity against *S. aureus* isolates of the SA phage, isolated from sewage water [71]. Iwano et al. using a mouse mastitis model, demonstrated that phage ΦSA012 reduced proliferation of *S. aureus* and inflammation in the mammary gland [72]. In a similar study, da Silva Duarte et al. evaluated the activity of the

T4virus vB_EcoM-UFV13 in an experimental *E. coli*-induced mastitis mouse model. The intramammary administration (multiplicity of infection; MOI 10) resulted in a 10-fold reduction in bacterial loads [73]. Despite all these studies, the success of phage therapy presents several limitations. Bacteria may acquire resistance to phages [74] and also induce an immune response [68]. Furthermore, some phages are unable to replicate in raw milk or even degraded/inactivated by the immune system [75]. For example, phage K, an anti-*Staphylococcus* phage, is inhibited by natural milk and udder secretions [76]. On the other hand, raw milk does not appear to hinder replication of *E. coli* phages, being this disadvantage limited to staphylococcal phages [77]. Another limitation is the strict host strain specificity, lytic phages are target specific and targets a narrow group of bacteria, often being strain specific. This situation is often proposed as a solution to prevent dysbiosis, normally associated with antibiotics. However, the complex multi-etiological nature of mastitis would require broad spectra solutions, which in this case would imply the use of multiple phages (bacteriophage cocktails) [78].

2.5. Endolysins

Endolysins, also known as enzybiotics, are specialized phage enzymes generated at the end of the lytic cycle with the aim of facilitating the release of new virions. These mureolytic enzymes target peptidoglycan and lyse cells from within, however they can also lyse bacteria upon exogenous application [79]. Depending on the mechanism of action, endolysins can be classified in different groups: amidases, endopeptidases, glucosidases, and transglycosylases [80]. In contrast to phages, no bacterial resistance against these enzymes has so far been reported, which is one of their main advantages [81]. Unlike chemical antibiotics, and as phages, phage lysins are selective and have a limited spectrum of action being only active against certain bacterial species or genus. This can be an advantage, since commensal flora is not affected, but also limits the applicability in cases where more than one bacterial specie is involved [82]. Furthermore, upon external application, lysins only affect gram-positive bacteria since these bacterial cells have no external membrane. In gram-negative bacteria, the outer membrane impedes endolysins to reach the inner peptidoglycan layer in the periplasmic space [83]. In this context, different approaches have intended to increase the membrane permeability to lysins [84], by combination with membrane destabilizing agents or by their direct modification [85].

Recently published studies have demonstrated the potential of these phage lytic proteins as a new strategy to prevent mastitis. Vander Elst et al. evaluated the antimicrobial activity of two

endolysins (i.e., PlySs2 and PlySs9), derived from *Streptococcus suis* serotype-2 and -9 prophages respectively, against to a panel of subclinical and clinical *S. uberis* milk isolates. The results showed that both endolysins were able to lyse all tested strains [86]. Other studies have involved the use of animal models. For example, in 2020, Gutiérrez et al. reported the characterization of endolysin LysRODI (encoded by staphylophage phiIPLA-RODI) and its application in a mastitis mice model. The endolysin LysRODI demonstrated great efficacy to prevent mammary infections induced by *S. aureus* and *S. epidermidis* [87]. In summary, these mureolytic enzymes show great potential for the treatment of infectious diseases. In contrasts to antibiotics, these antibacterial enzymes do not generate bacterial resistance, which is one of their main comparative advantages. However, their applicability is restricted due to their narrow range of action, limiting their use to some specific scenarios, and therefore curtailing their therapeutic use.

2.6. Antimicrobial peptides

Antimicrobial peptides (AMPs) are generally small cationic peptides (10 to 70 amino acids in length) with an amphipathic nature that have direct and indirect antimicrobial activity against gram-positive and gram-negative bacteria, fungi, and viruses [88]. Their anphipaticity is defined by the presence of positively charged and hydrophobic amino acid residues, which is indispensable to promote their intercalation into the phospholipid bilayer, creating pores, and leading to non-enzymatic cell disruption and osmotic lysis **(Figure 3)** [89,90]. Although bacterial membrane disruption is the main mechanism by which AMPs display their antibacterial activity, other intracellular targets have been described as those which inhibit gene expression and protein synthesis [91]. Moreover, other diverse functions have been attributed to AMPs such as immunostimulation, wound-healing, anti-inflammatory and anti-cancer properties, among others [81]. One of the main advantages of AMPs is that do not interact with specific targets, so the rate of resistance development of pathogens is relatively low [53].

Depending on the secondary structure, AMPs are typically classified into four groups: i) peptides with a α-helical structure; ii) peptides with a β-sheet structure; iii) extended linear peptides, with a random-coil structure in hydrophilic solutions and α-helix structure when they are in contact with hydrophobic environments such as the lipid bilayer membrane; and iv) peptides with a loop structure, besides, outside of this classification, we can also find peptides with cyclic and mixed structures [53]. Also, AMPs can be divided between those that are produced by eukaryotic organisms or by prokaryotic microorganisms. AMPs produced by eukaryotic organisms are a

principal component of innate immunity and are referred to as host defense peptides (HDPs) [92].

On the other hand, AMPs produced by bacteria (prokaryotic) are referred to bacteriocins and are aimed to defend their environmental niche against the competition by other related bacteria [93]. The major differences between these two types are the inhibition spectra and the immunomodulatory activities. HDPs usually exhibit broad-spectrum antimicrobial activity and immunomodulatory effects, while the bacterial spectrum range for bacteriocins tend to be narrow, often limited to bacterial strains or closely related bacteria [5].
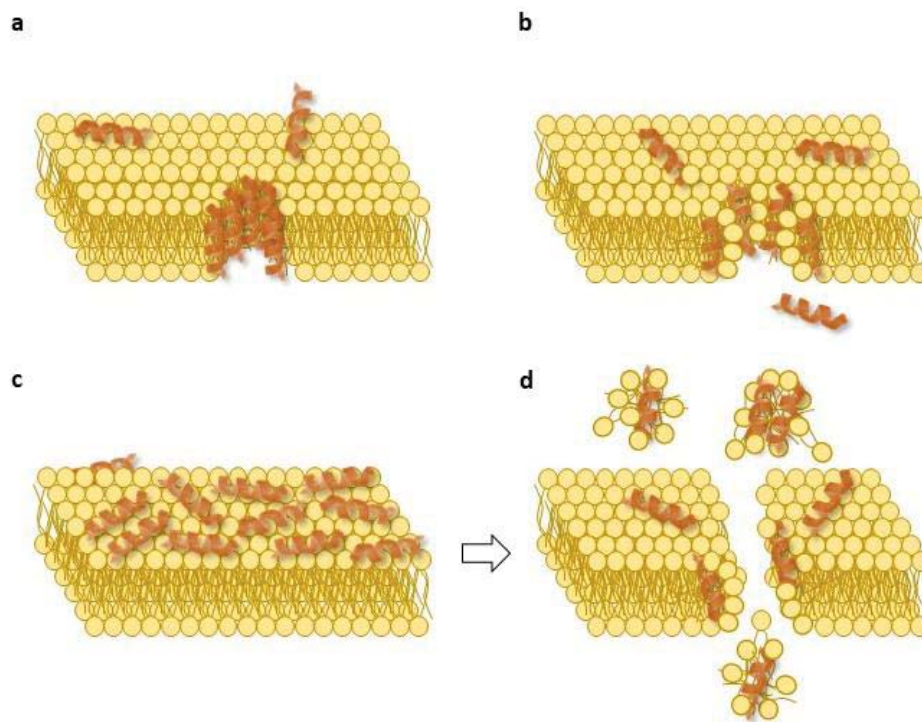
Figure 3. Proposed mechanism models of action for AMPs in bacterial membranes. **a**. **Barrel-stave model**, the AMPs are inserted perpendicularly into the lipid bilayer, then the lateral peptide-peptide interactions promote the formation of a barrel-shaped cluster that creates a transmembrane pore. **b**. **Toroidal pore model**, just as before, the peptides are inserted perpendicularly into the lipid bilayer, but without peptide-peptide interactions. The hydrophobic and hydrophilic arrangement of the lipid bilayer is disrupted, creating a positive curvature (invagination) that leads to the formation of a small hole. **c**. **Carpet model**, in this case AMPs are aligned parallel to the lipid bilayer, and after reaching a certain local concentration, an emulsion is formed which eventually disintegrates the membrane by forming micelles. The mechanism by which the lipid bilayer breaks into small pieces (micelles) is also known as the **detergent-like model** (**d**). Adapted from [90].

Bacteriocins are generally produced by gram-positive bacteria, especially LAB. These bacteriocins that are produced by LAB are considered to be generally recognized as safe (GRAS). However, some studies have reported the production of bacteriocins by gram-negative bacteria such as *E. coli* [94,95]. Bacteriocins are classified into two classes, class I, also called lantibiotics because they contain the modified amino acid lanthionine as part of their peptide chains, and

class II, where no post-translational modifications have been added (non-lantibiotics). Among bacteriocins, nisin is the most commonly studied. Nisin is a lantibiotic produced from *Lactococcus lactis* and is currently licensed as a food biopreservative on over 50 countries [96]. Furthermore, its application as an alternative for control and treatment of mastitis has been evaluated in different commercial products. For example, Amibicin N® (Applied Microbiology Inc., NY, USA) and Wipe Out® (ImmuCell Corporation, Portland, ME) are nisin-containing sanitizers used to clean, sanitize and dry the teat area and milker's hands before and during milking [97]. The intramammary administration of nisin in the treatment of subclinical mastitis in lactating cows has also been evaluated. In a study that involved 90 cows with subclinical mastitis, 46 received an intramammary infusion of nisin while the rest (44) received no treatment. The results indicated that nisin therapy had a bacteriological cure rate of 65.2 %, meanwhile, only 15.9 % of untreated cows spontaneously recovered [98].

One of the main advantages of AMPs is that selectively target bacteria without affecting eukaryotic cells. This is due to the different membrane composition of both cell types. The presence of a neutral net charge on eukaryotic cells prevents AMP interaction. On the other hand, the negative net charge on bacterial membrane drives the electrostatic interaction between this structure and the positively charged AMPs. However, in some cases, AMPs can be cytotoxic for various host cells, especially when administered at high concentrations. In this context, the direct peptide modification by amino acid substitutions has been proposed as a strategy to increase the antimicrobial properties of AMPs, decreasing the concentrations needed to achieve a therapeutic antimicrobial effect and therefore reducing the risk of cytotoxicity [99,100]. Another characteristic is that AMPs, mostly HDPs, exhibit a wide spectrum of action, however, this broad activity spectra do not discriminate between pathogenic and beneficial microorganisms, which can cause disruptions to the normal microbiota. Fusion designs including AMPs and pheromones (species-specific signaling molecules) have been proposed as a strategy to increase bacterial selectivity [101]. A recent example of peptide engineering applied to the treatment of mastitis is presented by Li et al., in which the generation of a dual-function antimicrobial peptide, consisting of a chimeric fusion of a *S. agalactiae* pheromone and a cell penetrating peptide, selectively killed *S. agalactiae* by disrupting the membrane structure and, more importantly, upon intramammary infusion, significantly reduced bacterial load in a mouse model of mastitis infection [102]. On the downside, AMPs are susceptible to the action of proteases, which potentially diminish their therapeutic application. In this regard, the rational design of AMPs offers an alternative to increase the stability and resistance against proteolysis. Different strategies have been proposed including cyclization [103], utilization

of non-natural amino acids [104], and replacement of L-amino acids for D-amino acids [105]. In this last case, the incorporation D-amino acids in the predicted cutting sites of the peptide structure conferred to these engineered AMPs resistance against specific proteases [106].

One example of *de novo* designed AMPs is GWH1, a cationic α-helical peptide of 20 amino acids which possess several characteristics that validate its future application for therapeutic purposes. In comparison with two other natural AMPs (magainin 2a and pleurocidin), GWH1 demonstrated enhanced antimicrobial activity, decreased hemolytic activity and improved selectivity, while maintaining broad-spectrum activity for gram-negative and gram-positive bacteria [107]. Apart from this, GWH1 peptide also present anti-tumoral activity through apoptotic pathways, demonstrating its potential use as an anticancer agent [108,109]. Furthermore, recent studies have showed that GWH1 nanostructuration into oligomeric complexes may be an appealing alternative for advanced treatments of bacterial infections [110,111].

The above notwithstanding, further investigation including the application of protein engineered technology and the incorporation of chemical modifications are required to develop custom designed peptide drugs with higher efficacy in therapeutic treatments. Furthermore, the high cost of production and difficult industrial scalability are other issues to be overcome before these peptides reach the market.

2.7. Cytokines

Cytokines are small intercellular regulatory proteins that play a central role in initiating, maintaining, and regulating the innate immune response [5]. Additionally, some cytokines act as immunostimulants, enhancing host's immunity and resistance toward infections through activation of any of the innate immune system components (phagocytes, neutrophils, complement system, and lysozyme activity). Under a normal state, cytokines are usually not produced, however, when the host immune system is compromised, as for example, during the invasion by pathogenic microorganisms, some of the most important produced cytokines are interleukin (IL)-1α, IL-1β, tumor necrosis factor alpha (TNFα), interferon gamma (IFN-γ), IL-12 and IL-18. In the specific case of IFN-γ, CD4+ T cells, NK cells and CD8+ T cells are responsible of its production [112]. The pivotal role of this cytokine in promoting protective immunity against infections has been fairly demonstrated in knock-out mice models with targeted disruptions of either IFN-γ gene or the IFN-γ receptor gene. In those cases, infected mice are unable to control

infections showing a rapid and fulminant bacterial growth [113–116]. These data have prompted many investigators to evaluate the beneficial effect of IFN-γ administration in a variety of experimental models of infection. For example, systemic administration of IFN-γ in animal infection models enhanced resistance against *Candida albicans* infection [117] and increased survival and decreased pathogenic bacterial loads in lungs of mice infected with *Cryptococcus neoformans* [118]. Furthermore, recombinant IFN-γ administration is an FDA approved treatment for disorders such as chronic granulomatous disease, which is characterized by a series of life-threatening recurrent infections by pyogenic bacteria. Patients treated with IFN-γ reduce the relative risk of infections by more than 70 %, without severe side effects [119]. And also, is a recommended treatment for other type of immunodeficiency syndromes, for example, the hyperimmunoglobulinemia E (hyper-IgE) syndrome [120].

Typically, an increase in the overall level of cytokines has been considered as an indicator of inflammation and a useful parameter in the diagnosis of mastitis [121]. However, other studies have focused their attention on the direct use of recombinant cytokines in the treatment of bovine mastitis. The majority of these studies are intended to investigate the capacity of cytokines to enhance bovine immune responses and to reduce or prevent intramammary infection. To date, recombinant IL-1, IL-2, IL-8, granulocyte colony stimulating factor (G-CSF), and IFN-γ have been investigated in *in vivo* models of mastitis [122]. In one of these studies, the intramammary administration of recombinant IL-1 and IL-2 increased the number of polymorphonuclear cells in milk, enhanced the inducible oxygen radical formation, and in the case of IL-2, enhanced the phagocytosis. Furthermore, the 52 % and 75 % of all *S. aureus* chronically infected mammary glands responded to the treatment with IL-2 and IL-1, respectively, completely clearing the infection [123]. In a different study, the efficacy of IFN-γ in cows experimentally induced with mastitis using *E. coli* as infective agent was evaluated. At the end of the experiment, all treated cows survived, while 42 % of non-treated cows died. These results suggest that intramammary infusion of IFN-γ can prevent the unrestricted growth of *E. coli* within the mammary gland reducing the severity of coliform mastitis [124].

As also mentioned for AMPs, one of the main disadvantages of cytokines is its limited half-life, strategies intended to regulate their action over time are highly desired. One example of this was presented by Canning et al., where the G-CSF was covalently bound to polyethylene glycol (PEG), the binding to this water-soluble polymer would increase the duration of cytokine activity by increasing the hemodynamic volume, reducing renal clearance and proteolytic degradation [125]. Animals treated with PEGylated G-CSF (pegbovigrastim) exhibited 4- to 5-fold

increase in circulating neutrophil numbers within 24 h of treatment initiation, and this increase persisted during a week. Additionally, the incidence of clinical mastitis in those treated animals was reduced by 35 % [126]. Currently, there is a commercial pegbovigrastim (Imrestor, Elanco, Greenfield, IN, USA) that is used to reduce the risk of clinical mastitis in periparturient cows.

2.8. Other alternatives

The above-mentioned alternatives can be included or categorized into different groups, based on the mechanism of action, properties, nature or because they have the same origin. Other type of compounds, cannot be categorized into a specific group or have not been especially designed for mastitis treatment. However, they have shown promising results in *in vitro* and *in vivo* approaches against some of the major mastitis-causing pathogens, therefore, further research in this area may result in novel therapies. One example is the use of single-chain variable region fragments (scFvs). Wang et al. developed a series of eight scFvs that specifically bound to *S. aureus* antigens and inhibited its growth in culture medium. Furthermore, the effectivity of this compound was evaluated in two *S. aureus*-induced mastitis models, murine and bovine, demonstrating a higher cure rate [127,128]. Other studies involve the use of mineral supplements. For example, Machado et al. demonstrated that the subcutaneous administration of different concentrations of selenium, copper, zinc, and manganese had a positive impact on udder health and reduced the cases of subclinical mastitis compared to the control group [129]. In this regard, the effect of different metal ions, as for example, silver and copper have also demonstrated an inhibitory action against various pathogens, including *E. coli* and *S. aureus* [130,131]. Photo dynamic therapy is another strategy with demonstrated effectivity when applied *in vivo* for subclinical bovine mastitis [132]. Finally, chitosan is a natural polysaccharide derived from chitin that displays broad spectrum antimicrobial activity against bacteria. Recent studies have demonstrated its potential as an antibiofilm agent against staphylococcal infections, being able to inhibit biofilm formation, and disrupt established biofilm [133]. Furthermore, the intramammary administration of chitosan at drying off, hastened the mammary gland involution and activated the immune response, demonstrating its immunostimulant properties [134].

3. RECOMBINANT PROTEIN PRODUCTION

Since the advent of recombinant DNA technology, advancement and development in the field of recombinant protein production has only progressed. Long gone are the days where kilograms of plant and animal tissues or large amounts of biological fluids were needed for the purification of a small amount of a given protein. Protein-based drugs involve the use of host cells where, after the introduction of an engineered or recombined DNA, the expression machinery is employed to produce the desired protein, which due to the DNA nature and origin, is termed "recombinant protein". The ability to produce large amounts of proteins in expression systems other than the source organisms opened the door for the development of industrial processes, as well as for the commercial production of such recombinant products. In the early 1980s, the first two approved biopharmaceuticals (recombinant human growth hormone and recombinant human insulin) entered the market, since then, hundreds of therapeutic protein products are currently on the market and many more are currently under development [135,136].

Moreover, some of the above-mentioned alternatives can be easily biosynthesized by using this technology. In the particular case of AMPs, chemical synthesis is the preferred method, however, this technology, although very efficient, is a complex and costly process [137] that may invalidate economically the manufacturing of the peptides [138,139]. Therefore, it is not an ideal platform for large-scale peptide production. High manufacturing cost is one of the major obstacles to the wide application of AMPs. In this context, recombinant DNA technology provides a more cost-effective means for large-scale manufacture of AMPs [140]. Indeed, many AMPs have been successfully obtained through recombinant production in various heterologous hosts [141,142]. And the same can be applied in the case of cytokines, where many examples of recombinant production can be found in the literature [143–146].

3.1. Microbial cell factories

Different expression systems can be used in order to produce proteins recombinantly (bacteria, yeast, filamentous fungi, unicellular algae, mammalian cell lines, and insect cell lines, among others). The choice will depend on several factors, but the most important one is the physicochemical properties of the desired recombinant protein. In cases where extensively post-translational modifications are needed for correct protein function, as for example protein glycosylation, the use of prokaryotic expression systems is not appropriate, due to its inability

to incorporate such modifications, in those cases, mammalian expression systems are the best option. However, when no complex post-translational modifications are needed, as it occurs with AMPs, or when the activity is not affected by its absence, bacteria are an excellent expression system [147]. Despite the inability to incorporate some post-translational modifications, the prokaryotic system is still the most widely used for protein overproduction in both laboratory and industrial scale. The reason for this is found in the different advantages provided by this system, such as the capacity to obtain large amounts of recombinant proteins in a short time, the simple bacterial cell culture conditions (media, additives), which are inexpensive and easily scalable, and the thorough understanding of the system.

3.2. Escherichia coli

Among bacteria, *E. coli* is the most commonly used for recombinant protein production, with around 30 % of all approved therapeutic proteins being produced in this host [135,148]. The advantages of this expression host **c**an be summarized in five different points:

- Fast growth kinetics: in rich media and with the optimal environmental conditions, *E. coli* strains can be duplicated in 20 minutes [149,150]. However, we have to considerer that protein expression implies a metabolic burden on the microorganism, therefore, growth kinetics may decrease accordingly.
- Cost-effectiveness: unlike mammalian cell lines, where complex nutritional requirements increase productions costs, bacterial production processes tend to be cheaper due to the inexpensive costs associated to rich complex media components.
- Genetic simplicity: *E. coli* is well characterized physiologically and metabolically, being one of the first organism to have its entire genome sequenced [151]. Therefore, the number of molecular tools available to genetically modify this microorganism are fairly abundant.
- High product yield associated with high cell densities in culture, which in best cases, may reach around 1×10^{10} and 1×10^{13} viable bacteria/mL [152,153].
- Easily scalable bioprocess development [154].

3.2.1. Strains

The deep knowledge about *E. coli* genome has provided the basis for different genetic modifications intended to enhance some of the drawbacks typically associated with this prokaryotic expression system. As a host for expression, *E. coli* includes numerous strains. The

BL21 (DE3) and its derivates are by far the most used strains for recombinant protein production. The preferred use of this strain lays on some genetic characteristics, for example, mutations in the genes of Lon protease (cytoplasm) and OmpT protease (outer membrane), whose deficiency decrease proteolysis during purification, especially after cell lysis [150]. A mutation in the *hsd*SB gen which increase plasmid stability and prevents its loss. The insertion in the bacterial genome of the λDE3 prophage, which contains the phage T7 RNA polymerase (T7 RNAP) gene under control of the lacUV5 promoter. For that reason, genes of interest are cloned under the control of a T7 promoter and induction can be initiated after the addition of isopropyl ß-D-1-thiogalactopyranoside (IPTG) [149].

Despite all this modifications, BL21 (DE3) cells still have some limitations such as the inability to produce correct disulfide bonds, codon usage bias and the presence of endotoxins, especially lipopolysaccharide (LPS) [155]. In order to address these limitations, different BL21 (DE3) derivatives have been developed, some of which are specially used in specific situations. BL21 (DE3) pLysS contains an additional plasmid to obtain more accurate control of protein basal expression and reduce possible deleterious effects of protein expression before induction [156]. BL21 (DE3) CodonPlus and Rosetta are carriers for plasmids containing extra copies of rare tRNAs genes for codon bias correction [149]. BL21 (DE3) Origami or SHuffle provide an oxidative environment that promotes disulfide bond formation thanks to inactivation of the thioredoxin reductase (*trxB*) and glutathione reductase (*gor*) genes [156].

Among bacteria selected for AMP expression, *E. coli*, particularly *E. coli* BL21 (DE3) strain has been the most popularly used [157–160]. On the other hand, a great variety of cytokines, including, G-CSF [161], IFN-γ [162], and IL-6 [146] have employed this expression host for their recombinant production.

3.2.2. Endotoxin-free *Escherichia coli*

One of the major limitations when working with *E. coli* strains is the presence of LPS. LPS is a major constituent of the outer membrane of almost all gram-negative bacteria. The presence of this endotoxin in therapeutic protein products may impair its effectivity and cause an innate immune response, limiting their biopharmaceutical applications. For that reason, removal techniques are required. However, these techniques tend to reduce protein yields and also increases the cost of the overall production process. For that reason, other alternative such as the generation of genetically modified LPS-free strains seems a more suitable strategy to

overcome this problem. Following this approach, Lucigen has generated a genetically modified *E. coli* strain which express an altered LPS version with unaltered viability and protein expression capabilities but reduced growth rate. This was accomplished by the incorporation of seven genetic deletions (*ΔgutQ, ΔkdsD, ΔlpxL, ΔlpxM, ΔpagP, ΔlpxP* and *ΔeptA)* and one additional compensating mutation (*msbA148*). This new line of *E. coli* cells, called ClearColi™ cells [163], does not trigger the endotoxic response in human cell lines, eliminates the risk of LPS contamination and the need for endotoxin removal, thus becoming a potential protein production platform for therapeutic proteins.

3.3. Gram-positive bacteria

Despite being the main choice, *E. coli* is not the only host used for recombinant protein production. In recent years, other bacterial species have increasingly attracted attention due to specifics characteristics that may surpass some of the disadvantages observed in other similar expression systems. In this context, gram-positive bacteria in contrast to gram-negative bacteria such as *E. coli,* does not contain endotoxins in their membrane, making these expression systems a much safer microbial alternative for recombinant protein production **(Figure 4)** [164,165]. Furthermore, recombinant proteins produced in gram-positive bacterial hosts, if needed, can be easily secreted to the growth medium due to the existence of secretion systems, facilitating their purification during downstream processing [166,167].
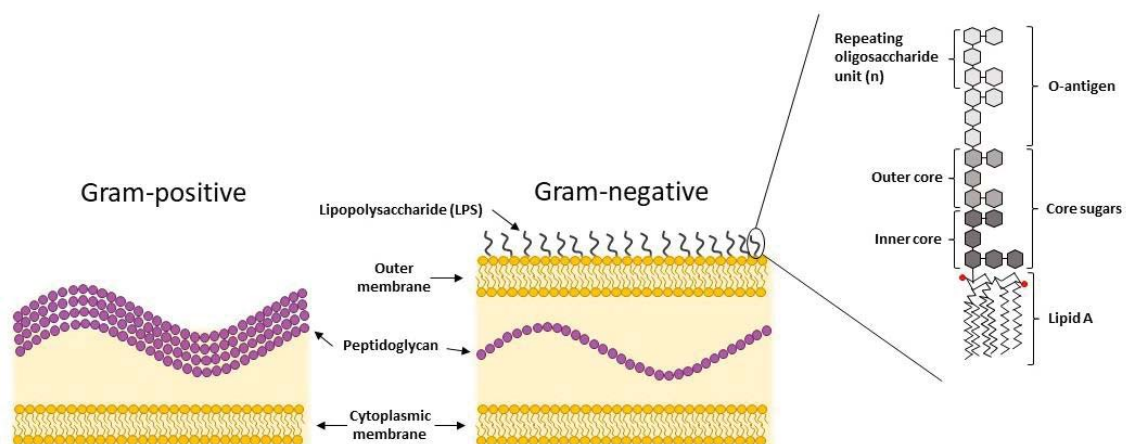
Figure 4. Differential membrane composition between gram-positive and gram-negative bacterial cells. In gram-negative bacteria, the outer membrane is coated with LPS. The basic structure of LPS consist on three differentiated regions, lipid A, core sugars and the highly variable O-antigen. Adapted from [165].

Several gram-positive bacteria possess the GRAS status. Some of them are *Bacillus subtilis*, which is widely used for expression of recombinant proteins in biotechnology [168–170]; *Corynebacterium glutamicum* which has been widely used for the industrial production of biochemicals including L-glutamate and L-lysine, and is now considered as a promising emerging host for protein production [171,172]; and LAB, whose most representative example is *Lactococcus lactis*, which has been used for centuries during fermentation processes and has been recently added to the GRAS list of microorganisms [173].

3.3.1. *Lactococcus lactis*

Several advantages including its well-known metabolism, genetics and the availability of molecular tools for genetic manipulation to favor protein expression make this expression system a competitive alternative to other gram-positive bacteria, or even depending on the application, a better option than their gram-negative counterpart, *E. coli* [167]. In contrast to other gram-positive bacteria such as *B. subtilis*, laboratory strains of *L. lactis* only possess two chromosomally encoded proteases, the extracellular HtrA and the intracellular ClpP, thereby reducing the possibility of degrading heterologous proteins [174]. Furthermore, genetically engineered strains without these proteases increase the stability and yields of recombinant proteins [167,175].

In terms of expression systems, inducible promoters have been fairly investigated and different options are available to provide a better controlled expression. The P170 promoter is turned on when the pH decreases below 6 during transition of culture from exponential to stationary phase, this expression system has the advantage of not requiring inducer, making it autoinducible [166,173]. However, the most widely used and studied expression system in *L. lactis* is the nisin-inducible controlled gene expression (NICE) system [176]. As has been mentioned in a previous section, nisin is a 34-amino acid bacteriocin produced by *L. lactis* to defend their environmental niche against the competition by other related bacteria. Expression of nisin is regulated by two genes, *nisR* and *nisK*. NisK act as a receptor for the mature nisin molecule, which upon binding activates NisR trough phosphorylation. After activation, NisR induces transcription of two promoters in the nisin gene cluster: PnisA and PnisF [177].

The most commonly used host strain for protein production purposes is NZ9000, which has been obtained with the insertion of both *nisK* and *nisR* genes into the chromosome of the nisin-

negative *L. lactis* subsp. *cremoris* MG1363 strain [178,179]. In expression plasmids based on NICE system, the DNA sequence encoding the protein of interest is cloned under the control of the inducible promoter PnisA and expression can be induced by the addition of sub-inhibitory amounts of nisin (0.1-5 ng/mL) to the culture medium [177]. To date, many recombinant proteins have been successfully produced using this expression systems, including lysostaphin [178], adjuvants and growth factors [180–182], prokaryotic and eucaryotic membrane proteins [183], matrix metalloproteinases [184], and cytokines [185–188]. Moreover, different studies have reported the suitability of *L. lactis* as an ideal vehicle for producing and secrete AMPs [189–191].

4. LIMITATIONS IN THE PRODUCTION OF RECOMBINANT PROTEINS

Even after carefully selecting the expression host and an appropriate expression system, the ideal situation would be obtaining the desired protein in high amounts and in a soluble and active state. However, during recombinant protein production several obstacles may impede reaching that goal. In most cases, protein expression may be compromised and no or low amounts of protein are produced. In this case, various situations may be responsible of this effect.

4.1. Protein toxicity

When the expressed protein has a detrimental function in the host cell, slow growth, low cell density and death are typically the normal outcome. In this case, the expressed protein can be considered as toxic and yields are reduced accordingly. However, when faced with this situation, different strategies can be employed to reduce as much as possible these effects. Lower the plasmid copy number, control the basal expression, regulate the level of induction, or direct the expressed protein to the periplasm or extracellularly are some of the strategies that have been proposed to deal with protein toxicity in host cells [149].

Due to its relevant importance in the protein recombinant production sector, most of these advances have been developed in the well-known *E. coli*. For example, as has been mentioned in the previous section, BL21 (DE3) pLysS contains an additional plasmid (pLysS) which express the T7 lysozyme. Before induction, T7 RNAP is degraded by this lysozyme, thereby leaky expression is completely avoided. After induction, T7 RNAP is produced in massive quantities surpassing the effect of the T7 lysozyme. This strategy ensures bacterial growth until induction.

However, after induction, other alternatives have been proposed, in the case of *E. coli*, a tunable expression can be achieved in certain strains. For example, in the Lemo21 (DE3) and the Tuner™ (DE3) strains, protein expression can be regulated by modifying the concentrations of the sugar L-rhamnose and the inducer IPTG, respectively. Another solution could be to secrete the protein to the periplasm or to the medium. This can be simply achieved by fusing a proper leader peptide to the recombinant protein. In *E. coli* there is a large variety of signal peptides [192]. However, the secretion machinery of *E. coli* has a limited capacity and can become overloaded [193], for that reason, the yields of secreted recombinant proteins in this expression system are often low [194]. However, gram-positive bacteria are a more suitable host for protein secretion due to the presence of a less complex cell wall that allow the direct secretion into the extracellular environment. In *L. lactis*, Usp45 is the only major protein secreted and its signal peptide is the most successful used for secretion [173].

4.2. Codon usage bias

Another factor that may influence the recombinant protein production yields is the codon usage bias. This phenomenon refers to the fact that different organisms have differences in the frequency of occurrence of synonymous codons. Therefore, a depletion of low-abundance tRNAs may occur in bacterial hosts expressing a foreign DNA, leading to amino acid misincorporation or truncation of the polypeptide chain and ultimately reducing the level of protein expression [195].

Two different strategies can be applied to solve this problem, first, modify the inserted foreign DNA by optimizing its sequence with the preferred codons of the expression host and second, supplement the bacterial expression host with those rare tRNAs. In the first case, the easiest way to address this approach is by replacing every amino acid by its most represented codon in the expression host, this strategy is known as "one amino acid-one codon" and has the advantage that can be applied to every expression host via *de novo* gene synthesis [196]. Codon optimization speed up the rate of translation elongation resulting in increased protein expression yields. However, folding of most proteins in bacteria occurs co-translationally, while the nascent peptide chains are synthesized [197]. For that reason, several studies have emphasized the role of translation kinetics in protein folding, considering codon usage as a new code within the genetic code that defines protein structures and expression levels (**Figure 5 a**) [198]. Based on this, when codon usage is not properly adapted, as for example in the case of codon

optimization, changes in elongation rate may lead to protein misfolding and loss of functionality (**Figure 5 b**) [199,200]. On the other hand, the increase in the availability of underrepresented tRNAs lays on studies based on specific expression systems, as has been mentioned in a previous section, two *E. coli* BL32 (DE3) derivatives, CodonPlus and Rosetta are strains specifically designed to provide extra genes for supplementation with tRNAs rarely used in *E. coli*.
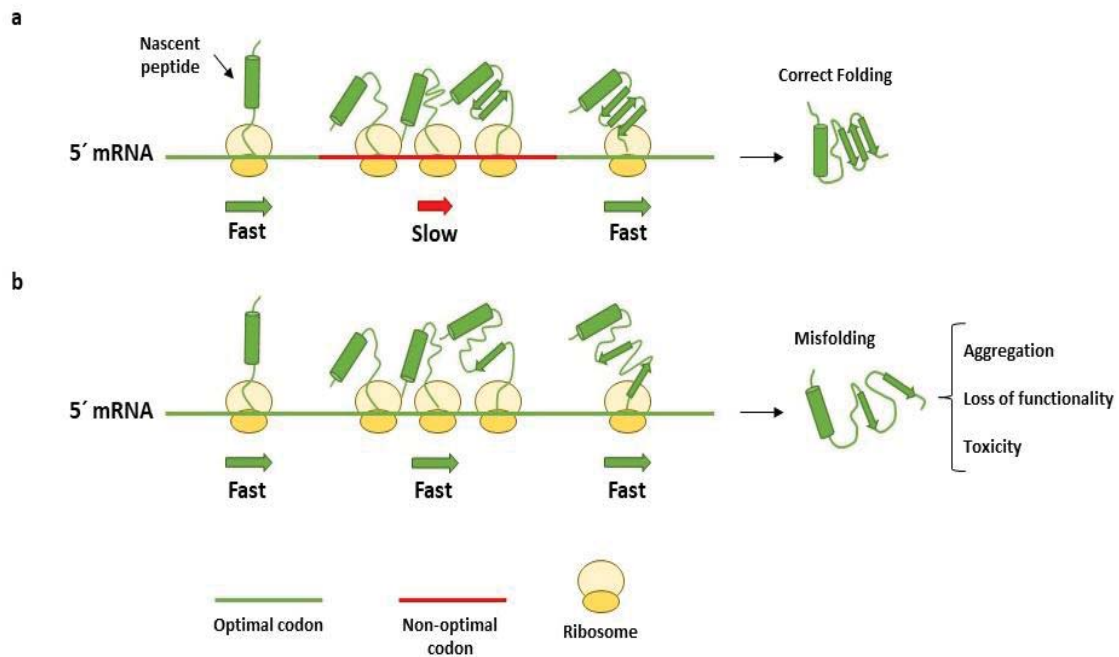
Figure 5. Role of codon usage on co-translational events. **a**. Codon usage adapted to co-translational folding process, the presence of non-optimal codon regions regulates the speed of translation elongation, promoting correct protein folding. **b**. Codon usage non-adapted to co-translational folding process, the speed of translation elongation proceeds uniformly, leading to protein misfolding. Adapted from [198].

4.3. Protein folding and aggregation

Even when the recombinant protein has no detrimental effects on bacterial metabolism and protein expression is effectively achieved, there is no guarantee that the protein will adopt its proper folded structure. Protein folding is a complex process where non-covalent interactions, especially hydrophobic effects, drives the conversion of a single amino acid chain into an intricated structure where the hydrophilic amino acids are exposed and hydrophobic ones are buried into the inner structure, far from the aqueous environment. For some proteins, these hydrophobic forces are enough to lead the proper folding of a specific protein into its native and functional version [201]. However, other proteins, with more complex structures, are not able to reach a proper folding by itself and require the assistance of specialized proteins, called

chaperones. In these cases, before reaching the native structure, proteins adopt a series of folding intermediates which are not kinetically favored, is at this point when non-native interaction may occur, leading to the formation of misfolded protein species **(Figure 6)** [202]. Therefore, a protein may adopt many different conformational states, and within this conformational diversity some protein conformers may expose interactive surfaces including aggregation-prone hydrophobic regions. Protein conformers bearing these exposed regions, tend to interact and associate in the crowned intracellular environment, leading to aggregation, and ultimately, the formation of inclusion bodies (IBs) in bacteria **(see Section 7)** [203,204].
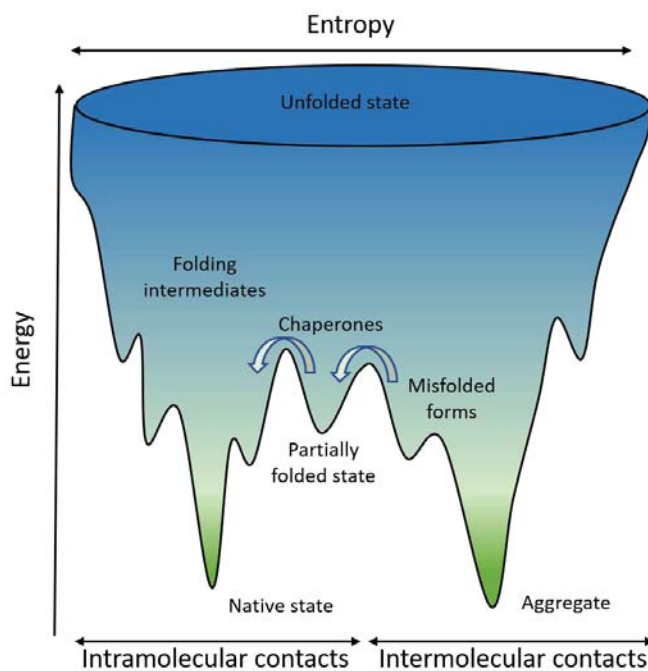
Figure 6. Funnel-like energy landscape of protein folding and aggregation. To achieve a thermodynamically favorable conformation, unfolded proteins need to cross substantial kinetic energy barriers. Chaperones assist protein folding by reducing intermolecular interactions and lowering the energy barriers. Adapted from [202].

During recombinant protein production in bacterial hosts, due the high levels of expression, polypeptides are synthetized in a rate faster than the rate of chaperone-mediated folding, this results in a saturation of the quality control mechanisms and the expressed protein aggregates consequently [205]. To increase the yields of soluble protein and avoid aggregation, different strategies have been proposed. Due to the overloading of the chaperone-mediated pathway, one strategy would be to enhance the availability of chaperones by increasing its quantities inside the cell. Therefore, co-expression of molecular chaperones along with the desired recombinant protein may be a solution to improve the conformational quality and yields of the produced protein [206,207]. However, given the broad variety of protein species, with completely different conformational structures, chaperone co-expression may lead to unpredictable and undesired results [208]. For that reason, this strategy cannot be applied as a general solution and needs to be optimized for each recombinant protein by a trial and error approach [135].

One of the simplest strategies to regulate protein aggregation consist on modifying culture conditions, especially growth temperature. At low temperatures protein biosynthesis is slowed down, thus protein quality control systems are not overwhelm and protein folding occurs at an adequate rate [209]. Additionally, hydrophobic interactions are not favored at low temperatures, which also contributes positively with protein folding [210].

Other strategies imply the direct manipulation of the recombinant protein. One that is traditionally used to increase protein solubility is the addition of solubility tags, at either N or C terminus, of the recombinant gene that is going to be synthetized. The most popular solubilization tags include N-utilization substance protein A (NusA), thioredoxin (Trx), small ubiquitin-like modifier (SUMO), maltose-binding protein (MBP) and glutathione S-transferase (GST) [149]. Additionally, these two latest elements can be used as affinity tags as well. Many of these fusion tags are large proteins, and may potentially interfere with the proper structure and function of the accompanying proteins. For that reason, in some cases, a tag removal process is required. However, tag removal has some associated drawbacks. The use of site-specific proteases for enzymatic cleavage is usually very expensive, accounting for a large portion of the manufacturing cost [211]. Furthermore, to obtain the cleaved protein, two affinity purification steps are needed, one to obtain the fusion protein and other to separate the cleaved protein from the solubilization tag as well as proteases [212]. This is a tedious and time-consuming process, that associated to inefficient enzymatic cleavage, may results in lower protein productivity due to protein loss during purification.

In that cases where protein aggregation is inevitable, some strategies are intended to favor protein aggregation to subsequently purify the resultant IBs and try to obtain the soluble protein from them **(see Section 7.5)**.

5. PROTEIN-BASED NANOFORMULATIONS FOR BIOTECHNOLOGICAL APPLICATIONS

Therapeutic proteins and peptides are very attractive from the pharmaceutical point of view due to their high potency and selectivity. Nonetheless, their efficacy is sometimes curtailed by their low stability and restricted bioavailability, limiting in most cases their therapeutic exploitation. In this sense, different technologies and strategies have been applied in order to overpass these limitations and improve the efficiency of these drugs after administration. Most of these strategies consist on the vehicularization of these proteins or peptides into superior complexes, providing a protective environment and allowing the possibility of deliver them to the right site. Different types of materials have been employed as nanocarriers including inorganic (gold, silver, silica, carbon nanotubes) and organic materials (lipids, polysaccharides, and proteins) [213]. Depending on the nature of the material, some properties of the nanoparticles such us size, drug release profile, solubility, stability, biodegradability and toxicity may differ [214]. In the specific case of protein-based nanoplatforms, certain properties such as biodegradability, biocompatibility, low toxicity and ease of modification makes them an attractive option for the nanoformulation of compounds with therapeutic potential [215].

Besides, the ability of proteins to interact with one another opens the possibility for the isolated monomeric forms to organize into supramolecular structures. In some cases, such interactions lead to the formation of protein aggregates, however, in other cases, protein may self-assemble into defined protein oligomers such as virus capsids, helicases or some chaperones. Although seemingly different, these small-scale complexes all originate from fundamental protein interactions and are driven by similar thermodynamic and kinetic factors [216]. Therefore, apart from the different conformational forms that a monomeric protein can adopt, there is also a diverse set of protein structural arrangements that can be achieved under certain conditions. For example, some proteins such as those that form the viral capsid, spontaneously self-assemble by design [217]. In other cases, environmental changes such as the decline of temperature [218], punctual mutations [219] or conformational changes [220] may be the initiators of this process, influencing the oligomeric state and functionality of the protein. In this context, a protein format can be defined as a superior structural arrangement that involves through directed or not directed interactions, the convergence of isolated protein forms. The different protein formats employed in this work **(Figure 7)** will be further discussed in the following sections.
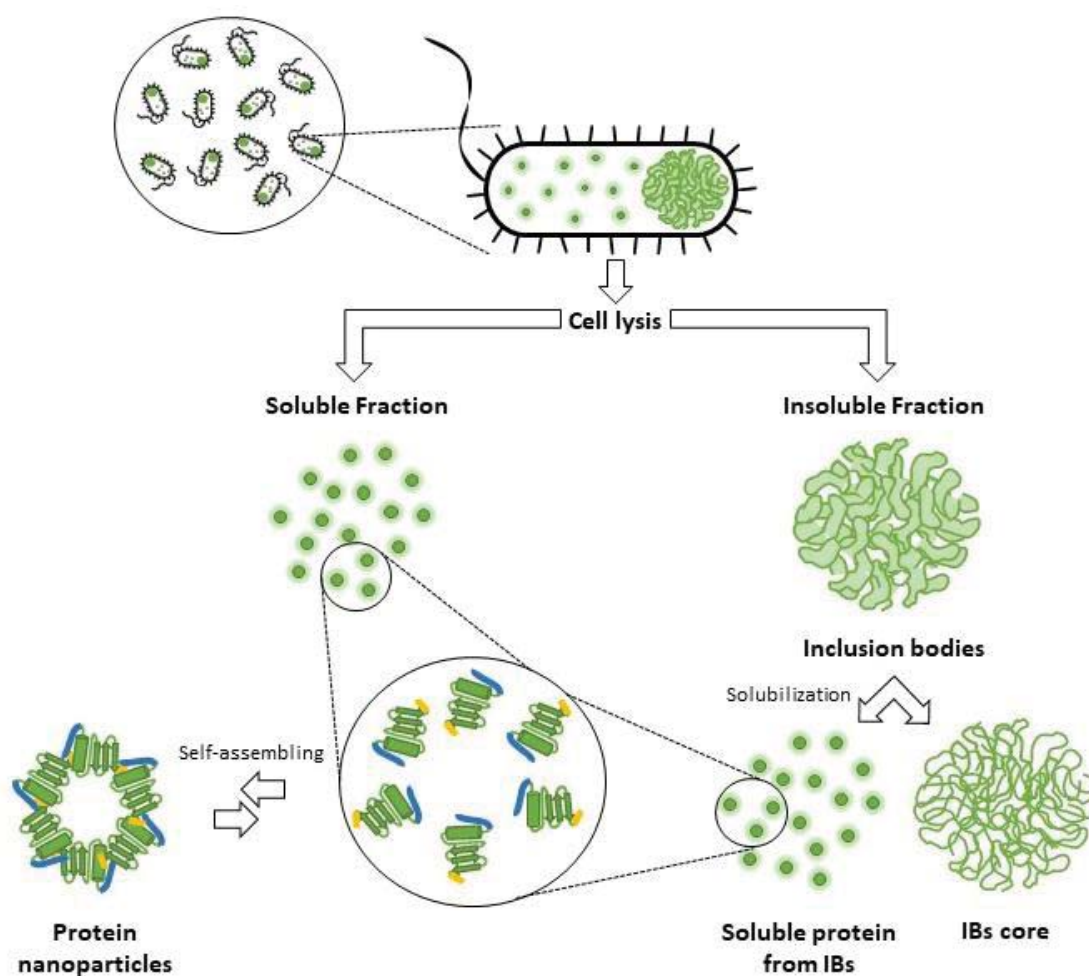
Figure 7. Schematic representation of the different protein formats employed in this work. In the case of large aggregates such as inclusion bodies (IBs), the accumulation of vast amounts of proteins leads the formation of a high-density protein format that can be isolated from the whole cell lysate by centrifugation. On the other hand, small oligomeric forms such as self-assembled nanoparticles would remain in the soluble fraction or may be extracted from the isolated IBs.

6. SOLUBLE FORMAT: PROTEIN NANOPARTICLES

The generation of sophisticated protein architectures based on non-covalent interactions between proteins is highly common in nature. One well-studied example are viruses, whereby the self-assembling capabilities of viral capsid proteins lead to the formation of their complex protective structures. These same structural proteins can be recombinantly expressed forming virus-like particles (VLPs), which lack the viral genetic material, and therefore, can be used for biomedical purposes, as for example, vaccine development [221] or as nanocarriers for drug delivery [222].

Self-assembling can be associated with modularity. In modular proteins, different amino acid sequences (proteins, protein domains or peptides) are gathered together in a single polypeptide chain that combines the properties of all the different individual elements. In our research group, it was described that the combination of two architectonic tags at both N and C-terminus (cationic and poly-histidine peptides, respectively) leads to the self-assembly of specific proteins into protein nanoparticles **(Figure 8)** [223]. In addition to promoting protein self-assembly, these peptides fulfil a dual role. Poly-histidine tags can also be used for purification purposes, and different functionalities have been described for cationic peptides. The number of positive charges in these cationic peptides seems to influence the final nanoparticle size, being those peptides that include more cationic residues responsible of the formation of larger nanoparticles [224].
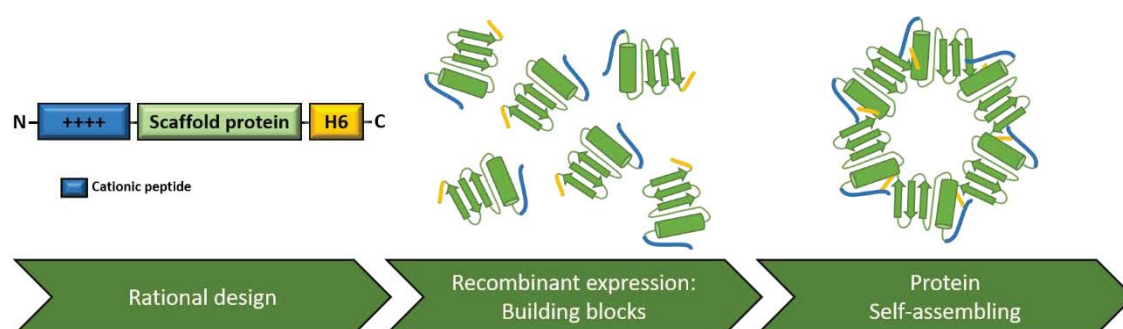
Figure 8. Protein-based nanoarchitectonic principle developed in our group. When the amino terminus of a his-tagged scaffold protein is fused to a cationic peptide, the resultant construct is able to self-assemble as protein only nanoparticles, where each individual monomer acts as a building block.

As an example of application, T22 which is an antagonist cationic peptide of the CXCR4 receptor (overexpressed in metastatic colorectal cancer stem cells) forms self-assembling protein nanoparticles when fused to a hexahistidine-tagged green fluorescent protein (GFP). The resultant nanoparticles are highly stable in human serum, show an estimated size of 12-13 nm by dynamic light scattering (DLS) [225], are observed under transmission electron microscopy (TEM) and field emission scanning electron microscopy (FESEM) as relatively monodispersed entities with a cyclic toroidal organization of the oligomer **(Figure 9)** [226,227], and most importantly, are able to target CXCR4-positive cancer stem cells [225].
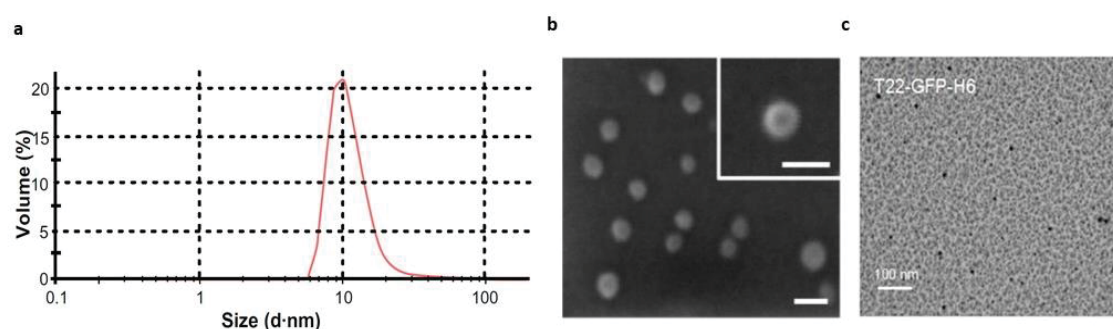
Figure 9. Characterization of T22-GFP-H6 protein nanoparticles. a) Dynamic light scattering (DLS) size analysis of T22-GFP-H6 nanoparticles. b) Field emission scanning electron microscopy (FESEM) images of T22-GFP-H6 nanoparticles showing the cyclic organization of the oligomer. Bars indicate 20 nm. c) Transmission electron microscopy (TEM) of T22-GFP-H6 nanoparticles. Bar indicates 100 nm. Adapted from [225, 226, 227].

This resulted in the development of different modular designs where the GFP was substituted by different protein scaffolds [228]. The addition of AMPs, and specifically GWH1 (with a remarkable content in cationic amino acids) [107], to this modular design has also confirmed the ability of this architectonic principle to lead to protein self-assembly while maintaining the capacity of GWH1 to selectively damage bacterial cells [111]. The self-assembling properties are maintained due to the cationic nature of most antimicrobial peptides. In this particular case, its role is three-fold, being responsible of protein oligomerization, bacterial specificity and antimicrobial activity.

All things considered, this modular design provide wide possibilities, as it is not restricted to any specific polypeptide. Therefore, different combinations may lead to the design of complex supramolecular arrangements with functional versatility.

7. INSOLUBLE FORMAT: INCLUSION BODIES

As previously mentioned, when a bacterial expression system, such as the one based on *E. coli*, is forced to overexpress a certain recombinant protein, the overwhelm of the protein quality control machinery leads to the formation of soluble and insoluble aggregates [229,230]. While IBs are usually recognized as completely formed insoluble aggregates, soluble aggregates can be considered as the initial forms of these large protein deposits. In most cases, these insoluble aggregates are observed inside the cell as large and refractile dense particles of approximately 0.2 - 1 μm. IBs are mainly composed of the expressed heterologous protein, although we can also find other host cell proteins, such as those related to the heat shock response (IbpA and IbpB), chaperones (DnaK) as well as other macromolecular contaminants, such as phospholipids from membranes and nucleic acids [231]. In *E. coli*, IBs are preferentially located at the poles, which is a non-occupied area of the cytoplasm, where they adopt their typical spherical or ovoid shape [232]. However depending on bacterial morphology, other distribution patterns can be observed [203]. During cell division, this particular distribution pattern results in a characteristic inheritance of aggregates between the two emerging cells. For example, in *E. coli*, after cell division, due to the specific location of the IBs within the cell, each daughter cell will receive one aggregate [233]. Within several generations, this process leads to an asymmetric inheritance, where most of the cells are free from aggregates, whereas only a few inherits all. This situation makes that under high-intensity stress, the asymmetric distribution increases the rate of cell division in those cells devoid of IBs, which results in a beneficial effect on the aging of the bacterial cell population [234,235].

7.1. Structural characteristics of IBs

Regarding the structure characteristics of IBs, they have been classically considered for years as amorphous elements devoid of any type of structural organization. However, studies done in the last decade have demonstrated that in these aggregates an amyloid structure coexist with properly or partially folded protein versions [236–238]. Using the fusion protein VP1GFP, which is composed of GFP as a scaffold and VP1 capsid protein of foot-and-mouth disease virus as an aggregation-promoting domain, Cano-Garrido et al. demonstrated that after a digestion process using proteinase K, the morphology as well as the size of these IBs was not affected, however, both the fluorescence emission and density decreased [239]. These results suggested that IBs have a "sponge-like structure" formed by an amyloidal fibrillar matrix, which acts as a scaffold,

43

providing mechanical stability and, in turn, allowing the entrapment of native or native-like protein structures responsible of the functional properties observed in most IBs [240]. Thus, these studies prove the existence of a structural heterogeneity in IBs, where a wide spectrum of possible conformational states of the recombinant protein (native, partially folded and unfolded state) coexists **(Figure 10)** [241].
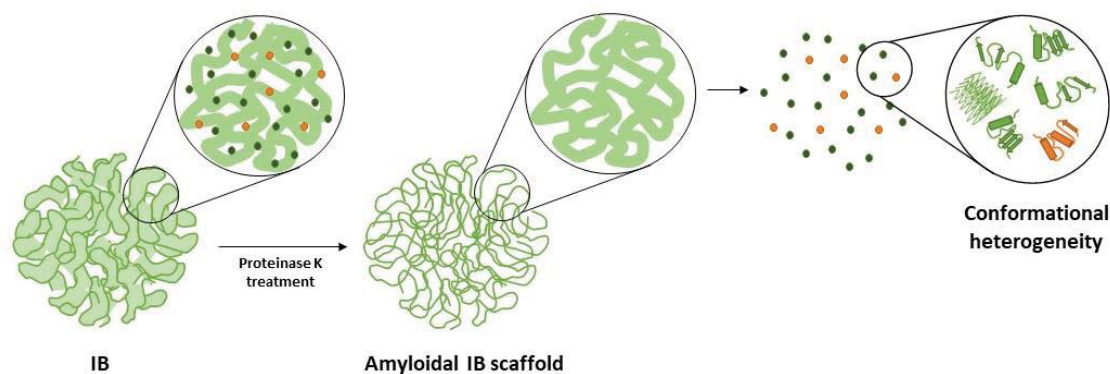
Figure 10. Supramolecular structure of IBs. Different protein conformational configurations, including properly folded, partially folded (dark green) and misfolded (orange), coexist into an amyloid fibrillar skeleton (light green). Adapted from [298].

7.2. Specificity in the aggregation process

The first insights of protein specificity during aggregation arise with the observation that mixed solutions of completely different proteins did not form hybrid co-aggregates after a renaturation process [242,243]. Subsequently, different studies have demonstrated that aggregation is a process that shows high specificity, favoring the interaction between those domains that show greater similarity. The initial studies that supported this idea were mainly based on *in vitro* observations under controlled aggregation conditions [244]. However, *in vivo* evidence of these intermolecular specific interactions between similarly protein domains was still lacking. In 2001 Kopito et al., using the eukaryotic cell line HEK293 as an expression system for the co-expression of two fluorescent proteins biosynthetically tagged to different aggregation-prone proteins demonstrated through fluorescence resonance energy transfer (FRET) experiments that the aggregation process *in vivo* was also highly specific [245]. Years later, a similar study was carried out using *E. coli* as a model expression system. In this case, two aggregation-prone polypeptides, the β-amyloid peptide (Aβ42) and the VP1 capsid protein of foot-and-mouth disease virus were fused to different fluorescent proteins [Blue Fluorescent Protein (BFP) and Green Fluorescent Protein (GFP)]. After analyzing the aggregation process by FRET, it was possible to observe a

greater specificity in the interaction of those fusion proteins that presented the same aggregation domain (Aβ42GFP-Aβ42BFP) compared to the interaction of those that presented different domains (VP1GFP-Aβ42BFP) **(Figure 11)** [237].
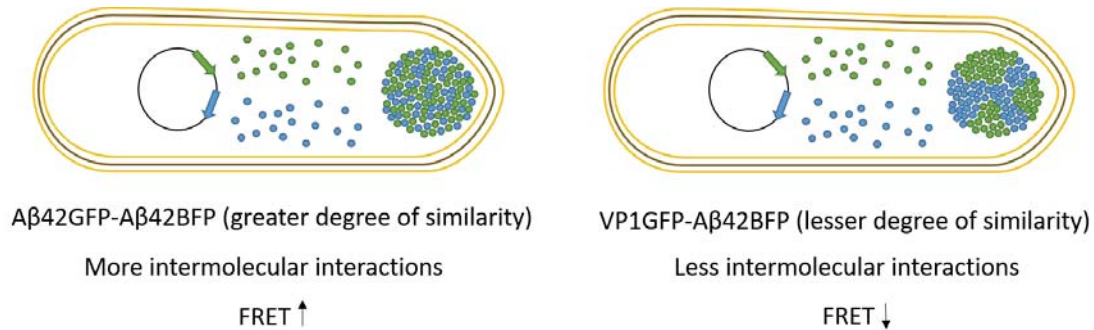
Figure 11. Simplified vision of protein specificity during aggregation process. Those proteins that share similar amino acid sequences, as for example by the addition of common aggregation tags, will tend to form closer intermolecular interactions in IBs. Adapted from [237].

7.3. Tailoring IBs

The generation of IBs is a process that is highly dependent of the physicochemical characteristics of each particular protein. However, different factors can be manipulated in order to favor protein aggregation. These factors can be divided into those that affect transcriptional and translational regulation and environmental factors. In the first case, gene dosage, promoter strength, and nature of the inducer are included. On the other hand, environmental factors that promote IBs formation include, high temperatures (≥ 37 °C), rapid bacterial growth rates, shorter culture times and low pH (< 5.5) [246].

In some cases, aggregation processes cannot be only promoted by indirect manipulations, as the ones mentioned before, and require direct modifications over the recombinant protein to induce IBs formation. Just as there exist solubility tags, so also there exist aggregation tags. This strategy consists on the generation of a fusion protein that contains two different parts, the heterologous protein and a protein domain or peptide which promotes aggregation. In particular, several protein domains have been shown to possess this capacity, including the foot-and-mouth disease virus capsid protein (VP1) [240], a variant of the human β-amyloid peptide (Aβ42 (F19D)) [237], a mutated version of the maltose-binding protein (MalE31) [247], and the cellulose-binding domain of *Clostridium cellulovorans* (CBDclos) [248]. Besides, during last years, several publications have demonstrated the ability of certain self-assembling peptides to

promote the *in vivo* aggregation of those proteins to which they are associated through a protein linker [249–252]. The process is generally driven by specific, non-covalent interactions that occur spontaneously between the different peptide molecules. Such interactions strongly depend on the three-dimensional conformation adopted by the peptides, as has been proven by studies carried out with the peptide 18A (EWLKAFYEKVLEKLKELF) and peptide ELK16 (LELELKLKLELELKLK) which, once expressed, spontaneously adopt an α-helix and β-sheet structure, respectively [251]. Other similar studies have involved the use of surfactant-like peptides (L6KD; LLLLLLKD) showing in the same way a great capacity to induce the formation of IBs in *E. coli* [252], or peptides mainly composed of hydrophobic amino acids (GFIL8; GFILGFIL), being in this case the hydrophobic interactions the main promoting force of aggregation [250].

The use of these self-assembling peptides presents a series of advantages compared to those aggregation tags traditionally used. The most evident is its short length, being constituted, at the very least, by eight amino acids [250]. This characteristic allows them to adopt simpler three-dimensional structures, and at the same time, makes them a much affordable option. On the other hand, in view of a possible therapeutic application, the use of these peptides is more advantageous, since they do not have a viral or bacterial origin, nor are they related to any conformational disease.

7.4. Functionality and applicability of IBs

Initially, IBs were defined as undesirable by-products resulting from protein overexpression. However, the concept of IB has evolved to the extent that it is today considered as a functional product to which multiple biotechnological applications are attributed **(Figure 12)** [253,254].

One of the main factors that has contributed to the development of biotechnological applications based on the use of IBs derives from the observation of biological activity in such aggregates. This is in contrast to the general perception of IBs as a source of non-active protein. However, this traditional belief began to change with the demonstration that IBs are partially composed by functional protein [240,255]. Furthermore, several studies proposed that functional protein content inside IBs can be modulated by temperature changes during protein production, being low temperatures those which favor a better conformational quality and thus, enhanced bioactivity [209,256,257] as it occurs with the soluble protein fraction. This functionality has allowed the use of this format for the immobilization of industrially important enzymes [258], which offers

an effective alternative with respect to the traditionally method, based on the immobilization of the enzyme (in a soluble state) to an inert surface. The immobilization of the soluble enzyme is a complex process during which certain enzymes can be inactivated with the consequent decrease in the overall catalytic activity. Furthermore, catalytically active IBs can be easily purified, and given its mechanical stability, recovered and reused in successive catalysis processes **(Figure 12 a)** [258].
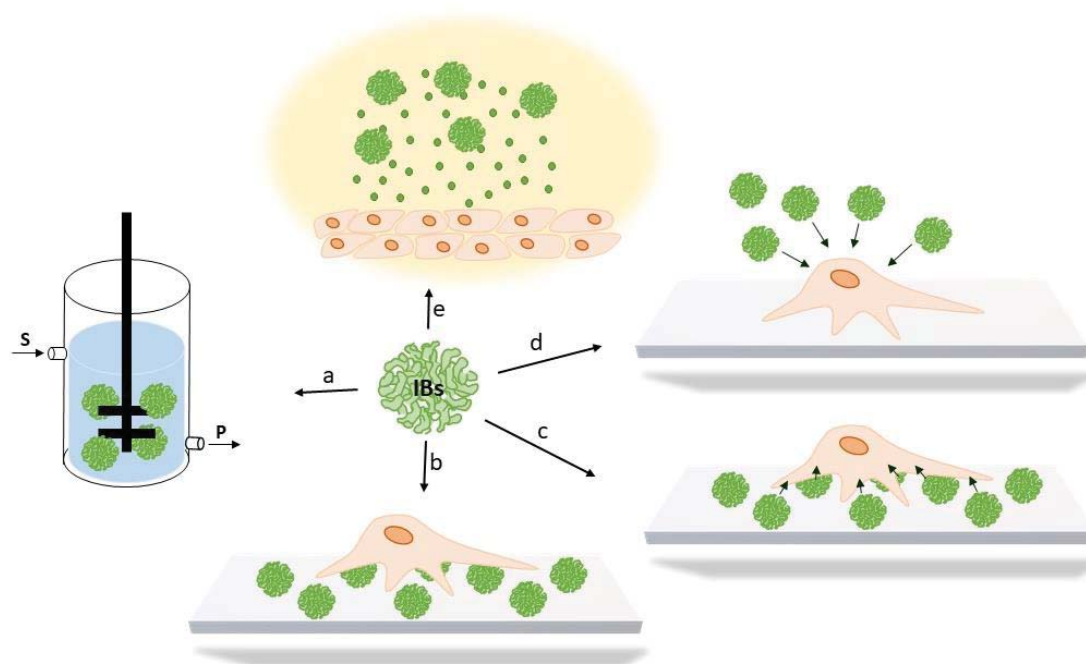
Figure 12. Principal applications attributed to bacterial IBs. IBs can be used as natural immobilized biocatalysts, converting substrates (S) to products (P) (**a**). IBs can be used as topographical agents, decorating flat surfaces and promoting cell adhesion and proliferation (**b**). IBs made of therapeutic proteins can be used as delivery systems in cell culture either by surface immobilization (**c**) or direct administration (**d**). IBs have also demonstrated the ability to act as efficient delivery system during *in vivo* applications, providing an excellent source of soluble bioactive protein (**e**). Adapted from [254].

A second application which has been gaining relevance in recent years, is the possible use of IBs for therapeutic purposes. Different individual observations have allowed the development of this idea: i) the capacity to produce these insoluble aggregates in endotoxin-free bacterial expression systems [259,260], which would reduce undesired immune responses, due to the absence of this contaminants; and ii) the existence of functional and structural similarities between bacterial IBs and secretory granules in the endocrine system. Secretory granules are functional amyloids which under physiological conditions act as hormone storage units, upon specific

stimuli, the retained protein is released with the assistance of cell chaperones [261]. In this context, IBs would act as mimetics of secretory granules, whereby the functional protein is sustainably released, as shown by previous studies carried out both *in vitro* **(Figure 12 b, c and d)** [257] and *in vivo* **(Figure 12 e)** [262]. Regarding *in vivo* application, different proteins including cytokines [263], antitumoral proteins [264], and matrix metalloproteinases [265] are some of the examples reported so far. The released protein can act extracellularly or intracellularly after incorporation into the cell [246]. Furthermore, IBs have demonstrated the ability to interact with cell membranes as well as to be internalized by them [266,267]. This last property, linked to the fact that IBs act as protein releasing materials and the ability to generate these products in endotoxin-free strains have served to define the nanopill concept, which considers those nanoparticles capable of releasing a certain protein with therapeutic effects in a controlled manner [262].

7.5. Recovery of bioactive protein from IBs

In those cases where the traditional soluble format is preferred over the direct utilization of IBs, and no soluble form is obtained during the recombinant production, the insoluble format may also act a source from which this soluble protein can be extracted. There are different types of strategies, one of them consist on classical denaturation and refolding procedures. This is based on the classical view of IBs, in which unfolded and/or misfolded polypeptide chains are not damaged, thus the information for a proper folding is still coded into its amino acid sequence. To obtain the recombinant protein, IBs need to be fully denatured with high concentrations of denaturants (e.g. urea or guanidinium chloride) and subsequently, after denaturant removal, refolded *in vitro* into its native folded version **(Figure 13)**. However, refolding is a protein dependent process that require different steps and the use of complex media composition. Therefore, protein refolding has to be carefully evaluated in every case, and even then, some proteins are not recovered after extensive trial-and-error approaches [135].

Another approach is based on the fact that IBs are composed, at least in part, by functional and therefore properly folded protein. For that reason, these types of procedures are simpler and do not require the disruption of the protein structure. In this sense, those strategies intended to release the entrapped functional protein from IBs are preferred over strategies that involve unfolding/refolding processes. The use of non-denaturing conditions for soluble protein extraction from IBs have been demonstrated in several studies for different proteins [255,257,268]. The use of mild solubilization agents, as for example, mild detergents or low concentrations of

chaotropes, allow an effective release of soluble protein from IBs without modifying the native-like protein structure **(Figure 13)**. In a recent work, the mild detergent N-lauroylsarcosine was used as solubilization agent to extract two functional proteins from *L. lactis* aggregates, the mammary serum amyloid A3 (M-SAA3) and metalloproteinase 9 (MMP-9), a difficult-to-purify and a prone-to-aggregate protein, respectively [184]. However other non-denaturing mild solubilization agents have been described (30 % trifluoroethanol, 5 % n-propanol, 5 % DMSO) [268,269].
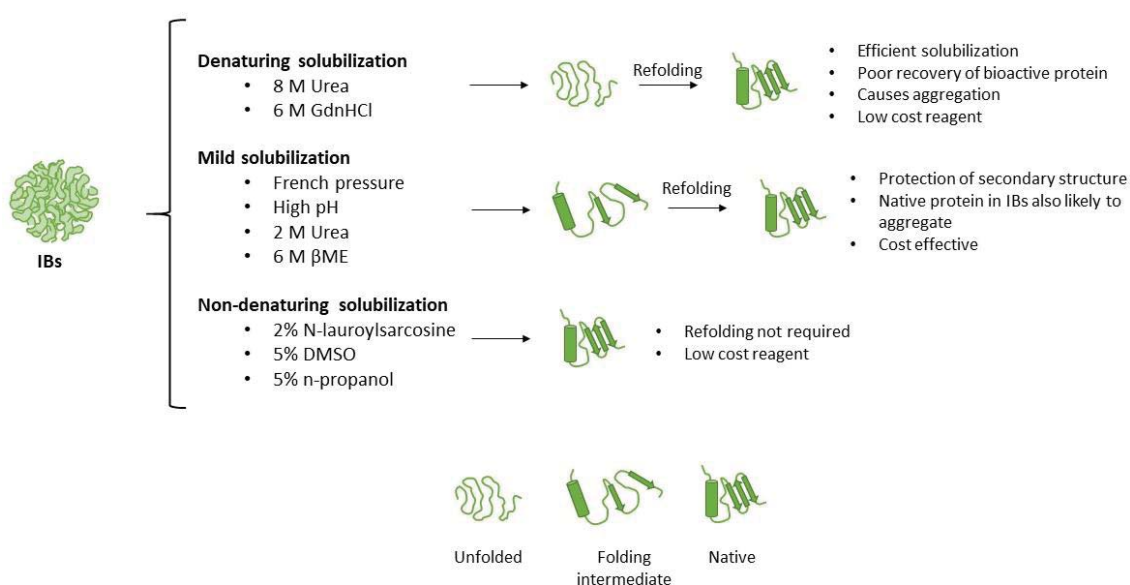
Figure 13. Schematic representation of the different IBs solubilization methods for protein recovery and their main characteristics. Adapted from [268].

OBJECTIVES

The use of certain proteins or peptides such us cytokines or AMPs, respectively, have been proposed as a potential alternative for the treatment of certain medical conditions, specifically those ones related with infectious diseases. In this thesis, the nanoformulation of these molecules into different protein formats including IBs and soluble self-assembling nanoparticles have been characterized and evaluated. In addition, some light has been shed on the forces that govern the aggregation process and how it can be modulated to promote the formation of IBs. For this purpose, different specific objectives have been addressed:

- To validate the importance of selecting the appropriate aggregation tag based on the protein properties to enhance the formation of IBs **(Study 1)**.

- To evaluate the underlying effect of specificity during the aggregation process and how this influences coaggregation **(Study 1)**.

- To test the influence of the addition of these aggregation tags with regard to protein expression levels, aggregation, releasing efficiencies, and functionality of the therapeutic IFN-γ protein **(Study 2)**.

- To explore the relationship between protein conformational diversity and conformational quality of protein subpopulations released from IBs **(Annex 1)**.

- To demonstrate the importance of the multivalent display of GWH1-GFP nanoparticles in terms of antimicrobial activity and its potential use in conjugation with other drugs such as 2′-deoxy-5-fluorouridine pentamer (5-FdU) **(Study 3 and Annex 3)**.

- To evaluate and compare in a mastitis mouse model the antimicrobial performance of the different protein formats containing the immunostimulant IFN-y and the GWH1 AMP and also to explore the synergy between them **(Study 3 and Annex 2)**.

- To review the most recent biotechnological innovations applied to AMPs in order to surpass some of the major disadvantages associated with this amino acid-based compounds **(Study 4)**.

RESULTS

STUDY 1

Insoluble proteins catch heterologous soluble proteins into inclusion bodies by intermolecular interaction of aggregating peptides

Jose Vicente Carratalá, Andrés Cisneros, Elijah Hellman, Antonio Villaverde and Neus Ferrer-Miralles

Microbial Cell Factories 20:30, 2021

Protein aggregation is a biological event observed in expression systems in which the recombinant protein is produced under stress conditions surpassing the homeostasis of the protein quality control system. This results in the formation of IBs in bacteria, a characteristic protein-based nanostructure to which different properties are attributed, and whose formation mechanism is of particular interest. However, the aggregation process is highly dependent of the physicochemical characteristics of each particular protein, being some proteins less prone to aggregation. In those cases, the promotion of protein aggregation can be achieved by the addition of aggregation prone stretches to the heterologous polypeptide chain, generating a fusion protein.

There is a wide variety of aggregation-prone peptides or polypeptides that can be employed as igniters of aggregation. These differ in origin and length, but in all cases, the intermolecular interactions that are stablished among them are the major driving force for these aggregation processes. However, contrary to general belief, the aggregation tag and the heterologous protein to which is fused, are not separate entities, and both elements contribute to the overall aggregation propensity. While the aggregation tag used may promote aggregation to a variable degree, the heterologous protein may have a positive, neutral or negative contribution to this process, suggesting that there is a net balance between the two components that needs to be studied for each combination.

In the present work, the aggregation efficiency of different aggregation tags over distinct heterologous proteins produced in *E. coli* was explored. Furthermore, a detailed analysis of the effect in aggregation propensity by the fusion of a series of L6K2-derived peptides to a specific protein (GFP) was also addressed. Finally, the importance of the stereospecific intermolecular interactions to promote coaggregation between proteins sharing a common aggregation tag was analyzed.

Microbial Cell Factories

RESEARCH

Open Access

Title: insoluble proteins catch heterologous soluble proteins into inclusion bodies by intermolecular interaction of aggregating peptides

Jose Vicente Carratalá[1,2,3], Andrés Cisneros[1,2], Elijah Hellman[1,2], Antonio Villaverde[1,2,3] and Neus Ferrer-Miralles[1,2,3*]

Abstract

Background: Protein aggregation is a biological event observed in expression systems in which the recombinant protein is produced under stressful conditions surpassing the homeostasis of the protein quality control system. In addition, protein aggregation is also related to conformational diseases in animals as transmissible prion diseases or non-transmissible neurodegenerative diseases including Alzheimer, Parkinson's disease, amyloidosis and multiple system atrophy among others. At the molecular level, the presence of aggregation-prone domains in protein molecules act as seeding igniters to induce the accumulation of protein molecules in protease-resistant clusters by intermolecular interactions.

Results: In this work we have studied the aggregating-prone performance of a small peptide (L6K2) with additional antimicrobial activity and we have elucidated the relevance of the accompanying scaffold protein to enhance the aggregating profile of the fusion protein. Furthermore, we demonstrated that the fusion of L6K2 to highly soluble recombinant proteins directs the protein to inclusion bodies (IBs) in *E. coli* through stereospecific interactions in the presence of an insoluble protein displaying the same aggregating-prone peptide (APP).

Conclusions: These data suggest that the molecular bases of protein aggregation are related to the net balance of protein aggregation potential and not only to the presence of APPs. This is then presented as a generic platform to generate hybrid protein aggregates in microbial cell factories for biopharmaceutical and biotechnological applications.

Keywords: Recombinant protein, Inclusion body formation, Protein aggregation, Intermolecular interaction, Antimicrobial peptides

Background

Protein aggregation is an event widespread distributed from bacteria to animals. In bacteria, it has been related to stress states with the deployment of a complex protein network to compensate for the reduction of the ability of the cells to cope with the conformational stress [1]. In contrast, in yeast, protein aggregation is an inheritable adaptive phenomenon [2]. In animals, protein

*Correspondence: neus.ferrer@uab.cat
[3] Bioengineering, Biomaterials and Nanomedicine Networking Biomedical Research Centre (CIBER-BBN), 08193 Bellaterra, Barcelona, Spain
Full list of author information is available at the end of the article

aggregation is also observed in pathological states related to conformational diseases [3], but is also associated to the formation of hormone aggregates in secretory granules [4].

During recombinant protein production, the detection of protein aggregates is a common outcome and is observed in both eukaryotic and prokaryotic expression systems [5, 6]. Bioinformatic tools are available for prediction of protein and peptide solubility and to identify aggregation-prone hot spots in the amino acid sequence, which can be modified during the design of recombinant genes [7–9]. However, changes in the primary structure of the natural proteins may lead to secondary effects as the appearance of immunogenic epitopes [10]. Therefore, the aggregation propensity of the produced protein may be reduced by lowering the transcription and translation rates of the gene, keeping intact the original amino acid sequence [11]. The main variables include the media composition, incubation temperature, promoter strength and inductor concentration among others [12].

In prokaryotes, the solubility of proteins is controlled by the protein quality control system, a complex network of protein factors involved in protein folding, unfolding and degradation [13]. In bacteria, aggregates, known as inclusion bodies (IBs), are dynamic protein clusters from which solubilized active protein conformers are released under physiological conditions [14–16]. In fact, recent experimental approaches have revealed the ability of active IBs to rescue enzymatic activities in cell cultures and to target cancer stem cells in cancer animal models [17–21]. Therefore, IBs are envisioned as depots of recombinant protein with the capacity to release the protein of interest from a complex and stable scaffold that protects the biological activity of the embed protein over time. Therefore, the enhancement of protein aggregation in this type of nanostructures is gaining interest. In fact, bioprocess design during recombinant protein production has been shown to impact the size of the IBs and the physicochemical quality of the recombinant protein achieving constant production of IBs [22–24]. In addition, aggregation propensity of recombinant proteins in expression systems may be enhanced by the addition of aggregation-prone peptides (APPs) in the design of the coding DNA sequence of the gene [25]. APP promote the establishment of intermolecular interactions between protein species enhancing the tendency of the resulting complexes to accumulate in the insoluble cell fraction [26]. Aggregation domains can be found in nature, in particular, several protein domains have been shown to possess such aggregation capacity, including a variant of the human β-amyloid peptide (Aβ42 (F19D)) [27], a mutant of the maltose binding protein (MalE31) [28], and the cellulose-binding domain of Clostridium cellulovorans

(CBDclos) [29], among others. Another peptide with high capacity to enhance protein aggregation is VP1, a peptide sequence present in the VP1 structural protein of the *Foot-and-mouth disease virus* [26]. Due to safety and regulatory purposes, the use of viral protein domains, as VP1, is not suitable for some applications. For that reason, the development of novel APPs is of great interest.

In this study, we have selected a small APP of 8 amino acids in length (L6K2) to study the potential of this type of peptides to enhance the aggregation propensity of soluble proteins [30]. In addition, we have amplified its aggregating potential by protein engineering and demonstrated the antimicrobial activity of this type of amphipathic alpha-helices. We have also analyzed the role of stereospecific interactions in the aggregation of heterologous recombinant proteins in the presence of L6K2-containing peptides, providing a platform to obtain hybrid IBs inside the cells. These results have relevant implications in the biopharmaceutical and biotechnological applications of IBs.

Results and discussion
Modulation of recombinant protein solubility in *ClearColi* cells

In order to study the performance of APP fused to recombinant proteins in the endotoxin free *ClearColi*™ expression system, two model soluble proteins; iRFP (near-infrared fluorescent protein) and GFP (green fluorescence protein) were selected as scaffolds and fused to the surfactant-like peptide L6K2, previously described as APP (Fig. 1a) [14].

In transformed *ClearColi* cells, recombinant H6iRFP protein was equally distributed in both soluble and insoluble cell fractions (Fig. 1b, c). As expected, upon L6K2 fusion, a different distribution pattern was observed, where most of the protein was located in the insoluble cell fraction, suggesting an increased aggregation tendency for this fusion protein (Fig. 1b, c). The change in solubility pattern was achieved within 1 h of induction and was maintained for up to 5 h (Fig. 1b). As a model APP, with high ability to enhance aggregation tendency of recombinant proteins, VP1 from the capsid protein of the *Foot-and-mouth disease virus* [26, 27] was fused to GFP (Fig. 1a). As expected, most of the protein signal in the sample was detected in the insoluble cell fraction (Fig. 1b, c). In contrast, the recombinant H6GFPL6K2 was mostly detected in the soluble cell fraction (Fig. 1b, c). These results indicated that the aggregation propensity of a recombinant protein may be modulated by APP although the solubility tendency of the scaffold protein may counteract this effect (compare solubility of iRFP and GFP when fused to L6K2 in Fig. 1b, c). In the case of VP1, the aggregation tendency overcome the high solubility of the

Fig. 1 Effect of the addition of L6K2 in the aggregation propensity of fluorescent proteins. **a** Schematic representation of the recombinant genes is shown displaying protein domains by separate squares. H6 indicates the presence of a Hisx6 tag. PT corresponds to a linker with the indicated amino acid sequence. **b** Comparative aggregation propensity of iRFP and GFP in the presence of L6K2. VP1GFPH6 corresponds to a GFP fused to VP1 considered as positive control of the experiment. **c** Relative solubility (%) of recombinant proteins detailed in panel **a** analyzed by Western Blotting. Equivalent number of transformed *ClearColi* cells were lysed and soluble and insoluble cells fractions were separated. All proteins were detected with anti-his antibody

GFP, while GFP solubility was not affected by the L6K2 addition (compare solubility of GFP when fused to VP1 or L6K2 in Fig. 1b, c).

Impact of APP length on protein solubility in *ClearColi* cells
As the ability of L6K2 to reduce solubility of GFP was not significant while it was effective in iRFP, we decided to evaluate the effect of peptide length in the solubility of GFP. For that, we redesigned the H6GFPL6K2 recombinant gene to add at the C-terminus of the GFP sequence, different versions of the surfactant-like peptide L6K2 (Fig. 2a). The aggregating potential of L6K2 peptide was amplified by reiteration of leucine and lysine repeats in different positions (see Table 1) and analyzed by AGGRESCAN software [8]. Selected peptides displayed higher hot spot area (HSA) than the original L6K2 peptide. However, only L12K4 and L18K6 showed increased normalized hot spot area (NHSA) and increased average aggregation-propensity hot spot (a^{4}vAHS).
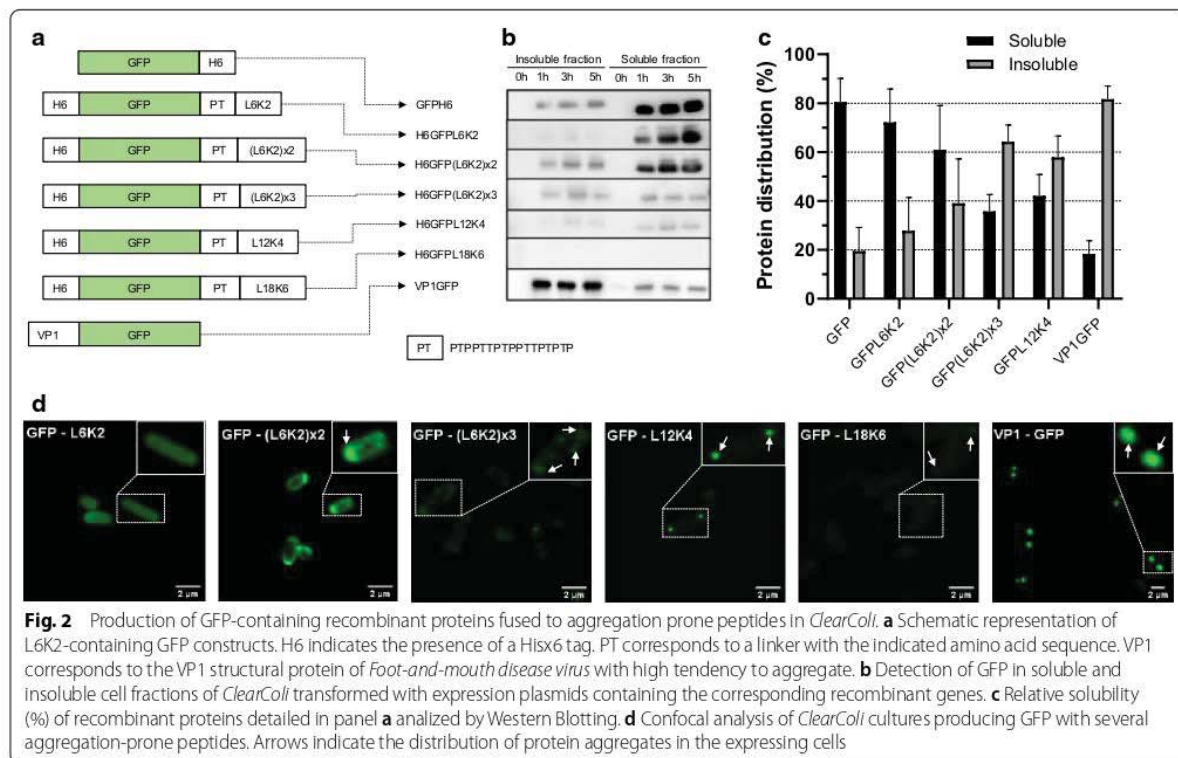
As previously observed, H6GFPL6K2 was detected in the soluble cell fraction of transformed *ClearColi* cells (Fig. 2b, c) and consequently, the emitted fluorescence was homogenously distributed in the cytosol (Fig. 2d). The addition of the L6K2 derived peptides had a positive impact in protein aggregation tendency. As expected, the distribution of fluorescence in the transformed cells was detected in protein clusters (IBs; Fig. 2d and Additional file 1: Fig S1a). In fact, we detected two different aggregation patterns in the L6K2 derived constructs. On the one hand, the proteins containing serial L6K2 repeats ((L6K2)x2 and (L6K2)x3) were preferentially detected in periplasmic areas around the cells, while the constructs containing longer Leucine/Lysine tracks (L12K4 and L18K6) were detected as fluorescent cellular pole aggregates. Therefore, the serial L6K2 repeats acted both as APP and periplasm localization signals since the fluorescence pattern revealed the clustering of signal in discrete aggregates on the periphery of the cell cytoplasm. In addition, the aggregation tendency in L6K2 repeats increased with the number of repeats while L12K4 presented an aggregation pattern like the observed in cells expressing the positive control VP1GFP. This aggregation tendency was not recorded in Western Blot analysis of the soluble and insoluble cell fractions (Fig. 2b, c), indicating that the aggregation tendency of the L6K2-derived peptides may be sensitive to the tested experimental conditions of protein extraction. This was not the case of the aggregation pattern of VP1GFP construct that was perfectly replicated under confocal laser scanning microscopy and SDS-PAGE (Compare VP1GFP data in Fig. 2b–d).

Antimicrobial activity of L6K2-containing recombinant proteins
During recombinant gene expression experiments of L6K2-containing constructs, the growth of transformed *E. coli* cells was compromised, especially in the case of L18K6 (data not shown). At that point, we reasoned whether the peptides were toxic to the cell by displaying antimicrobial activity. The modeling of the L6K2 derived peptides with PEP-FOLD 3 [31–33] displayed amphipathic alpha helices in all cases (Additional file 2: Figure S2a). The preferred conformation of the L6K2-containing peptides was maintained in the presence of the PT

Fig. 2 Production of GFP-containing recombinant proteins fused to aggregation prone peptides in *ClearColi*. **a** Schematic representation of L6K2-containing GFP constructs. H6 indicates the presence of a Hisx6 tag. PT corresponds to a linker with the indicated amino acid sequence. VP1 corresponds to the VP1 structural protein of *Foot-and-mouth disease virus* with high tendency to aggregate. **b** Detection of GFP in soluble and insoluble cell fractions of *ClearColi* transformed with expression plasmids containing the corresponding recombinant genes. **c** Relative solubility (%) of recombinant proteins detailed in panel **a** analized by Western Blotting. **d** Confocal analysis of *ClearColi* cultures producing GFP with several aggregation-prone peptides. Arrows indicate the distribution of protein aggregates in the expressing cells

Table 1 Predictions of "hot spots (HS)" of aggregation in aggregating polypeptides by AGGRESCAN [8]

Name	HS region	HS size	Sequence	HSA	NHSA	a⁴vAHS	Ref.
L6K2	1–6	6	LLLLLLKK	6.211	1.035	0.949	[22]
(L6K2)x2	1–14	14	LLLLLLKKLLLLLLKK	12.789	0.913	0.865	This study
(L6K2)x3	1–22	22	LLLLLLKKLLLLLLKKLLLLLLKK	19.367	0.880	0.842	This study
L12K4	1–13	13	LLLLLLLLLLLLKKKK	14.625	1.125	1.074	This study
L18K6	1–19	19	LLLLLLLLLLLLLLLLLLKKKKKK	23.025	1.212	1.171	This study

HS hot spot, *HSA* hot spot area, *NHSA* normalized HSA, *a4vAHS* average aggregation-propensity in each HS

linker, which has been described as a flexible peptide for separating protein domains (Additional file 2: Fig. S2b) [34]. This configuration has been described in naturally produced or synthetic cationic antimicrobial peptides (AMP) which have been proposed as a potential new class of antimicrobial drugs [35]. The production of small peptides is difficult to be reached by recombinant technologies due to reduced stability, and alternative strategies have been taken to overcome such a main bottleneck [36]. One possibility is the fusion of AMP to partner proteins for a potential dual effect on the final product. First, the reduction of the toxicity of the AMP over the expressing host, and the improvement in the stability

of the peptide in expression systems [37]. However, the study of their activity when fused to reporter proteins by genetic engineering has not been explored in depth. Examples of this strategy include the fusion between GWH1 [38] and GFPH6 [14, 39] and the secretory production of AMP-containing fusion partners [40]. In those studies, the fusion of the AMP to the N-terminus of recombinant protein preserved the bactericidal activity of the AMP even though with its C-terminus anchored by the fusion. Therefore, we analyzed the putative antimicrobial activity of the purified soluble versions of H6GFPL6K2 and H6GFP(L6K2)X2 proteins and compared these data with that obtained for purified GWH1GFPH6.

The results indicated that the antimicrobial activity of L6K2-containing recombinant proteins is strain specific (Fig. 3), being comparable to the antimicrobial activity of GWH1 peptide fused to GFP in *E. coli* cultures (Fig. 3b). In addition, the position of the peptide at each end of the scaffold protein did not appear to be relevant to the antimicrobial activity. On the other hand, the incubation of *S. aureus* with the proteins containing amphipathic alpha-helices had only a slight effect on cell viability under the tested conditions (Fig. 3a). Interestingly, the antimicrobial activity of the recombinant proteins was completely different when *Micrococcus luteus* cells were challenged. The addition of the purified proteins had a positive effect on cell viability at lower concentrations while at the highest protein concentration (8 μmol/L) the cell viability dropped drastically (Fig. 3c).

As observed in Fig. 3b, the antimicrobial activity of the L6K2-containing constructs was detected in *E. coli* cultures at low protein concentrations. This mechanism may explain the cell growth inhibition observed in *ClearColi* cultures transformed with expression vectors with cloned L6K2-derived genes. Small cationic or amphipathic molecules, similar to the ones described in this work, have been described as produced by prokaryotes and eukaryotic organisms as defense against infectious agents. These molecules belong to a non-specific ancient system of innate immunity and they perform their activity through direct interaction with membranes, nucleic acids, protein or even activate autolysins [41–44]. In the case of interacting with membranes, they cause the destabilization of the cytoplasmic membrane by forming pores or by their arrangement parallel to the membrane surface, disrupting the proton motive force and provoking the leakage of vital molecules which lead to cell death. However, even

though their mechanism of action is nonspecific, it has been described a differential efficacy of the same antimicrobial peptide between Gram-negative and Gram-positive bacteria [45, 46]. In the case of Gram-positive bacteria, apart from membrane disruption, the reaction requires further interactions with the cell wall [45].

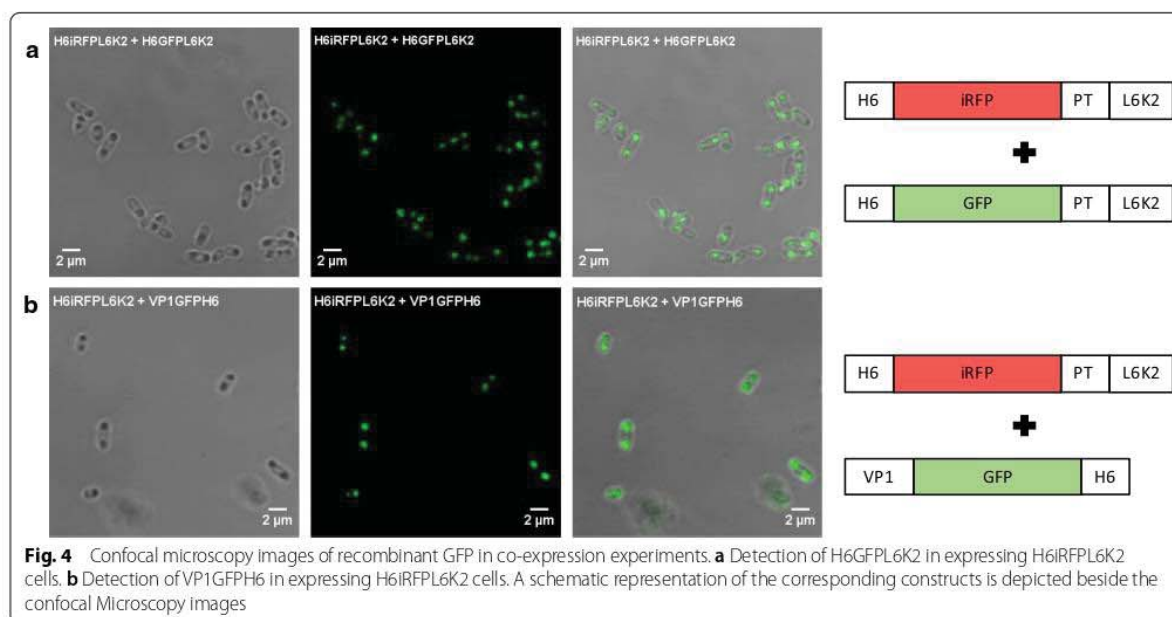## Pull-down effect on aggregation tendency of H6GFPL6K2

Aggregation of different proteins may be enhanced by the stereospecific interaction of APP in bacteria [26]. In that context, we reasoned that the aggregation ability of a recombinant protein with the same APP may enhance the aggregation tendency of H6GFPL6K2 when produced simultaneously in cells. For that purpose, we generated a dual expression vector including the gene encoding for H6iRFPL6K2, which displayed a high tendency to aggregate beside the gene coding for H6GFPL6K2 to be simultaneously expressed. In cells expressing at the same time the aggregation prone H6iRFPL6K2 construct and the soluble H6GFPL6K2 construct, the fluorescence of the GFP shifted from the cytoplasm to polar protein aggregates (IBs) (Fig. 4). The green fluorescence distribution in expressing cells was similar to the pattern observed when co-expressing VP1GFPH6 and H6iRFPL6K2.

The change in the aggregation propensity of the H6GFPL6K2 seemed to be directed by the pull-down ability of the L6K2 peptide present in the H6iRFPL6K2 construct. The intermolecular interactions between L6K2 present in the two proteins enhances the aggregation tendency of GFP. In the expressing cells, the newly formed H6GFPL6K2, when interacting with H6iRFPL6K2 with a high tendency to aggregate was dragged to the insoluble cell fraction. Therefore, it may be hypothesized that when two different proteins share aggregation prone domains, even
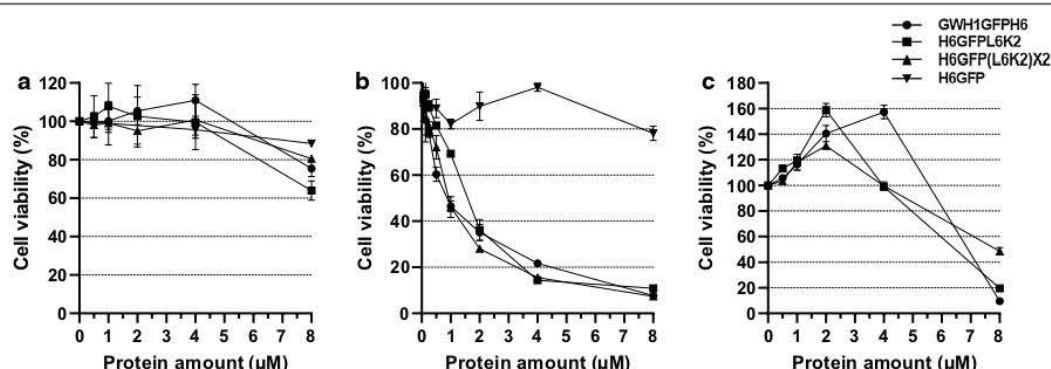
Fig. 3 Survival curves of microbial cells in the presence of putative antimicrobial peptides fused to GFP protein. **a** *Staphylococcus aureus*, **b** *Escherichia coli* and **c**. *Micrococcus luteus*. The results are presented as mean of two replicas for each analyzed point with corresponding standard error bar. Similar CFU where seeded on 96-well plates and the indicated protein concentrations were added to evaluate its effect on cell metabolism

Fig. 4 Confocal microscopy images of recombinant GFP in co-expression experiments. **a** Detection of H6GFPL6K2 in expressing H6iRFPL6K2 cells. **b** Detection of VP1GFPH6 in expressing H6iRFPL6K2 cells. A schematic representation of the corresponding constructs is depicted beside the confocal Microscopy images

if one of the proteins is still soluble, the protein with the highly aggregation propensity may lead the accompanying soluble protein to the insoluble cell fraction through coexpression. However, although the secondary structure of the iRFP and GFP proteins is not similar (Additional file 3: Figure S3), the effect of the iRFP scaffold protein in the aggregation enhancement of H6GFPL6K2 may not be ruled out. For that reason, a spectral variant of GFP (EBFP2; highly similar in amino acid sequence and secondary structure) was fused to VP1 domain generating VP1EBFP2H6 construct (Additional file 4: Figure S4). Predictably, when produced recombinantly, this protein was mainly accumulated in the insoluble cell fraction (Additional file 5: Figure S5).
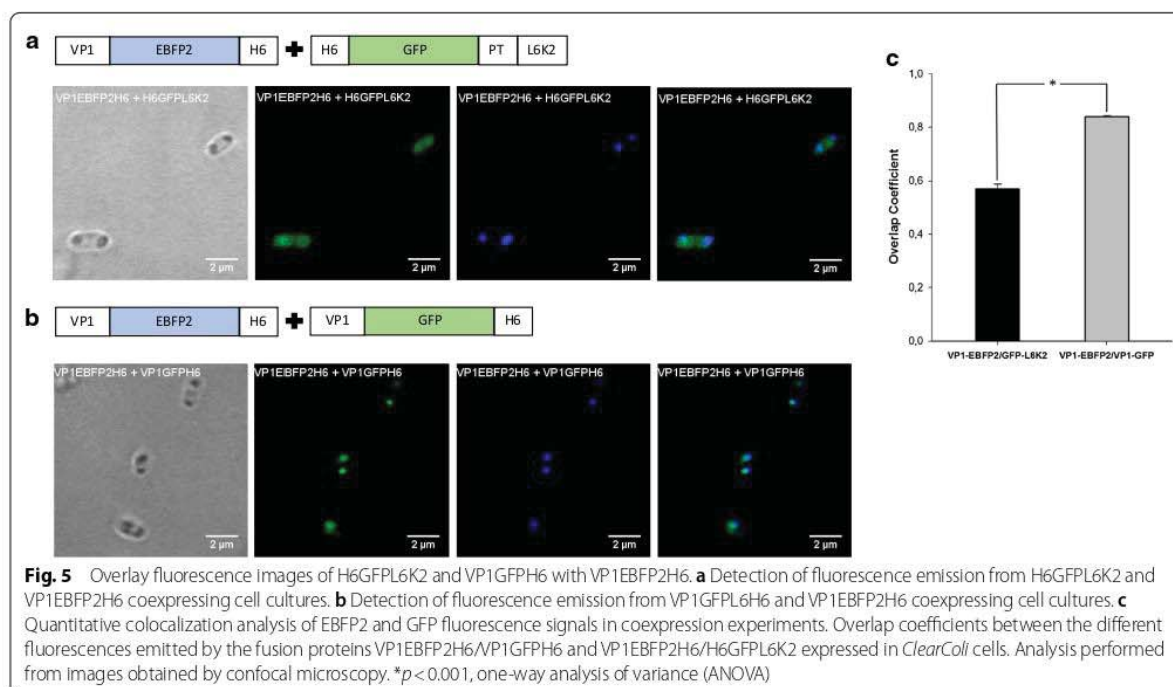
The distribution of the GFP fluorescence in cells simultaneously transformed with plasmids coding H6GFPL6K2 and VP1EBFP2H6 was homogeneously distributed in the cytoplasm of the cells, in agreement with the data obtained in the expression experiment of H6GFPL6K2 alone (compare the distribution of GFP fluorescence in Figs. 2c and 5a, and Additional file 1: Fig. S1b). On the other hand, the fluorescence emitted by EBFP2 fused to VP1 in those cells was mainly detected in polar IBs as expected. When VP1GFPH6 was expressed along with VP1EBFP2H6, the GFP fluorescence was located exclusively at the poles of the cells, as IBs (Fig. 5b and Additional file 1: Fig. S1b). The colocalization analysis of the fluorescence emission from both proteins indicated the preference of H6GFPL6K2 to aggregate in the presence of the same APP (Fig. 5c) ruling out an aggregating

role of the scaffold protein in this process. Therefore, this result has a direct application for biopharmaceutical and biotechnological applications through protein engineering. In fact, these protein nanoclusters have been described as a source of soluble active protein obtained upon incubation in non-denaturing conditions [14–16] and have also been administered as biocompatible depots for tumor targeting of therapeutic proteins [17–21]. Furthermore, protein aggregation seems to be a common mechanism described in most of the expression systems [47–49] that opens up the possibility of expanding this type of strategy to proteins that are difficult to produce in prokaryotes. Therefore, the fusion of common APP to different therapeutic recombinant proteins can induce the colocalization of two recombinant proteins in IBs, obtaining protein formulations with potential synergic activities.

Conclusions

Protein aggregation is a universal event which is associated to conformational diseases in eukaryotes. In bacteria, although it has been described as a symptom of metabolic stress resistance, some studies suggest the relevance of protein aggregation in physiological adaptation to stress [1]. In most of the recombinant protein production experiments described so far, a variable portion of the protein accumulated in bacterial IBs. In recent years, the use of IBs as active protein deposits has begun to be explored for biopharmaceutical and biotechnological applications [22, 50]. The current study highlighted

Fig. 5 Overlay fluorescence images of H6GFPL6K2 and VP1GFPH6 with VP1EBFP2H6. **a** Detection of fluorescence emission from H6GFPL6K2 and VP1EBFP2H6 coexpressing cell cultures. **b** Detection of fluorescence emission from VP1GFPL6H6 and VP1EBFP2H6 coexpressing cell cultures. **c** Quantitative colocalization analysis of EBFP2 and GFP fluorescence signals in coexpression experiments. Overlap coefficients between the different fluorescences emitted by the fusion proteins VP1EBFP2H6/VP1GFPH6 and VP1EBFP2H6/H6GFPL6K2 expressed in *ClearColi* cells. Analysis performed from images obtained by confocal microscopy. *$p < 0.001$, one-way analysis of variance (ANOVA)

the ability to enhance protein aggregation by the fusion of APPs to recombinant proteins used as baits for the capture of soluble proteins. This effect was even observed for highly soluble proteins as GFP. In addition, hybrid IBs, enriched in two different recombinant proteins, were formed through stereospecific interactions between common APP. Therefore, the presented data described the potential of APP in the control of the aggregation propensity of recombinant proteins in biological formulations based on IBs and open up the possible exploration of synergic activities of hybrid protein aggregates, produced in bacterial cell factories, for biomedical and nanobiotechnological purposes.

Methods
Molecular cloning
All protein designs were cloned in pETDuet™-1 plasmid (Novagen), except for H6iRFP, GFPH6 an GWH1GFPH6, which were cloned into *Nde*I and *Hind*III sites of plasmid pET22b (Novagen). For all pETDuet™-1 derived expression vectors, protein-coding DNA fragments were inserted in either, MCS1 or MCS2 of pETDuet™-1 plasmid. In the case of H6GFPL6K2, H6GFP(L6K2)X2, H6GFP(L6K2)X3, H6GFPL12K4, H6GFPL18K6 and VP1GFPH6, digestion was performed with *Nde*I and *Xho*I and insertion into the MCS2. On the other hand, H6iRFPL6K2 and VP1EBFP2H6 were digested

with *Nco*I and *Hind*III and inserted into the MCS1. For dual expression plasmids, H6iRFPL6K2 + H6GFPL6K2, H6iRFPL6K2 + VP1GFPH6, VP1EBFP2H6 + VP1GFPH6 and VP1EBFP2H6 + H6GFPL6K2 a two-step cloning strategy was followed. After the generation of the MCS2 cloning plasmids (pETDuet-H6GFPL6K2 and pETDuet-VP1GFPH6), H6iRFPL6K2 and VP1EBFP2H6 fragments were inserted into the MCS1 after digestion with *Nco*I and *Hind*III. All L6K2-containing protein versions included a linker (PT) between GFP and the L6K2 peptide or derivatives as previously described [30].

Expression of recombinant proteins in *ClearColi* cells
ClearColi BL21 (DE3) was selected as expression host for the different versions of the fluorescent proteins. The same conditions were applied in all cases. Briefly, after transformation with the corresponding expression vector, bacterial cells were allowed to growth in lysogenic broth (LB) medium supplemented with 100 µg/ml ampicillin in a shake flask (250 rpm) at 37 ºC. When cultures reached an optical density of approximately 0.5–0.6, protein expression was induced by adding 1 mmol/L isopropyl-β-D-thiogalactopyranoside (IPTG). Protein samples were taken at the indicated times (h) postinduction. In all cases, bacterial OD was measured and adjusted to 1, subsequently cells were collected by centrifugation (5 minutes, 1,200 *g*). Resuspended cells were processed for

confocal microscopy visualization or to evaluate the relative protein distribution between the insoluble and soluble cell fractions, in those cases, the expression time was set at 3 h.

Evaluation of protein aggregation propensity

Bacterial pellets harboring the expressed proteins were resuspended in 1 mL of PBS until a homogeneous suspension was achieved. Bacterial cell disruption was carried out by sonication (1 round of 1 min at 10 % amplitude and 1 round of 1 min at 15 % amplitude). Then, the soluble and insoluble cell fractions were separated by centrifugation (15 min, 15,000 g at 4 °C). The insoluble cell fraction, containing the cell debris, was resuspended in 1 mL of PBS, after that, a small aliquot of both fractions, soluble and insoluble, was mixed (1:1) with Laemmli buffer. Soluble samples were boiled at 90 °C for 10 min, while the insoluble samples were boiled for 40 min. The processed samples were charged on SDS-PAGE gels and analyzed by Western Blotting with an anti-His monoclonal antibody (His Tag Antibody, mAb, Mouse, Genscript). Images were acquired with the ChemiDoc™ Touch Imaging System (Bio-Rad) and further processing was performed with Image Lab Software. Percentage of aggregation was calculated based on the numerical band intensity value obtained from blotting membrane images. For each expression time, the total amount of protein (100 %) was considered as the sum of the band intensities in both, soluble and insoluble cell fractions. Therefore, percentage of aggregation can be estimated from the band intensity value in the insoluble cell fraction.

Visualization of recombinant proteins in *ClearColi* cells

Bacterial pellets harboring the expressed proteins were resuspended in 500 μL of PBS containing 4 % formaldehyde. Then, resuspended samples were incubated 10 minutes at RT and washed twice with PBS. In a glass slide, a small drop of ProLong™ Gold Antifade Mountant (Thermo) was mixed with 5 μL of the bacterial suspension. The resultant solution was covered with a coverslip and fixed to avoid dehydration. The observation of the fluorescent proteins inside bacteria was recorded by TCS-SP5 confocal laser scanning microscopy (Leica Microsystems). Images were processed using the ImageJ software. Colocalization analysis of fluorescent proteins in *ClearColi* cells were performed by measuring the overlap coefficients of 10 regions of interest (ROIs) which were compared by one-way analysis of variance (ANOVA).

Purification of soluble recombinant proteins fused to APP

For purification of H6GFPL6K2, H6GFP(L6K2)X2 and GWH1GFPH6, protein expression was induced with 0.1 mmol/L isopropyl-β-D-thiogalactopyranoside (IPTG) at 20 °C, overnight. The cell pellet was collected (6000 *g*, 4 °C, 15 minutes) and resuspended in wash buffer (20 mmol/L Tris-HCl, pH 8.0, 500 mmol/L NaCl, 10 mmol/L imidazole) with ethylenediamine tetra-acetic acid-free protease-inhibitor (complete EDTA-Free, Roche). Cells were then disrupted by sonication (1 round of 2 min at 10 % amplitude and 10 rounds of 2 min at 15 % of amplitude) and cell debris was separated from soluble fraction by centrifugation (15,000 *g* at 4 °C, 45 minutes). After filtration (0.22 μm), the His-tagged proteins were purified from the soluble fraction by His tag affinity chromatography using HiTrap Chelatin HP 1 ml column (GE Healthcare) in an ÄKTA purifier FPLC (GE Healthcare). The purified fraction was obtained after elution with a linear gradient of 20 mmol/L Tris-HCl pH 8.0, 500 mmol/L NaCl, 500 mmol/L imidazole. The purity of the different samples was analyzed by TGX gel chemistry and Western Blotting. The selected fractions were mixed and dialyzed against sodium bicarbonate buffer with salt (166 mmol/L NaHCO3, pH 8.0, 333 mmol/L NaCl) and protein amounts were quantified by Bradford assay.

Antimicrobial activity of APP-containing recombinant proteins

The antimicrobial activity of H6GFPL6K2, H6GFP(L6K2)X2 and GWH1GFPH6 was evaluated against three bacterial species, *E. coli*, *S. aureus*, and *M. luteus*, using the broth micro-dilution method. Different two-fold dilutions of the proteins, ranging from 0.06 to 8 μmol/L, were seeded in 96-well plates for each bacterial species. After that, 10^6 CFU/mL of the corresponding bacteria were inoculated in each well. Maximal growth was achieved in control wells with no protein. Each concentration was evaluated in technical duplicates. Wells with 100 μL of Mueller Hinton Broth Cation-adjusted medium (MHB-2, Sigma-Aldrich) were considered as blank solution. Growth conditions were stablished in 18 h at 37 °C. The bacterial viability was evaluated using the commercially available BacTiter-Glo™ Microbial Cell Viability Assay (Promega) following the manufacturer's instructions. Luminescence was measured using the Multilabel Plater Reader VICTOR3 (PerkinElmer).

Supplementary Information

The online version contains supplementary material available at https://doi.org/10.1186/s12934-021-01524-3.

Additional file 1: Figure S1. Extended confocal microscopy visualization of *E. coli ClearColi* cells producing the recombinant fluorescent proteins. **a** Visual field of cells producing L6K2-containing constructs and VP1GFPH6 (aggregation control) analyzed in Fig. 2. **b** Visual fields of cells producing simultaneously GFP and EBFP2 constructs analyzed in Fig 5. Scale bar indicates 4 μm.

Additional file 2: Figure S2. PEP-FOLD server-generated models of aggregation prone peptides fused to GFP scaffold protein. **a** Regular polypeptide helices in a right-handed alpha-helical conformation are shown. All structures are reproduced at the same scale. **b** Helical conformation of two L6K2-containing peptides (blue) in the presence of PT linker (grey).

Additional file 3: Figure S3. DNA sequences of recombinant genes H6iRFPL6K2 and H6GFPL6K2 used in the study. Translate tool from Expasy was used to obtain corresponding amino acid sequences. Clustalw was run to align amino acid sequences and Swiss Model to display 3D structures of the recombinant proteins.

Additional file 4: Figure S4. DNA sequence of recombinant gene VP1EB-FP2H6 used in the study. Translate tool from Expasy was used to obtain corresponding amino acid sequence. Clustalw was run to align amino acid sequence of GFP and EBFP2. Swiss Model was used to display 3D structure of EBFP2 protein.

Additional file 5: Figure S5. Relative solubility (%) of recombinant proteins. Detection of H6GFPL6K2, VP1GFPH6 and VP1EBFP2H6 in the soluble and insoluble cell fractions of *ClearColi* analyzed by Western Blotting. Equivalent number of transformed *ClearColi* cells were lysed and soluble and insoluble cells fractions were separated. All proteins were detected with anti-his antibody. Data are presented as mean ± STD of biological triplicate measurements.

Abbreviations
IBs: Inclusion bodies; APP: Aggregation-prone peptide; iRFP: Near-infrared fluorescent protein; GFP: Green fluorescence protein; HS: Hot spot; HAS: Hot spot area; NHSA: Normalized HAS; a⁴vAHS: Average aggregation-propensity in each HS; AMP: Antimicrobial peptide.

Authors' contributions
JVC and NFM designed the experiments. JVC, AC and EH performed the experiments. JVC and NFM analyzed and interpreted the data. NFM wrote the manuscript. AVC, EH and JVC revised the manuscript. All authors read and approved the final manuscript.

Availability of data and materials
The datasets used and/or analyzed during the current study are available from the corresponding author on reasonable request.

Ethics approval and consent to participate
Not applicable.

Consent for publication
Not applicable.

Competing interests
The authors declare that they have no competing interests.

Author details
[1] Institute for Biotechnology and Biomedicine, Autonomous University of Barcelona, 08193 Bellaterra, Barcelona, Spain. [2] Department of Genetics and Microbiology, Autonomous University of Barcelona, 08193 Bellaterra, Barcelona, Spain. [3] Bioengineering, Biomaterials and Nanomedicine Networking Biomedical Research Centre (CIBER-BBN), 08193 Bellaterra, Barcelona, Spain.

References
1. Schramm FD, Schroeder K, Jonas K. Protein aggregation in bacteria. FEMS Microbiol Rev. 2020;44:54–72.
2. Wallace EWJ, Kear-Scott JL, Pilipenko EV, Schwartz MH, Laskowski PR, Rojek AE, et al. Reversible, specific, active aggregates of endogenous proteins assemble upon heat stress. Cell. 2015;162:1286–98.
3. Chiti F, Dobson CM. Protein misfolding, amyloid formation, and human disease: a summary of progress over the last decade. Annu Rev Biochem. 2017;86:27–68.
4. Dannies PS. Prolactin and growth hormone aggregates in secretory granules: the need to understand the structure of the aggregate. Endocr Rev. 2012;33:254–70.
5. Corchero JL. Eukaryotic aggresomes: from a model of conformational diseases to an emerging type of immobilized biocatalyzers. Appl Microbiol Biotechnol. 2016;100:559–69.
6. Singh A, Upadhyay V, Upadhyay AK, Singh SM, Panda AK. Protein recovery from inclusion bodies of *Escherichia coli* using mild solubilization process. Microb Cell Fact. 2015;14:41.
7. Kuriata A, Iglesias V, Pujols J, Kurcinski M, Kmiecik S, Ventura S. Aggrescan3D (A3D) 2.0: prediction and engineering of protein solubility. Nucleic Acids Res. 2019;47:W300–7.
8. Conchillo-Solé O, de Groot NS, Avilés FX, Vendrell J, Daura X, Ventura S. AGGRESCAN: a server for the prediction and evaluation of "hot spots" of aggregation in polypeptides. BMC Bioinformatics. 2007;8:65.
9. Tsolis AC, Papandreou NC, Iconomidou VA, Hamodrakas SJ. A consensus method for the prediction of "aggregation-prone" peptides in globular proteins. PLoS One. 2013;8:e54175.
10. Singh SK. Impact of product-related factors on immunogenicity of biotherapeutics. J Pharm Sci. 2011;100:354–87.
11. Schlesinger O, Chemla Y, Heltberg M, Ozer E, Marshall R, Noireaux V, et al. Tuning of recombinant protein expression in *Escherichia coli* by manipulating transcription, translation initiation rates, and incorporation of noncanonical amino acids. ACS Synth Biol. 2017;6:1076–85.
12. Rosano GL, Ceccarelli EA. Recombinant protein expression in *Escherichia coli*: advances and challenges. Front Microbiol. 2014;5:172.
13. Calloni G, Chen T, Schermann SM, Chang H-C, Genevaux P, Agostini F, et al. DnaK functions as a central hub in the *E. coli* chaperone network. Cell Rep. 2012;1:251–64.
14. Carratalá JV, Cano-Garrido O, Sánchez J, Membrado C, Pérez E, Conchillo-Solé O, et al. Aggregation-prone peptides modulate activity of bovine interferon gamma released from naturally occurring protein nanoparticles. N Biotechnol. 2020;57:11–9. https://doi.org/10.1016/j.nbt.2020.02.001.
15. Peternel S, Grdadolnik J, Gaberc-Porekar V, Komel R. Engineering inclusion bodies for non denaturing extraction of functional proteins. Microb Cell Fact. 2008;7:34.
16. Pesarrodona M, Fernández Y, Foradada L, Sánchez-Chardi A, Conchillo-Solé O, Unzueta U, et al. Conformational and functional variants of CD44-targeted protein nanoparticles bio-produced in bacteria. Biofabrication. 2016;8:025001.
17. Céspedes MV, Cano-Garrido O, Álamo P, Sala R, Gallardo A, Serna N, et al. Engineering secretory amyloids for remote and highly selective destruction of metastatic foci. Adv Mater. 2020;32:e1907348.
18. Unzueta U, Seras-Franzoso J, Céspedes MV, Saccardo P, Cortés F, Rueda F, et al. Engineering tumor cell targeting in nanoscale amyloidal materials. Nanotechnology. 2017;28:015102.
19. Unzueta U, Cespedes MV, Sala R, Alamo P, Sánchez-Chardi A, Pesarrodona M, et al. Release of targeted protein nanoparticles from functional bacterial amyloids: A death star-like approach. J Control Release. 2018;279:29–39.

20. Vázquez E, Corchero JL, Burgueño JF, Seras-Franzoso J, Kosoy A, Bosser R, et al. Functional inclusion bodies produced in bacteria as naturally occurring nanopills for advanced cell therapies. Adv Mater. 2012;24:1742–7.

21. Pesarrodona M, Jauset T, Díaz-Riascos ZV, Sánchez-Chardi A, Beaulieu M-E, Seras-Franzoso J, et al. Targeting antitumoral proteins to breast cancer by local administration of functional inclusion bodies. Adv Sci. 2019;6:1900849.

22. Slouka C, Kopp J, Spadiut O, Herwig C. Perspectives of inclusion bodies for bio-based products: curse or blessing? Appl Microbiol Biotechnol. 2019;103:1143–53.

23. Kopp J, Kolkmann A-M, Veleenturf PG, Spadiut O, Herwig C, Slouka C. Boosting Recombinant Inclusion Body Production-From Classical Fed-Batch Approach to Continuous Cultivation. Front Bioeng Biotechnol. 2019;7:297.

24. Kopp J, Slouka C, Strohmer D, Kager J, Spadiut O, Herwig C. Inclusion body bead size in *E. coli* controlled by physiological feeding. Microorganisms. 2018;6:116.

25. Wang X, Zhou B, Hu W, Zhao Q, Lin Z. Formation of active inclusion bodies induced by hydrophobic self-assembling peptide GFIL8. Microb Cell Fact. 2015;14:88.

26. Morell M, Bravo R, Espargaró A, Sisquella X, Avilés FX, Fernàndez-Busquets X, et al. Inclusion bodies: specificity in their aggregation process and amyloid-like structure. Biochim Biophys Acta. 2008;1783:1815–25.

27. García-Fruitós E, González-Montalbán N, Morell M, Vera A, Ferraz RM, Arís A, et al. Aggregation as bacterial inclusion bodies does not imply inactivation of enzymes and fluorescent proteins. Microb Cell Fact. 2005;4:27.

28. Arié J-P, Miot M, Sassoon N, Betton J-M. Formation of active inclusion bodies in the periplasm of *Escherichia coli*. Mol Microbiol. 2006;62:427–37.

29. Nahalka J, Nidetzky B. Fusion to a pull-down domain: a novel approach of producing *Trigonopsis variabilis* D-amino acid oxidase as insoluble enzyme aggregates. Biotechnol Bioeng. 2007;97:454–61.

30. Zhou B, Xing L, Wu W, Zhang X-E, Lin Z. Small surfactant-like peptides can drive soluble proteins into active aggregates. Microb Cell Fact. 2012;11:10.

31. Lamiable A, Thévenet P, Rey J, Vavrusa M, Derreumaux P, Tufféry P. PEP-FOLD3: faster de novo structure prediction for linear peptides in solution and in complex. Nucleic Acids Res. 2016;44:W449-54.

32. Shen Y, Maupetit J, Derreumaux P, Tufféry P. Improved PEP-FOLD approach for peptide and miniprotein structure prediction. J Chem Theory Comput. 2014;10:4745–58.

33. Thévenet P, Shen Y, Maupetit J, Guyon F, Derreumaux P, Tufféry P. PEP-FOLD: an updated de novo structure prediction server for both linear and disulfide bonded cyclic peptides. Nucleic Acids Res. 2012;40:W288-93.

34. Poon DKY, Withers SG, McIntosh LP. Direct demonstration of the flexibility of the glycosylated proline-threonine linker in the Cellulomonas fimi Xylanase Cex through NMR spectroscopic analysis. J Biol Chem United States. 2007;282:2091–100.

35. Huang Y, Huang J, Chen Y. Alpha-helical cationic antimicrobial peptides: relationships of structure and function. Protein Cell. 2010;1:143–52.

36. Gaglione R, Pane K, Dell'Olmo E, Cafaro V, Pizzo E, Olivieri G, et al. Cost-effective production of recombinant peptides in *Escherichia coli*. N Biotechnol. 2019;51:39–48.

37. Zhao Q, Xu W, Xing L, Lin Z. Recombinant production of medium- to large-sized peptides in *Escherichia coli* using a cleavable self-aggregating tag. Microb Cell Fact. 2016;15:136.

38. Chou HT, Kuo TY, Chiang JC, Pei MJ, Yang WT, Yu HC, et al. Design and synthesis of cationic antimicrobial peptides with improved activity and selectivity against *Vibrio* spp. Int J Antimicrob Agents. 2008;32:130–8.

39. Serna N, Sánchez-García L, Sánchez-Chardi A, Unzueta U, Roldán M, Mangues R, et al. Protein-only, antimicrobial peptide-containing recombinant nanoparticles with inherent built-in antibacterial activity. Acta Biomater. 2017;60:256–63.

40. Yu H, Li H, Gao D, Gao C, Qi Q. Secretory production of antimicrobial peptides in *Escherichia coli* using the catalytic domain of a cellulase as fusion partner. J Biotechnol. 2015;214:77–82.

41. Gordon YJ, Romanowski EG, McDermott AM. A review of antimicrobial peptides and their therapeutic potential as anti-infective drugs. Curr Eye Res. 2005;30:505–15.

42. Raheem N, Straus SK. Mechanisms of Action for Antimicrobial Peptides With Antibacterial and Antibiofilm Functions. Front Microbiol. 2019;10:2866.

43. Kumar P, Kizhakkedathu JN, Straus SK. Antimicrobial peptides: diversity, mechanism of action and strategies to improve the activity and biocompatibility in vivo. Biomolecules. 2018;8:4.

44. Wimley WC. Describing the mechanism of antimicrobial peptide action with the interfacial activity model. ACS Chem Biol. 2010;5:905–17.

45. Torcato IM, Huang Y-H, Franquelim HG, Gaspar D, Craik DJ, Castanho MARB, et al. Design and characterization of novel antimicrobial peptides, R-BP100 and RW-BP100, with activity against Gram-negative and Gram-positive bacteria. Biochim Biophys Acta Netherlands. 2013;1828:944–55.

46. Elliott AG, Huang JX, Neve S, Zuegg J, Edwards IA, Cain AK, et al. An amphipathic peptide with antibiotic activity against multidrug-resistant Gram-negative bacteria. Nat Commun. 2020;11:3184.

47. Martínez-Alonso M, Toledo-Rubio V, Noad R, Unzueta U, Ferrer-Miralles N, Roy P, et al. Rehosting of bacterial chaperones for high-quality protein production. Appl Environ Microbiol. 2009;75:7850–4.

48. Rueda F, Gasser B, Sánchez-Chardi A, Roldán M, Villegas S, Puxbaum V, et al. Functional inclusion bodies produced in the yeast *Pichia pastoris*. Microb Cell Fact. 2016;15:1–2.

49. Rodríguez-Carmona E, Mendoza R, Ruiz-Cánovas E, Ferrer-Miralles N, Abasolo I, Schwartz S, et al. A novel bio-functional material based on mammalian cell aggresomes. Appl Microbiol Biotechnol. 2015;99:7079–88.

50. Jäger VD, Kloss R, Grünberger A, Seide S, Hahn D, Karmainski T, et al. Tailoring the properties of (catalytically)-active inclusion bodies. Microb Cell Fact. 2019;18:33.

Publisher's note

STUDY 2

Aggregation-prone peptides modulate activity of bovine interferon gamma released from naturally occurring protein nanoparticles

Jose Vicente Carratalá, Olivia Cano-Garrido, Julieta Sánchez, Cristina Membrado, Eudald Pérez, Oscar Conchillo-Solé, Xavier Daura, Alejandro Sánchez-Chardi, Antonio Villaverde, Anna Arís, Elena Garcia-Fruitós, Neus Ferrer-Miralles

Cytokines are small intercellular regulatory proteins that play a central role in initiating, maintaining, and regulating the innate immune response. Specifically, IFN-γ has a pivotal role in promoting protective immunity against infections, for that reason, the development of strategies involving this protein may be a complementary alternative to reduce antibiotic usage and tackle with the emerge of resistant bacteria. However, one of the main disadvantages associated with cytokines is their low stability, therefore, strategies intended to improve their limited half-life and to regulate their action over time are highly desired.

In this context, the IB format may overcome these limitations by providing a stable environment where functionally active cytokines can be protected from degradation and sustainedly released over time, increasing the duration of cytokine activity. The use of aggregation-prone peptides seems an appealing alternative to promote the formation of these naturally occurring aggregates. However, as presented in the previous study, the heterologous protein must be considered in the overall aggregation process. For that reason, the screening of different aggregation-prone peptides seems a logical alternative in order to select the one that best matches the aggregation capabilities of the heterologous protein of interest.

In the present study, peptides of different amino acid length (L6K2, CYOB and HALRU) were biosynthetically fused to IFN-γ and their effect on promoting protein aggregation and functionality was evaluated and compared. In all cases the formation of IBs was promoted, however, the aggregation tag had a major influence on the overall functionality. Specifically, the L6K2 aggregation-prone peptide not only promoted aggregation, but increased the heterologous protein functionality to which was fused to. These results suggest that depending on the aggregation tag, the aggregation process can be modulated in order to obtain IBs with the desired properties for their application.

Contents lists available at ScienceDirect

New BIOTECHNOLOGY

Full Length Article

Aggregation-prone peptides modulate activity of bovine interferon gamma released from naturally occurring protein nanoparticles

José Vicente Carratalá[a,b], Olivia Cano-Garrido[a,b,c,1], Julieta Sánchez[a,2], Cristina Membrado[a,b], Eudald Pérez[a,b], Oscar Conchillo-Solé[a], Xavier Daura[a,d], Alejandro Sánchez-Chardi[e], Antonio Villaverde[a,b,c], Anna Arís[f], Elena Garcia-Fruitós[f], Neus Ferrer-Miralles[a,b,c,*]

[a] Institute for Biotechnology and Biomedicine, Autonomous University of Barcelona, Bellaterra, Barcelona, Spain
[b] Department of Genetics and Microbiology, Autonomous University of Barcelona, Barcelona, Spain
[c] Bioengineering, Biomaterials and Nanomedicine Networking Biomedical Research Centre (CIBER-BBN), Bellaterra, Barcelona, Spain
[d] Catalan Institution for Research and Advanced Studies, Barcelona, Spain
[e] Microscopy Service, Autonomous University of Barcelona, Bellaterra, Barcelona, Spain and Department of Evolutionary Biology, Ecology and Environmental Sciences, Faculty of Biology, University of Barcelona, Barcelona, Spain.
[f] Department of Ruminant Production, Institute of Agrifood Research and Technology (IRTA), Caldes de Montbui, Barcelona, Spain

ABSTRACT

Efficient protocols for the production of recombinant proteins are indispensable for the development of the biopharmaceutical sector. Accumulation of recombinant proteins in naturally-occurring protein aggregates is detrimental to biopharmaceutical development. In recent years, the view of protein aggregates has changed with the recognition that they are a valuable source of functional recombinant proteins. In this study, bovine interferon-gamma (rBoIFN-γ) was engineered to enhance the formation of protein aggregates, also known as protein nanoparticles (NPs), by the addition of aggregation-prone peptides (APPs) in the generally recognized as safe (GRAS) bacterial *Lactococcus lactis* expression system. The L6K2, HALRU and CYOB peptides were selected to assess their intrinsic aggregation capability to nucleate protein aggregation. These APPs enhanced the tendency of the resulting protein to aggregate at the expense of total protein yield. However, fine physico-chemical characterization of the resulting intracellular protein NPs, the protein released from them and the protein purified from the soluble cell fraction indicated that the compactability of protein conformations was directly related to the biological activity of variants of IFN-γ, used here as a model protein with therapeutic potential. APPs enhanced the aggregation tendency of fused rBoIFN-γ while increasing compactability of protein species. Biological activity of rBoIFN-γ was favored in more compacted conformations. Naturally-occurring protein aggregates can be produced in GRAS microorganisms as protein depots of releasable active protein. The addition of APPs to enhance the aggregation tendency has a positive impact in overall compactability and functionality of resulting protein conformers.

Introduction

The efficient production and purification of recombinant proteins in a wide range of expression hosts has driven the launch of a large number of biopharmaceutical products. One of the most-studied and most-used gene expression systems for biopharmaceutical products is *Escherichia coli* [1,2]. Prokaryotic endotoxin-free expression systems are being explored to avoid the presence pro-inflammatory contamination by lipopolysaccharide (LPS) components of the outer leaflet of the outer membrane of *E. coli*, including *E. coli* LPS mutant strains [3,4] and Generally Recognized As Safe (GRAS) microorganisms, such as *Lactococcus lactis* [5–7].

Fig. 1. IFN-γ constructs produced in *E. coli* and *L. lactis* (a) The general organization of IFN-γ constructs is configured (IFN-γ)-Linker-APP-H6. The amino acid sequences of the linker and the APPS are shown below the schematic representation of the protein designs. (b) Quantification of the production of IFN-γ in IB-like nanoparticles in *L. lactis* (top) and solubility (bottom) of IFN-γ in *L. lactis*. Significant results are shown as * $p \leq 0.05$ and ** $p \leq 0.005$.

During recombinant gene expression, the stress imposed on the protein quality control machinery leads, in most cases, to the accumulation of the recombinant protein in aggregates that form intracellular nanoparticles (NPs), known as inclusion bodies (IBs) [8–10]. These are dynamic and complex nanostructures with a variable content of recombinant protein [11–13]. The trapped protein was formerly thought to be biologically inactive due to aberrant protein conformations or inactive partially folded species incompatible with biological activity. The recombinant protein can often be recovered, with low efficiency, from the insoluble cell fraction by *in vitro* denaturing/refolding processes [14]. However, this view of naturally occurring protein aggregates has changed radically since the detection of biologically active protein embedded in these aggregates [15–17]. The classic view of protein aggregates as mere inactive folding intermediates has been transformed into one of heterogeneous porous multimeric structures stabilized by a scaffold of cross beta-sheet structures containing conformers of the recombinant protein in which a spectrum of species containing quasi-native conformations are incorporated [9]. It has been reported that biologically active protein species can be extracted from IBs, indicating the biologically active nature of proteins forming these aggregates [18]. Hence, IBs are envisionaged as non-toxic, biocompatible and mechanically stable materials from which biologically active molecules of the recombinant protein can be released under mild solubilization and physiological conditions [13,16,18–21].

Interest in the possibility of controlling the aggregation of recombinant proteins in these types of nanostructures is increasing, and several aggregation-prone peptides (APPs) have been identified for fusion with recombinant proteins to enhance the aggregation process in the producing cell [22]. In this study, interferon (IFN)-γ was selected as a model protein in order to study the effect of the addition of APPs in naturally occurring protein aggregates due to interest in this activity in biomedicine and its potential use in animal health. IFN-γ is the sole type II IFN. IFN-γ secretion by natural killer (NK) cells and antigen-presenting cells enhances the innate immune response, while T-lymphocytes are involved in the secretion of IFN-γ in the adaptive immune response [23,24]. The activity of IFN-γ depends on its interaction, as a dimer, with the IFN-γ receptor (IFNGR). Approved recombinant human IFN-γ can be obtained from the *E. coli* expression system, but novel protein formulations need to be developed in GRAS expression systems due to safety concerns. In most reported studies of the expression and purification of IFN-γ, the recombinant protein is recovered from the purified IBs through extensive denaturation-refolding processes [25–28].

In this work, the mature form of bovine IFN-γ (rBoIFN-γ) protein (UniProtKB P07353, residues 24 to 166) was produced in GRAS lactic acid bacteria (*L. lactis*) in the form of protein NPs. The ability of APPs fused to rBoIFN-γ to enhance the aggregation propensity of the recombinant cytokine was analyzed and the link assessed between the biological activities contained in protein NPs of IFN-γ variants and their physicochemical characteristics. It was found that the activity of the IBs is related to the specific biological activity of the recombinant protein they contain, whereas the proportion of released protein is not the main factor. The data presented illustrate the potential of endotoxin-free protein NPs as active biomaterials to formulate, at the nanoscale level, releasable proteins of biomedical interest.

Table 1

Selection of APPs from predictions of "hot spots (HS)" of aggregation in polypeptides by AGGRESCAN [31]. CYOB: Cytochrome bo₃ ubiquinol oxidase subunit 1 from *E. coli*, HALRU: Aragonite protein AP7. NA: Not applicable. HS: hot spot. HSA: hot spot area. NHSA: normalized HSA. a4vAHS: average aggregation-propensity in each HS.

Name	UniProtKB	HS region	HS size	Sequence	HSA	NHSA	a⁴vAHS	Ref
CYOB	P0ABI8	591-629	39	AGIVIAAFSTIFGFAMIWHI WWLAIVGFAGMIITWIVKS	30.696	0.787	0.767	This study
HALRU	Q9BP37	1-17	17	MTYMCSILICLVLILCA	15.842	0.932	0.904	This study
L6K2	NA	1-6	6	LLLLLLKK	6.211	1.035	0.949	[30]

Materials and methods

Bacterial strains and plasmids

E. coli MC4100 (StrepR) [29] was used for cloning genes for protein production in *L. lactis*. *E. coli* DH5α was used for cloning genes in *E. coli*. *L. lactis cremoris* NZ9000 (Boca Scientific, MA, USA), and *ClearColi®* BL21(DE3) (Lucigen, WI, USA) were used in experiments for each expression system. Gene sequences were codon optimized for the *L. lactis* expression host (Geneart, MA; USA, Suppl. Fig. S1). For *L. lactis* expression vectors, IFN-γ of bovine origin (*Bos Taurus*; NM_ 174086.1 in Suppl. Fig. S1) was cloned into the CmR pNZ8148 plasmid (MoBiTech, Goettingen, Germany) as described in Supplementary Materials and Methods and [6]. In addition, fusions of rBoIFN-γ with APPs were constructed (rBoIFN-γ_L6K2, rBoIFN-γ_HALRU and rBoIFN-γ_CYOB; Fig. 1). L6K2 is a surfactant-like peptide with aggregating properties [30]. HALRU and CYOB are aggregating-prone peptides; CYOB is from cytochrome bo3 ubiquinol oxidase subunit 1 from *E. coli* (UniProtKB P0ABI8) and HALRU from aragonite protein AP7 (UniProtKB Q9BP37) selected with AGGRESCAN [31] (see Table 1). For Clearcoli®, the *L. lactis* codon-optimized bovine IFN-γ gene was cloned into pETDuet-1 (Novagen, WI, USA) (Suppl. Fig. S2 and Supplementary Materials and Methods). The recombinant proteins were produced as the mature form of the IFN-γ (from Gln24 to Thr166; NP_776511.1) (Fig. S2). All genes were C-terminally fused to a His-tag for detection and quantification by western blot analysis and a linker with a predicted random coil conformation was positioned between the IFN-γ and APP as previously described [30].

Selection of APPs

APPs were selected by scanning the Disprot v6.02 database [32] with AGGRESCAN software [31]. The selection was based on the assumption that APPs in solvent-exposed regions were the best candidates for the purposes of this study. Two unstructured regions were selected from CYOB and HALRU (see above). CYOB was selected as the peptide displaying the highest hot spot area (HSA). HALRU showed a high normalized hot spot area (NHSA) and average aggregation-propensity hot spot (a4vAHS) while maintaining a significantly high HSA value relative to the other identified peptides. L6K2 was selected based on previous experimental results [30] after analysis with AGGRESCAN showed that this peptide had a high normalized HSA (NHSA) and high average aggregation-propensity hot spot (a⁴vAHS) despite having shorter sequence (Table 1 and Fig. 1a).

Production and purification of rBoIFN-γ protein from the soluble cell fraction

Cultures of *ClearColi®* BL21 (DE3) cells transformed with the plasmid pETDuet-rBoIFN-γ (Supplementary Materials and Methods) were incubated in a shake flask at 37 °C and 250 rpm in LB medium supplemented with 100 μg/ml ampicillin. Protein expression was induced by adding 1 mM isopropyl-β-D-thiogalactopyranoside IPTG. The cultures were then incubated at 20 °C and 250 rpm overnight for protein production. Cells were collected by centrifugation 15 min, 6,000 ×

g, 4 °C), and soluble rBoIFN-γ protein was purified as described in Supplementary Materials and Methods. Protein expression of *L. lactis* cells transformed with plasmid containing the rBoIFN-γ gene was induced and purified as described in Supplementary Materials and Methods and [6]. The control protein rBoIFN-γ_Std, produced in *E. coli* was obtained from R&D Systems (2300-BG-025, R&D Systems, MN, USA).

Production and purification of rBoIFN-γ protein nanoparticles

L. lactis cells transformed with expression plasmids (pNZ8148-rBoIFN-γ, pNZ8148-rBoIFN-γ_L6K2, pNZ8148-rBoIFN-γ_HALRU and pNZ8148-rBoIFN-γ_CYOB) were grown as above. NP production was induced by adding 12.5 ng/ml nisin (Sigma-Aldrich, MO, USA) to *L. lactis* cultures. After induction, the cultures were grown for 5 h. The protein NPs were purified using the protocol described previously (Supplementary Materials and Methods and [6]).

Quantitative protein analysis

Recombinant proteins were quantified by denaturing SDS-PAGE as described previously (Supplementary Materials and Methods and [33]). In addition, the yields of purified proteins in each of the formats are shown in Table S1.

Ultrastructural characterization

To characterize the morphometry of the NPs, microdrops of protein aggregate suspensions were deposited for 2 min on silicon wafers (Ted Pella Inc.), air-dried and observed in a near-native state under a field emission scanning electron microscope (FESEM) Zeiss Merlin (Zeiss, Obercochen, Germany) operating at 1 kV. Micrographs were acquired with a high-resolution in-lens secondary electron (SE) detector. Images were taken at magnifications ranging from 20,000x to 80,000 × .
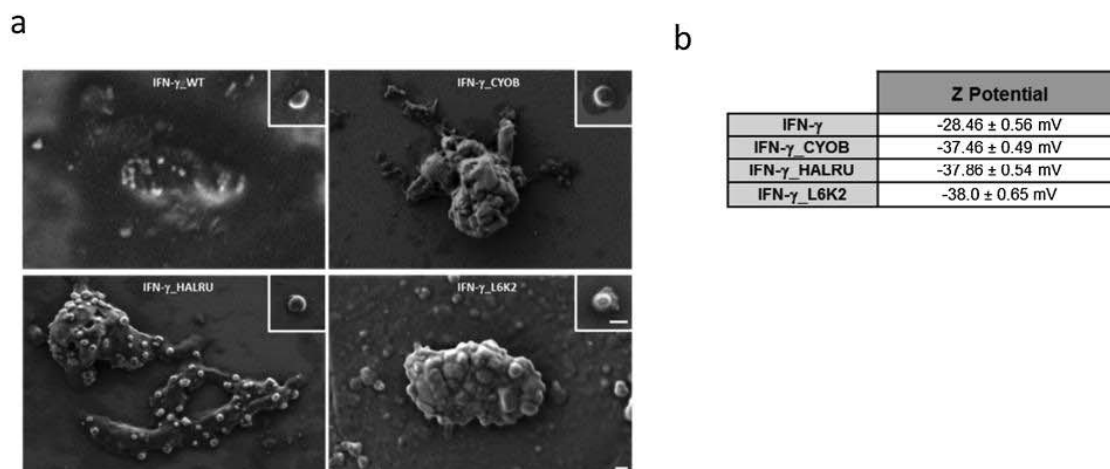
Z potential analysis

Z potential (ZP) characterization of each kind of protein NP was carried out by Dynamic Light Scattering (DLS) (Zetasizer Nano ZS, Malvern Instruments Ltd, Malvern, UK). To prevent the electrodes from burning, the samples were prepared in deionized (MilliQ) water. Each sample was analyzed in triplicate.

Determination of rBoIFN-γ biological activity in bovine cells

The different rBoIFN-γ formulations described here were analyzed by a modified kynurenine bioassay (Supplementary Materials and Methods and [34]). The antiproliferative activity of IFN-γ in this assay is related to the induction of the expression of the indoleamine 2,3-dioxygenase 1 (*IDO1*) gene, which is the first and rate-limiting enzyme in tryptophan catabolism. IDO1 catalyzes oxidative cleavage of tryptophan to N-formylkynurenine. Following a hydrolysis step, the latter is transformed into L-kynurenine by Ehrlich's reagent, giving a yellow-colored compound absorbing at 490 nm [35]. The absorbance vs IFN-γ concentration (nmol/L) curves were adjusted to Eq. (1) [20]. Abs*490* is

a

b

	Z Potential
IFN-γ	-28.46 ± 0.56 mV
IFN-γ_CYOB	-37.46 ± 0.49 mV
IFN-γ_HALRU	-37.86 ± 0.54 mV
IFN-γ_L6K2	-38.0 ± 0.65 mV

Fig. 2. (a) Ultrastructural characterization by FESEM of protein aggregates and purified protein nanoparticles of rBoIFN-γ, rBoIFN-γ_CYOB, rBoIFN-γ_HARLU and rBoIFN-γ_L6K2. Scale bars correspond to 200 nm. (b) ZP of purified protein nanoparticles.

the absorbance at 490 nm, which represents an indirect measurement of IFN-γ binding to the receptor, Absmax is the maximal binding of IFN-γ to the receptor, and K_D is the equilibrium dissociation constant. A low value of K_D indicates high IFN-γ affinity to the receptor.

$$Abs490 = \frac{Absmax \times IFN\gamma}{[IFN\gamma] + K_D} \quad (1)$$

Assay of protein solubilization from protein nanoparticles

The rBoIFN-γ protein NPs (rBoIFN-γ_L, rBoIFN-γ_L6K2, rBoIFN-γ_CYOB and rBoIFN-γ_HALRU) were solubilized in PBS. In all cases, the concentration was adjusted to 1 μmol/L. After manual agitation, each sample was incubated at 37 °C for 96 h to reproduce the conditions used during the biological activity analysis. Protein concentration was quantified and the biological activity determined at a single concentration (0.72 nmol/L) as described in previous section.

Interferon size determination

The volume size distribution of IFN-γ was determined by DLS. A 60-μl aliquot (stored at -80 °C) was thawed, and the volume size distribution of each protein format was immediately determined at 633 nm (Zetasizer Nano ZS, Malvern Instruments Ltd, Malvern, UK).

Analysis of protein conformation by intrinsic tryptophan fluorescence

Fluorescence spectra were recorded on a Cary Eclipse spectro-fluorometer (Agilent Technologies, CA, USA). A quartz cell with a 10-mm path length and a thermostatic holder was used. The excitation and emission slits were set at 5 nm. The excitation wavelength (λ_{ex}) was set at 295 nm. Emission spectra were acquired within a range from 310 to 550 nm. The protein concentration was 14 μmol/L in PBS DEFINE. To evaluate conformational differences between the proteins, the center of spectral mass (CSM), was applied, the weighted average of the fluorescence spectrum peak. The CSM was calculated for each of the fluorescence emission spectra [36] according to Eq. (2), where I_i is the fluorescence intensity measured at wavelength λ_i.

$$\lambda = \frac{\sum \lambda_i \cdot I_i}{\sum I_i} \quad (2)$$

CSM values were analyzed at room temperature and under thermal heating at 5 °C/min rate.

Statistical analysis

Prior to the use of parametric tests, normality and homogeneity of variances were tested using the Shapiro-Wilk test for all quantitative data or the Levene test for raw or transformed data. Divergences between groups were tested with one-way ANOVA, and pairwise comparisons were made with Student's t tests. The results were expressed as the arithmetic mean for non-transformed data ± the standard error of the mean ($\bar{x}$ ± SEM), except otherwise stated.

The least squares method was applied to fit functions through a regression analysis to determine the K_D values according to Eq. (1). Significance was accepted at $p < 0.05$, and Bonferroni correction was applied for sequential comparisons. All statistical analyses were performed with SPSS v. 18 for Windows.

Results and discussion

Production of rBoIFN-γ in L. lactis

In *L. lactis*, most of the rBoIFN-γ protein was detected in the soluble cell fraction in the absence of any APP (Fig. 1b, upper panel). This observation is in agreement with previous results for the expression of the natural DNA sequence of the bovine IFN-γ gene in *E. coli* [37]. The presence of the APPs in the recombinant protein caused a noticeable shift of the final products toward the insoluble cell fraction, as expected (Fig. 1b, lower panel). The purity of the protein aggregates ranged between 50–60 % in all constructs (Suppl. Fig. S3). The APP resulting in the highest aggregation tendency was the L6K2 peptide. In addition, the presence of an APP tag also had a negative effect on the total recombinant protein produced in the cell (Fig. 1a, upper panel). The best APP in terms of aggregation propensity and protein yield in the insoluble cell fraction, corresponded to the IFN-γ L6K2 formulation. The performance of this surfactant-like peptide exceeded the predicted aggregation-prone capabilities of CYOB and HALRU peptides (Table 1).

Nanoarchitectonic characterization of protein nanoparticles

The morphometry of purified protein NPs of the rBoIFN-γ variants

14
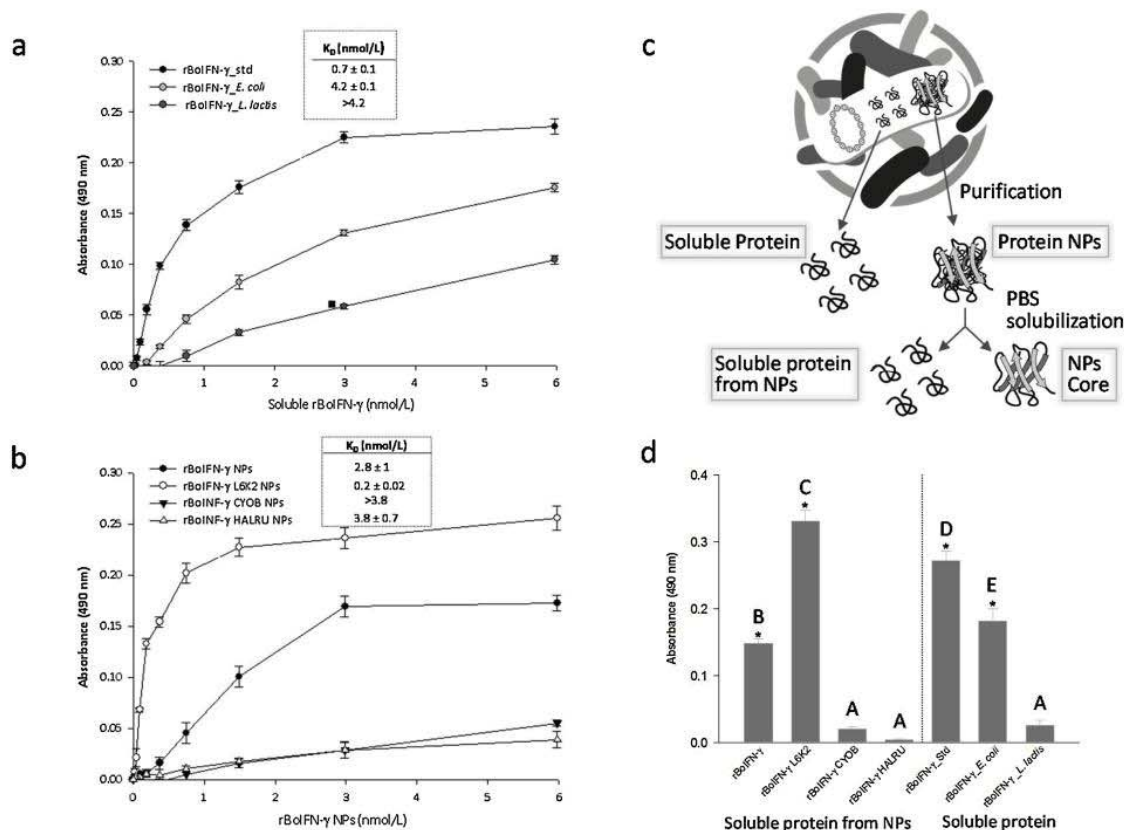
Fig. 3. Kynurenine levels measured by absorbance at 490 nm after treatment of EBTr cells for 96 h with increasing amounts of rBoIFN-γ from different origins. (a) Soluble rBoIFN-γ produced in the indicated expression system. (b) Protein nanoparticles of rBoIFN-γ produced in *L. lactis*. The K_D values are indicated in the plot. (c) Schematic representation of the protein samples used in the activity assays: soluble protein obtained from the soluble cell fraction, protein NPs purified from the insoluble cell fraction, soluble protein obtained from the protein NPs, and the NP core after a resolubilization procedure. (d) Comparison of the activity between rBoIFN-γ protein obtained from solubilization of protein NPs and purified rBoIFN-γ from the soluble cell fraction as indicated at 0.72 nmol/L. Different letters depict differences between proteins ($p <$ 0.001) except rBoIFN-γ from protein NPs and rBoIFN-γ_E ($p =$ 0.024).

was examined by FESEM (Fig. 2a). The images revealed the presence of multimeric complexes comprising discrete NPs in addition to isolated protein NPs (inset Fig. 2a). The NPs were similar to rBoIFN-γ protein NPs obtained previously in this expression system [6]. ZP measurements showed that all of the NPs presented negatively charged surfaces with negative values ranging from − 38 to − 28 mV (Fig. 2b), indicating the stability of the NP suspension. The higher values of ZP obtained for the IFN-γ variants provide information about particle stability, as NPs displaying higher ZP values (> +30 mV or < − 30 mV) exhibit increased stability due to greater electrostatic repulsion between particles [38].

Biological activity of soluble IFN-γ and NPs of IFN-γ

The activity of IFN-γ is usually determined by an antiviral assay [39]. However, alternative assays have been developed to simplify the procedure. One approach to evaluate IFN-γ activity mediated by IFN-γ receptor binding is the detection of L-kynurenine. The activity of IFN-γ is highly species-specific and, a specific assay for the bovine IFN-γ was developed and validated in this study [34]. For validation, the activity of three soluble rBoIFN-γ proteins was tested (Fig. 3a). rBoIFN-γ_Std exhibited the lowest dissociation constant (K_D) among the proteins purified from the soluble cell fraction (Fig. 3a) similar to the value

determined for human IFN-γ [40]. The difference in this parameter with in-house IFN-γ produced in *Clearcoli* (rBoIFN-γ_*E. coli*) may be related to the absence of C-terminal variants in this sample, the effect of the fused His-tag at the C-terminus, or other variables [41]. The protein obtained from the *L. lactis* expression system displayed less activity, which may be due to differences in the folding efficiency during the production process among prokaryotic expression systems [42,43]. Once the activity assay was validated, the biological activity contained in the IFN-γ protein NPs produced in *L. lactis* was determined. The results showed that all cells were able to elicit responses to the presence of the protein NPs, and the IFN-γ_L6K2 formulation displayed the highest initial rate and kynurenine production (Fig. 3b). The addition of HALRU and CYOB APP to IFN-γ had a moderate effect on the cell response. It is of interest to know why the sample corresponding to protein NPs of IFN-γ_L6K2 had the highest activity and initial rate, even compared with commercial IFN-γ. Consistent with this observation, a previous analysis of the activity of recombinant β-galactosidase produced in *E. coli* in the form of protein NPs revealed higher specific activity than the corresponding soluble version of the protein [15]. However, protein NPs obtained from *E. coli* have not been characterized in detail. The activity displayed by *E. coli* IBs has been attributed to the release of a spectrum of conformers of the recombinant protein, which leaves a scaffold that is resistant to proteolysis and has an extensive cross-beta-pleated sheet

conformation [44,45]. For protein NPs of rBoIFN-γ produced in *L. lactis*, 30–40 % of the material is resistant to proteolysis, indicating that the protein NPs obtained in this expression system follow similar principles to the *E. coli* system [6]. Thus, the activities displayed by the protein NPs are probably due to the partial release of the IFN-γ that forms part of the macromolecular complex [46]. To evaluate better the ability of the protein NPs to release protein, they were incubated in PBS for 96 h to emulate the protein release conditions established during the biological activity assay (see the experimental design used to obtain the different protein samples in Fig. 3c). Release of 52.67 %, 5.30 %, 0.42 % and 0.46 % was observed for IFN-γ, IFN-γ_L6K2, IFN-γ_HALRU and IFN-γ_CYOB NPs, respectively. In order to analyze the specific activity of the proteins released from the protein NPs, an activity assay was performed and the results compared with proteins obtained directly from the soluble cell fraction (Fig. 3d). The results showed that the maximal specific activity corresponded to the IFN-γ_L6K2 protein released from NPs. In addition, the comparison of the specific activity of the rBoIFN-γ protein produced in *L. lactis* and purified from the soluble cell fraction with that of the corresponding protein released from NPs suggested that the released protein elicited better conformational performance (compare the second and last bars in Fig. 3d).

The addition of APPs to the rBoIFN-γ protein improved the aggregation profile of the produced protein (Fig. 1b). However, the presence of this type of peptide had a negative effect on the overall production of the protein and, in the case of HALRU and CYOB, a major impact on biological activity (Fig. 3). From this, AGGRESCAN software is able to predict the propensity of the resulting APP-containing recombinant IFN-γ to aggregate and is a reliable tool for analyzing solubility performance in the design of recombinant genes [31].

Physicochemical characterization of soluble IFN-γ and nanoparticles of IFN-γ

The precise physicochemical analysis of recombinant proteins is important for safety concerns [47,48]. To further analyze the protein in different formats, DLS measurements were performed (Fig. 4a–d). The rBoIFN-γ_Std exhibited a peak with a maximum at 7.6 nm, similar to the peak at 6.13 nm for the IFN-γ produced in *L. lactis*. This configuration ($6-8$ nm) might correspond to the dimeric form of the cytokine. However, the IFN-γ obtained from *E. coli* showed a tendency towards a larger size. Therefore, the specific activity of the different rBoIFN-γ formats is not simply linked to the dimeric configuration, which is the functional conformation when binding to the cell receptor, and some other variables might be involved. When analyzing the size of the purified NPs, a peak above 1,000 nm was detected, exceeding the upper sensitivity limit of the equipment (Fig. 4b). The NPs were clustered in higher-order complexes from monomeric versions of 200 nm (Fig. 2a). All samples exhibited the same profile. After solubilization of the protein embedded in the NPs, the size of the remaining material remained above 1,000 nm since the scaffold of the NPs retained the overall structure after the protein was released (Fig. 4d). The released protein showed a narrow dispersion ranging from the dimeric size of the protein identified in the samples obtained from the commercial IFN-γ or the soluble version purified from *L. lactis* detected in the upper panel of Fig. 4a (Fig. 4c). In addition, the polydispersity index (PI) of these samples was higher than that of the soluble IFN-γ versions. The PI corresponds to an estimate of the width of the distribution, and higher values of PI are consistent with the data showing a pool of conformers in the folding of recombinant proteins when the proteins are produced in the cell [49]. In contrast, in the protein versions purified from the soluble cell fraction, the downstream processing based on affinity chromatography selects only a narrow collection of conformers (only those that are able to bind to the Ni^{2+} in the resin). This indicates that the protein obtained during solubilization assays from protein NPs is more representative of the diversity in conformations of a single protein that are produced in the expression system.

To further analyze the link between the physicochemical properties and the specific activity of the proteins, the fluorescence emission of Trp was recorded. Each fluorescence emission spectrum was transformed into a CSM value. This parameter is related to the relative exposure of the Trp to the protein environment. The maximum red-shift in the CSM of the Trp spectrum is compatible with large solvent accessibility [50–52], whereas the blue shift in the CSM corresponds to a Trp hidden in a more hydrophobic milieu [53]. The mature form of BoIFN-γ has a unique Trp at position 36, which is partially buried in the 3D structure of the protein (PDB 1D9C) [54] and is not involved in either monomer or in cytokine-receptor interactions, as shown in the 3D structure of the human tetrameric complex of the cytokine dimer with the receptor (PDB 1FG9) [55]. A remarkable aspect of the intrinsic fluorescence analysis is that all the rBoIFN-γ variants within the NPs or after solubilization from the protein NPs exhibited lower CSM values than the samples obtained from the soluble fraction (Table 2). These results suggest that the protein forming part of the NPs and the protein solubilized from the aggregates have a more compact conformation than the soluble version. The most active IFN-γ soluble version corresponded to the commercial IFN-γ, which had the lowest CMS due to its highly compacted structure. The proteins obtained from the soluble fraction of *E. coli* and *L. lactis* exhibited higher CMS values than the commercial protein. These differences might be related to the distinct sizes detected (Fig. 4a). The rBoIFN-γ_*E. coli* was approximately three times larger than the same protein produced in *L lactis*, indicating that the Trp residue was located in a more polar environment compared with the *L lactis* form (Table 2). For the protein originating from the particulate form, a blue shift was observed compared with the soluble versions, and the CSM increased as it was resolubilized (lines 4 and 6 of Table 2). The CSM value of the solubilized rBoIFN-γ_*L. lactis* protein sample did not reach that of the soluble counterpart (lines 3 and 4 of Table 2). When the APPs were incorporated in the engineered protein constructs, the solubilized proteins showed a decrease in the CSM values compared with the protein NPs samples (lines 5 and 7). This behavior suggests a possible self-arrangement of the tag within the protein that could replace water molecules and increase the hydrophobicity of the Trp environment. The CYOB construct (line 6 of Table 2) required a specific analysis as this tag contributes five additional Trp residues to the whole protein structure. In this case, the solubilized protein spectrum exhibited a modest red shift (higher CMS value) compared with the particulate form, indicating that the solubilization process exposed some of the Trp residues to a hydrophilic environment. The CSM values of the CYOB and HALRU protein NPs remained unaltered after solubilization (Table 2, lines 6 and 7). These data are in accordance with the higher stability of the particulate forms, which exhibited low levels of protein release.

The NP form of IFN-γ also favored the specific activity (insets, Fig. 3, *L. lactis* and non-tagged rBoIFN). This phenomenon is not only due to more active conformation of the protein (Fig. 4 and Table 2, line 3 vs line 4) [56] but also to the heterogeneous distribution of the protein and the ability of the protein NPs to increase the effective concentration of protein in the proximity of the receptor. Moreover, the formulation containing L6K2 was the most efficient, even compared with the commercial protein. Solubilization clearly conferred the most active and altered conformation of the protein without the tag. Although a low percentage of protein was released from the NPs containing L6K2, at least in PBS, this released protein seems to be sufficient to surpass the activity of the released protein without a tag (Fig. 3). Furthermore, the CSM thermal profile of the released proteins demonstrated that L6k2 tag not only confers the highly compact structure (low CSM value, Table 2) but also contribute to a unique and complete thermal unfolding profile (Fig. S4).

Another interesting aspect is the effect of the size of the tag on the structure-function of the protein. The incorporation of a tag larger than 17 amino acids beyond the linker (Fig. 1a) could generate steric problems preventing the interaction of tagged IFN-γ with the receptor. As shown in Fig. 1, L6K2 is only 8 amino acids, compared with 17 amino
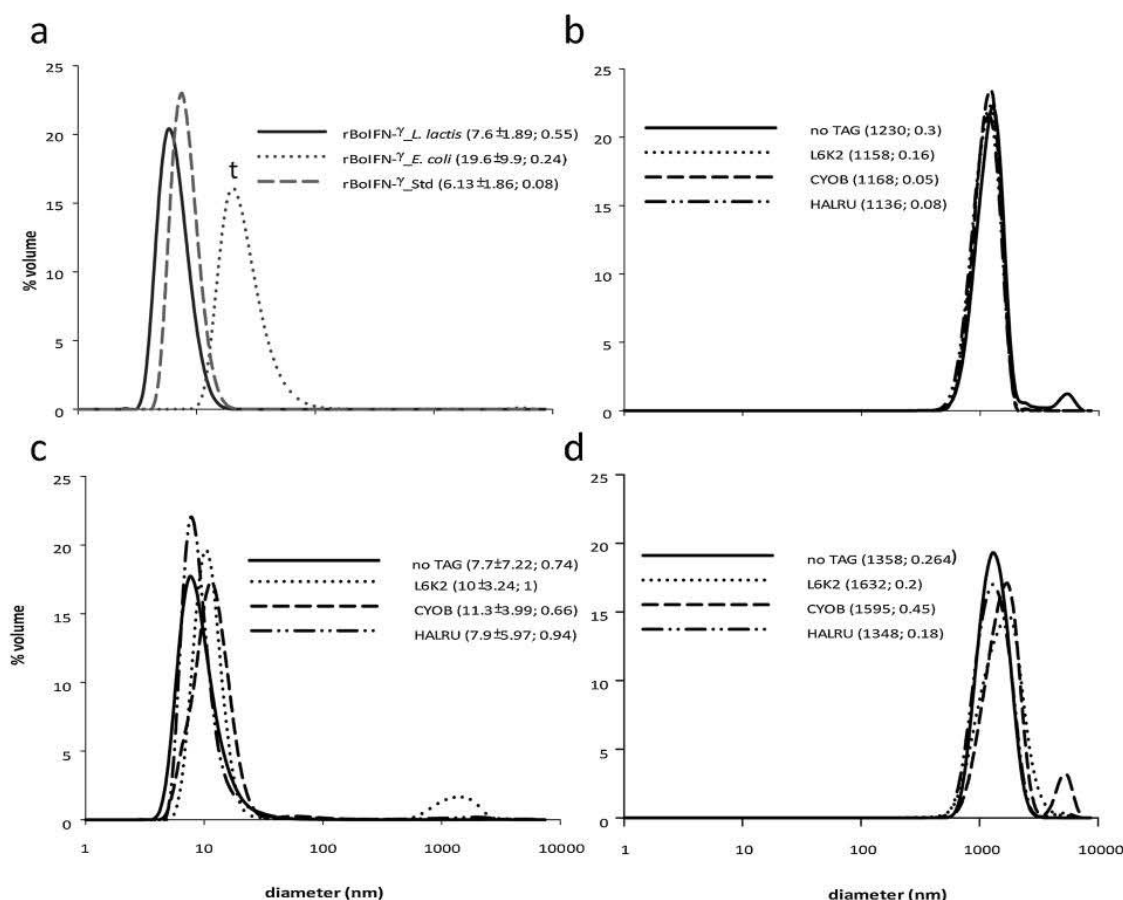
Fig. 4. Recombinant IFN-γ sizes in different supramolecular arrangements (purified soluble IFN-γ and INF-γ IBs). (a) Soluble rBoIFN-γ from different origins: commercial rBoIFN-γ_Std, in-house rBoIFN-γ from *E. coli* and *L. lactis*. (b) rBoIFN-γ IBs produced in *L. lactis*. (c) PBS solubilized rBoIFN-γ from IBs after interferon release. (d) Scaffold of rBoIFN-γ IBs incubated for 96 h at 37 °C. The mean size and polydispersity index are indicated in brackets. The average size data of the soluble proteins were analyzed by one-way ANOVA (^{t} corresponds to $P < 0.07$).

Table 2

Center of spectral mass (CSM) of IFN-γ protein preparations in soluble formats or in protein NPs analyzed before and after the resolubilization protocol.

		Soluble rBoIFN-γ	rBoIFN-γ NPs		Soluble rBoIFN-γ from NPs
			CSM (nm)		
		Soluble	Protein NPs	NP core	Resolubilized
1	rBoINF-γ_Std	356.5			
2	rBoIFN-γ_ *E. coli*	358.1			
3	rBoIFN-γ_ *L. lactis*	357.4			
4	rBoIFN-γ_*L. lactis*		**352.4**	353.6	**354.2**
5	rBoIFN-γ_L6K2_*L. lactis*		**352.7**	353.6	**351.7**
6	rBoIFN-γ_CYOB_*L. lactis*		353.1	353.1	354
7	rBoIFNγ_HALRU_*L. lactis*		354.2	354.2	352

acids for HALRU and 38 amino acids for CYOB. The short size of the L6K2 tag might reduce the difficulty of the interaction between L6K2-IFN-γ and the receptor compared with the longer IFN-γ tags since the C-terminal end of the protein, where the APPs are fused, is located in close proximity to the receptor in the 3D structure in PDB 1FG9.

In the recombinant protein production platform, the general consensus for improving protein yield is to improve the solubility of the protein. However, solubility and conformational quality are not necessarily coincident parameters [57]. The functionalities of the protein obtained from the soluble cell fraction or the protein NPs of rBoIFN-γ_*L. lactis* in the present work supported these previous findings, as the protein obtained from the soluble cell fraction was less active than that recovered from the protein NPs. The compactabilities of the conformations of these proteins were in agreement with their dissimilar biological activity. Therefore, results obtained in this study may indicate that the compactability of protein conformations is a significant parameter related to stability and function [58,59].

Conclusions

In this study, it has been demonstrated that the addition of APPs promoted the production of naturally occurring protein NPs of IFN-γ in the GRAS *Lactococcus lactis* expression system. The fine physico-chemical characterization of the resulting proteins revealed that conformational compactability was directly related to the biological performance of the recombinant IFN-γ.

Author contributions

E. Garcia-Fruitós and N. Ferrer-Miralles designed and supervised the experiments. J.V. Carratalà, O. Cano-Garrido, J. Sánchez, C. Membrado, E. Pérez, O. Conchillo-Solé and A. Sánchez-Chardi performed the experiments. J. V. Carratalà, O. Cano-Garrido, J. Sánchez and N. Ferrer-Miralles analyzed the data. All authors edited the manuscript. N. Ferrer-Miralles wrote the paper.

Appendix A. Supplementary data

Supplementary material related to this article can be found, in the online version, at doi:https://doi.org/10.1016/j.nbt.2020.02.001.

References

[1] Baeshen MN, Al-Hejin AM, Bora RS, Ahmed MM, Ramadan HA, Saini KS, et al. Production of biopharmaceuticals in *E. coli*: current scenario and future perspectives. J Microbiol Biotechnol 2015;25:953–62. https://doi.org/10.4014/jmb.1412.12079.

[2] Sanchez-Garcia L, Martin L, Mangues R, Ferrer-Miralles N, Vazquez E, Villaverde A. Recombinant pharmaceuticals from microbial cells: a 2015 update. Microb Cell Fact 2016;15:33. https://doi.org/10.1186/s12934-016-0437-3.

[3] Rueda F, Cespedes MV, Sanchez-Chardi A, Seras-Franzoso J, Pesarrodona M, Ferrer-Miralles N, et al. Structural and functional features of self-assembling protein nanoparticles produced in endotoxin-free *Escherichia coli*. Microb Cell Fact 2016;15:59. https://doi.org/10.1186/s12934-016-0457-z.

[4] Mamat U, Wilke K, Bramhill D, Schromm AB, Lindner B, Kohl TA, et al. Detoxifying *Escherichia coli* for endotoxin-free production of recombinant proteins. Microb Cell Fact 2015;14:57. https://doi.org/10.1186/s12934-015-0241-5.

[5] Garcia-Fruitos E. Lactic acid bacteria: a promising alternative for recombinant protein production. Microb Cell Fact 2012;11:157. https://doi.org/10.1186/1475-2859-11-157.

[6] Cano-Garrido O, Sanchez-Chardi A, Pares S, Giro I, Tatkiewicz WI, Ferrer-Miralles N, et al. Functional protein-based nanomaterial produced in microorganisms recognized as safe: a new platform for biotechnology. Acta Biomater 2016;43:230–9. https://doi.org/10.1016/j.actbio.2016.07.038.

[7] Ferrer-Miralles N, Villaverde A. Bacterial cell factories for recombinant protein production; expanding the catalogue. Microb Cell Fact 2013;12:113. https://doi.org/10.1186/1475-2859-12-113.

[8] Kopito RR. Aggresomes, inclusion bodies and protein aggregation. Trends Cell Biol 2000;10:524–30.

[9] Rinas U, Garcia-Fruitos E, Corchero JL, Vazquez E, Seras-Franzoso J, Villaverde A. Bacterial inclusion bodies: discovering their better half. Trends Biochem Sci 2017;42:726–37. https://doi.org/10.1016/j.tibs.2017.01.005.

[10] Rodriguez-Carmona E, Mendoza R, Ruiz-Canovas E, Ferrer-Miralles N, Abasolo I, Schwartz Jr S, et al. A novel bio-functional material based on mammalian cell aggresomes. Appl Microbiol Biotechnol 2015;99:7079–88. https://doi.org/10.1007/s00253-015-6684-0.

[11] Garcia-Fruitos E. Inclusion bodies: a new concept. Microb Cell Fact 2010;9:80. https://doi.org/10.1186/1475-2859-9-80.

[12] Jurgen B, Breitenstein A, Urlacher V, Buttner K, Lin H, Hecker M, et al. Quality control of inclusion bodies in *Escherichia coli*. Microb Cell Fact 2010;9:41. https://doi.org/10.1186/1475-2859-9-41.

[13] Singh A, Upadhyay V, Upadhyay AK, Singh SM, Panda AK. Protein recovery from inclusion bodies of *Escherichia coli* using mild solubilization process. Microb Cell Fact 2015;14:41. https://doi.org/10.1186/s12934-015-0222-8.

[14] Yamaguchi H, Miyazaki M. Refolding techniques for recovering biologically active recombinant proteins from inclusion bodies. Biomolecules 2014;4:235–51. https://doi.org/10.3390/biom4010235.

[15] Garcia-Fruitos E, Gonzalez-Montalban N, Morell M, Vera A, Ferraz RM, Aris A, et al. Aggregation as bacterial inclusion bodies does not imply inactivation of enzymes and fluorescent proteins. Microb Cell Fact 2005;4:27. https://doi.org/10.1186/1475-2859-4-27.

[16] Jevsevar S, Gaberc-Porekar V, Fonda I, Podobnik B, Grdadolnik J, Menart V. Production of nonclassical inclusion bodies from which correctly folded protein can be extracted. Biotechnol Prog 2005;21:632–9. https://doi.org/10.1021/bp0497839.

[17] Nahalka J, Nidetzky B. Fusion to a pull-down domain: a novel approach of producing *Trigonopsis variabilis* D-amino acid oxidase as insoluble enzyme aggregates. Biotechnol Bioeng 2007;97:454–61. https://doi.org/10.1002/bit.21244.

[18] Gifre-Renom L, Cano-Garrido O, Fabregas F, Roca-Pinilla R, Seras-Franzoso J, Ferrer-Miralles N, et al. A new approach to obtain pure and active proteins from *Lactococcus lactis* protein aggregates. Sci Rep 2018;8:13917. https://doi.org/10.1038/s41598-018-32213-8. 10.1038/s41598-018-32213-8 [pii].

[19] Cespedes MV, Fernandez Y, Unzueta U, Mendoza R, Seras-Franzoso J, Sanchez-Chardi A, et al. Bacterial mimetics of endocrine secretory granules as immobilized in vivo depots for functional protein drugs. Sci Rep 2016;6:35765. https://doi.org/10.1038/srep35765.

[20] de Jong LA, Uges DR, Franke JP, Bischoff R. Receptor-ligand binding assays: technologies and applications. J Chromatogr B Analyt Technol Biomed Life Sci 2005;829:1–25. https://doi.org/10.1016/j.jchromb.2005.10.002.

[21] Peternel S, Komel R. Active protein aggregates produced in *Escherichia coli*. Int J Mol Sci 2011;12:8275–87. https://doi.org/10.3390/ijms12118275.

[22] Krauss U, Jager VD, Diener M, Pohl M, Jaeger KE. Catalytically-active inclusion bodies-carrier-free protein immobilizates for application in biotechnology and biomedicine. J Biotechnol 2017;258:136–47. https://doi.org/10.1016/j.jbiotec.2017.04.033.

[23] Le PC, Genin P, Baines MG, Hiscott J. Interferon activation and innate immunity. Rev Immunogenet 2000;2:374–86 ncbi.nlm.nih.gov/pubmed/11256746.

[24] Schoenborn JR, Wilson CB. Regulation of interferon-gamma during innate and adaptive immune responses. Adv Immunol 2007;96:41–101. https://doi.org/10.1016/S0065-2776(07)96002-2.

[25] Khalilzadeh R, Shojaosadati SA, Maghsoudi N, Mohammadian-Mosaabadi J, Mohammadi MR, Bahrami A, et al. Process development for production of recombinant human interferon-gamma expressed in *Escherichia coli*. J Ind Microbiol Biotechnol 2004;31:63–9. https://doi.org/10.1007/s10295-004-0117-x.

[26] Perez L, Vega J, Chuay C, Menendez A, Ubieta R, Montero M, et al. Production and characterization of human gamma interferon from *Escherichia coli*. Appl Microbiol Biotechnol 1990;33:429–34.

[27] Vaiphei ST, Pandey G, Mukherjee KJ. Kinetic studies of recombinant human interferon-gamma expression in continuous cultures of *E. coli*. J Ind Microbiol Biotechnol 2009;36:1453–8. https://doi.org/10.1007/s10295-009-0632-x.

[28] Kumar M, Singh M, Singh SB. Optimization of conditions for expression of recombinant interferon-gamma in *E. coli*. Mol Biol Rep 2014;41:6537–43. https://doi.org/10.1007/s11033-014-3537-3.

[29] Thomas JG, Baneyx F. Roles of the *Escherichia coli* small heat shock proteins IbpA and IbpB in thermal stress management: comparison with ClpA, ClpB, and HtpG in vivo. J Bacteriol 1998;180:5165–72.

[30] Zhou B, Xing L, Wu W, Zhang XE, Lin Z. Small surfactant-like peptides can drive soluble proteins into active aggregates. Microb Cell Fact 2012;11:10. https://doi.org/10.1186/1475-2859-11-10.

[31] Conchillo-Sole O, de Groot NS, Aviles FX, Vendrell J, Daura X, Ventura S. AGGRESCAN: a server for the prediction and evaluation of "hot spots" of aggregation in polypeptides. BMC Bioinformatics 2007;8:65. https://doi.org/10.1186/1471-2105-8-65.

[32] Piovesan D, Tabaro F, Micetic I, Necci M, Quaglia F, Oldfield CJ, et al. DisProt 7.0: a major update of the database of disordered proteins. Nucleic Acids Res 2017;45:D219–27. https://doi.org/10.1093/nar/gkw1056.

[33] Cano-Garrido O, Rueda FL, Sanchez-Garcia L, Ruiz-Avila L, Bosser R, Villaverde A, et al. Expanding the recombinant protein quality in *Lactococcus lactis*. Microb Cell Fact 2014;13:167. https://doi.org/10.1186/s12934-014-0167-3.

[34] Spekker K, Czesla M, Ince V, Heseler K, Schmidt SK, Schares G, et al. Indoleamine 2,3-dioxygenase is involved in defense against *Neospora caninum* in human and bovine cells. Infect Immun 2009;77:4496–501. https://doi.org/10.1128/IAI.00310-09.

[35] Boyanova M, Tsanev R, Ivanov I. A modified kynurenine bioassay for quantitative determination of human interferon-gamma. Anal Biochem 2002;308:178–81.

[36] Lakowicz JR, Kusba J, Wiczk W, Gryczynski I, Szmacinski H, Johnson ML. Resolution of the conformational distribution and dynamics of a flexible molecule

using frequency-domain fluorometry. Biophys Chem 1991;39:79–84.

[37] Li GY, Xiao ZZ, Lu HP, Li YY, Zhou XH, Tan X, et al. A simple method for recombinant protein purification using self-assembling peptide-tagged tobacco etch virus protease. Protein Expr Purif 2016;128:86–92. https://doi.org/10.1016/j.pep.2016.08.013.

[38] Bhattacharjee S. DLS and zeta potential - what they are and what they are not? J Control Release 2016;235:337–51. https://doi.org/10.1016/j.jconrel.2016.06.017.

[39] Meager A. Biological assays for interferons. J Immunol Methods 2002;261:21–36.

[40] Bomsztyk K, Stanton TH, Smith LL, Rachie NA, Dower SK. Properties of interleukin-1 and interferon-gamma receptors in B lymphoid cell line. J Biol Chem 1989;264:6052–7.

[41] Hess AK, Saffert P, Liebeton K, Ignatova Z. Optimization of translation profiles enhances protein expression and solubility. PLoS One 2015;10:e0127039 https://doi.org/10.1371/journal.pone.0127039.

[42] Boumaiza M, Colarusso A, Parrilli E, Garcia-Fruitos E, Casillo A, Aris A, et al. Getting value from the waste: recombinant production of a sweet protein by *Lactococcus lactis* grown on cheese whey. Microb Cell Fact 2018;17:126. https://doi.org/10.1186/s12934-018-0974-z.

[43] Marini G, Luchese MD, Argondizzo AP, de Goes AC, Galler R, Alves TL, et al. Experimental design approach in recombinant protein expression: determining medium composition and induction conditions for expression of pneumolysin from *Streptococcus pneumoniae* in *Escherichia coli* and preliminary purification process. BMC Biotechnol 2014;14:1. https://doi.org/10.1186/1472-6750-14-1.

[44] Garcia-Fruitos E, Aris A, Villaverde A. Localization of functional polypeptides in bacterial inclusion bodies. Appl Environ Microbiol 2007;73:289–94. https://doi.org/10.1128/AEM.01952-06.

[45] Upadhyay AK, Murmu A, Singh A, Panda AK. Kinetics of inclusion body formation and its correlation with the characteristics of protein aggregates in *Escherichia coli*. PLoS One 2012;7:e33951 https://doi.org/10.1371/journal.pone.0033951.

[46] Unzueta U, Cespedes MV, Sala R, Alamo P, Sanchez-Chardi A, Pesarrodona M, et al. Release of targeted protein nanoparticles from functional bacterial amyloids: a death star-like approach. J Control Release 2018;279:29–39. https://doi.org/10.1016/j.jconrel.2018.04.004.

[47] Hunig T. The storm has cleared: lessons from the CD28 superagonist TGN1412 trial. Nat Rev Immunol 2012;12:317–8. https://doi.org/10.1038/nri3192.

[48] Suntharalingam G, Perry MR, Ward S, Brett SJ, Castello-Cortes A, Brunner MD, et al. Cytokine storm in a phase 1 trial of the anti-CD28 monoclonal antibody TGN1412. N Engl J Med 2006;355:1018–28. https://doi.org/10.1056/NEJMoa063842.

[49] Yu Z, Reid JC, Yang YP. Utilizing dynamic light scattering as a process analytical technology for protein folding and aggregation monitoring in vaccine manufacturing. J Pharm Sci 2013;102:4284–90. https://doi.org/10.1002/jps.23746. S0022-3549(15)30802-9 [pii].

[50] Li TM, Hook III JW, Drickamer HG, Weber G. Plurality of pressure-denatured forms in chymotrypsinogen and lysozyme. Biochemistry 1976;15:5571–80.

[51] Mohana-Borges R, Silva JL, Ruiz-Sanz J, de Prat-Gay G. Folding of a pressure-denatured model protein. Proc Natl Acad Sci U S A 1999;96:7888–93.

[52] Ruan K, Weber G. Hysteresis and conformational drift of pressure-dissociated glyceraldehydephosphate dehydrogenase. Biochemistry 1989;28:2144–53.

[53] Sanchez JM, Nolan V, Perillo MA. Beta-galactosidase at the membrane-water interface: a case of an active enzyme with non-native conformation. Colloids Surf B Biointerfaces 2013;108:1–7. https://doi.org/10.1016/j.colsurfb.2013.02.019.

[54] Randal M, Kossiakoff AA. The 2.0 A structure of bovine interferon-gamma; assessment of the structural differences between species. Acta Crystallogr D Biol Crystallogr 2000;56:14–24.

[55] Thiel DJ, le Du MH, Walter RL, D'Arcy A, Chene C, Fountoulakis M, et al. Observation of an unexpected third receptor molecule in the crystal structure of human interferon-gamma receptor complex. Structure 2000;8:927–36.

[56] Flores SS, Nolan V, Perillo MA, Sanchez JM. Superactive beta-galactosidase inclusion bodies. Colloids Surf B Biointerfaces 2019;173:769–75. https://doi.org/10.1016/j.colsurfb.2018.10.049.

[57] Martinez-Alonso M, Garcia-Fruitos E, Villaverde A. Yield, solubility and conformational quality of soluble proteins are not simultaneously favored in recombinant *Escherichia coli*. Biotechnol Bioeng 2008;101:1353–8. https://doi.org/10.1002/bit.21996.

[58] Ghobadi S, Ashrafi-Kooshk MR, Mahdiuni H, Khodarahmi R. Enhancement of intrinsic fluorescence of human carbonic anhydrase II upon topiramate binding: some evidence for drug-induced molecular contraction of the protein. Int J Biol Macromol 2018;108:240–9. https://doi.org/10.1016/j.ijbiomac.2017.12.011.

[59] Wang L, Dong Q, Zhu Q, Tang N, Jia S, Xi C, et al. Conformational characteristics of rice hexokinase OsHXK7 as a moonlighting protein involved in sugar signalling and metabolism. Protein J 2017;36:249–56. https://doi.org/10.1007/s10930-017-9718-x.

Supplementary material

Aggregation-prone peptides modulate activity of bovine interferon gamma released from naturally occurring protein nanoparticles

José Vicente Carratalá[a,b], Olivia Cano-Garrido[a,b,c,1], Julieta Sánchez[a,2], Cristina Membrado[a,b], Eudald Pérez[a,b], Oscar Conchillo-Solé[a], Xavier Daura[a,d], Alejandro Sánchez-Chardi[e], Antonio Villaverde[a,b,c], Anna Arís[f], Elena Garcia-Fruitós[f], Neus Ferrer-Miralles[a,b,c]#

[a]Institute for Biotechnology and Biomedicine, Autonomous University of Barcelona, Bellaterra, Barcelona, Spain

[b]Department of Genetics and Microbiology, Autonomous University of Barcelona, Bellaterra, Barcelona, Spain

[c]Bioengineering, Biomaterials and Nanomedicine Networking Biomedical Research Centre (CIBER-BBN), Bellaterra, Barcelona, Spain

[d]Catalan Institution for Research and Advanced Studies, Barcelona, Spain

[e]Department of Evolyutionary Biology, Ecology and Environmental Sciences, Faculty of Biology, University of Barcelona, Barcelona, Spain.

[f]Department of Ruminant Production, Institute of Agrifood Research and Technology (IRTA), Caldes de Montbui, Barcelona, Spain

#Address correspondence to Neus Ferrer-Miralles, neus.ferrer@uab.cat.

[1]Present address: Nanoligent SL. Eureka Building. Campus of the Autonomous University of Barcelona. Bellaterra, Barcelona, Spain

[2]Permanent address: National University of Cordoba, Faculty of Exact, Physical and Natural Sciences, ICTA and Chemistry Department, CONICET Institute of Biological and Technological Research (IIByT) Cordoba Argentina

Figure S1. Nucleotide sequence of BoIFN-γ genes

A) Nucleotide sequence of *Bos taurus* IFN-γ gene (ORF 1; NM_ 174086.1). **B)** Nucleotide sequence of IFN-γ gene codon optimized for *L. lactis* (Geneart). Additional A codon is labeled in red. For both sequences, only coding sequence of the mature protein is shown (residues 24-166).

Figure S2. Amino acid sequences of rBoIFN-γ recombinant proteins.

A) Sequence alignment of the amino acid sequence of *Bos taurus* IFN-γ protein (NP_776511) and recombinant IFN-γ used in the study. An additional A (in red) was introduced during the cloning process associated with the use of the *Nco*I restriction site. C-terminal 6 x His tag and additional K are marked in yellow. Signal peptide of the native IFN-γ sequence is shown in bold. **B)** Amino acid sequence of the rIFN-γ fused to aggregation peptides L6K2, HALRU and CYOB (highlighted in green). Linker between IFN-γ and aggregation peptides are highlighted in grey. **C)** Amino acid sequence of protein variants of rBoIFN-γ used as control protein (2300-BG-025, R&D Systems). This sample corresponded to a mixture of bovine IFN-γ Gln24-Thr166 and Gln24-Arg162, both with an N-terminal methionine. Note that in the rBoIFN-γ variants produced in-house, a K residue was included at the N-terminus of the His-tag for putative elimination of the tag by exopeptidases.

Figure S3. Analysis of the relative abundance of rBoIFN-γ in protein nanoparticles. Protein bands were separated and revealed in denaturing TGX stain-free gels (Bio-Rad) in triplicate. Quantification analysis were performed using Quantity one software (BioRad). Relative purity of positive protein bands is displayed below the corresponding lanes (%)

Figure S4. Center of spectral mass (CSM) versus temperature of rBoIFN-γ proteins resolubilized from NPs. Change in CSM (weighted average of the fluorescence spectrum peak) at 550 nm of resolubilized rBoIFN-γ, released form protein nanoparticles, as a function of temperature.

A)

ATGCAGGGCCAATTTTTTAGAGAAATAGAAAACTTAAAGGAGTATTTTAATGCAAGTAGCCCA
GATGTAGCTAAGGGTGGGCCTCTCTTCTCAGAAATTTTGAAGAATTGGAAAGATGAAAGTGAC
AAAAAAATTATTCAGAGCCAAATTGTCTCCTTCTACTTCAAACTCTTTGAAAACCTCAAAGAT
AACCAGGTCATTCAAAGGAGCATGGATATCATCAAGCAAGACATGTTTCAGAAGTTCTTGAAT
GGCAGCTCTGAGAAACTGGAGGACTTCAAAAAGCTGATTCAAATTCCGGTGGATGATCTGCAG
ATCCAGCGCAAAGCCATAAATGAACTCATCAAAGTGATGAATGACCTGTCACCAAAATCTAAC
CTCAGAAAGCGGAAGAGAAGTCAGAATCTCTTTCGAGGCCGGAGAGCATCAACG

B)

ATGGCACAAGGTCAATTCTTTCGTGAAATTGAAAATCTTAAAGAATATTTTAATGCTAGTAGT
CCTGATGTTGCTAAAGGTGGTCCATTGTTTTCAGAAATTTTGAAAAATTGGAAAGATGAATCT
GATAAGAAAATTATTCAATCTCAAATTGTTAGTTTTTATTTTAAATTGTTTGAAAATCTTAAA
GATAATCAAGTTATTCAACGTTCAATGGATATTATTAAACAAGATATGTTTCAAAAATTTCTT
AATGGATCATCTGAAAAATTGGAAGATTTTAAAAAATTGATTCAAATTCCAGTTGATGATTTA
CAAATTCAAAGAAAAGCTATTAATGAACTTATTAAAGTTATGAATGATCTTAGTCCTAAATCA
AATTTGCGTAAAAGAAAACGTTCACAAAATCTTTTTCGTGGTCGTCGTGCTTCAACT

Figure S1

84

A)

```
BOV_NP_776511.  MKYTSYFLALLLCGLLGFSGSYGQGQFFREIENLKEYFNASSPDVAKGGPLFSEILKNWK 60
rBoIFN-γ        --------------------MAQGQFFREIENLKEYFNASSPDVAKGGPLFSEILKNWK 39
                .**************************************
```

```
NP_776511.1     DESDKKIIQSQIVSFYFKLFENLKDNQVIQRSMDIIKQDMFQKFLNGSSEKLEDFKKLIQ 120
rBoIFN-γ        DESDKKIIQSQIVSFYFKLFENLKDNQVIQRSMDIIKQDMFQKFLNGSSEKLEDFKKLIQ 99
                ************************************************************
```

```
NP_776511.1     IPVDDLQIQRKAINELIKVMNDLSPKSNLRKRKRSQNLFRGRRAST------- 166
rBoIFN-γ        IPVDDLQIQRKAINELIKVMNDLSPKSNLRKRKRSQNLFRGRRASTKHHHHHH 152
                *********************************************
```

B)

rBoIFN-γ_L6K2 (20,388.55 Da)

MAQGQFFREI ENLKEYFNAS SPDVAKGGPL FSEILKNWKD ESDKKIIQSQ IVSFYFKLFE NLKDNQVIQR SMDIIKQDMF
QKFLNGSSEK LEDFKKLIQI PVDDLQIQRK AINELIKVMN DLSPKSNLRK RKRSQNLFRG RRAST PTPPTTPTPPTTPTPTP
LLLLLLKK HHHHHH

rBoIFN-γ_HALRU (21,466.90 Da)

MAQGQFFREI ENLKEYFNAS SPDVAKGGPL FSEILKNWKD ESDKKIIQSQ IVSFYFKLFE NLKDNQVIQR SMDIIKQDMF
QKFLNGSSEK LEDFKKLIQI PVDDLQIQRK AINELIKVMN DLSPKSNLRK RKRSQNLFRG RRAST PTPPTTPTPPTTPTPTP
MTYMCSIL ICLVLILCA K HHHHHH

rBoIFN-γ_CYOB (23,902.71 Da)

MAQGQFFREI ENLKEYFNAS SPDVAKGGPL FSEILKNWKD ESDKKIIQSQ IVSFYFKLFE NLKDNQVIQR SMDIIKQDMF
QKFLNGSSEK LEDFKKLIQI PVDDLQIQRK AINELIKVMN DLSPKSNLRK RKRSQNLFRG RRAST PTPPTTPTPPTTPTPTP
AGIVIAAF STIFGFAMIWHIWWLAIVGF AGMIITWIVKS K HHHHHH

C)

rBoIFN-γ_Std (variant M24-166)

MQGQFFREI ENLKEYFNAS SPDVAKGGPL FSEILKNWKD ESDKKIIQSQ IVSFYFKLFE NLKDNQVIQR SMDIIKQDMF
QKFLNGSSEK LEDFKKLIQI PVDDLQIQRK AINELIKVMN DLSPKSNLRK RKRSQNLFRG RRAST

rBoIFN-γ_Std (variant M24-164)

MQGQFFREI ENLKEYFNAS SPDVAKGGPL FSEILKNWKD ESDKKIIQSQ IVSFYFKLFE NLKDNQVIQR SMDIIKQDMF
QKFLNGSSEK LEDFKKLIQI PVDDLQIQRK AINELIKVMN DLSPKSNLRK RKRSQNLFRG RRA

Figure S2
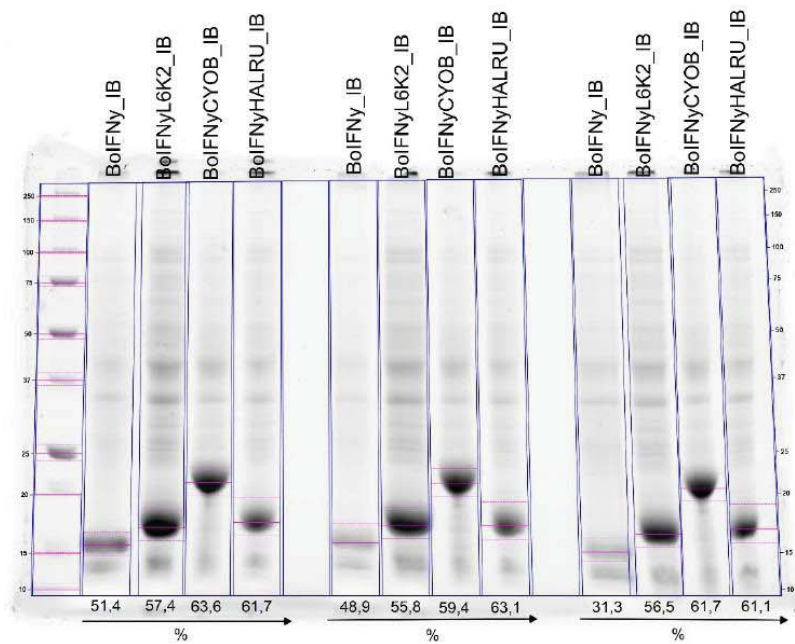
Figure S3
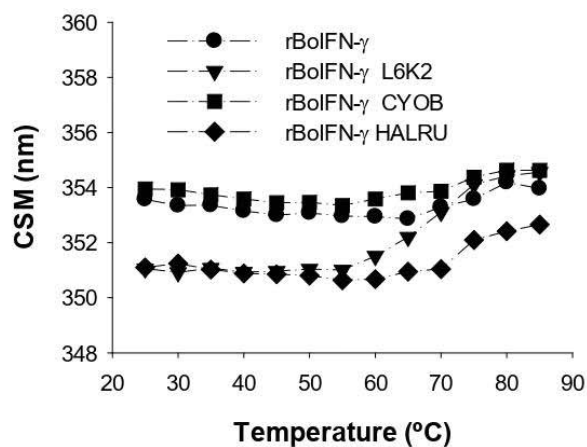
Figure S4

Table S1. Yield of rBoIFN-γ purified proteins obtained in different formats.

Name	Format	Expression system	Yield (mg/L)	Comments
rBoIFN-γ	soluble	*Clearcoli®*	10.46	Purified by IMAC
rBoIFN-γ	soluble	*L. lactis*	15.5	
rBoIFN-γ	Nanoparticle	*L. lactis*	24.73	Purified from insoluble cell fraction
rBoIFN-γ_L6K2	Nanoparticle	*L. lactis*	20.22	
rBoIFN-γ_HALRU	Nanoparticle	*L. lactis*	11.64	
rBoIFN-γ_CYOB	Nanoparticle	*L. lactis*	11.74	
rBoIFN-γ	soluble	*L. lactis*	13.03	Solubilized from nanoparticles
rBoIFN-γ_L6K2	soluble	*L. lactis*	1.07	
rBoIFN-γ_HALRU	soluble	*L. lactis*	0.05	
rBoIFN-γ_CYOB	soluble	*L. lactis*	0.05	

Supplementary Materials and Methods

Bacterial strains and plasmids

In the **cloning** of bovine IFN-γ genes in **L. lactis**, *Nco*I/*Xba*I digestion products (IFN-γ, IFN-γ _L6K2, IFN-γ _HALRU and IFN-γ_CYOB) were ligated into the expression plasmid **pNZ8148**. Ligation products were **transformed** by electroporation into *L. lactis cremoris* NZ9000 (Boca Scientific) competent cells. Electroporation was carried out using Gene Pulser (Bio-rad) at 2500 V, 200 Ω and 25 μF in a pre-cooled 2 cm electroporation cuvette. After this, samples were supplemented with 900 μL M17 broth with 0.5 % glucose and incubated for 2 h at 30 °C. The electroporation mix was centrifuged for 10 min at 10,000 x *g* at 4 °C and the pellet was resuspended in 100-200 μL of M17 media and plated.

In the **cloning** of IFN-γ gene in **ClearColi®** BL21(DE3) (Lucigen), *Nco*I/*Hin*dIII digestion product was ligated into the expression plasmid **pETDuet-1** (Novagen) *ClearColi®* BL21(DE3). For **ClearColi® BL21 (DE3) transformation**, 1 μL of ligated DNA was mixed into a chilled electroporation 0.2 cm gap cuvette with 100 μL of thawed cells. Electroporation was carried out at 25 μF, 750 Ω and 2,400 V. 10 seconds after the electroporation, 900 μL of LB medium was added into the cuvette, mixed and transferred to a sterile tube. The cells were then incubated in a shaking incubator at 150 rpm for 1 hour at 37 °C. After that, 100 μL of the growing culture was spread in a plate (containing 100 μg/mL of Ampicillin). This procedure was done in triplicate. The plates were incubated for 32-40 hours at 37 °C.

For all clones, in the sequence design we added an *Nco*I restriction site at the 5' end, followed by the nucleotides CA to restore the reading frame. These additional nucleotides resulted in the addition of amino acid A beside the initial M of the polypeptide (marked in red in Figs. S1 and S2)

All genes were C-terminally fused to a His-tag for detection and quantification by western blot analysis. Furthermore, an additional codon that specifies the amino acid Lys was included at the N-terminus of the His-tag for putative elimination of the tag by exopeptidases.

Production and purification of rBoIFN-γ protein from the soluble cell fraction

For **protein purification** in *L. lactis*, approximately 5 g of an *L. lactis* pellet was solubilized in 30 mL of wash buffer (Tris 20 mmol/L pH 8.0, 500 mmol/L NaCl, 10 mmol/L Imidazole) and one tablet of cOmplete, EDTA-free Protease Inhibitor (Roche). **Cell lysis** was carried out in a French press (3 cycles at 1,500 psi, Thermo FA-078A) in ice coating. The resultant solution was centrifuged (15,000 x *g*, 40 min, 4 °C) and the soluble cell fraction was filtered by 0.22 μm and kept on ice until the purification step. **Protein purification** was performed by immobilized metal affinity chromatography (IMAC) using a HiTrap Chelating HP 1-ml column (GE Healthcare) with an ÄKTA purifier FPLC system (GE Healthcare). The eluted proteins were then dialyzed against phosphate-buffered saline (PBS) buffer. Elution of the protein was performed with a linear gradient of 20 CV of elution buffer (Tris 20 mmol/L pH 8.0, 500 mmol/L NaCl, 500 mmol/L Imidazole). A single positive protein peak was detected at 50 % elution profile. Final protein concentration was 2.99 mg/mL with a yield of 15.5 mg/L.

For **protein purification** in *Clearcoli®*, approximately 5 g of an *E. coli* pellet (1.3 L of cell culture) was solubilized in 25 mL of wash buffer (Tris 20 mmol/L pH 8.0, 500 mmol/L NaCl, 10 mmol/L Imidazole) and one tablet of cOmplete, EDTA-free Protease Inhibitor (Roche). **Cell lysis** was performed by sonication (1 round of 3 min at 10 % amplitude and 5 rounds of 3 minutes at 15 % amplitude; Branson 450 Digital Sonicator). The resultant solution was centrifuged (15,000 x *g*, 40 min, 4 °C) in order to separate cell debris from soluble elements, after that, the soluble cell fraction was filtered by 0.22 μm and kept on ice until the purification step. **Protein purification** was carried out by His tag affinity chromatography using ÄKTA purifier FPLC (GE Healthcare) and HiTrap Chelating HP 1 mL column (GE Healthcare). The sample was charged into the column at a flow rate of 1 mL/min, after that, the column was washed with five column volumes and elution was set with a linear gradient of 20 CV at a flow rate of 1 mL/min (Elution buffer: Tris 20 mmol/L pH 8.0, 500 mmol/L NaCl, 500 mmol/L Imidazole). All fractions were collected and analyzed by TGX technology (Bio-Rad) and western blot. The positive IFN-γ fractions (13 mL) were eluted in a single peak, pulled and dialyzed against phosphate-buffered saline (PBS) buffer overnight at 4 °C. The final

protein concentration was determined by Bradford´s protein assay, yielding 0.80 mg/mL. Samples of 100 µL were stored at - 80 °C until its activity evaluation by the kynurenine assay. The final **yield** was 10.46 mg/L.

From this point, the same protocol was followed for all protein constructs. The soluble and insoluble cell fractions were separated by centrifugation (40 min, 15,000 x g, 4 °C). The recombinant protein in the soluble cell fraction was purified by immobilized metal affinity chromatography (IMAC) using a HiTrap Chelating HP 1-ml column (GE Healthcare) with an ÄKTA purifier FPLC system (GE Healthcare). The eluted proteins were then dialyzed against phosphate-buffered saline (PBS) buffer.

Production and purification of rBoIFN-γ protein nanoparticles.

The first step in the **purification** of protein nanoparticles of was to resuspend the cell pellet in PBS 1 x (every 50 mL cell pellet in 30 mL PBS). Then, mechanical disrupt the sample by French press (Thermo FA-078A) at 3 cycles at 1,500 psi.

After that, lysozyme (10 µg/mL) (Roche: 10 837 059 001) was added and incubated 2 h at 250 rpm and 37 °C and after this it was frozen at -80 °C O/N. After thawing the mixture, Triton X-100 (0.4 mL/100 mL sample) (Roche: 10 789 704 001) was added and the sample was incubated at RT 1 h under gentle agitation. At this point, bacterial contamination was tested by inoculating 100 µL of the mixture on M17B + 0.5 % glucose plates, that were incubated O/N at 30 °C. Freeze/thaw cycles were repeated until obtaining no viable cells on LB plates. Then, Nonidet P-40 (25 µL/100 mL sample) (Roche: 11 754 599 001) was added and the mixture was incubated 1 h under gentle agitation at 4 °C. Following this, $MgSO_4$ (60 µL/100 mL sample) and DNAse I (60 µL/100 mL sample) (Roche: 10 104 159 001) were added and the sample was incubated 1 h under gentle agitation at 37 °C. Finally, the pellet was resuspended in lysis buffer + Triton X-100 (5 mL/100 mL initial sample) and harvested at 15,000 x g for 15 min at 4 °C. Another freeze/thaw cycle was done, NPs were harvested at 15,000 x g for 15 min at 4 °C, the supernatant was

discarded and NPs were diluted and resuspended 1:10 in PBS. The protocol was performed under sterile conditions.

Quantitative protein analysis

Unless otherwise stated, soluble and protein NPs were analyzed by denaturing SDS-PAGE (10 % acrylamide). Samples were resuspended with denaturing buffer (Laemli 4 x: Tris base 1.28 g, glycerol 8 mL, SDS 1.6 g, β-mercaptoethanol 4 mL, urea 9.6 g in 100 mL). Protein samples were boiled for 5 and 45 min respectively and loaded onto the gel. SDS-PAGE protein bands were electroblotted onto nitrocellulose membranes and identified using a commercial polyclonal serum against the histidine tag (#A00186-100 Genscript) and an anti-mouse secondary antibody (#170-6516, Bio-Rad). The recombinant protein yield was estimated by comparison with a standard curve of known amounts of a purified GFP-H6 protein quantified by the Bradford assay. Quantification was performed with Quantity One software (Bio-Rad).

Determination of rBoIFN-γ biological activity in bovine cells

Bovine fibroblast-like cells (EBTr cells), (87090202 Sigma-Aldrich) were cultured in Dulbecco's modified Eagle's medium (Gibco) with 10 % fetal bovine serum (FBS). For activity analysis, the cells were seeded in 96-well flat-bottom microtiter plates (5000 cells per well) in medium supplemented with 100 µg/ml L-Trp. Serial dilutions of both, the soluble and NP forms of rBoIFNy at quantities ranging from 6 nmol/L to 0.024 nmol/L were incubated with cells for 96 h at 37 °C. The presence of L-kynurenine was detected by the addition of Ehrlich's reagent 4-(dimethylamino) benzaldehyde (156477, Sigma-Aldrich) and measuring the absorbance at 490 nm in a conventional luminometer and VICTOR3V 1420 multilabel reader (PerkinElmer).

STUDY 3

In vivo bactericidal efficacy of GWH1 antimicrobial peptide displayed on protein nanoparticles, a potential alternative to antibiotics

Jose Vicente Carratalá, Eric Brouillette, Naroa Serna, Alejandro Sánchez-Chardi, Julieta M. Sánchez, Antonio Villaverde, Anna Arís, Elena Garcia-Fruitós, Neus Ferrer-Miralles, François Malouin

To tackle with the development of bacterial resistance against traditional antibiotics, novel alternative therapies are urgently needed. The use of cytokines such as IFN-γ described in Study 2 could be a potential strategy to reduce antibiotic usage. On the other hand, antimicrobial peptides (AMPs) such as GWH1 have been already proposed as another potential solution. However, more studies are needed in order to fully develop innovative nanotherapeutics in the treatment of microbial infections, considering the need to also increase the stability of these amino acid-based compounds.

The self-arrangement of individual protein forms into superior structural complexes leads to the formation of different protein formats which could potentially contribute to increase protein stability. While the IB format, analyzed in detail in Study 1 and Study 2, act as an insoluble natural depot of proteins, providing a complex environment by which functional protein is sustainably released, other self-assembled oligomeric forms such as soluble protein nanoparticles (NPs) tend to present a defined multimeric structure that also have a huge potential for the production of cytokines and AMPs in a stable form.

The ability of IFN-γ to retain activity upon release of naturally occurring IBs observed in Study 2, and its relevant role on promoting and efficient immune response against infectious agents, such as bacteria, leads us to further test its performance in an *in vivo* murine model of mastitis. Furthermore, in order to increase the antimicrobial capabilities of this cytokine, a fusion design containing GWH1 was also evaluated. On the other hand, the self-arrangement of AMP-containing proteins into nanoparticles, such as GWH1-GFP, has been proposed as a novel strategy to fight against bacterial infections. However, an *in vivo* approach was still lacking to demonstrate its potential therapeutic effect.

In this context, different protein designs including IFN-γ, GWH1-IFN-γ, GFP and GWH1-GFP in different protein nanoformats were tested and compared in an *in vivo* mouse model of mastitis.

pharmaceutics

MDPI

Article

In Vivo Bactericidal Efficacy of GWH1 Antimicrobial Peptide Displayed on Protein Nanoparticles, a Potential Alternative to Antibiotics

Jose V. Carratalá [1,2,3], Eric Brouillette [4,5], Naroa Serna [1,2,3], Alejandro Sánchez-Chardi [6,7], Julieta M. Sánchez [1,2,†], Antonio Villaverde [1,2,3], Anna Arís [8], Elena Garcia-Fruitós [8], Neus Ferrer-Miralles [1,2,3,*] and François Malouin [4,5,*]

[1]   Institute for Biotechnology and Biomedicine, Autonomous University of Barcelona, Bellaterra, 08193 Barcelona, Spain; JoseVicente.Carratala@uab.cat (J.V.C.); naroa.serna@uab.cat (N.S.); jsanchezqa@gmail.com (J.M.S.); antonio.villaverde@uab.cat (A.V.)

[2]   Department of Genetics and Microbiology, Autonomous University of Barcelona, Bellaterra, 08193 Barcelona, Spain

[3]   Bioengineering, Biomaterials and Nanomedicine Networking Biomedical Research Centre (CIBER-BBN), C/Monforte de Lemos 3-5, 28029 Madrid, Spain

[4]   Centre d'Étude et de Valorisation de la Diversité Microbienne (CEVDM), Département de Biologie, Université de Sherbrooke, 2500 Boul. Université, Sherbrooke, QC J1K 2R1, Canada; eric.brouillette@usherbrooke.ca

[5]   Mastitis Network and Regroupement de Recherche Pour un Lait de Qualité Optimale (Op+Lait), Université de Montréal, 2900 Edouard Montpetit Blvd, Montréal, QC H3T 1J4, Canada

[6]   Microscopy Service, Autonomous University of Barcelona, Bellaterra, 08193 Barcelona, Spain; Alejandro.Sanchez.Chardi@uab.cat

[7]   Departament of Evolutionary Biology, Ecology and Environmental Sciences, University of Barcelona, Avda Diagonal 643, 08028 Barcelona, Spain

[8]   Department of Ruminant Production, Institute of Agriculture and Agrifood Research and Technology (IRTA), Caldes de Montbui, 08140 Barcelona, Spain; anna.aris@irta.cat (A.A.); elena.garcia@irta.cat (E.G.-F.)

*   Correspondence: neus.ferrer@uab.cat (N.F.-M.); francois.malouin@usherbrooke.ca (F.M.)

†   Permanent address: Faculty of Exact, Physical and Natural Sciences, ICTA and Chemistry Department, CONICET Institute of Biological and Technological Research (IIByT), National University of Cordoba, Velez Sarsfield Avenue 1611, X 5016GCA Córdoba, Argentina.

check for updates

Abstract: Oligomerization of antimicrobial peptides into nanosized supramolecular complexes produced in biological systems (inclusion bodies and self-assembling nanoparticles) seems an appealing alternative to conventional antibiotics. In this work, the antimicrobial peptide, GWH1, was N-terminally fused to two different scaffold proteins, namely, GFP and IFN-γ for its bacterial production in the form of such recombinant protein complexes. Protein self-assembling as regular soluble protein nanoparticles was achieved in the case of GWH1-GFP, while oligomerization into bacterial inclusion bodies was reached in both constructions. Among all these types of therapeutic proteins, protein nanoparticles of GWH1-GFP showed the highest bactericidal effect in an in vitro assay against *Escherichia coli*, whereas non-oligomerized GWH1-GFP and GWH1-IFN-γ only displayed a moderate bactericidal activity. These results indicate that the biological activity of GWH1 is specifically enhanced in the form of regular multi-display configurations. Those in vitro observations were fully validated against a bacterial infection using a mouse mastitis model, in which the GWH1-GFP soluble nanoparticles were able to effectively reduce bacterial loads.

1. Introduction

Novel antimicrobial and engineering approaches are urgently needed to cope with antibiotic resistance. Antimicrobial peptides (AMPs), a class of naturally occurring small (generally less than 50 amino acids) and positively charged peptides [1], have attracted attention in clinical research because of their broad-spectrum activity against a diverse group of microorganisms, including antibiotic-resistant pathogens [2]. On the other hand, cytokines are a group of small immunomodulatory proteins that play a central role in host defense by orchestrating the antimicrobial functions and conferring greater protection against different infectious agents [3]. One of the most studied cytokines is interferon-gamma (IFN-γ), which has proven to be a potent immunoprophylactic agent [4,5].

However, under physiological conditions, AMPs are subjected to proteolytic degradation and peptide inactivation by nonspecific interactions with anionic substances, which result in the low bioavailability and poor in vivo stability of these small molecules [6]. Furthermore, most cytokines, including IFN-γ, have very short half-lives, so their immunological function is limited [3]. Therefore, the accumulation of these proteins in naturally occurring bacterial inclusion bodies (IBs) and soluble self-assembling protein-only nanoparticles (PNPs) seems an appealing alternative to overcome these limitations. In 2017, Serna et al. described for the first time the use of PNPs as antibacterial agents [7]. These soluble PNPs were obtained following a modular protein design based on the fusion of a cationic peptide to a C-terminal his-tagged scaffold protein [8]. This modular configuration was presented as a transversal platform which has been replicated with several scaffold proteins [9,10]. The cationic α-helical GWH1 antimicrobial peptide [11], once fused to the amino terminus of green fluorescent protein (GFP), promoted the oligomerization in PNPs of around 50 nm size which showed a wide bactericidal effect against different pathogenic bacteria in cell cultures [7]. Due to the functional and structural versatility of this system, we wondered whether the fusion design between GWH1 and IFN-γ could also lead to the formation of these highly stable nanosized oligomers (PNPs). Besides, bacterial IBs, once considered as waste by-products derived from recombinant protein production, now provide a useful source of ready-to-use active protein. Inside these structures, therapeutic proteins are stored in native and native-like conformations and are released under physiological conditions [12–14]. The benefits of this system lie in the protective effect against degradation and the sustained release of the protein, which in both cases can significantly increase their half-lives.

The aim of the present study is to characterize and to evaluate, in an in vivo mastitis mice model, the direct and non-direct antibacterial effects of two different protein designs (GWH1-GFP and GWH1-IFN-γ) assembled in two protein formats, namely, PNPs and IBs. Furthermore, we wanted to test the synergy of both activities, immunomodulation and bactericidal effect, in a single polypeptide with the potential to form PNPs. The results obtained here could throw some light on the development of new protein-based mastitis therapies but with transversal applicability in any clinical problem needing unconventional antimicrobial therapies.

2. Materials and Methods

2.1. Protein Design and Production

All DNA sequences (GWH1-GFP, GWH1-IFN-γ, IFN-γ and GFP) were codon optimized (*Escherichia coli*), synthetized and cloned in pET22b plasmids by GeneArt (Waltham, MA, USA). IFN-γ from mouse origin was selected in sequence designs due to the species-specific nature of this protein. *E. coli* BL21 (DE3) (Novagen, Madison, WI, USA) was chosen as expression host. Protein production was performed in 2 L volume flasks containing 500 mL of LB medium with 100 μg/mL ampicillin (plasmid resistance). Cells were incubated at 37 °C until the culture reached an optical density of around 0.5, at this point 0.1 mmol/L of isopropyl β-D-1-thiogalactopyranoside (IPTG) was added to each culture and expression temperature was set at 20 °C for 5 h. For IBs, production times were established for 3 h at 37 °C. Cells were harvested by centrifugation (20 min, 5000 rpm) and stored at −80 °C.

2.2. Protein Purification

For soluble protein, purification procedures were performed as described before [9], with some modifications. The cell pellet was resuspended in wash buffer (Tris 20 mmol/L, pH 8.0, NaCl 500 mmol/L, imidazole 10 mmol/L) with DNase (1 mg/mL) (Thermo-Scientific, Waltham, MA, USA) and ethylenediamine tetra-acetic acid-free protease-inhibitor (complete EDTA-Free, F. Hoffmann-La Roche AG, Basel, Switzerland). French press was selected as disruption method for cell lysis (3 rounds at 1200 psi). The protein amount was quantified by Bradford, aliquoted and stored at $-80\ ^{\circ}$C for further experiments. A schematic representation of the different types of bioactive materials obtained after protein purification is outlined in Scheme 1. Purified recombinant protein from the soluble cell fraction by affinity chromatography generated two types of protein samples depending on macromolecular organization (unassembled and assembled proteins (PNPs)). Purified proteins were stored in sodium bicarbonate buffer containing 166 mmol/L NaHCO$_3$ and 333 mmol/L NaCl. Bacterial IBs were purified and quantified as described earlier [15]. An additional step of French Press disruption (3 rounds at 1200 psi) was included at the beginning of the process. Sterile conditions were maintained throughout the process. Pelleted IBs were resuspended in sodium bicarbonate buffer prior to its use. Purification productivity of analyzed recombinant proteins as well as protein solubility is detailed in Supplementary Table S1.
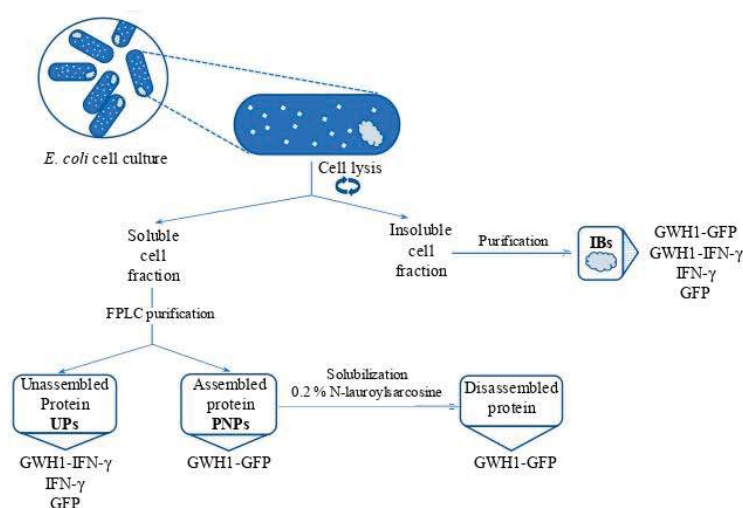
Scheme 1. Schematic representation of the protein formats used through the study. During protein production, recombinant protein was accumulated inside *E. coli* cells as insoluble aggregates (inclusion bodies—IBs) or in a soluble state. After cell lysis and centrifugation, IBs were recovered from the cell debris. Supernatant was used for soluble protein purification purposes. Positive protein peaks were analyzed by dynamic light scattering (DLS) and protein samples were categorized as unassembled protein versions or assembled protein versions. Assembled protein GWH1-GFP was transformed into disassembled protein by incubation with mild detergent. The names of the protein samples used in the mastitis mice model are labeled beside or below the protein versions enclosed in a light blue box.

2.3. Nanoparticle Size Characterization

Size distribution of protein samples was determined by dynamic light scattering (DLS). Average values were obtained after the independent measurement of protein samples in triplicates at 633 nm in a Zetasizer Nano ZS (Malvern Instruments Ltd., Malvern, UK). Nanoscale morphological characterization of isolated IBs was performed with two high resolution electron microscopy techniques adapted to this type of biomaterial [16–23]. Sample preparation for the field emission scanning electron microscope (FESEM) observation was described previously [12]. Pellets of the same four isolated

IBs were processed following conventional transmission electron microscopy (TEM) procedures as previously described [16,17].

2.4. Bactericidal Activity Assay

The effect of the different antimicrobial candidates was evaluated against *E. coli* ATCC 25922 and *Staphylococcus aureus* ATCC 29737. The assay was performed using a broth micro-dilution method. In 96-well plates, after a two-fold dilution process in 50 μL, each well contained a specific amount of the corresponding protein, ranging from 6 to 0.4 μmol/L. After protein distribution, 50 μL of Mueller Hinton Broth Cation-adjusted medium (MHB-II, Sigma-Aldrich, Saint Louis, MO, USA) containing 10^6 CFU/mL (colony forming units per mL) of *E. coli* or *S. aureus* was inoculated in each well. Maximal growth was achieved in control wells with no protein. Each concentration was evaluated in duplicates. After microorganism inoculation, the 96-well plates were gently agitated and then incubated without agitation at 37 °C for 18 h. Bacterial viability was evaluated using the commercially available BacTiter-Glo™ Microbial Cell Viability Assay (Promega, Madison, WI, USA) following the manufacturer's instructions. Luminescence was measured using the Multilabel Plater Reader VICTOR3 (PerkinElmer, Waltham, MA, USA).

2.5. Disassembling of Soluble Nanoparticles

GWH1-GFP PNPs were disassembled after the addition of the mild-solubilization agent N-lauroylsarcosine 0.2% (Sigma-Aldrich, Saint Louis, MO, USA) (see Scheme 1). The disassembling process was evaluated by DLS at 633 nm in a Zetasizer Nano ZS (Malvern Instruments Ltd., Malvern, UK). Bactericidal activity of assembled and disassembled GWH1-GFP proteins was evaluated as described in Section 2.4, apart from the protein concentration range, that in this case ranged from 0.5 to 8 μmol/L.

2.6. Protein Solubilization from IBs

The different protein IBs (GWH1-GFP, GWH1-IFN-γ, IFN-γ and GFP) were resuspended in 250 μL of sodium bicarbonate buffer. The conditions for solubilization were established at 37 °C for 18 h with agitation. After the incubation, the solubilized protein in the supernatant was recovered by centrifugation (15 min, 15,000× *g*). Size distribution of the solubilized protein was evaluated by DLS and the amount of protein released from the IBs was determined by Western blot, as detailed [12].

2.7. Determination of Murine IFN-γ Biological Activity

The procedure for the activity evaluation of IFN-γ was adapted from a nitric oxide (NO)-based bioassay [24]. Detailed modifications are described as follows. Serial dilutions of the different IFN-γ constructs (commercial *E. coli*-derived murine IFN-γ (R&D systems, Minneapolis, MN, USA), recombinant in-house murine IFN-γ and GWH1-IFN-γ) at quantities ranging from 6 to 120 nmol/L were incubated with murine microglial cells (BV-2) for 48 h at 37 °C. No protein was added in control wells. To study the specificity of the NO response, a specific concentration (120 nmol/L) of a commercial recombinant mouse IFN-γ was evaluated in the absence and presence of 500 μmol/L L-NMA (Sigma-Aldrich, Sant Louis, MO, USA), an inhibitor of nitric oxide synthase (i-NOS).

2.8. Mouse Model of Infectious Mastitis

The mouse mastitis model was previously described [25–27]. CD-1 lactating micewere used. Experiment specifications are briefly reported here. A total of 100 μL of bacteria (100 CFUs of either *E. coli* ATCC 25922 or *S. aureus* ATCC 29737) and 100 μL of the corresponding protein compound (assembled PNPs, unassembled soluble protein or IBs) were administered in each mammary gland pair. A minimum of three mice (6 mammary glands) were employed to test each protein compound. Protein concentrations in all cases were adjusted to 60 μmol/L after dilution (unassembled versions

and PNPs) or resuspension (IBs) with sodium bicarbonate buffer with salt. In experimental controls, 100 μL of sodium bicarbonate buffer with salt was administered instead of the protein-containing solutions. At relevant time points post-inoculation (6, 12 and 24 h for kinetics growth studies and 8 h for compound efficacy studies), mice were sedated and euthanized. Bacterial CFU contained in samples were evaluated by plating serial dilutions of gland homogenates on tryptic soy agar (TSA) plates and raw CFU counts converted into base 10 logarithm values. The animal experiments were performed in accordance with the guidelines of the Canadian Council on Animal Care and approved by the ethics committee on animal experimentation of the Faculté des Sciences of Université de Sherbrooke (protocol 2017–1966 FM2017-01B).

2.9. Statistical Analysis

All statistical analyses were conducted in GraphPad Prism version 8.0.0 for Windows (GraphPad Software, San Diego, CA, USA) with at least three independent replicates unless otherwise indicated. Bars in figures are expressed as mean ± standard deviation. Quantitative data were tested for normality and equality of variances with Kolmogorov–Smirnov and Levene tests, respectively, prior to analyses. Depending on the experiment, statistical divergences were evaluated using one-way ANOVA with Tukey's multiple comparisons test or two-tailed unpaired Student's *t* test. Statistical significance in relevant results is indicated in figures as $* p < 0.05$, $** p < 0.01$, and $*** p < 0.001$.

3. Results

3.1. Characterization of Self-Assembling Nanoparticles

In the modular protein designs, GWH1 was N-terminally fused to two different his-tagged protein scaffolds (Figure 1A), namely, the previously reported GWH1-GFP [7] and the new design, GWH1-IFN-γ. After purification of recombinant proteins accumulated in the soluble cell fraction, high purity was reached with all protein designs (Figure 1(B1)). Self-assembling of monomers into soluble protein nanoparticles (PNPs) is driven by the fusion of a cationic peptide (GWH1) with His6-tagged scaffolds [10]. However, under the tested experimental conditions, protein oligomerization in soluble PNPs was only achieved with GWH1-GFP (Figure 1D) as previously described [7]. In DLS analysis, the peak size for this oligomer was around 35 nm. The high polydispersity showed by the sample could indicate the presence of a diverse mixture of PNPs with different oligomeric states (Figure 1D). Modular protein GWH1-IFN-γ showed an average size of around 10 nm (Figure 1D). When compared to IFN-γ, only a slight difference in size was observed, suggesting that protein oligomerization was not achieved with this fusion protein design. As expected, GFP and IFN-γ did not form PNPs (Figure 1D).

3.2. In Vitro Evaluation of Antibacterial Activity

The antimicrobial potential of soluble GWH1-GFP (PNPs) and soluble GWH1-IFN-γ (unassembled protein (UP) forms) was evaluated in an in vitro assay against two of the most common pathogens involved in mastitis, *S. aureus* and *E. coli*. GFP and IFN-γ were used as controls for their antimicrobial peptide carrier counterparts. GWH1-GFP showed a dose-dependent antibacterial activity against *E. coli* reducing cell viability by up to 90% (Figure 2A). On the other hand, GWH1-IFN-γ UPs did not follow the same pattern, only showing antibacterial activity at the highest concentration, reducing bacterial viability by 40%. As expected, GFP and IFN-γ had no significant effect on cell viability (Figure 2A). On *S. aureus*, a dose-dependent pattern was observed again with GWH1-GFP PNPs (Figure 2B). However, its effect on cell viability was not as pronounced as that observed with *E. coli*. GWH1-IFN-γ UPs had a similar effect, reducing cell viability by 40% at the highest concentration. Control proteins, GFP and IFN-γ, showed an unspecific effect on cell viability, reducing bacterial loads to the same extent as that observed for the GWH1 carrier versions (Figure 2B).
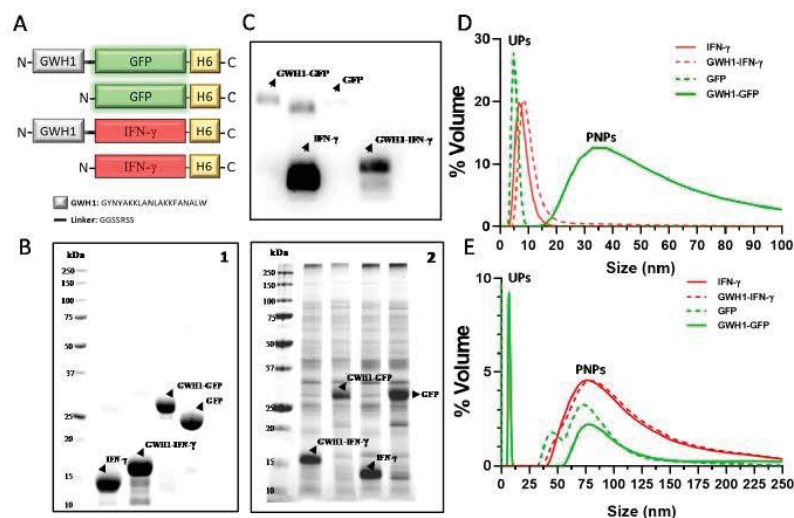
Figure 1. Characterization of the different protein formats employed in this study. (**A**) Schematic representation of multimeric fusion proteins. The presence of a cationic peptide (GWH1) in the N-terminus, plus the His6 tag in C-terminus, may induce the formation of protein-only nanoparticles (PNPs). A linker between GWH1 and the scaffold protein was added in order to increase flexibility and facilitate self-assembling process. (**B**) TGX Stain-free^TM analysis showing the purity of the different protein designs in both, soluble proteins (**B1**) and IBs (**B2**). (**C**) Western blot showing the qualitative amount of protein released from the different IBs. (**D**) Evaluation of self-assembling capabilities of purified soluble proteins by size determination using DLS. PNPs: protein nanoparticles; UPs: unassembled proteins. (**E**) Size distribution of the protein samples obtained after solubilization from different IBs analyzed by DLS.
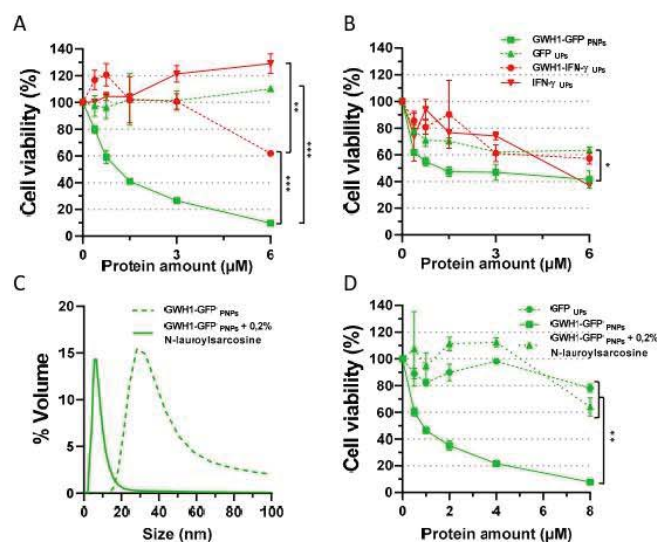

Figure 2. Antimicrobial activity of assembled (PNPs) and unassembled soluble proteins (UPs) in vitro. (**A**) Effect on cell viability of increasing amounts of GWH1-GFP and GWH1-IFN-γ against *E. coli* and (**B**) *S. aureus* (**C**). Dynamic light scattering (DLS) analysis showing the nanoparticle disassembling of GWH1-GFP in presence of 0.2% N-lauroylsarcosine. (**D**) Comparative effect on cell viability of disassembled (promoted in presence of 0.2% N-lauroylsarcosine) and assembled GWH1-GFP against *E. coli* in vitro. IFN-γ and GFP were used as controls. Significant results are shown as * $p \leq 0.05$, ** $p \leq 0.01$ and *** $p \leq 0.001$, multiple *t* test. All experiments were performed in duplicates. Bars represent the the mean ± standard deviation.

3.3. Importance of Nanoparticle Format on Antibacterial Activity

Given that the nanoparticulated format seems to properly display the antimicrobial activity, the PNPs formed by GWH1-GFP were incubated with a mild solubilization agent (N-lauroylsarcosine) in order to disassemble the oligomeric format while preserving the native-like protein structure [28]. The presence of monomers of 5 nm size after achieving the final concentration of 0.2% N-lauroylsarcosine was observed by DLS (Figure 2C). In *E. coli*, the monomeric version of GWH1-GFP lacked the dose-dependent antimicrobial behavior showed by the PNP version, only acting at the highest concentration by reducing cell viability by 40%, a low antimicrobial effect compared with its fully active version, which reduced viability by more than 90% (Figure 2D).

3.4. Bioactivity Evaluation of IFN-γ-Based Proteins

The measurement of nitric oxide (NO) produced by the murine microglial cell line BV-2, in the presence of IFN-γ, provides a simple method for detection of bioactive mouse IFN-γ. The use of a selective inhibitor of iNOS, NG-monomethyl-L-arginine (L-NMA) allows one to evaluate the specificity of the response. An inhibition in the NO production by BV-2 cells was observed when L-NMA was added in the presence of commercial mouse IFN-γ (Figure 3A). The activity of the two mouse IFN-γ designs (IFN-γ and GWH1-IFN-γ UPs) was compared to a standard calibrated mouse IFN-γ. BV-2 cells produced nitrite in a dose-dependent manner in response to IFN-γ at protein concentrations between 6 and 120 nmol/L. The biological activity of the standard mouse IFN-γ was significantly higher than that of the recombinant IFN-γ produced in this study. Surprisingly, GWH1-IFN-γ UPs did not show any response in that range of concentrations, while recombinant in-house INF-γ was effective from 12 nmol/L (Figure 3B).
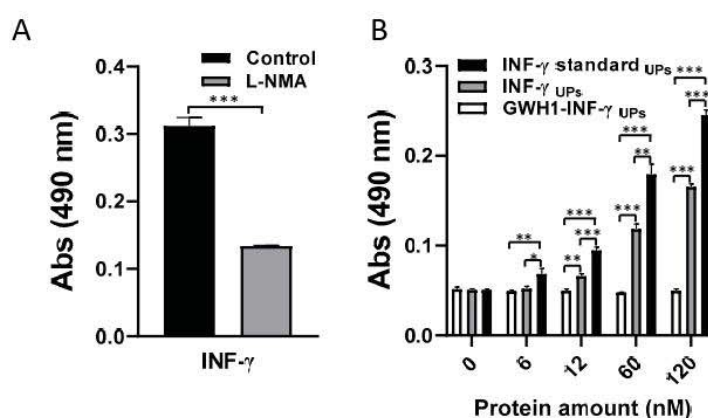

Figure 3. Nitric oxide (NO)-based bioassay for mouse IFN-γ activity evaluation in the murine microglial cell line BV-2. (**A**) Inhibitory effect of L-NMA (NG-monomethyl-L-arginine) on nitric oxide production by BV-2 in presence of a commercial recombinant mouse IFN-γ (120 nmol/L). Significant results are shown as *** $p \leq 0.001$, unpaired Student's *t* test. (**B**) Nitric oxide production (measured by its absorbance at 490 nm) for increasing amounts of the different IFN-γ-based constructs using, as standard, a commercial recombinant mouse IFN-γ. Significant results are shown as * $p \leq 0.05$, ** $p \leq 0.01$ and *** $p \leq 0.001$, multiple *t* test. All experiments were performed in triplicates and data are represented as mean ± standard deviation.

3.5. Growth Kinetics of E. coli in the Mastitis Mice Model

The intramammary infection (IMI) was monitored in a time course experiment (Figure 4). The medians of bacterial loads were 1.2×10^5 CFU, 3.8×10^7 CFU and 7.8×10^9 CFU per g of gland after 6, 12 and 24 h, respectively. Results demonstrated a steady growth and since higher bacterial loads

affected the general health of the animals, an infection time of 8 h was selected as the experimental condition for therapeutic efficacy studies.
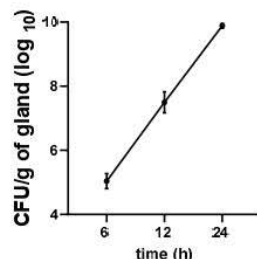
Figure 4. Growth kinetics of *E. coli* in the mouse mammary gland at 6, 12 and 24 h after the administration of 100 CFU through the teat channel. The bacterial loads for each time point were evaluated in 8 individual mammary glands (4 mice). Bars represent the mean ± standard deviation.
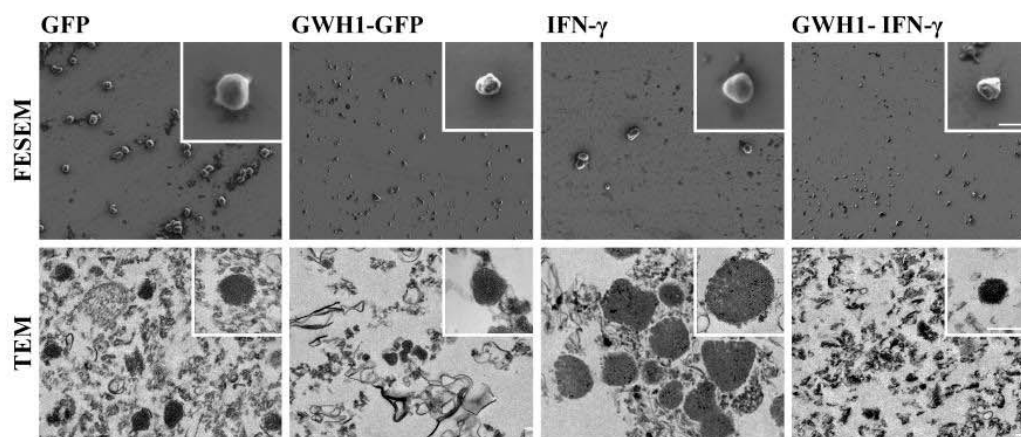
3.6. Characterization of IBs

Recombinant protein production in bacteria induces the formation of discrete protein clusters usually located at the cellular poles. These supramolecular complexes, known as IBs, contain functional recombinant protein. Released recombinant proteins tend to co-purify with other cellular proteins using IBs purification methods. In any case, in this study, a representative amount of the produced recombinant protein was observed in all cases (Figure 1(B2)). IFN-γ IBs showed the best releasing efficiency, being the amount of protein observed qualitatively different from the other candidates (Figure 1C). On the other hand, just a faint band was observed for GFP-based proteins, indicating a poor releasing process (Figure 1C). The size distribution of the solubilized protein was also evaluated (Figure 1E). Although soluble aggregates were mainly released from all protein designs, only GWH1-GFP included a monomeric distribution, which indicated the presence of two populations of different sizes. The ultrastructural characteristics of the IBs were analyzed by electronic microscopy (EM) (Figure 5). The results showed the presence of round-shaped IBs with a similar electrodensity in all samples but with marked differences between GWH1-based IBs and the GWH1-free (IFN-γ and GFP) IBs (Figure 5). Interestingly, in *E. coli*, IFN-γ formed a high amount of IBs with similar size and shape than GFP IBs. Conversely, GWH1-GFP and GWH1-IFN-γ IBs showed a shape–size distribution completely different from those observed for the well-formed GFP IBs. In addition, a high variability in size can be observed between these samples, suggesting the presence of not completely formed IBs (Figure 5).

3.7. Therapeutic Effect of PNPs and IBs in the Mouse Mastitis Model

A single dose of 60 µmol/L of each different protein design, in both soluble (UPs or PNPs) and insoluble (IBs) formats, was administered just after the intramammary inoculation of *E. coli*. The soluble PNPs of GWH1-GFP and the soluble UP versions of IFN-γ and GWH1-IFN-γ provoked a significant decrease in bacterial loads in comparison to both the control (sodium bicarbonate buffer) or GFP treatments (Figure 6A). The presence of GFP had, however, some negative effect on *E. coli* growth (Figure 6A). IFN-γ and GWH1-IFN-γ UPs caused a decrease in bacterial loads by 2.8 and 2 times greater than that caused by GFP, respectively. Nevertheless, the strongest bactericidal effect was obtained by the nanoparticle-forming protein GWH1-GFP, which decreased the bacterial loads by 35 times in comparison to the control treatment and by 11.5 times compared with the GWH1-free GFP. On the other hand, the same protein designs produced as IBs showed a different outcome (Figure 6B). The GFP IBs had a similar effect on bacterial loads than that observed for GFP UPs. Surprisingly, IFN-γ IBs showed a significant effect, diminishing bacterial loads by almost 6 times when compared to GFP IBs and by 11 times compared to the control. The IB format for the GWH1 carrier proteins, GWH1-IFN-γ and GWH1-GFP, showed a significant effect over bacterial loads in control glands, causing a decrease

of 6.4 and 5.2 times, respectively. However, for these two samples only a numerically decrease in bacterial loads by 3.2 and 2.7 times in comparison to GFP IBs was observed, respectively.


Figure 5. Ultrastructural characterization and analysis by electronic microscopy of purified inclusion bodies. Representative images of general fields and nanoparticle detail of entire IBs of GFP, GWH1-GFP, IFN-γ and GWH1-IFN-γ at two different magnifications, 11,000×/150,000× (FESEM) and 3000×/10,000× (TEM). Magnifications are equivalent in each micrograph to allow comparative visualization. The scale bars represent 500 nm.
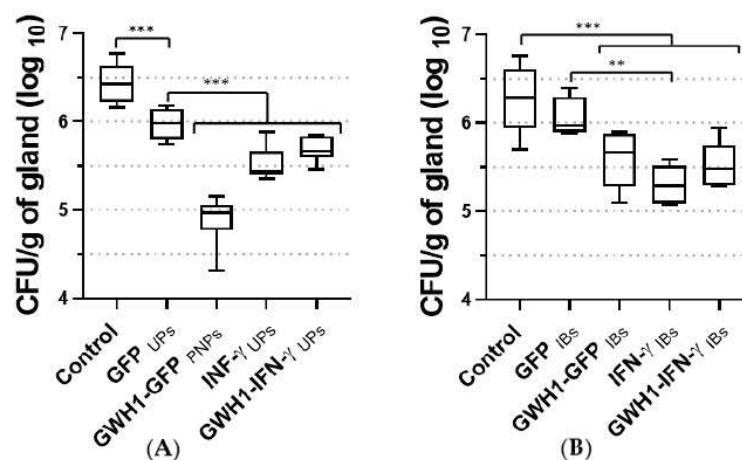
Figure 6. Bacterial loads (*E. coli* CFU/g of gland log10) measured after the administration of therapeutic and non-therapeutic protein formats into infected mammary glands. (**A**) Effect of unassembled protein forms (UPs) and assembled protein-only nanoparticles (PNPs) 8 h after the challenge with 100 CFU of *E. coli*. (**B**) Effect of the inclusion body (IB) format 8 h after the challenge with 100 CFU of *E. coli*. In all cases, 60 µM of the different protein formats were administered just after the infection with *E. coli*. Sodium bicarbonate buffer (166 mmol/L $NaHCO_3$, 333 mmol/L NaCl) and GFP were used as controls. The middle bars indicate median values for each group of glands (at least 6 glands) whereas the boxes specify quartiles Q1-Q3. Experiments were performed with at least three independent replicates. Significant results are shown as ** $p \leq 0.01$ and *** $p \leq 0.001$, one-way analysis of variance (ANOVA) followed by Tukey's multiple comparisons test.

The performance of the GWH1-GFP construct forming PNPs prompted us to expand our in vivo study in *S. aureus*-challenged mice. In that case, GWH1-GFP PNPs caused a significant decrease in bacterial loads, showing 3.3 times less bacteria within the glands than the control (Figure 7).

However, there was no difference when compared to the GFP UPs treatment, which also reduced *S. aureus* colonization.
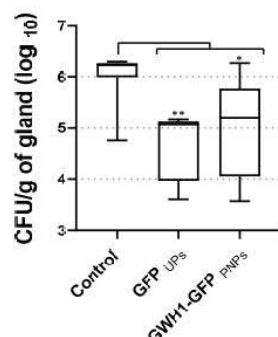
Figure 7. Antimicrobial effect of GFP and GWH1-GFP (PNPs) over *S. aureus*-infected mammary glands in vivo. Mammary glands were harvested and processed 8 h after the simultaneous administration of 100 CFU of *S. aureus* and 60 μmol/L of protein, respectively. Sodium bicarbonate buffer (166 mmol/L $NaHCO_3$, 333 mmol/L NaCl) was used as control. The middle bars indicate median values for each group of glands (at least 6 glands) whereas the boxes specify quartiles Q1-Q3. The experiment was performed in triplicates. Significant results are shown as * $p \leq 0.05$, ** $p \leq 0.01$, one-way analysis of variance (ANOVA), followed by Tukey's multiple comparisons test.

4. Discussion

Novel therapies are urgently needed to tackle the reduced cure rates related to the development of bacterial resistance [29]. One alternative includes the use of alpha-helical AMPs [30]. However, large-scale production of synthetic small peptides is challenging [31] and recombinant protein production in prokaryotic host is presented here as a promising alternative. Several experimental strategies have been explored to cope with the inherent toxicity of such peptides, when recombinantly produced, towards the prokaryotic host, including the fusion to partner proteins that seem to mask the antimicrobial activity [32–34], as well as the accumulation in the insoluble cell fraction of AMPs fused to scaffold proteins [35]. In any case, regardless of the mechanism of action of alpha-helical AMPs against microorganisms, the recombinant production of these peptides might be achieved by the neutralization of their net charge by fusion to solubility-enhancing proteins [36–38] or by enhancing formation of IBs in producing cells by the fusion to aggregation-prone proteins [39].

In the present work, we have designed GWH1-containing recombinant proteins, with the idea of building bifunctional molecules where each individual part of the recombinant fusion design could maintain its original function, and at the same time, act as a building block for protein self-assembling [8,10]. In that sense, it has been demonstrated that GFP, toxins and pro-apoptotic proteins are able to act as scaffold partners for protein self-assembling while retaining their biological activity [9,40]. Protein production was affected by the expression of these AMP carrying proteins. The addition of GWH1 provoked a drastic decrease in protein yields in comparison to the non-AMP-containing counterparts, see Supplementary Table S1. However, proteins were produced in enough amounts to allow an effective purification process. Still, in the tested conditions, GWH1-IFN-γ arrangement was unable to promote the formation of soluble PNPs (Figure 1D), suggesting the inability of the mouse IFN-γ to act as a scaffold domain for protein oligomerization. Mature mouse IFN-γ forms noncovalently linked homodimers of 20–25 kDa [41]. The formation of dimers in both, IFN-γ and GWH1-IFN-γ could explain the bigger sizes observed by DLS and the bigger size of GWH1-IFN-γ over IFN-γ due to the presence of the GWH1 peptide. Moreover, the N-terminal addition of the GWH1 antimicrobial peptide has somehow diminished or truncated the mouse IFN-γ functionality as observed when comparing the activity of the IFN-γ and GWH1-IFN-γ proteins (Figure 3B). This fact is not surprising, since there is evidence that the N-terminus region of mouse IFN-γ plays an important

role in receptor binding. Therefore, the failure to bind prevents internalization and later events that result in the induction of the immune response [42,43].

Surprisingly, antimicrobial performance of GWH1-containing proteins in different hosts, showed an inhibitory activity against *E. coli*, whereas *S. aureus* was more resistant to the treatment (Figure 2A,B). The different membrane composition may influence the mechanism of action of α-helical AMPs, especially for Gram-negative and Gram-positive bacteria [44]. In this sense, the GWH1 constructs produced in this work, not only have displayed a preferred antimicrobial activity against the Gram-negative *E. coli*, but, most importantly, the antimicrobial performance in this microorganism was enhanced when the GWH1-fusion proteins formed nanoparticles (Figure 2A). The main mechanism of action of AMPs is membrane permeabilization and structural disruption. To achieve the antimicrobial effect, a minimal AMP concentration is required in the target surface. Such characteristic is described as the threshold concentration [45] and is experimentally expressed as the peptide-to-lipid ratio (P/L). The propensity of GWH1-GFP to self-assemble in multimeric complexes could enhance the proximity of effective monomeric units on cell surface, diminishing the local peptide concentration required to reach higher P/L values. As the P/L ratio increases, the peptides start to insert and traverse the membrane. AMP monomeric forms require higher concentrations to achieve threshold concentrations. This was demonstrated in the case of the monomeric GWH1-GFP, which lacked a dose-dependent antimicrobial activity, only showing antimicrobial effect at the highest concentration, suggesting the need to reach a critical concentration in order to display its activity (Figure 2D). A similar result was observed with the unassembled GWH1-IFN-γ (Figure 2A). The presented evidence validates the multimeric format as a more effective arrangement than the monomeric format, when it comes to antimicrobial activity.

In order to explore the influence of the multiple display configuration of AMPs in the in vivo settings, we analyzed the performance of the engineered protein nanoparticles in a mouse mastitis model. Infectious mastitis is one of the most relevant diseases in dairy cattle, and antibiotic usage is the leading strategy for its treatment and prevention, since this disease is the costliest for dairy producers [46]. Despite the high antimicrobial activity showed by the multimeric format of GWH1-GFP, in vitro assays do not always correlate with in vivo efficacies inside the mammary gland [47,48]. Various aspects are influenced by the complex milk environment [25], and, therefore, a proof of concept in vivo approach is necessary. To date, different studies have used mouse models to assess the effect of antimicrobials [48–51]. However, most of these studies were dedicated to the Gram-positive pathogen *S. aureus* [25] and only few of them characterized the efficacy of antimicrobial agents on other relevant mastitis-causing pathogens such as *E. coli* [52,53]. To the best of our knowledge, this is the first study in which the antimicrobial capacity of AMP-containing nanoparticles has been determined in an in vivo mouse mastitis model of *E. coli* infection. Based on the in vitro assays for GWH1-GFP PNPs, a single dose of 60 μmol/L, i.e., ten times the MIC measured in vitro for GWH1-GFP in *E. coli* (Figure 2A), was selected for the intramammary administration after the bacterial challenge. As a result, the GWH1-GFP PNPs further reduced by 1-Log the bacterial burden in glands when compared with the non-AMP-containing counterpart, GFP (Figure 6A). This difference can be explained by the presence of the GWH1 antimicrobial peptide, which validates the functionality of this format in the milk environment and its efficacy as a promising anti-mastitis candidate. However, in *S. aureus* challenged animals, GWH1-GFP PNPs reduced bacterial load at the same level as control GFP (UPs) (Figure 7). In accordance with this, antimicrobial activity of GWHI-GFP PNPs in in vitro experiments against *S. aureus* was lower than that observed against *E. coli* (Figure 2A). As previously mentioned, the differences in the structure and physical properties of the bacterial membrane might account for the dissimilar activity of the same AMP in Gram-negative and Gram-positive bacteria [54]. On the other hand, in *E. coli*, GWH1-IFN-γUPs were not as effective as GWH1-GFP PNPs (Figure 6A), which supports the idea that the multimeric format is of utmost significance for reducing the local concentration of AMP necessary to achieve a deleterious membrane disruption, and, consequently, to increase the efficacy of the compound.

The IB format provides a protective environment against short-time degradation and a sustainable release of recombinant protein that may improve the effect over time [55–57]. However, as it has been described before [12], the amount of protein that can be released from IBs can vary depending on the IB-forming protein and the used experimental conditions during protein production process [58]. All this, associated with the fact that IFN-γ IBs have previously demonstrate activity, even at higher level than the soluble counterpart [12], urged us to test the efficacy of this format in an in vivo approach. The antimicrobial efficacy for GWH1-GFP IBs was partially reduced, showing a more disperse pattern which was not significant when compared to GFP IBs. This observation could be in accordance with the studied characteristics of GWH1-GFP IBs. The low availability of protein due to the poor release (Figure 1C) associated with the fact that part of the released protein can be found in a monomeric state (Figure 1E), which has been demonstrated here whereby bactericidal activity is reduced, may explain the low efficacy of this format in terms of antimicrobial activity. GWH1-IFN-γ and IFN-γ IBs slightly reduced the bacterial burden, being this latter statistically significant when compared to GFP IBs. This behavior could be associated with the increased release showed by both protein designs from IBs, especially for IFN-γ IBs (Figure 1C). Additionally, it is well known that IFN-γ has a very short half-life and therefore its immunological function in the mammary gland is limited [3]. The protective behavior provided by this oligomeric format may enhance its stability and merits further research. In fact, previous results showed that the activity of IFN-γ is preserved in protein released from IBs after a 96 h incubation at 37 °C [12]. The cytokine embedded in IBs could be less sensitive towards proteolytic degradation, which could then result in a better immunological performance inside the mammary gland. In fact, in the in vivo assays, the activity of the proteins containing IFN-γ displayed a higher activity when administered in IB format.

Altogether, the results presented in this work show a better antimicrobial performance of the multimeric AMP format against the monomeric configuration, and, most importantly, provided significant data for considering the AMP-containing nanoparticles as a promising alternative for treatment of mastitis. However, it should be noted that efficacy studies in mice should only be considered as an intermediate proxy to predict efficacy in dairy cows [51]. Overall, the versatility of the nanoparticle self-assembling format provides a valuable tool for testing a diversity of AMP with different scaffold proteins that could generate possible synergies or provide antimicrobial activity against other pathogens of interest.

5. Conclusions

The extensive use of antibiotics for the treatment and prevention of bacterial infections increases the selective pressure for appearance of resistant bacteria. Previously, we have described the antimicrobial activity of peptides fused to a scaffold protein and displayed in various copies on soluble PNPs. We have also analyzed the potential of naturally occurring protein supramolecular complexes, in particular IBs, to release biologically active soluble protein nanoparticles in in vivo approaches. In this work, we explored the relevance of the oligomeric state of antimicrobial peptides in such protein nanoparticles and studied their efficiency in vitro and in vivo against different mastitis causing pathogens. The results presented here indicate the potential of multiple displays of peptides in protein nanoparticles for the development of novel antimicrobial peptide-based formulations.

References

1. Ciumac, D.; Gong, H.; Hu, X.; Lu, J.R. Membrane targeting cationic antimicrobial peptides. *J. Colloid Interface Sci.* **2019**, *537*, 163–185. [CrossRef] [PubMed]
2. Seo, M.D.; Won, H.S.; Kim, J.H.; Mishig-Ochir, T.; Lee, B.J. Antimicrobial peptides for therapeutic applications: A review. *Molecules* **2012**, *17*, 12276–12286. [CrossRef] [PubMed]
3. Aitken, S.L.; Corl, C.M.; Sordillo, L.M. Immunopathology of mastitis: Insights into disease recognition and resolution. *J. Mammary Gland Biol. Neoplasia* **2011**, *16*, 291–304. [CrossRef] [PubMed]
4. Sordillo, L.M.; Babiuk, L.A. Controlling acute *Escherichia coli* mastitis during the periparturient period with recombinant bovine interferon gamma. *Vet. Microbiol.* **1991**, *28*, 189–198. [CrossRef]
5. Pighetti, G.; Sordillo, L. Specific immune responses of dairy cattle after primary inoculation with recombinant bovine interferon-gamma as an adjuvant when vaccinating against mastitis. *Am. J. Vet. Res.* **1996**, *57*, 819–824.
6. Lei, R.; Hou, J.; Chen, Q.; Yuan, W.; Cheng, B.; Sun, Y.; Jin, Y.; Ge, L.; Ben-Sasson, S.A.; Chen, J.; et al. Self-assembling myristoylated human α-defensin 5 as a next-generation nanobiotics potentiates therapeutic efficacy in bacterial infection. *ACS Nano* **2018**, *12*, 5284–5296. [CrossRef]
7. Serna, N.; Sánchez-García, L.; Sánchez-Chardi, A.; Unzueta, U.; Roldán, M.; Mangues, R.; Vázquez, E.; Villaverde, A. Protein-only, antimicrobial peptide-containing recombinant nanoparticles with inherent built-in antibacterial activity. *Acta Biomater.* **2017**, *60*, 256–263. [CrossRef] [PubMed]
8. Serna, N.; Céspedes, M.V.; Saccardo, P.; Xu, Z.; Unzueta, U.; Álamo, P.; Pesarrodona, M.; Sánchez-Chardi, A.; Roldán, M.; Mangues, R.; et al. Rational engineering of single-chain polypeptides into protein-only, BBB-targeted nanoparticles. *Nanomed. Nanotechnol. Biol. Med.* **2016**, *12*, 1241–1251. [CrossRef] [PubMed]
9. Serna, N.; Céspedes, M.V.; Sánchez-García, L.; Unzueta, U.; Sala, R.; Sánchez-Chardi, A.; Cortés, F.; Ferrer-Miralles, N.; Mangues, R.; Vázquez, E.; et al. Peptide-based nanostructured materials with intrinsic proapoptotic activities in CXCR4+ solid tumors. *Adv. Funct. Mater.* **2017**, *27*, 1–9. [CrossRef]
10. Unzueta, U.; Ferrer-Miralles, N.; Cedano, J.; Zikung, X.; Pesarrodona, M.; Saccardo, P.; García-Fruitós, E.; Domingo-Espín, J.; Kumar, P.; Gupta, K.C.; et al. Non-amyloidogenic peptide tags for the regulatable self-assembling of protein-only nanoparticles. *Biomaterials* **2012**, *33*, 8714–8722. [CrossRef]
11. Chou, H.; Kuo, T.; Chiang, J.; Pei, M.; Yang, W.; Yu, H.; Lin, S.; Chen, W. Design and synthesis of cationic antimicrobial peptides with improved activity and selectivity against *Vibrio* spp. *Int. J. Antimicrob. Agents* **2008**, *32*, 130–138. [CrossRef] [PubMed]
12. Carratalá, J.V.; Cano-garrido, O.; Sánchez, J.; Membrado, C.; Pérez, E.; Conchillo-solé, O.; Daura, X.; Sánchez-chardi, A. Aggregation-prone peptides modulate activity of bovine interferon gamma released from naturally occurring protein nanoparticles. *N. Biotechnol.* **2020**, *57*, 11–19. [CrossRef] [PubMed]
13. Pesarrodona, M.; Jauset, T.; Díaz-Riascos, Z.V.; Sánchez-Chardi, A.; Beaulieu, M.-E.; Seras-Franzoso, J.; Sánchez-García, L.; Baltà-Foix, R.; Mancilla, S.; Fernández, Y.; et al. Targeting antitumoral proteins to breast cancer by local administration of functional inclusion bodies. *Adv. Sci.* **2019**, *6*, 1900849. [CrossRef] [PubMed]
14. Céspedes, M.V.; Cano-Garrido, O.; Álamo, P.; Sala, R.; Gallardo, A.; Serna, N.; Falgàs, A.; Voltà-Durán, E.; Casanova, I.; Sánchez-Chardi, A.; et al. Engineering secretory amyloids for remote and highly selective destruction of metastatic foci. *Adv. Mater.* **2020**, *32*, e1907348. [CrossRef] [PubMed]

15. Ferrer-Miralles, N.; Saccardo, P.; Corchero, J.L.; Xu, Z.; García-Fruitós, E. General introduction: Recombinant protein production and purification of insoluble proteins. *Methods Mol. Biol.* **2015**, *1258*, 1–24. [CrossRef] [PubMed]

16. Seras-Franzoso, J.; Sánchez-Chardi, A.; Garcia-Fruitós, E.; Vázquez, E.; Villaverde, A. Cellular uptake and intracellular fate of protein releasing bacterial amyloids in mammalian cells. *Soft Matter* **2016**, *12*, 3451–3460. [CrossRef] [PubMed]

17. Cano-Garrido, O.; Sánchez-Chardi, A.; Parés, S.; Giró, I.; Tatkiewicz, W.I.; Ferrer-Miralles, N.; Ratera, I.; Natalello, A.; Cubarsi, R.; Veciana, J.; et al. Functional protein-based nanomaterial produced in microorganisms recognized as safe: A new platform for biotechnology. *Acta Biomater.* **2016**, *43*, 230–239. [CrossRef]

18. Céspedes, M.V.; Fernández, Y.; Unzueta, U.; Mendoza, R.; Seras-Franzoso, J.; Sánchez-Chardi, A.; Álamo, P.; Toledo-Rubio, V.; Ferrer-Miralles, N.; Vázquez, E.; et al. Bacterial mimetics of endocrine secretory granules as immobilized in vivo depots for functional protein drugs. *Sci. Rep.* **2016**, *6*, 1–10. [CrossRef]

19. Genís, S.; Sánchez-Chardi, A.; Bach, À.; Fàbregas, F.; Arís, A. A combination of lactic acid bacteria regulates *Escherichia coli* infection and inflammation of the bovine endometrium. *J. Dairy Sci.* **2017**, *100*, 479–492. [CrossRef]

20. De Pinho Favaro, M.T.; Sánchez-García, L.; Sánchez-Chardi, A.; Roldán, M.; Unzueta, U.; Serna, N.; Cano-Garrido, O.; Azzoni, A.R.; Ferrer-Miralles, N.; Villaverde, A.; et al. Protein nanoparticles are nontoxic, tuneable cell stressors. *Nanomedicine* **2018**, *13*, 255–268. [CrossRef]

21. Cano-Garrido, O.; Garcia-Fruitós, E.; Villaverde, A.; Sánchez-Chardi, A. Improving Biomaterials Imaging for Nanotechnology: Rapid Methods for Protein Localization at Ultrastructural Level. *Biotechnol. J.* **2018**, *13*, 1–8. [CrossRef]

22. Unzueta, U.; Cespedes, M.V.; Sala, R.; Alamo, P.; Sánchez-Chardi, A.; Pesarrodona, M.; Sánchez-García, L.; Cano-Garrido, O.; Villaverde, A.; Vázquez, E.; et al. Release of targeted protein nanoparticles from functional bacterial amyloids: A death star-like approach. *J. Control. Release* **2018**, *279*, 29–39. [CrossRef] [PubMed]

23. Sánchez, J.M.; López-Laguna, H.; Álamo, P.; Serna, N.; Sánchez-Chardi, A.; Nolan, V.; Cano-Garrido, O.; Casanova, I.; Unzueta, U.; Vazquez, E.; et al. Artificial inclusion bodies for clinical development. *Adv. Sci.* **2019**, *1902420*, 1–7. [CrossRef]

24. Malu, S.; Srinivasan, S.; Maiti, P.K.; Rajagopal, D.; John, B.; Nandi, D. IFN-γ bioassay: Development of a sensitive method by measuring nitric oxide production by peritoneal exudate cells from C57BL/6 mice. *J. Immunol. Methods* **2003**, *272*, 55–65. [CrossRef]

25. Brouillette, E.; Malouin, F. The pathogenesis and control of *Staphylococcus aureus*-induced mastitis: Study models in the mouse. *Microbes Infect.* **2005**, *7*, 560–568. [CrossRef] [PubMed]

26. Asli, A.; Brouillette, E.; Ster, C.; Ghinet, M.G.; Brzezinski, R.; Lacasse, P.; Jacques, M.; Malouin, F. Antibiofilm and antibacterial effects of specific chitosan molecules on *Staphylococcus aureus* isolates associated with bovine mastitis. *PLoS ONE* **2017**, *12*, e0176988. [CrossRef] [PubMed]

27. Mordmuang, A.; Brouillette, E.; Voravuthikunchai, S.P.; Malouin, F. Evaluation of a Rhodomyrtus tomentosa ethanolic extract for its therapeutic potential on *Staphylococcus aureus* infections using in vitro and in vivo models of mastitis. *Vet. Res.* **2019**, *50*, 49. [CrossRef]

28. Singh, A.; Upadhyay, V.; Upadhyay, A.K.; Singh, S.M.; Panda, A.K. Protein recovery from inclusion bodies of *Escherichia coli* using mild solubilization process. *Microb. Cell Fact.* **2015**, *14*, 1–10. [CrossRef]

29. Boireau, C.; Cazeau, G.; Jarrige, N.; Calavas, D.; Madec, J.-Y.; Leblond, A.; Haenni, M.; Gay, É. Antimicrobial resistance in bacteria isolated from mastitis in dairy cattle in France, 2006–2016. *J. Dairy Sci.* **2018**, *101*, 9451–9462. [CrossRef]

30. Carratalá, J.V.; Serna, N.; Villaverde, A.; Vázquez, E.; Ferrer-Miralles, N. Nanostructured antimicrobial peptides: The last push towards clinics. *Biotechnol. Adv.* **2020**, *44*, 107603. [CrossRef]

31. Bray, B.L. Large-scale manufacture of peptide therapeutics by chemical synthesis. *Nat. Rev. Drug Discov.* **2003**, *2*, 587–593. [CrossRef] [PubMed]

32. Meiyalaghan, S.; Latimer, J.M.; Kralicek, A.V.; Shaw, M.L.; Lewis, J.G.; Conner, A.J.; Barrell, P.J. Expression and purification of the antimicrobial peptide GSL1 in bacteria for raising antibodies. *BMC Res. Notes* **2014**, *7*, 777. [CrossRef] [PubMed]

33. Sun, B.; Wibowo, D.; Sainsbury, F.; Zhao, C.-X. Design and production of a novel antimicrobial fusion protein in Escherichia coli. *Appl. Microbiol. Biotechnol.* **2018**, *102*, 8763–8772. [CrossRef] [PubMed]

34. Yu, H.; Li, H.; Gao, D.; Gao, C.; Qi, Q. Secretory production of antimicrobial peptides in *Escherichia coli* using the catalytic domain of a cellulase as fusion partner. *J. Biotechnol.* **2015**, *214*, 77–82. [CrossRef]

35. Soundrarajan, N.; Cho, H.-S.; Ahn, B.; Choi, M.; Thong, L.M.; Choi, H.; Cha, S.-Y.; Kim, J.-H.; Park, C.-K.; Seo, K.; et al. Green fluorescent protein as a scaffold for high efficiency production of functional bacteriotoxic proteins in Escherichia coli. *Sci. Rep.* **2016**, *6*, 20661. [CrossRef]

36. Zhou, Q.-F.; Luo, X.-G.; Ye, L.; Xi, T. High-level production of a novel antimicrobial peptide perinerin in Escherichia coli by fusion expression. *Curr. Microbiol.* **2007**, *54*, 366–370. [CrossRef]

37. Li, J.F.; Zhang, J.; Zhang, Z.; Kang, C.T.; Zhang, S.Q. SUMO mediating fusion expression of antimicrobial peptide CM4 from two joined genes in Escherichia coli. *Curr. Microbiol.* **2011**, *62*, 296–300. [CrossRef]

38. Wei, X.; Wu, R.; Zhang, L.; Ahmad, B.; Si, D.; Zhang, R. Expression, Purification, and Characterization of a Novel Hybrid Peptide with Potent Antibacterial Activity. *Molecules* **2018**, *23*, 1491. [CrossRef]

39. Lee, J.H.; Kim, J.H.; Hwang, S.W.; Lee, W.J.; Yoon, H.K.; Lee, H.S.; Hong, S.S. High-level expression of antimicrobial peptide mediated by a fusion partner reinforcing formation of inclusion bodies. *Biochem. Biophys. Res. Commun.* **2000**, *277*, 575–580. [CrossRef]

40. Sánchez-García, L.; Serna, N.; Álamo, P.; Sala, R.; Céspedes, M.V.; Roldan, M.; Sánchez-Chardi, A.; Unzueta, U.; Casanova, I.; Mangues, R.; et al. Self-assembling toxin-based nanoparticles as self-delivered antitumoral drugs. *J. Control. Release* **2018**, *274*, 81–92. [CrossRef]

41. Gray, P.W.; Goeddel, D.V. Cloning and expression of murine immune interferon cDNA. *Proc. Natl. Acad. Sci. USA* **1983**, *80*, 5842–5846. [CrossRef]

42. Ahmed, C.M.I.; Burkhart, M.A.; Subramaniam, P.S.; Mujtaba, M.G.; Johnson, H.M. Peptide Mimetics of Gamma Interferon Possess Antiviral Properties against Vaccinia Virus and Other Viruses in the Presence of Poxvirus B8R Protein. *J. Virol.* **2005**, *79*, 5632–5639. [CrossRef] [PubMed]

43. Magazine, H.I.; Carter, J.M.; Russell, J.K.; Torres, B.A.; Dunn, B.M.; Johnson, H.M. Use of synthetic peptides to identify an N-terminal epitope on mouse γ interferon that may be involved in function. *Proc. Natl. Acad. Sci. USA* **1988**, *85*, 1237–1241. [CrossRef]

44. Torcato, I.M.; Huang, Y.-H.; Franquelim, H.G.; Gaspar, D.; Craik, D.J.; Castanho, M.A.R.B.; Troeira Henriques, S. Design and characterization of novel antimicrobial peptides, R-BP100 and RW-BP100, with activity against Gram-negative and Gram-positive bacteria. *Biochim. Biophys. Acta* **2013**, *1828*, 944–955. [CrossRef] [PubMed]

45. Melo, M.N.; Ferre, R.; Castanho, M.A.R.B. Antimicrobial peptides: Linking partition, activity and high membrane-bound concentrations. *Nat. Rev. Microbiol.* **2009**, *7*, 245–250. [CrossRef] [PubMed]

46. Aghamohammadi, M.; Haine, D.; Kelton, D.F.; Barkema, H.W.; Hogeveen, H.; Keefe, G.P.; Dufour, S. Herd-Level Mastitis-Associated Costs on Canadian Dairy Farms. *Front. Vet. Sci.* **2018**, *5*, 100. [CrossRef] [PubMed]

47. Apparao, M.D.; Ruegg, P.L.; Lago, A.; Godden, S.; Bey, R.; Leslie, K. Relationship between in vitro susceptibility test results and treatment outcomes for gram-positive mastitis pathogens following treatment with cephapirin sodium. *J. Dairy Sci.* **2009**, *92*, 2589–2597. [CrossRef]

48. Demon, D.; Ludwig, C.; Breyne, K.; Guédé, D.; Dörner, J.-C.; Froyman, R.; Meyer, E. The intramammary efficacy of first generation cephalosporins against *Staphylococcus aureus* mastitis in mice. *Vet. Microbiol.* **2012**, *160*, 141–150. [CrossRef]

49. Li, L.; Wang, L.; Gao, Y.; Wang, J.; Zhao, X. Effective antimicrobial activity of plectasin-derived antimicrobial peptides against *Staphylococcus aureus* infection in mammary glands. *Front. Microbiol.* **2017**, *8*, 2386. [CrossRef]

50. Wei, W.; Dejie, L.; Xiaojing, S.; Tiancheng, W.; Yongguo, C.; Zhengtao, Y.; Naisheng, Z. Magnolol inhibits the inflammatory response in mouse mammary epithelial cells and a mouse mastitis model. *Inflammation* **2015**, *38*, 16–26. [CrossRef]

51. Schmelcher, M.; Powell, A.M.; Camp, M.J.; Pohl, C.S.; Donovan, D.M. Synergistic streptococcal phage λSA2 and B30 endolysins kill streptococci in cow milk and in a mouse model of mastitis. *Appl. Microbiol. Biotechnol.* **2015**, *99*, 8475–8486. [CrossRef]

52. Notebaert, S.; Demon, D.; Vanden Berghe, T.; Vandenabeele, P.; Meyer, E. Inflammatory mediators in *Escherichia coli*-induced mastitis in mice. *Comp. Immunol. Microbiol. Infect. Dis.* **2008**, *31*, 551–565. [CrossRef] [PubMed]

pharmaceutics

MDPI

Supplementary Materials: In Vivo Bactericidal Efficacy of GWH1 Antimicrobial Peptide Displayed on Protein Nanoparticles, a Potential Alternative to Antibiotics

Jose V. Carratalá, Eric Brouillette , Naroa Serna, Alejandro Sanchez-Chardi,
Julieta M. Sanchez, Antonio Villaverde, Anna Arís, Elena Garcia-Fruitós,
Neus Ferrer-Miralles * and François Malouin *

Table S1. Solubility and productivity of recombinant proteins produced in the study. Soluble versions were produced at 20 °C for 5 h and IBs were produced at 37 °C for 3 h. Values represent mean and SEM when available. Not determined (n.d.).

Protein name	Soluble version (20 °C)		IBs (37 °C)	
	Solubility (%)	Productivity (mg/L)	Solubility (%)	Productivity (mg/L)
IFN-γ	60.20	26.6 ± 2.40	69.20	48.48 ± 15.73
GWH1-GFP	63.60	3.26 ± 0.81	16.90	13.40 ± 11.66
GWH1- IFN-γ	62.80	1.80 ± 1.92	51	22.67 ± 18.10
GFP	80.50 ± 9.68	92	n.d.	101.18 ± 27.29

STUDY 4

Nanostructured antimicrobial peptides: The last push towards clinics

Jose Vicente Carratalá, Naroa Serna, Antonio Villaverde, Esther Vázquez, Neus Ferrer-Miralles

Biotechnology Advances 44, 2020

AMPs represent excellent drug candidates for clinical exploitation. These cationic peptides have their own advantages over conventional antibiotics, with a broad-spectrum antibacterial, antifungal and antivirus activities, the ability to favorably modulate the host immune response and the reduced possibility of inducing bacterial drug resistance.

To date, several AMPs have been approved by the FDA and are already on the market. However, their clinical translation is in most cases hampered due to the presence of certain structural and functional limitations including cytotoxicity, hemolytic activity, low stability, susceptibility to proteolytic degradation, high production costs, and difficult industrial scalability. These are some of the issues that must be circumvented before more AMP-based products reach the market.

This review is intended to explore some of the most novel mechanisms developed to surpass some of the drawbacks associated to AMPs. Through the application of protein engineering technology, the incorporation of chemical modifications, and the use of different protein-based formats among others, different studies aim to shed light on the future clinical application of AMP-based compounds taking into account the most available advanced tools.

Research review paper

Nanostructured antimicrobial peptides: The last push towards clinics

Jose Vicente Carratalá[a,b,c,1], Naroa Serna[a,b,c,*,1], Antonio Villaverde[a,b,c,*], Esther Vázquez[a,b,c,*], Neus Ferrer-Miralles[a,b,c]

[a] Institut de Biotecnologia i de Biomedicina, Universitat Autònoma de Barcelona, Bellaterra, Barcelona 08193, Spain
[b] Departament de Genètica i de Microbiologia, Universitat Autònoma de Barcelona, Bellaterra, Barcelona 08193, Spain
[c] CIBER de Bioingeniería, Biomateriales y Nanomedicina (CIBER-BBN), Bellaterra, Barcelona 08193, Spain

ARTICLE INFO

ABSTRACT

Peptide drugs hold great potential for the treatment of infectious diseases due to their unconventional mechanisms of action, biocompatibility, biodegradability and ease of synthesis and modification. The increasing rising of bacterial strains resistant to classical antibiotics have pushed the development of new peptide-based antimicrobial therapies. In this context, over the past few years, different approaches have reached a clinical approval. Furthermore, the application of nanotechnological principles to the design of antimicrobial peptide-based composites increases even more the already known benefits of antimicrobial peptides as competent protein drugs. Then, we provide here an overview of the current strategies for antimicrobial peptide discovery and modification and the status of such peptides already under clinical development. In addition, we summarize the innovative formulation strategies for their application, focusing on the controlled self-assembly for the fabrication of antimicrobial nanostructures without the assistance of external nanocarriers, and with emphasis on bioengineering, design of ultra-short peptides and rising insights in bacterial selectivity.

1. Introduction: Do we really need new antimicrobials?

The pharmaceutical industry facilitates the immediate availability of antibiotics, which remain one of the most commonly prescribed classes of drugs (both for humans and animals) (Fuentes et al., 2018). However, easy access and mass use have led to their overuse, prompting bacteria to develop resistances. Infections caused by antimicrobial-resistant (AMR) bacteria have emerged as a major problem in global healthcare. The Review on Antimicrobial Resistance commissioned by David Cameron and chaired by Jim O'Neill indicates that annually, over 700,000 people die worldwide due to the infections caused by multidrug resistant (MDR) pathogens. It also warns that if no effective action is taken, the world could be facing 10 million deaths per year due to AMR by 2050, surpassing the number of deaths caused by cancer (Shankar, 2016). This situation urged to find biomedical solutions to AMR through the development of new generation medicaments. To this end, specific action plans have been developed in many countries, starting with Obama's National Action Plan for Combating Antibiotic-Resistant Bacteria in the US and following with EU's European One Health Action Plan against AMR.

The analysis of the U.S. Food and Drug Administration (FDA) approved drugs indicates that only eight new antibiotics have been approved from 2017 to 2019, most of these being derivatives of known conventional classes (Fig. 1A) (World Health Organization, 2019). Moreover, the current global clinical pipeline for infectious diseases is still dominated by broad spectrum β-lactam-based drugs, mostly in combination with β-lactamase inhibitors (Theuretzbacher et al., 2019a). Other drugs in development are also modified versions of old-class well-known antibiotics (Fig. 1B). These new molecules usually provide improvements for selected class-specific resistance mechanisms, but are limited by cross-resistance to existing drugs (Mamatha and Shanthi, 2018).

In this context, the antibiotic resistance crisis requires a multi-faceted approach that includes the development of novel antimicrobials (Spellberg et al., 2015; Stein, 2017). Fortunately, the preclinical pipeline overview is much more diverse with new scientifically interesting

---

Fig. 1. Overview of the FDA-approved agents and clinical and preclinical pipeline of infectious diseases. A) Antibiotics that gained market authorization between 2017 and 2019. MOA: new mode of action. NCR: no cross-resistance to other antibiotics classes. CC: new chemical class. T: new target. B) General clinical and preclinical pipeline. The group of old targets are derivatives of conventional antibiotics that includes β-lactams and other inhibitors of penicillin-binding proteins, fluoroquinolones, bacterial topoisomerase inhibitors, aminoglycosides, polymyxins and macrolides. New targets include synthetic and natural AMPs, natural products and enzyme inhibitors of the bacterial fatty acid biosynthesis pathway. Other strategies involve antibiotic hybrids or nanoparticles among others (World Health Organization, 2019; Theuretzbacher et al., 2019a).

approaches mainly focused on the development of antimicrobial peptides (AMPs) and a narrow-spectrum or pathogen-specific antibacterial agents such as antibodies, engineered phages and antivirulence factors (Fig. 1B) (Theuretzbacher et al., 2019b). The pharmaceutical industry is undertaking a paradigm shift to more tailored therapies, becoming more similar to the development of cancer-targeted drugs.

2. Antimicrobial peptides

AMPs represent excellent drug candidates for clinical exploitation (Kang et al., 2017). Besides the broad action spectrum showed by conventional antibiotics, AMPs are less subject to development of resistances and also act as immunomodulating and antiviral agents (Otvos, 2016; Raheem and Straus, 2019). AMPs, by themselves, represent the first line of defense against invading pathogens, being a key part of the innate immune system in a wide range of organisms. These small peptides are defined as small pore-forming proteins that target the negatively charged bacterial membranes by permeation, exerting cell lysis. Due to the potential AMP resistance and their clinical relevance, mechanisms of such resistance, that in some cases has been already observed, have been recently explored at the molecular level and a few of them identified. For instance, some bacteria show intrinsic resistance to AMPs by the exposure of positively charged lipids on their membrane (Mwangi et al., 2019a). In Gram-negative bacteria the incorporation of 4-aminoarabinose (Ar4N) or palmitoylation of lipid A makes LPS less negative and prevent the interaction with AMPs. In Gram-positive bacteria, many modifications have also been detected in

the cell wall teichoic acid (TA), which is a primary binding site of AMPs. Despite of such evidences for microbial resistance to AMPs, those mechanisms were mainly studied under the classical consideration of a single drug target, which makes sense for conventional antibiotics, but that could hardly provide conclusive data in the case of multiple-targeting AMPs (Bechinger and Gorr, 2017; Mwangi et al., 2019a). On the other side, the multiple sites of AMP action (membrane target, damage to intracellular biomolecules and oxidative damage) that do not involve specific protein binding, and also the rapid drug action make the acquisition of AMP resistance a very difficult event (Bechinger and Gorr, 2017; Mwangi et al., 2019b). Furthermore, AMPs show potent activity against biofilms that develop resistance to traditional antibiotics (Chung and Khanum, 2017). In addition, in most cases, these cationic peptides neutralize the effects of endotoxins and control inflammation, that might repair damaged tissue in the patient and facilitate wound closure by promoting wound neovascularization and re-epithelialization of healing skin (Liu et al., 2017; Zhang et al., 2019).

2.1. Commercialized AMPs

More than 5000 natural and synthetic AMPs have been discovered so far (Data Repository of Antimicrobial Peptides, DRAMP, http://dramp.cpu-bioinfor.org/). Among them, only eight have been approved by the FDA, namely Colistin, Polymyxin B, Vancomycin, Gramicidin, Bacitracin, Daptomycin, Enfuvirtide and Telaprevir. Three Vancomycin-derived lipoglycopeptides have also been commercialized as Telavancin, Oritavancin and Dalbavancin (Table 1).

2

Table 1
Antimicrobial peptides approved by FDA (up to April 2020).

Name	Approved by FDA	Trade name	Administration	Peptide type	Application	Antimicrobial activity
Colistin	1962	Coly-Micins	Intravenous	Cyclic lipopeptide	Bacterial infections	Gram-negative bacteria
Polymyxin B	1964	Poly-Rx	Intravenous Intramuscular	Cyclic peptide	Bacterial infections	Gram-negative bacteria
Vancomycin	1983	Vancocin	Oral	Heptapeptide	Bacterial infections	Gram-positive bacteria
Gramicidin D	1995	Neosporin	Topical	Mixture of 3 peptides	Bacterial conjuntivitis	Gram-positive bacteria
Bacitracin	1997	Baciim	Topical	Cyclic polypopeptide	Skin and eye infections	Gram-positive bacteria
Daptomycin	2003	Cubicin	Intravenous	Cyclic lipopeptide	Bacterial skin infections	Gram-positive bacteria
Enfuvirtide	2003	Fuzeon	Sucutaneous	Polypeptide	HIV-1 infection	Virus
Telavancin	2009	Vibativ	Intravenous	Lipoglycopeptide (vancomycin derived)	Acute bacterial skin infections	Gram-positive bacteria
Telaprevir	2011	Incivo	Oral	Peptide	Hepatitis C	Virus
Oritavancin	2014	Orbactiv	Intravenous	Lipoglycopeptide (vancomycin derived)	Acute bacterial skin infections	Gram-positive bacteria
Dalbavancin	2014	Dalvance	Intravenous	Lipoglycopeptide (vancomycin derived)	Acute bacterial skin infections	Gram-positive bacteria

These commercialized peptides have been mostly utilized for topical administration (skin infections, pink eye, or wounds). However, some lipopeptide derivatives have been approved for direct injection into the human body such as Coly-Mycins, Cubicin, Vibativ, Orbactiv and Dalvance (Chen and Lu, 2020; Lei et al., 2019), since these agents show long elimination half-life and improved pharmacokinetics (Shi et al., 2017). Nonetheless, there are some drawbacks hampering their regular and future use. Vibativ may cause toxicity at high doses and kidney damage in some patients (Cavanaugh et al., 2019). Cubicin triggers serious side effects including hypersensitivity reactions or eosinophilic pneumonia (Higashi et al., 2018; Kido et al., 2019). Orbactiv and Dalvance show low effectiveness against drug-resistant Gram-positive microorganisms (Morrisette et al., 2019). Coly-Mycins, may cause damage to the central nervous system and kidneys in adult patients along with the selection of colistin-resistant bacteria (Caniaux et al., 2017; Karaiskos et al., 2017).

This scenario suggests that the design of AMPs as human medicines must focus on reducing their toxicity and avoiding such side effects. Additionally, most of the commercialized AMPs (except colistin) are used for treating Gram-positive bacterial infections, being the development of AMPs to treat infections caused by Gram-negative bacteria an urgent need.

2.2. Current clinical pipeline of AMPs

To date, there are around 75 AMP-based drugs under development (http://dramp.cpu-bioinfor.org/) (Kang et al., 2019). Even though the majority of developmental projects are focused on their antibacterial performance, a few are starting to explore other interesting applications such as antiviral and wound healing activity (Fig. 2A). Importantly, among those studies focused on the enhancement of antibacterial activity, great efforts are made leading Gram-negative active AMPs to clinics, overcoming the lack of approved effective peptides in this area (Fig. 2B). However, as mentioned above, the interest in AMPs has been compromised by a generically poor pharmacokinetics and the rather constant toxicity profiles (AB Naafs, 2018). Their hemolytic activity and slight toxicity towards mammalian cells along with protease susceptibility, low hydro-solubility and rapid renal filtration are limiting factors that have restricted their therapeutic use as antibacterial agents. To open to the clinical applicability, long-lasting AMP analogues need to be developed to overcome these disadvantages (Kumar et al., 2018; Mahlapuu et al., 2016).

In view of this need and as shown in the preclinical pipeline, several strategies are being conducted to improve AMP functionality (AB Naafs, 2018). Chemical modification of natural AMPs and development of peptidomimetics are the leading strategies to enhance the *in vivo* stability and to avoid enzymatic degradation (Fig. 2C) (World Health Organization, 2019; Koo and Seo, 2019). Although these encouraging strategies minimize proteolysis and enhance stability *in vivo*, additional approaches that improve pharmacokinetic profiles, increase the local concentration of AMPs and overcome toxicity problems are still urgent (Kumar et al., 2018). In this context, nanotechnology as well as approaches to gain targeting abilities represent the most promising alternatives to the direct application of these agents and push them towards clinical trials.

3. Rational engineering of AMPs

#### 3.1. The importance of single modifications; less is more

Multiple physico-chemical properties endowed antimicrobial peptides with its antibacterial effects. For instance, length, hydrophobicity, hydrophobic moment, net charge, amphipathicity and helicity are key factors that influence the deleterious peptide activity over bacterial membranes and its selectivity. All these properties are interrelated, and the antimicrobial activity is the result of a delicate balance among them. For this reason, there is no convention about the ideal modifications that would result into an optimal functionality, and modulating the biophysical features to favor antimicrobial potency or selectivity have to be empirically determined for each peptide.

During the last years, important progresses have been made in this area, and the rough influences of each peptide property have been defined, giving the opportunity to rationally modify the global AMP performance. Regarding length, in 2017, Gagnon et al. demonstrated that the antimicrobial activity was clearly dependent on the peptide length (Gagnon et al., 2017). After evaluating a different set of peptides that differed in length, the authors concluded that only the peptides that were long enough to span the hydrophobic width of the lipid bilayer were able to generate an antimicrobial effect. Therefore, depending on the membrane thickness, any tested peptide requires a certain minimal length to be active (Gagnon et al., 2017). However, as the peptide length increases, so does the net positive charge and hydrophobicity.

The net positive charge and hydrophobicity are key parameters that define the amphipathicity of α-helical peptides, clearly describing the hydrophilic and hydrophobic portions in the helical structure. The net positive charge or cationicity is an essential property responsible for the initial electrostatic interactions of AMPs with the negatively charged lipopolysaccharides and phospholipids on the cell membrane (Liscano et al., 2019; Liu et al., 2019). On the other hand, hydrophobicity controls the extent to which the peptide can be inserted into the hydrophobic membrane core (Liscano et al., 2019).

Interestingly, those physicochemical properties can be modulated by single modifications in the amino acid sequence of the AMP. There are several recent reports demonstrating that a single Lys substitution in the polar face of the peptides has a positive effect on the antimicrobial properties (Gong et al., 2020; Liu et al., 2019; Pedron et al., 2019; Rončević et al., 2019; Torres et al., 2018). However, multiple amino acid substitutions in the hydrophilic portion (≥ 2) may lead to undesired and unexpected results. In 2019, Pedron et al. showed that

3
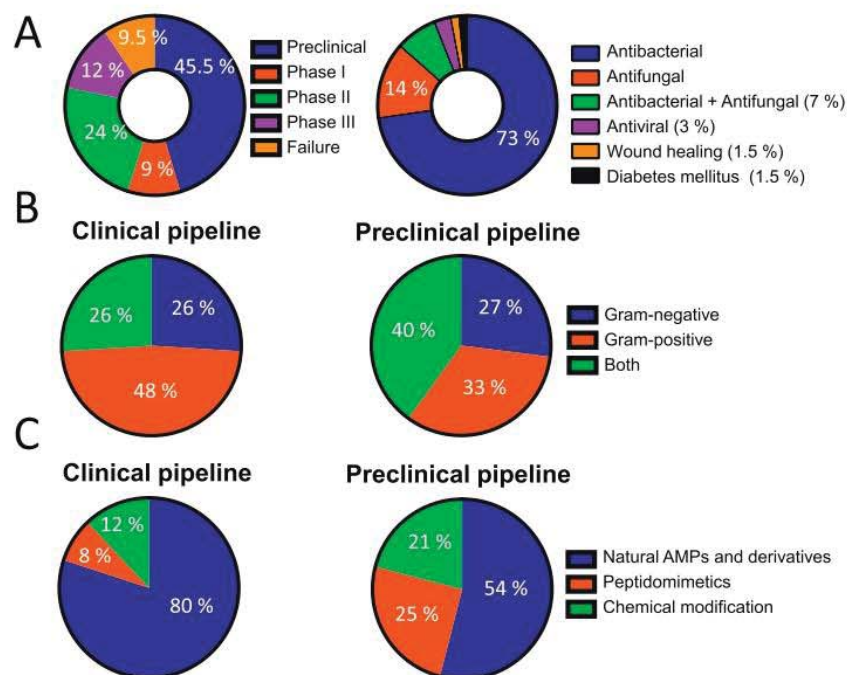
Fig. 2. Development phase, target organisms and advancement approaches of AMPs. A) Current development phase of AMPs and their indicated activity. B) Target bacterial organisms. The majority of AMPs currently in clinical trials target Gram-positive bacteria. In the preclinical pipeline there are more molecules aimed at both Gram-negative bacteria and Gram-positive bacteria. C) The most commonly pursued approaches in preclinical pipeline are peptidomimetics and chemical modifications that include macrocyclation, incorporation of non-canonical amino and D-amino acids, acetylation, amidation, glycosylation and lipidation (Koo and Seo, 2019). Information obtained from DRAMP, http://dramp.cpu-bioinfor.org/.

simultaneous Lys substitutions (2–3) in the hydrophilic portion of the helical structure increased the antimicrobial and anticancer activities compared to the unmodified peptide, but that they also increased the hemolytic activity (Pedron et al., 2019). In a different work, Liscano et al. modified the Alyteserin 1c peptide through the substitution of hydrophobic amino acids located on the polar face by hydrophilic amino acids, increasing the net charge ($+2 > +5$). The modified peptide dramatically lost its activity against Gram-negative bacteria, but instead, it showed increased activity against Gram-positive bacteria and enhanced hemolytic activity (Liscano et al., 2019). On the other hand, those modifications intended to modify the hydrophobic portion with positively charged amino acids leads to a diminished antimicrobial activity due to a decreased hydrophobicity and hydrophobic moment and an altered amphipathicity (Pedron et al., 2019; Torres et al., 2018).

These results suggest that there is no completely linear relationship between positive net charge and antimicrobial activity (Liscano et al., 2019; López Cascales et al., 2018). Therefore, rather than just increasing the net charge, it appears more important to carefully evaluate where these positives charges (the positively charged amino acids) are going to be introduced into the peptide sequence, which amino acids are going to be substituted and the extent of these changes in the global hydrophobicity, hydrophobic moment, amphipathicity and helicity of the peptide. The higher the changes, the higher the risk to modify the balance between those properties and the possibility to render unexpected and undesired results. For all these reasons, some authors have concluded that increasing the appropriate amount of positive net charge in specific positions (hydrophilic face), while maintaining hydrophobicity within a reasonable range, may be a predictably strategy to enhance the potential antimicrobial activity without maximizing the cytotoxicity until an unacceptable extent (Gong et al., 2020; Liu et al., 2019; Torres et al., 2018).

3.2. Resistance to proteolytic degradation

Susceptibility to proteolytic degradation is one of the major drawbacks of AMPs, as degradation reduces their half-life and limits their potential therapeutic applications. To overcome this bottleneck,

different strategies have been proposed including cyclization (Rozek et al., 2003), replacement of L-amino acids for D-amino acids (Zhao et al., 2016) and utilization of non-natural amino acids in the AMP synthesis (Oliva et al., 2018).

Recently, additional chemical modifications have been implemented in AMP development. For instance, the staple strategy is a new cyclization method which consists on the covalent cross-linking between the side chains of two amino acids, generating a conformational-constrained α-helix with improved proteolytic stability (Li et al., 2018, 2019). Very recently, Li et al. created a series of lysine-tethered cyclic peptides with strong antimicrobial activity, low hemolysis and high proteolytic stability. In their study they demonstrated that the introduction of a cross-link on the hydrophilic AMP face lowered the risk of hemolysis while the position of the cross-linked lysines strongly determined the proteolytic resistance (Li et al., 2020). However, chemical modifications add complexity and increase production costs, being a limitation for development and commercial application.

The appropriate arrangement of natural amino acids to protect protease cleavage sites is a promising cost-effective approach to reduce hydrolysis (Shao et al., 2019). As an example, Wang and coworkers constructed an antitrypsin/antichymotrypsin peptide structure which consisted on the (XYPX)n repeat, where X represents Ile, Leu or Val, Y represents Arg or Lys, and P represents Pro (Wang et al., 2019a). Pro at the C terminus of Arg and Lys protects from cleavage by trypsin, while Ile and Val placed at both termini prevent degradation by chymotrypsin. Among the different combinations, the peptide (IRPI)7 showed excellent resistance to trypsin/chymotrypsin even after 8 h of incubation (Wang et al., 2019b). Furthermore, both appropriate formulation and chemical modification are not mutually exclusive and they can be combined in the AMP design.

The incorporation of D-amino acids into the AMP structure is also a suitable approach to enhance the stability of the drug. However, there is no universal rule on how to incorporate these modifications. In a recent study, the WLBU2 peptide, intended to be applied to the treatment of respiratory infections, was modified by L-Val to D-Val enantiomerization, which are the predicted cutting sites of neutrophil elastase, a common protease in this type of infection (Di et al., 2020).
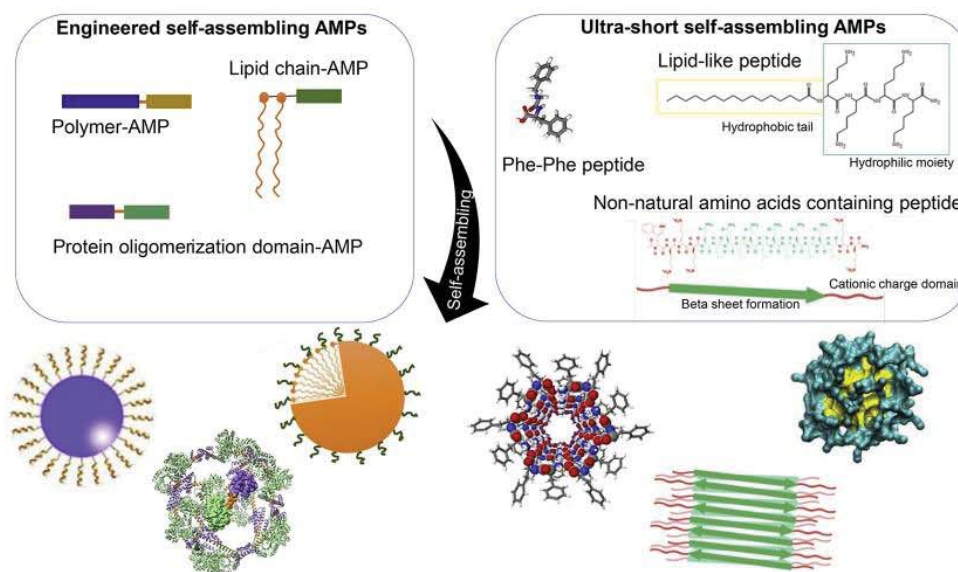
4

Fig. 3. Strategies for the development of AMP-based multimers through self-assembling reached by protein engineering and by the use of ultra-short peptides. Reproduced with permission from (Glover and Clark, 2016; Sikorska et al., 2014; Silva et al., 2013; Xu et al., 2018; Zhao et al., 2017).

Different designs were generated, which differed in the number on modified valine residues. The variant D8, with a complete L-Val to D-Val enantiomerization, not only showed enhanced resistance to protease digestion but it also reduced host toxicity and improved the antimicrobial activity (Di et al., 2020).

Taken together, the identification and application of the correct modifications (natural or non-natural) into the most susceptible digestion sites of the peptide structure allows to rationally designing application-specific AMPs with reduced sensitivity to proteases *in vivo*.

4. Nanotechnology of AMPs

The nanoscale size provides half-life extension and stability, and it exploits multivalency and multispecificity to increase target selectivity (Huh and Kwon, 2011; Walvekar et al., 2019). Gaining nanostructure is expected to enhance the intrinsically antimicrobial properties of AMPs, preventing renal clearance and allowing the material to fully exploit the enhanced retention and permeability effect (EPR) (Azzopardi et al., 2013). Most of nanostructured drugs that reached the clinic are based on such EPR strategy, and this effect can be also exploited for AMPs delivery. At infection sites, the release and accumulation of bacterial components (mainly bacterial proteases and lipopolysaccharide or lipoteichoic acid) trigger various inflammatory mediators that directly stimulate vascular permeability and also activate immune cells that interact with vascular endothelia (Abdulkhaleq et al., 2018; Azzopardi et al., 2013; Fenaroli et al., 2018). This fact results in barrier dysfunction and gap widening, leading to the accumulation of nanoparticles at the infection sites.

4.1. Gaining nanoscale size: self-assembling AMPs

Drug delivery systems are engineered nanoscale platforms for the targeted delivery and controlled release of therapeutic agents. Several types of carriers are currently used in research for AMP delivery such as metal nanoparticles (Aderibigbe, 2017; Yuan et al., 2018), carbon nanotubes (Assali et al., 2017; Tondro et al., 2019), lipid-based nanoparticles (Hallaj-Nezhadi and Hassan, 2015; Nisini et al., 2018; Thakur et al., 2018) and polymer-based nanostructures (Mhlwatika and Aderibigbe, 2018). There is a variety of recently published review

articles focused on the different nanosystems used to deliver AMPs to the infection sites, showing an increased therapeutic potential and decreased toxicity and hemolytic activity of these agents (Dube, 2019; Martin-Serrano et al., 2019; Radaic et al., 2020; Teixeira et al., 2020).

From an applied point of view, these carriers show very interesting uses in areas such as electronics, environmental or medical sciences. However, as drug delivery systems, most of them raise severe biocompatibility concerns such as poor water solubility and high toxicity (Dusinska et al., 2017). Indeed, certain carriers may induce allergic sensitization, can modulate cytokine production and thus display proinflammatory effects (Elsabahy and Wooley, 2013). Importantly, they show poor biodegradability as are poorly metabolized by human enzymes. Therefore, they tend to accumulate in lysosomes (Feliu et al., 2016; Vlasova et al., 2016) or they can be secreted by urine being a matter of environmental concern, especially for metal-based nanocarriers (Wilson, 2018). In this context, the introduction of novel biocompatible and biodegradable materials has been pursued. Among them, protein materials, based on natural non-toxic macromolecules, show special interest in clinics (Serna et al., 2018; Verma et al., 2018; Wang et al., 2019c; Sanchez et al., 2020). Peptides are intriguing building blocks for a variety of applications in nanotechnology as they can self-assemble into well-ordered nanostructures with appealing physical properties such as adhesiveness and elasticity, and with regulatable stiffness, flexibility and mechanical strength (Unzueta et al., 2017, 2015; López-Laguna et al., 2020). The advantage of peptides over alternative building blocks is that they are highly versatile materials, fully biocompatible and biodegradable (De Frates et al., 2018).

4.1.1. Engineering of self-assembling AMPs

Protein engineering allows the formulation of AMPs with tailored modifications to achieve self-assembling properties and to reach nanoscale size (Carmona-Ribeiro, 2018; Lombardi et al., 2019a, 2019b). For this purpose, different strategies have been developed including conjugation with biodegradable polymers and lipid moieties or the incorporation of protein oligomerization domains (Fig. 3, Table 2).

4.1.1.1. Polymer-protein conjugates. The exploitation of biodegradable materials including synthetic and natural polymers, has progressively become an appealing source of biomaterials for medicine (Konai et al.,

Table 2
Most representative examples of engineered self-assembling AMPs. VRSA:Vancomycin resistant S. aureus, MRSA: Methicillin resistant S. aureus.

AMP	Self assembling domain	Fusion peptide	Tested microorganisms	Production	Ref
Hep	Protein polymer: Spider silk domain (SSD)	H6-6SSD-Hep H6-12SSD-Hep	P. aeruginosa, E. coli, Methicillin resistant S. aureus, VRSA, E.feacalis, B. pumillus, C. albicans	Recombinant: E. coli BL21	(Franco et al., 2018)
Human Neutrophil peptide 1 (HNP1)	Protein polymer: Spider silk domain (SSD)	H6-6SSD-HNP1 H6-12SSD-HNP1	P. aeruginosa, E. coli, MRSA, Vancomycin resistant S. aureus, E. feacadis, B. pumillus, C. albicans	Recombinant: E. coli BL21	(Franco et al., 2018)
Bacitracin A	Synthetic polymer: poly(D,L-lactic-co-glycolic acid) (PLGA)	BA-PLGA BA-PEG-PLGA BA-PEG-PLGA-BA	E. coli, S. Aureus, P. Aeruginosa, S. pyogenes, A. pyogenes, S. Typhimurium.	Synthetic	(Hong et al., 2018)
WMR peptide, (Myxinidin derivative)	Aliphatic residues containing a lipidic tail (PA)	WMR-PA	P. aeruginosa, C. albicans	Synthetic	(Lombardi et al., 2019a, 2019b)
GWH1	Protein domains: Cationic peptide at amino terminus of a scaffold protein and a poly-histidine tag at the carboxy terminus	GWH1-GFP-H6	S. aureus, M. luteus E. coli, P. aeruginosa	Recombinant: E. coli Origami B	(Serna et al., 2017)
Melittin	Protein domain: β-sheet-forming synthetic peptide	(QL)6- Mel	E. coli	Synthetic	(Chen et al., 2019)

2018). Collagen, gelatin and silk are commonly used natural protein-based polymers as scaffolds for the generation of self-assembling materials. In this sense, Franco et al. (2018), genetically engineered a spider silk protein fused to three human AMPs (namely human neutrophil defensin 2, human neutrophil defensin 4, and hepcidin), thus obtaining self-assembling nanostructures that demonstrated bactericidal activity against Gram-negative and Gram-positive bacteria and low toxicity on mammalian cells (Franco et al., 2018). Regarding to synthetic biodegradable polymers, aliphatic polyesters such as polylactide (PLA), polyglycolide (PGA), and their copolymer poly(lactide-co-glycolide) (PLGA) are the most frequently used and importantly, they are among the few synthetic polymers approved by the FDA for human clinical applications (Blasi, 2019; Hirenkumar and Steven, 2012). Based on this fact, PLGA copolymers were selected for conjugation with the N-terminus of bacitracin A in a study by Hong et al. (2018). The developed PEGylated self-assembled nano-bacitracin A showed enhanced antibacterial potency against Gram-negative and Gram-positive bacteria and high solubility in the treatment of invasive infections (Hong et al., 2018).

4.1.1.2. Lipid-protein conjugates. Lipopeptides are amphiphilic molecules based on one or more lipid chains attached to a peptide. These molecules have the ability to self-assemble into a wide variety of structures (Hutchinson et al., 2017). Self-assembly processes of amphiphiles have been widely used to mimic biological systems, such as assembly of proteins (Qiu et al., 2018; Zhang, 2017). In this sense, Lombardi et al. (2019a) used the antimicrobial WMR peptide, which is a modification of the native sequence of the myxinidin, linked to a peptide segment of aliphatic residues containing a lipidic tail to generate a peptide amphiphile (named WMR PA). The designed WMR PA was able to self-assemble into stable nanofiber structures that integrate on their surface the antibacterial peptide (Lombardi et al., 2019b). These nanoassemblies highly affected biofilm formation and eliminated the already formed biofilms of *P. aeruginosa* and *C. albicans* when compared to the native WMR peptide (Lombardi et al., 2019b).

4.1.1.3. Multifunctional proteins. Another approach is the empowering of AMPs with protein domains that promote the oligomerization of AMPs in form of nanostructures (Chiesa et al., 2020; Liu and Hudalla, 2019; Vázquez and Villaverde, 2010). The construction of these protein assemblies relies on the controlled oligomerization of individual polypeptides, which act as building blocks of complex arrangements allowing the generation of self-assembled nanostructures. In this context, a new engineering oligomerization strategy has been developed in our team. Such strategy allows obtaining fully functional nanostructures based on the combined use of non-amyloidogenic architectonic tag pairs, consisting in a cationic peptide at amino terminus of a scaffold protein along with a poly-histidine tag at the carboxy terminus (López-Laguna et al., 2019; Serna et al., 2019; Unzueta et al., 2012). Under this concept, Serna et al. (2017) engineered the synthetic AMP GWH1 as self-assembling protein-only nanoparticles that showed multivalent display of the AMP, high antimicrobial activity against Gram-negative and Gram-positive bacteria and absence of cytotoxicity in mammalian cells. In these GWH1-GFP-H6 nanoparticles, the cationic GWH1 acted as antimicrobial peptide as well as oligomerization domain together with the H6 tag, while the green fluorescent protein acted as scaffold protein (Serna et al., 2017). In another recent example, Chen et al. (2019) associated a natural AMP (Mellitin) with a β-sheet-forming synthetic peptide. The polypeptide self-assembled to form a supramolecular nanofiber that displayed mellitin at the nanofiber-solvent interface in a precisely controlled manner (Chen et al., 2019). The AMP-displaying nanofiber showed high antibacterial activity without compromising biological safety over mammalian cells (Chen et al., 2019).

6

J.V. Carratalá, et al.

Table 3
Most representative examples of ultra-short self-assembling AMPs.

Peptide	Sequence	Tested microorganisms	Self-assembling	Ref
Diphenylalanine peptide	FF	E. coli	FF core	(Schnaider et al., 2017)
Fmoc-peptide gelators	FmocFF, FmocFFKK, FmocFFFKK and FmocFFOO	S. aureus, S. epidermidis, E. coli, P. aeruginosa	FF core	(McCloskey et al., 2017)
Modified diphenylalanine peptides	NH₂-FF-COOH, NH₂-FF-COOH and NH₂-FF-NH₂	S. aureus	FF core	(Porter et al., 2018)
FF8	KRRFFRRK	E. coli, S. aureus	FF core	(Shen et al., 2020)
DW362	dWdk3(QL)6dK2	E. coli	Introduction of non natural amino acids	(Xu et al., 2018)
α/β-pentapeptide	Lys-βAla-βAla-Lys-βAla	P. aeruginosa, E. coli, S. aureus, B. cereus	Introduction of non natural amino acids	(Goel et al., 2018)
Arg-rich tetrapeptides	C16-RRRR-NH2, C14-RRRR-NH2, C12-RRRR-NH2, and C16-PRRR-NH2	S. aureus, S. Epidermidis, E. Coli, P. Aeruginosa, C. albicans	Lipopeptide	(Sikorska et al., 2018)
Lys-rich tripeptides	(C₁₀₋₁₆)₂Dab-KKK-NH2 and (C₁₀₋₁₆)₂Dap-KKK-NH2	S. aureus, S. Epidermidis, E. Coli, P. Aeruginosa, C. albicans	Lipopeptide	(Stachurski et al., 2019)

4.1.2. Ultra-short self-assembling AMPs

Recently, the design of ultra-short peptides that are able both, to self-assemble and display antimicrobial activity, has emerged as a robust strategy (Fig. 3, Table 3, Choudhury et al., 2020; Eckert et al., 2006b; He et al., 2009; Kim et al., 2016; Wang et al., 2020; Ng et al., 2018; Thota et al., 2020).

4.1.2.1. Diphenilalanine (FF) core.
Diphenylalanine (FF) is known as the core motif for the ß-amyloid self-assembling sequence and it is frequently employed as a backbone to design short peptide-based hydrogelators. Generally, an aromatic capping group is also added on the N-terminus of the FF sequence, as this fact enhances intramolecular interactions and favors hydrogel formation. Fluorenylmethyloxycarbonyl (Fmoc), a protecting group widely used in solid phase synthesis, is one of the most investigated capping group for generating short peptide-based hydrogelators (Wei et al., 2017). In this context, Schnaider et al. (2017) presented the FF peptide as the minimal model for antibacterial supramolecular polymers, that upon self-assembling as nanotubes showed high antibacterial activity against E. coli (Schnaider et al., 2017). Later, McCloskey et al. (2017) designed ultrashort Fmoc-peptide gelators (FmocFF peptides) that formed surfactant-like soft gels. These gels eradicated established bacterial biofilms implicated in a variety of medical device infections (McCloskey et al., 2017). Moreover, Porter et al. (2018) modified terminal functional groups of diphenylalanine peptide to amino or carboxylic acid. The resulting peptide nanotubes showed different antibacterial selectivity against S. aureus and mammalian cell toxicity profiles that depend on the precise modification (Porter et al., 2018). Recently, Shen et al. (2020) synthetized a novel AMP named FF8, which is a cationic octapeptide composed of arginine, lysine, and phenylalanine. The FF8 was found to self-assemble into nanofibers that exhibited enhanced anti-bacterial activity against E. coli and S. aureus (Shen et al., 2020).

4.1.2.2. Non-natural amino acids.
The incorporation of unnatural amino acids into peptides also promotes their assembling in form of macroscopic hydrogels (Melchionna et al., 2016). Interestingly, apart from providing supramolecular organization, D-amino acids can also enhance the antimicrobial activity and selectivity of AMPs (Jia et al., 2017; Kumar et al., 2018; Oliva et al., 2018). In this context, Dawei Xu et al. (2018) designed a peptide named DW362 consisting in a central (QL)6 domain in the L-form, flanked by D-lysine residues at both termini. The DW362 nanofibers displayed high antimicrobial activity against E. coli while having, at the same time, greatly reduced cytotoxicity compared to some natural monomeric AMPs (Xu et al., 2018). In another example, Goel et al. (2018) fabricated nanostructures from a mixed α/β-pentapeptide, which majorly contain non-natural β-alanine residues in the backbone. The amphiphilic pentapeptide showed the ability to self-assemble into cationic nanovesicles in an aqueous solution and promoted toxicity against both Gram-negative and Gram-positive bacterial strains (Goel et al., 2018).

4.1.2.3. Lipopeptides.
Short cationic lipopeptides seem to represent a promising alternative against invading microorganisms (Carmona-Ribeiro, 2018). These peptides mimic the structure–function relationship of natural lipopeptides. Therefore, owing to the surfactant-like structure, they are capable to undergo self-assembly in solution. In this sense, Sikorska et al. (2018) synthetized short lipopeptides composed of a fatty acid covalently attached to the N-terminus of Arg-rich tetrapeptides that self-assembled into micelles. The shortening of the acyl chain results in compounds with an enhanced antimicrobial activity against Gram-positive bacteria and a lower haemolytic activity (Sikorska et al., 2018). Recently, Stachurski et al. (2019) conjugated two fatty acid tails with a three-lysine peptide. The presence of cationic lysine residues and fatty acid tails resulted in a total positive charge and anphipaticity. These lipopeptides self-assembled, and showed high antimicrobial activity against Gram-

7

positive and Gram-negative bacteria, in addition to low hemolytic activity in absence of any detectable effect on mammalian cells (Stachurski et al., 2019).

5. New developments on bacterial selectivity

One of the major drawbacks of AMPs is the non-specific toxicity on host cells. The positively charge density on AMPs is the driven force for bacterial selectivity. However, this strategy can be a "double edged sword" due to the undesired hemolytic activity or cytotoxicity on eukaryotic membranes. In this context, different approaches have been proposed to reduce or even avoid these undesired side effects. Increased selectivity of AMPs can be achieved by either reducing the intrinsic toxicity towards eukaryotic cells, or increasing the antibacterial activity while the cytotoxicity is maintained under a safe threshold. As discussed above, the direct peptide modification by amino acid substitutions is a powerful tool that may endow AMPs with increased antimicrobial properties and at the same time enhance their selectivity. In 2018, Torres and coworkers generated a series of derivatives of the peptide polybia-CP, where every single amino acid in the sequence was substituted by an Alanine residue and the resulting species finally evaluated (Torres et al., 2018). This strategy allowed discriminating among the amino acids that substantially contributed to the helical structure and antimicrobial function. After the screening, the selected non-contributing amino acids were sequentially substituted by Lys residues. Among the engineered variants, the Gly to Lys analog ($[Lys]_7$-Pol-CP-NH$_2$) was the most selective peptide towards a large variety of microorganisms, basically due to its higher antimicrobial activity (Torres et al., 2018). However, this broad activity spectra do not discriminate between pathogenic and beneficial microorganism, which can cause disruptions to the normal microbiota leading to numerous adverse side effects (Eckert et al., 2006a).

5.1. Targeted hybrid AMPs

In recent years, several studies have focused on the design of AMPs through hybridization. The chimeric fusion of two known AMPs may result in the design of novel antimicrobial agents that combine the main advantages of the individual parent peptides while reducing the AMP associated drawbacks (Al Tall et al., 2019; Dong et al., 2018; Jiang et al., 2019; Wanmakok et al., 2018; Wei et al., 2018; Yang et al., 2020). However, a significant part of these studies have focused on combining two membrane-permeabilizing peptides, and few of them have investigated the possible synergies that may result from the combination of peptides with different functionalities.

In 2006, Eckert et al. (2006b) described for the first time the selectively targeted antimicrobial peptide (STAMPs) strategy, which consisted on the design of highly species-specific antimicrobial peptides through the independent fusion of two functional components, a broad-spectrum AMP and a targeting peptide, by using a small linker (Eckert et al., 2006b). To date, many studies have employed this strategy in the design of hybrid AMPs, targeted to one single microbial species (Eckert et al., 2006a; Kim et al., 2020; Mai et al., 2011; Qiu et al., 2003; Xu et al., 2020) or directed against an specific group (Choudhury et al., 2020; Eckert et al., 2006b; He et al., 2009; Kim et al., 2016; Wang et al., 2020) (Table 4).

Different pathogen surface determinants have been used for the selective targeting of this type of hybrid AMPs, as for example, pheromone receptors and cell wall components. In this latter case, the chimeric combination of LPS-targeting peptides to potent broad spectrum AMPs led to the generation of dual-function candidates with increased antimicrobial activity, selectivity against Gram-negative bacteria, and LPS-neutralizing activities (Kim et al., 2016; Wang et al., 2020). On the other hand, bacterial peptide pheromones are species-specific signaling molecules that can transverse the cell wall and bind to the cognate membrane receptors with high affinities (Xu et al., 2020). The

effectivity and high specificity of these pheromone-containing hybrid AMPs have been widely investigated elsewhere (Eckert et al., 2006a; Mai et al., 2011; Qiu et al., 2003; Xu et al., 2020).

Nonetheless, despite the high selectivity of these hybrid peptides, non-specific bactericidal effects are still observed is some cases. Indeed, in the STAMPs strategy, the killing component of these fusion peptides remains unchanged, being then able to interact via electrostatic interaction with the negatively charged membrane components. This fact may explain the untargeted bactericidal effects. In this context, the rational redesign of the constituent components in those hybrid peptides could be a complementary approach. In 2020, Xu et al. (2020) enhanced the target specificity of a pheromone-containing hybrid peptide by decreasing the net positive charge within the killing domain from (+6) to (+4). This modification did not affect the membrane permeabilization activity and therefore, their antimicrobial effect remained unaltered (Xu et al., 2020).

6. pH-responsive AMP-based systems

During bacterial infection, the accumulation of metabolic-derived acidic compounds may induce a pH decrease at infection sites (pH 5.5) (Chen et al., 2020; Gontsarik et al., 2019; Pranantyo et al., 2019). This fact provides an opportunity to design pH-responsive antimicrobial nanosystems able to display selective bactericidal effects at infection sites while remain stealthy under physiological conditions (pH 7.4) (Pranantyo et al., 2019). The development of AMP-based pH-targeted delivery systems have been previously investigated in the context of anticancer therapies (Cao et al., 2017). However, just few studies have evaluated their functionality for antibacterial purposes.

In a recent study, Pranantyo et al. (2019) designed a pH-switchable negative to positive nanosystem consisting on AMP-coated gold nanoclusters functionalized with citraconic anhydride (Fig. 4A). This anionic compound interacted with the cationic amines of the peptide, switching from positive to negative net charge. Under acidic condition, citraconyl amides are easily hydrolyzed switching to cationic mode and displaying the antimicrobial effect (Pranantyo et al., 2019). In a similar study, Gontsarik et al. (2019) designed a pH-responsive lipid-based nanocarrier based on the self-assembly of oleic acid with the antimicrobial peptide LL-37 (Fig. 4B). This combination led to peptide coated cylindrical micelles, which showed negligible antimicrobial activity at physiological pH (pH 7.0). However, under acidic environments (pH 5.0), the gradual protonation of the oleic acid induced the oligomerization of the cylindrical micelles into superior structures (branched thread micelles and aggregates), which showed increased antimicrobial activity (Gontsarik et al., 2019). Recently, Chen et al. (2020) developed a smart delivery system based on AMP loaded titanium nanotubes that in acidic conditions behaves like a Pandora's box (Fig. 4C). In this approach, poly (methacrylic acid) (PMAA) served as a pH-responsive molecular gate, which under physiological conditions (pH 7.4) could swell to close the opening of the nanotubes. However, when bacterial infection occurs (pH < 6.0) it collapses, leading to a sustainable delivery of the AMPs to ultimately kill bacteria (Chen et al., 2020).

The afore mentioned strategies involve the use of interfaces as carriers for the delivery of antimicrobial peptides that may raise biocompatibility concerns. At the same time, in most cases, the pH-dependent behavior is provided by the close interaction with other intermediate compounds, which imply an increased complexity during manufacturing. Therefore, the design of peptide-only pH-responsive antimicrobials is highly desirable in order to reduce all possible disadvantages of other materials. In this context, Xiong et al. (2017) developed a pH-sensitive antimicrobial polypeptide able to undergo a transition from random coiled to helical conformation under acidic pH. The polypeptide exhibited potent antimicrobial activity against *H. pylori* under the acidic environment of the stomach, while showed low toxicity against normal tissues and commensal bacteria at neutral pH

8

Table 4
Summary of the different antimicrobial and targeting peptides employed in STAMPs strategy.

Killing domain			Targeting domain		Hybrid peptide[a]	MIC (μM)	Target	ref
Name	Sequence	MIC (μM)	Name	Sequence				
novispirin G10	KNLRRIIRKGIHIIKKYG	2.6	KH	KKHRKHRKHRKH	KKHRKHRKHRKH**GGGSGGS**KNLRRIIRKGIHIIKKYG	2.8	*Pseudomonas spp.*	(Eckert et al., 2006b)
G2	KNLRIIRKGIHIIKKY	12.1	CSP_C16	TFFRLFNRSFTQALGK	TFFRLFNRSFTQALGK**GGG**KNLRIIRKGIHIIKKY	3.0	*Streptococcus mutans*	(Eckert et al., 2006a)
			CSP_MB	TFFRLFNR	TFFRLFNR**GGG**KNLRIIRKGIHIIKKY	3.2		
S6L3–33	FKKFWKWFRRF	7.0	CSP_C16	TFFRLFNRSFTQALGK	TRRRLFNRSFTQALGK**SGGG**FKKFWKWFRRF	2.5		
			CSP_MB	TFFRLFNR	TFFRLFNR**SGGG**FKKFWKWFRRF	2.5		
BD2.20	FIRKFLKWLL	14.4	KH	KKHRKHRKHRKH	TFFRLFNR**GGG-K**FIRKFLKKWLL KKHRKHRKHRKH**GGG**	11.9	*Pseudomonas aeruginosa* / *Streptococcus mutans*	(He et al., 2009)
		2.8	CSP_MB	TFFRLFNR		6.2		
NRC-4	GWGSFFKKAAHVGKL	1.0	CSP	TFFRLFNR	TFFRLFNR**GGG**WGSFFKKAAHVGKL	2.8	*Streptococcus mutans*	(Mai et al., 2011)
GNU7	RLLRPLLQLLKQKLR	16–32	Syn	GLRRLLRKIRGRWK	GLRRLLRKIRGRWK**GGG**RLLRPLLQLLKQKLR	0.5–1	Gram-negative bacteria	(Kim et al., 2016)
N6	GFAWNVCVYRNGVRVCHRRAN	0.4	LBP14	RVQGRWKVRASFFK	RVQGRWKVRASFFK**EAAAKEAAAK**GFAWNV CVYRNGVRVCHRRAN	1.5	*Escherichia coli*	(Wang et al., 2020)
GNU7	RLLRPLLQLLKQKLR	32	PA2	SQRKLAAKLTSK	SQRKLAAKLTSK**GGG**RLLRPLLQLLKQKLR	2.0	*Pseudomonas aeruginosa*	(Kim et al., 2020)
plectasin	GFGCGNPWDEDDMQCHNHC KSIKGYKGGYCAKGGFVCKCY	9–19	A12C	VHMVAGPGREPT	VHMVAGPGREPT**GGGHMG**FGCNGPWDED DMQCHNHCKSIKGYKGGYCAKGGFVCKCY	7–25	*Staphylococcus spp.*	(Choudhury et al., 2020)
eurocin	GFGCPGDAYQCSEHCRALGG GRTGGYCAGPWYLGHPTCTCSF	6–12			VHMVAGPGREPT**GGGHMG**FGCPGDAYQC SEHCRALGGGRTGGYCAGPWYLGHPTCTCSF	8–24		
C4	WKWKWENGKWKWKW	64	cCF10	LVTLVFV	LVTLVFV**GGG**WKWKWENGKWKWKW	8	*Enterococcus faecalis*	(Xu et al., 2020)

[a] Linker peptides inside the hybrid designs are indicated in bold.
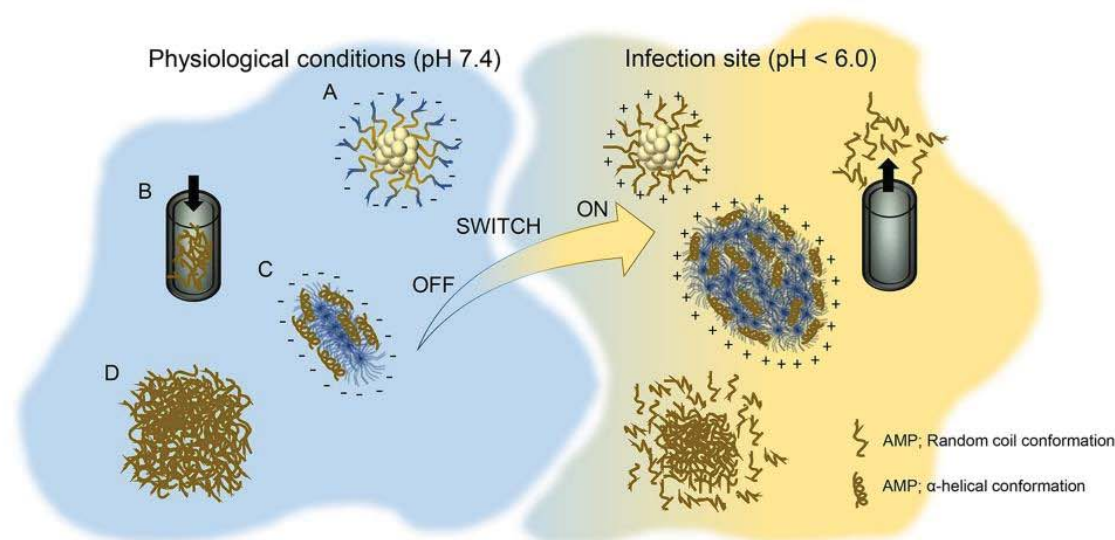
Fig. 4. Scheme of the most representative AMP-based pH-responsive strategies. pH transitional modifications from inactive (left, neutral pH) to active (right, acidic pH) are shown. A. AMP coated gold nanoclusters (AuNCs) functionalized with citraconic anhydride (Pranantyo et al., 2019). B. AMP loaded titanium nanotubes (Ti-NTs) sealed with poly (methacrylic acid) (Chen et al., 2020). C. AMP-coated cylindrical micelles (Gontsarik et al., 2019). D. AMP consisting in supramolecular hydrogels (Wang et al., 2019a). (For interpretation of the references to colour in this figure legend, the reader is referred to the web version of this article.)

(Xiong et al., 2017). However, despite the high conditional specificity, these *de novo* designed polypeptides are still subjected to the traditional drawbacks associated with the applications of AMP *in vivo*, and therefore an engineering approach should be provided in order to gain nanoscale size. Interestingly, Wang et al. (2019a) designed a pH-responsive conformation transitional peptide, able to self-assemble into hydrogels (Fig. 4D). The *de novo* designed octapeptide IKFQFHFD combined two properties, namely the adoption of a molecular structure similar to that of AMP in acidic conditions (pH 5.5) and the ability to self-assemble at neutral pH (pH 7.4). This fact resulted in the formation of pH-switchable supramolecular hydrogels able to remain biocompatible at physiological pH and to disassemble on demand under acidic conditions, releasing the peptide, which possesses antimicrobial activity at such acidic pH (Wang et al., 2019b).

7. Conclusion

The development of novel drugs against multidrug resistant bacterial pathogens is an unquestionable and urgent need. Natural and synthetic antimicrobial peptides are proposed as a potential and valuable alternative to conventional antibiotics. However, poor pharmacokinetic profiles and associated side toxicities have compromised the generic applicability of these compounds. The application of nanotechnologies to AMP development, while highly promising, has so far offered moderate improvements and rendered still insufficiently competent drugs. This is mainly due to the limited biocompatibility of the materials used as nanocarrier systems and to their undesired harmful effects. In this context, some emerging bioengineering concepts open a door to the generic design of nanostructured drugs in absence of carriers. In this context, peptide-based materials resulting from the regulated self-assembling of individual protein segments simultaneously provide optimal nanoscale size, multivalent display of the functional peptide and a potent antimicrobial activity. Then, a relevant number of self-assembling strategies have already proved the feasibility to recruit such high functional complexity in structurally simple protein-based entities. The expanding catalogues of self-assembling protein domains, AMPs and targeting ligands, together with newly developed nanobiotechnological approaches, are expected to result, in a short term, in a

new generation of rationally optimized antimicrobial drugs. Such constructs might be excellent competitors or even full alternatives to conventional antibiotics in the biopharma market for safer, highly efficient and more selective treatments of bacterial infection.

Declaration of Competing Interest

The authors declare no conflict of interest.

References

Shankar, P., 2016. Book review: tackling drug-resistant infections globally. Arch. Pharm. Pract. 7, 110. https://doi.org/10.4103/2045-080x.186181.

AB Naafs, M., 2018. The antimicrobial peptides: ready for clinical trials? Biomed. J. Sci. Tech. Res. 7, 6038–6042. https://doi.org/10.26717/bjstr.2018.07.001536.

Abdulkhaleq, L.A., Assi, M.A., Abdullah, R., Zamri-Saad, M, Taufiq-Yap, Y.H., Hezmee, M.N.M., 2018. The crucial roles of inflammatory mediators in inflammation: a review. Vet. World 11, 627–635. https://doi.org/10.14202/vetworld.2018.627-635.

Aderibigbe, B.A., 2017. Metal-based nanoparticles for the treatment of infectious diseases. Molecules 22, 1370. https://doi.org/10.3390/molecules22081370.

Al Tall, Y., Abualhaijaa, A., Alsaggar, M., Almaaytah, A., Masadeh, M., Alzoubi, K.H., 2019. Design and characterization of a new hybrid peptide from LL-37 and BMAP-27. Infect. Drug Resist. 12, 1035–1045. https://doi.org/10.2147/IDR.S199473.

Assali, M., Zaid, A.N., Abdallah, F., Almasri, M., Khayyat, R., 2017. Single-walled carbon

10

nanotubes-ciprofloxacin nanoantibiotic: strategy to improve ciprofloxacin antibacterial activity. Int. J. Nanomedicine 12, 6647–6659. https://doi.org/10.2147/IJN.S140625.

Azzopardi, E.A., Ferguson, E.L., Thomas, D.W., 2013. The enhanced permeability retention effect: a new paradigm for drug targeting in infection. J. Antimicrob. Chemother. 68, 257–274. https://doi.org/10.1093/jac/dks379.

Bechinger, B., Gorr, S.U., 2017. Antimicrobial peptides: mechanisms of action and resistance. J. Dent. Res. 96, 254–260. https://doi.org/10.1177/0022034516679973.

Blasi, P., 2019. Poly(lactic acid)/poly(lactic-co-glycolic acid)-based microparticles: an overview. J. Pharm. Investig. 49, 337–346. https://doi.org/10.1007/s40005-019-00453-z.

Caniaux, I., van Belkum, A., Zambardi, G., Poirel, L., Gros, M.F., 2017. MCR: modern colistin resistance. Eur. J. Clin. Microbiol. Infect. Dis. 36, 415–420. https://doi.org/10.1007/s10096-016-2846-y.

Cao, J., Zhang, Y., Shan, Y., Wang, J., Liu, F., Liu, H., Xing, G., Lei, J., Zhou, J., 2017. A pH-dependent antibacterial peptide release nano-system blocks tumor growth in vivo without toxicity. Sci. Rep. 7, 1–13. https://doi.org/10.1038/s41598-017-11687-y.

Carmona-Ribeiro, A.M., 2018. Self-assembled antimicrobial nanomaterials. Int. J. Environ. Res. Public Health 15, 1408. https://doi.org/10.3390/ijerph15071408.

Cavanaugh, C., Moeckel, G.W., Perazella, M.A., 2019. Telavancin - associated acute kidney injury. Clin. Nephrol. 91, 187–191. https://doi.org/10.5414/CN109651.

Chen, C.H., Lu, T.K., 2020. Development and challenges of antimicrobial peptides for therapeutic applications. Antibiotics 9, 24. https://doi.org/10.3390/antibiotics9010024.

Chen, W., Yang, S., Li, S., Lang, J.C., Mao, C., Kroll, P., Tang, L., Dong, H., 2019. Self-assembled peptide nanofibers display natural antimicrobial peptides to selectively kill bacteria without compromising cytocompatibility. ACS Appl. Mater. Interfaces 11, 28681–28689. https://doi.org/10.1021/acsami.9b09583.

Chen, J., Shi, X., Zhu, Y., Chen, Y., Gao, M., Gao, H., Liu, L., Wang, L., Mao, C., Wang, Y., 2020. On-demand storage and release of antimicrobial peptides using Pandora's box-like nanotubes gated with a bacterial infection-responsive polymer. Theranostics 10, 109–122. https://doi.org/10.7150/thno.38388.

Chiesa, G., Kiriakov, S., Khalil, A.S., 2020. Protein assembly systems in natural and synthetic biology. BMC Biol. 18, 1–18. https://doi.org/10.1186/s12915-020-0751-4.

Choudhury, A., Islam, S.M.A., Ghidey, M.R., Kearney, C.M., 2020. Repurposing a drug targeting peptide for targeting antimicrobial peptides against Staphylococcus. Biotechnol. Lett. 42, 287–294. https://doi.org/10.1007/s10529-019-02779-y.

Chung, P.Y., Khanum, R., 2017. Antimicrobial peptides as potential anti-biofilm agents against multidrug-resistant bacteria. J. Microbiol. Immunol. Infect. 50, 405–410. https://doi.org/10.1016/j.jmii.2016.12.005.

De Frates, K., Markiewicz, T., Gallo, P., Rack, A., Weyhmiller, A., Jarmusik, B., Hu, X., 2018. Protein polymer-based nanoparticles: fabrication and medical applications. Int. J. Mol. Sci. 19, 1–20. https://doi.org/10.3390/ijms19061717.

Di, Y.P., Lin, Q., Chen, C., Montelaro, R.C., Doi, Y., Deslouches, B., 2020. Enhanced therapeutic index of an antimicrobial peptide in mice by increasing safety and activity against multidrug-resistant bacteria. Sci. Adv. 6. https://doi.org/10.1126/sciadv.aay6817.

Dong, N., Li, X.R., Xu, X.Y., Lv, Y.F., Li, Z.Y., Shan, A.S., Wang, J.L., 2018. Characterization of bactericidal efficiency, cell selectivity, and mechanism of short interspecific hybrid peptides. Amino Acids 50, 453–468. https://doi.org/10.1007/s00726-017-2531-1.

Dube, A., 2019. Nanomedicines for infectious diseases. Pharm. Res. 36, 10–11. https://doi.org/10.1007/s11095-019-2603-x.

Dusinska, M., Tulinska, J., El Yamani, N., Kuricova, M., Liskova, A., Rollerova, E., Rundén-Pran, E., Smolkova, B., 2017. Immunotoxicity, genotoxicity and epigenetic toxicity of nanomaterials: new strategies for toxicity testing? Food Chem. Toxicol. 109, 797–811. https://doi.org/10.1016/j.fct.2017.08.030.

Eckert, R., He, J., Yarbrough, D.K., Qi, F., Anderson, M.H., Shi, W., 2006a. Targeted killing of Streptococcus mutans by a pheromone-guided "smart" antimicrobial peptide. Antimicrob. Agents Chemother. 50, 3651–3657. https://doi.org/10.1128/AAC.00622-06.

Eckert, R., Qi, F., Yarbrough, D.K., He, J., Anderson, M.H., Shi, W., 2006b. Adding selectivity to antimicrobial peptides: rational design of a multidomain peptide against Pseudomonas spp. Antimicrob. Agents Chemother. 50, 1480–1488. https://doi.org/10.1128/AAC.50.4.1480-1488.2006.

Elsabahy, M., Wooley, K.L., 2013. Cytokines as biomarkers of nanoparticle immunotoxicity. Chem. Soc. Rev. 42, 5552–5576. https://doi.org/10.1039/c3cs60064e.

Feliu, N., Docter, D., Heine, M., Del Pino, P., Ashraf, S., Kolosnjaj-Tabi, J., Macchiarini, P., Nielsen, P., Alloyeau, D., Gazeau, F., Stauber, R.H., Parak, W.J., 2016. In vivo degeneration and the fate of inorganic nanoparticles. Chem. Soc. Rev. 45, 2440–2457. https://doi.org/10.1039/c5cs00699f.

Fenaroli, F., Repnik, U., Xu, Y., Johann, K., Van Herck, S., Dey, P., Skjeldal, F.M., Frei, D.M., Bagherifam, S., Kocere, A., Haag, R., De Geest, B.G., Barz, M., Russell, D.G., Griffiths, G., 2018. Enhanced permeability and retention-like extravasation of nanoparticles from the vasculature into tuberculosis granulomas in zebrafish and mouse models. ACS Nano 12, 8646–8661. https://doi.org/10.1021/acsnano.8b04433.

Franco, A.R., Palma Kimmerling, E., Silva, C., Rodrigues, F.J., Leonor, I.B., Reis, R.L., Kaplan, D.L., 2018. Silk-based antimicrobial polymers as a new platform to design drug-free materials to impede microbial infections. Macromol. Biosci. 18, 1–15. https://doi.org/10.1002/mabi.201800262.

Fuentes, A., Pineda, M., Venkata, K., 2018. Comprehension of top 200 prescribed drugs in the US as a resource for pharmacy teaching, training and practice. Pharmacy 6, 43. https://doi.org/10.3390/pharmacy6020043.

Gagnon, M.C., Strandberg, E., Grau-Campistany, A., Wadhwani, P., Reichert, J., Bürck, J., Rabanal, F., Auger, M., Paquin, J.F., Ulrich, A.S., 2017. Influence of the length and

charge on the activity of α-helical amphipathic antimicrobial peptides. Biochemistry 56, 1680–1695. https://doi.org/10.1021/acs.biochem.6b01071.

Glover, D.J., Clark, D.S., 2016. Protein calligraphy: a new concept begins to take shape. ACS Cent. Sci. 2, 438–444. https://doi.org/10.1021/acscentsci.6b00067.

Goel, R., Garg, C., Gautam, H.K., Sharma, A.K., Kumar, P., Gupta, A., 2018. Fabrication of cationic nanostructures from short self-assembling amphiphilic mixed α/β-pentapeptide: potential candidates for drug delivery, gene delivery, and antimicrobial applications. Int. J. Biol. Macromol. 111, 880–893. https://doi.org/10.1016/j.ijbiomac.2018.01.079.

Gong, Z., Pei, X., Ren, S., Chen, X., Wang, L., Ma, C., Xi, X., Chen, T., Shaw, C., Zhou, M., 2020. Identification and rational design of a novel antibacterial peptide dermaseptin-AC from the skin secretion of the red-eyed tree frog Agalychnis callidryas. Antibiotics 9, 243. https://doi.org/10.3390/antibiotics9050243.

Gontsarik, M., Yaghmur, A., Ren, Q., Maniura-Weber, K., Salentinig, S., 2019. From structure to function: pH-switchable antimicrobial nano-self-assemblies. ACS Appl. Mater. Interfaces 11, 2821–2829. https://doi.org/10.1021/acsami.8b18618.

Hallaj-Nezhadi, S., Hassan, M., 2015. Nanoliposome-based antibacterial drug delivery. Drug Deliv. 22, 581–589. https://doi.org/10.3109/10717544.2013.863409.

He, J., Anderson, M.H., Shi, W., Eckert, R., 2009. Design and activity of a "dual-targeted" antimicrobial peptide. Int. J. Antimicrob. Agents 33, 532–537. https://doi.org/10.1016/j.ijantimicag.2008.11.013.

Higashi, Y., Nakamura, S., Tsuji, Y., Ogami, C., Matsumoto, K., Kawago, K., Tokui, K., Hayashi, R., Sakamaki, I., Yamamoto, Y., 2018. Daptomycin-induced eosinophilic pneumonia and a review of the published literature. Intern. Med. 57, 253–258. https://doi.org/10.2169/internalmedicine.9010-17.

Hirenkumar, M., Steven, S., 2012. Poly lactic-co-glycolic acid (PLGA) as biodegradable controlled drug delivery carrier. Polymers (Basel). 3, 1–19. https://doi.org/10.3390/polym3031377.Poly.

Hong, W., Zhao, Y., Guo, Y., Huang, C., Qiu, P., Zhu, J., Chu, C., Shi, H., Liu, M., 2018. PEGylated self-assembled nano-bacitracin A: probing the antibacterial mechanism and real-time tracing of target delivery in vivo. ACS Appl. Mater. Interfaces 10, 10688–10705. https://doi.org/10.1021/acsami.8b00135.

Huh, A.J., Kwon, Y.J., 2011. "Nanoantibiotics": a new paradigm for treating infectious diseases using nanomaterials in the antibiotics resistant era. J. Control. Release 156, 128–145. https://doi.org/10.1016/j.jconrel.2011.07.002.

Hutchinson, J.A., Burholt, S., Hamley, I.W., 2017. Peptide hormones and lipopeptides: from self-assembly to therapeutic applications. J. Pept. Sci. 23, 82–94. https://doi.org/10.1002/psc.2954.

Jia, F., Wang, J., Peng, J., Zhao, P., Kong, Z., Wang, K., Yan, W., Wang, R., 2017. D-amino acid substitution enhances the stability of antimicrobial peptide polybia-CP. Acta Biochim. Biophys. Sin. Shanghai 49, 916–925. https://doi.org/10.1093/abbs/gmx091.

Jiang, J., Qian, K., Liu, G., Sun, L., Zhou, G., Li, J., Fang, X., Ge, H., Lv, Z., 2019. Design and activity study of a melittin–thanatin hybrid peptide. AMB Express 9, 14. https://doi.org/10.1186/s13568-019-0739-z.

Kang, H.K., Kim, C., Seo, C.H., Park, Y., 2017. The therapeutic applications of antimicrobial peptides (AMPs): a patent review. J. Microbiol. 55, 1–12. https://doi.org/10.1007/s12275-017-6452-1.

Kang, X., Dong, F., Shi, C., Liu, S., Sun, J., Chen, J., Li, H., Xu, H., Lao, X., Zheng, H., 2019. DRAMP 2.0, an updated data repository of antimicrobial peptides. Sci. Data 6, 148. https://doi.org/10.1038/s41597-019-0154-y.

Karaiskos, I., Souli, M., Galani, I., Giamarellou, H., 2017. Colistin: still a lifesaver for the 21st century? Expert Opin. Drug Metab. Toxicol. 13, 59–71. https://doi.org/10.1080/17425255.2017.1230200.

Kido, K., Oyen, A.A., Beckmann, M.A., Brouse, S.D., 2019. Musculoskeletal toxicities in patients receiving concomitant statin and daptomycin therapy. Am. J. Heal. Pharm. 76, 206–210. https://doi.org/10.1093/ajhp/zxy036.

Kim, H., Jang, J.H., Kim, S.C., Cho, J.H., 2016. Enhancement of the antimicrobial activity and selectivity of GNU7 against Gram-negative bacteria by fusion with LPS-targeting peptide. Peptides 82, 60–66. https://doi.org/10.1016/j.peptides.2016.05.010.

Kim, H., Jang, J.H., Kim, S.C., Cho, J.H., 2020. Development of a novel hybrid antimicrobial peptide for targeted killing of Pseudomonas aeruginosa. Eur. J. Med. Chem. 185, 111814. https://doi.org/10.1016/j.ejmech.2019.111814.

Konai, M.M., Bhattacharjee, B., Ghosh, S., Haldar, J., 2018. Recent progress in polymer research to tackle infections and antimicrobial resistance. Biomacromolecules 19, 1888–1917. https://doi.org/10.1021/acs.biomac.8b00458.

Koo, H.B., Seo, J., 2019. Antimicrobial peptides under clinical investigation. Pept. Sci. 111, e24122. https://doi.org/10.1002/pep2.24122.

Kumar, P., Kizhakkedathu, J.N., Straus, S.K., 2018. Antimicrobial peptides: diversity, mechanism of action and strategies to improve the activity and biocompatibility in vivo. Biomolecules 8, 4. https://doi.org/10.3390/biom8010004.

Lei, J., Sun, L.C., Huang, S., Zhu, C., Li, P., He, J., Mackey, V., Coy, D.H., He, Q.Y., 2019. The antimicrobial peptides and their potential clinical applications. Am. J. Transl. Res. 11, 3919–3931.

Li, Y., Wu, M., Chang, Q., Zhao, X., 2018. Stapling strategy enables improvement of antitumor activity and proteolytic stability of host-defense peptide hymenochirin-1B. RSC Adv. 8, 22268–22275. https://doi.org/10.1039/c8ra03446j.

Li, Y., Zhang, Y., Wu, M., Chang, Q., Hu, H., Zhao, X., 2019. Improving selectivity, proteolytic stability, and antitumor activity of hymenochirin-1B: a novel glycosylated staple strategy. ACS Chem. Biol. 14, 516–525. https://doi.org/10.1021/acschembio.9b00046.

Li, H., Hu, Y., Pu, Q., He, T., Zhang, Q., Wu, W., Xia, X., Zhang, J., 2020. Novel stapling by lysine tethering provides stable and low hemolytic cationic antimicrobial peptides. J. Med. Chem. 63, 4081–4089. https://doi.org/10.1021/acs.jmedchem.9b02025.

Liscano, Y., Salamanca, C.H., Vargas, L., Cantor, S., Laverde-Rojas, V., Oñate-Garzón, J., 2019. Increases in hydrophilicity and charge on the polar face of alyteserin 1c helix

change its selectivity towards gram-positive bacteria. Antibiotics 8, 1–16. https://doi.org/10.3390/antibiotics8040238.

Liu, R., Hudalla, G.A., 2019. Using self-assembling peptides to integrate biomolecules into functional supramolecular biomaterials. Molecules 24, 15–21. https://doi.org/10.3390/molecules24081450.

Liu, S., Long, Q., Xu, Y., Wang, J., Xu, Z., Wang, L., Zhou, M., Wu, Y., Chen, T., Shaw, C., 2017. Assessment of antimicrobial and wound healing effects of Brevinin-2Ta against the bacterium Klebsiella pneumoniae in dermally-wounded rats. Oncotarget 8, 111369–111385. https://doi.org/10.18632/oncotarget.22797.

Liu, Y., Du, Q., Ma, C., Xi, X., Wang, L., Zhou, M., Burrows, J.F., Chen, T., Wang, H., 2019. Structure–activity relationship of an antimicrobial peptide, phylloseptin-PHa: balance of hydrophobicity and charge determines the selectivity of bioactivities. Drug Des. Devel. Ther. 13, 447–458. https://doi.org/10.2147/DDDT.S191072.

Lombardi, L., Falanga, A., Del Genio, V., Galdiero, S., 2019a. A new hope: self-assembling peptides with antimicrobial activity. Pharmaceutics 11, 166. https://doi.org/10.3390/pharmaceutics11040166.

Lombardi, L., Shi, Y., Falanga, A., Galdiero, E., De Alteriis, E., Franci, G., Chourpa, I., Azevedo, H.S., Galdiero, S., 2019b. Enhancing the potency of antimicrobial peptides through molecular engineering and self-assembly. Biomacromolecules 20, 1362–1374. https://doi.org/10.1021/acs.biomac.8b01740.

López Cascales, J.J., Zenak, S., García De La Torre, J., Lezama, O.G., Garro, A., Enriz, R.D., 2018. Small cationic peptides: influence of charge on their antimicrobial activity. ACS Omega 3, 5390–5398. https://doi.org/10.1021/acsomega.8b00293.

López-Laguna, H., Unzueta, U., Conchillo-Solé, O., Sánchez-Chardi, A., Pesarrodona, M., Cano-Garrido, O., Voltà, E., Sánchez-García, L., Serna, N., Saccardo, P., Mangues, R., Villaverde, A., Vázquez, E., 2019. Assembly of histidine-rich protein materials controlled through divalent cations. Acta Biomater. 83, 257–264. https://doi.org/10.1016/j.actbio.2018.10.030.

López-Laguna, H., Sánchez-García, L., Serna, N., Voltà-Duran, E., Sánchez, J.M., Sánchez-Chardi, A., Unzueta, U., Łoś, M., Villaverde, A., Vázquez, E., 2020. Engineering protein nanoparticles out from components of the human microbiome engineering. Small. https://doi.org/10.1002/smll.202001885. in press.

Mahlapuu, M., Håkansson, J., Ringstad, L., Björn, C., 2016. Antimicrobial peptides: an emerging category of therapeutic agents. Front. Cell. Infect. Microbiol. 6, 1–12. https://doi.org/10.3389/fcimb.2016.00194.

Mai, J., Tian, X.L., Gallant, J.W., Merkley, N., Biswas, Z., Syvitski, R., Douglas, S.E., Ling, J., Li, Y.H., 2011. A novel target-specific, salt-resistant antimicrobial peptide against the cariogenic pathogen Streptococcus mutans. Antimicrob. Agents Chemother. 55, 5205–5213. https://doi.org/10.1128/AAC.05175-11.

Mamatha, H.G., Shanthi, V., 2018. Baseline resistance and cross-resistance among fluoroquinolones in multidrug-resistant Mycobacterium tuberculosis isolates at a national reference laboratory in India. J. Glob. Antimicrob. Resist. 12, 5–10. https://doi.org/10.1016/j.jgar.2017.08.014.

Martin-Serrano, Á., Gómez, R., Ortega, P., La Mata, F.J.D., 2019. Nanosystems as vehicles for the delivery of antimicrobial peptides (Amps). Pharmaceutics 11, 1–24. https://doi.org/10.3390/pharmaceutics11090448.

McCloskey, A.P., Draper, E.R., Gilmore, B.F., Laverty, G., 2017. Ultrashort self-assembling Fmoc-peptide gelators for anti-infective biomaterial applications. J. Pept. Sci. 23, 131–140. https://doi.org/10.1002/psc.2951.

Melchionna, M., Styan, K., Marchesan, S., 2016. The unexpected advantages of using D-amino acids for peptide self-assembly into nanostructured hydrogels for medicine. Curr. Top. Med. Chem. 16, 2009–2018. https://doi.org/10.2174/1568026616666160215155136.

Mhlwatika, Z., Aderibigbe, B.A., 2018. Application of dendrimers for the treatment of infectious diseases. Molecules 23, 2205. https://doi.org/10.3390/molecules23092205.

Morrisette, T., Miller, M.A., Montague, B.T., Barber, G.R., McQueen, R.B., Krsak, M., 2019. On- and off-label utilization of dalbavancin and oritavancin for Gram-positive infections. J. Antimicrob. Chemother. 74, 2405–2416. https://doi.org/10.1093/jac/dkz162.

Mwangi, J., Hao, X., Lai, R., Zhang, Z.Y., 2019a. Antimicrobial peptides: new hope in the war against multidrug resistance. Zool. Res. 40, 488–505. https://doi.org/10.24272/j.issn.2095-8137.2019.062.

Mwangi, J., Hao, X., Lai, R., Zhang, Z.Y., 2019b. Antimicrobial peptides: new hope in the war against multidrug resistance. Zool. Res. 40, 488–505. https://doi.org/10.24272/j.issn.2095-8137.2019.062.

Ng, S.M.S., Yap, J.M., Lau, Q.Y., Ng, F.M., Ong, E.H.Q., Barkham, T., Teo, J.W.P., Alfatah, M., Kong, K.W., Hoon, S., Arumugam, P., Hill, J., Chia, C.S.B., 2018. Structure-activity relationship studies of ultra-short peptides with potent activities against fluconazole-resistant Candida albicans. Eur. J. Med. Chem. 150, 479–490. https://doi.org/10.1016/j.ejmech.2018.03.027.

Nisini, R., Poerio, N., Mariotti, S., De Santis, F., Fraziano, M., 2018. The multirole of liposomes in therapy and prevention of infectious diseases. Front. Immunol. 9, 155. https://doi.org/10.3389/fimmu.2018.00155.

Oliva, R., Chino, M., Pane, K., Pistorio, V., De Santis, A., Pizzo, E., D'Errico, G., Pavone, V., Lombardi, A., Del Vecchio, P., Notomista, E., Nastri, F., Petraccone, L., 2018. Exploring the role of unnatural amino acids in antimicrobial peptides. Sci. Rep. 8, 1–16. https://doi.org/10.1038/s41598-018-27231-5.

Otvos, L., 2016. Immunomodulatory effects of anti-microbial peptides. Acta Microbiol. Immunol. Hung. 63, 257–277. https://doi.org/10.1556/030.63.2016.005.

Pedron, C.N., de Oliveira, C.S., da Silva, A.F., Andrade, G.P., da Silva Pinhal, M.A., Cerchiaro, G., da Silva Junior, P.I., da Silva, F.D., Torres, M.D.T., Oliveira, V.X., 2019. The effect of lysine substitutions in the biological activities of the scorpion venom peptide VmCT1. Eur. J. Pharm. Sci. 136, 104952. https://doi.org/10.1016/j.ejps.2019.06.006.

Porter, S.L., Coulter, S.M., Pentlavalli, S., Thompson, T.P., Laverty, G., 2018. Self-

assembling diphenylalanine peptide nanotubes selectively eradicate bacterial biofilm infection. Acta Biomater. 77, 96–105. https://doi.org/10.1016/j.actbio.2018.07.033.

Pranantyo, D., Liu, P., Zhong, W., Kang, E.T., Chan-Park, M.B., 2019. Antimicrobial peptide-reduced gold nanoclusters with charge-reversal moieties for bacterial targeting and imaging. Biomacromolecules 20, 2922–2933. https://doi.org/10.1021/acs.biomac.9b00392.

Qiu, X.Q., Wang, H., Lu, X.F., Zhang, J., Li, S.F., Cheng, G., Wan, L., Yang, L., Zuo, J.Y., Zhou, Y.Q., Wang, H.Y., Cheng, X., Zhang, S.H., Ou, Z.R., Zhong, Z.C., Cheng, J.Q., Li, Y.P., Wu, G.Y., 2003. An engineered multidomain bactericidal peptide as a model for targeted antibiotics against specific bacteria. Nat. Biotechnol. 21, 1480–1485. https://doi.org/10.1038/nbt913.

Qiu, F., Chen, Y., Tang, C., Zhao, X., 2018. Amphiphilic peptides as novel nanomaterials: design, self-assembly and application. Int. J. Nanomedicine 13, 5003–5022. https://doi.org/10.2147/IJN.S166403.

Radaic, A., de Jesus, M.B., Kapila, Y.L., 2020. Bacterial anti-microbial peptides and nanosized drug delivery systems: the state of the art toward improved bacteriocins. J. Control. Release 321, 100–118. https://doi.org/10.1016/j.jconrel.2020.02.001.

Raheem, N., Straus, S.K., 2019. Mechanisms of action of antimicrobial peptides with antibacterial and antibiofilm functions. Front. Microbiol. 10, 1–14. https://doi.org/10.3389/fmicb.2019.02866.

Rončević, T., Vukičević, D., Krce, L., Benincasa, M., Aviani, I., Maravić, A., Tossi, A., 2019. Selection and redesign for high selectivity of membrane-active antimicrobial peptides from a dedicated sequence/function database. Biochim. Biophys. Acta Biomembr. 1861, 827–834. https://doi.org/10.1016/j.bbamem.2019.01.017.

Rozek, A., Powers, J.P.S., Friedrich, C.L., Hancock, R.E.W., 2003. Structure-based design of an indolicidin peptide analogue with increased protease stability. Biochemistry 42, 14130–14138. https://doi.org/10.1021/bi035643g.

Sanchez, J.M., López-Laguna, H., Álamo, P., Serna, N., Sánchez-Chardi, A., Nolan, V., Cano-Garrido, O., Casanova, I., Unzueta, U., Vazquez, E., Mangues, R., Villaverde, A., 2020. Artificial inclusion bodies for clinical development. Adv. Sci. 7, 1902420. https://doi.org/10.1002/advs.201902420.

Schnaider, L., Brahmachari, S., Schmidt, N.W., Mensa, B., Shaham-Niv, S., Bychenko, D., Adler-Abramovich, L., Shimon, L.J.W., Kolusheva, S., Degrado, W.F., Gazit, E., 2017. Self-assembling dipeptide antibacterial nanostructures with membrane disrupting activity. Nat. Commun. 8, 1365. https://doi.org/10.1038/s41467-017-01447-x.

Serna, N., Sánchez-García, L., Sánchez-Chardi, A., Unzueta, U., Roldán, M., Mangues, R., Vázquez, E., Villaverde, A., 2017. Protein-only, antimicrobial peptide-containing recombinant nanoparticles with inherent built-in antibacterial activity. Acta Biomater. 60, 256–263. https://doi.org/10.1016/j.actbio.2017.07.027.

Serna, N., Sánchez-García, L., Unzueta, U., Díaz, R., Vázquez, E., Mangues, R., Villaverde, A., 2018. Protein-based therapeutic killing for cancer therapies. Trends Biotechnol. 36, 318–335. https://doi.org/10.1016/j.tibtech.2017.11.007.

Serna, N., Sánchez, J.M., Unzueta, U., Sánchez-García, L., Sánchez-Chardi, A., Mangues, R., Vázquez, E., Villaverde, A., 2019. Recruiting potent membrane penetrability in tumor cell-targeted protein-only nanoparticles. Nanotechnology 30, 115101. https://doi.org/10.1088/1361-6528/aaf959.

Shao, C., Zhu, Y., Lai, Z., Tan, P., Shan, A., 2019. Antimicrobial peptides with protease stability: progress and perspective. Future Med. Chem. 11, 2047–2050. https://doi.org/10.4155/fmc-2019-0167.

Shen, Z., Guo, Z., Zhou, L., Wang, Y., Zhang, J., Hu, J., Zhang, Y., 2020. Biomembrane induced in situ self-assembly of peptide with enhanced antimicrobial activity. Biomater. Sci. 8, 2031–2039. https://doi.org/10.1039/c9bm01785b.

Shi, S., Hashemi, V., Wang, S.C., Yang, J., Yang, M., Semple, A., Narasimhan, C., Antochshuk, V., 2017. Overcoming challenges with intravenous administration of an investigational protein therapeutic. J. Pharm. Sci. 106, 3465–3473. https://doi.org/10.1016/j.xphs.2017.07.018.

Sikorska, E., Dawgul, M., Greber, K., Iłowska, E., Pogorzelska, A., Kamysz, W., 2014. Self-assembly and interactions of short antimicrobial cationic lipopeptides with membrane lipids: ITC, FTIR and molecular dynamics studies. Biochim. Biophys. Acta Biomembr. 1838, 2625–2634. https://doi.org/10.1016/j.bbamem.2014.06.016.

Sikorska, E., Stachurski, O., Neubauer, D., Małuch, I., Wyrzykowski, D., Bauer, M., Brzozowski, K., Kamysz, W., 2018. Short arginine-rich lipopeptides: from self-assembly to antimicrobial activity. Biochim. Biophys. Acta Biomembr. 1860, 2242–2251. https://doi.org/10.1016/j.bbamem.2018.09.004.

Silva, R.F., Araújo, D.R., Silva, E.R., Ando, R.A., Alves, W.A., 2013. L -Diphenylalanine microtubes as a potential drug-delivery system: characterization, release kinetics, and cytotoxicity. Langmuir 29, 10205–10212. https://doi.org/10.1021/la4019162.

Spellberg, B., Bartlett, J., Wunderink, R., Gilbert, D.N., 2015. Novel approaches are needed to develop tomorrow's antibacterial therapies. Am. J. Respir. Crit. Care Med. 191, 135–140. https://doi.org/10.1164/rccm.201410-1894OE.

Stachurski, O., Neubauer, D., Małuch, I., Wyrzykowski, D., Bauer, M., Bartoszewska, S., Kamysz, W., Sikorska, E., 2019. Effect of self-assembly on antimicrobial activity of double-chain short cationic lipopeptides. Bioorg. Med. Chem. 27, 115129. https://doi.org/10.1016/j.bmc.2019.115129.

Stein, R.A., 2017. Mugs of the bugs: the most wanted ones. Int. J. Clin. Pract. 71, e12963. https://doi.org/10.1111/ijcp.12963.

Teixeira, M.C., Carbone, C., Sousa, M.C., Espina, M., Garcia, M.L., Sanchez-Lopez, E., Souto, E.B., 2020. Nanomedicines for the delivery of antimicrobial peptides (Amps). Nanomaterials 10, 560. https://doi.org/10.3390/nano10030560.

Thakur, K., Sharma, G., Katare, B.S., 2018. Topical drug delivery of anti-infectives employing lipid-based nanocarriers: dermatokinetics as an important tool. Curr. Pharm. Des. https://doi.org/10.2174/1381612825666190118155843.

Theuretzbacher, U., Gottwalt, S., Beyer, P., Butler, M., Czaplewski, L., Lienhardt, C., Moja, L., Paul, M., Paulin, S., Rex, J.H., Silver, L.L., Spigelman, M., Thwaites, G.E., Paccaud, J.P., Harbarth, S., 2019a. Analysis of the clinical antibacterial and antituberculosis pipeline. Lancet Infect. Dis. 19, e40–e50. https://doi.org/10.1016/S1473-3099(18)

30513-9.

Theuretzbacher, U., Outterson, K., Engel, A., Karlén, A., 2019b. The global preclinical antibacterial pipeline. Nat. Rev. Microbiol. 18, 275–285. https://doi.org/10.1038/s41579-019-0288-0.

Thota, C.K., Berger, A.A., Harms, B., Seidel, M., Böttcher, C., von Berlepsch, H., Xie, C., Süssmuth, R., Roth, C., Koksch, B., 2020. Short self-assembling cationic antimicrobial peptide mimetics based on a 3,5-diaminobenzoic acid scaffold. Pept. Sci. 112, e24130. https://doi.org/10.1002/pep2.24130.

Tondro, G.H., Behzadpour, N., Keykhaee, Z., Akbari, N., Sattarahmady, N., 2019. Carbon@polypyrrole nanotubes as a photosensitizer in laser phototherapy of *Pseudomonas aeruginosa*. Colloids Surf. B: Biointerfaces 180, 481–486. https://doi.org/10.1016/j.colsurfb.2019.05.020.

Torres, M.D.T., Pedron, C.N., Higashikuni, Y., Kramer, R.M., Cardoso, M.H., Oshiro, K.G.N., Franco, O.L., Silva Junior, P.I., Silva, F.D., Oliveira Junior, V.X., Lu, T.K., de la Fuente-Nunez, C., 2018. Structure-function-guided exploration of the antimicrobial peptide polybia-CP identifies activity determinants and generates synthetic therapeutic candidates. Commun. Biol. 1, 1–16. https://doi.org/10.1038/s42003-018-0224-2.

Unzueta, U., Ferrer-Miralles, N., Cedano, J., Zikung, X., Pesarrodona, M., Saccardo, P., García-Fruitós, E., Domingo-Espín, J., Kumar, P., Gupta, K.C., Mangues, R., Villaverde, A., Vazquez, E., 2012. Non-amyloidogenic peptide tags for the regulatable self-assembling of protein-only nanoparticles. Biomaterials 33, 8714–8722. https://doi.org/10.1016/j.biomaterials.2012.08.033.

Unzueta, U., Céspedes, M.V., Vázquez, E., Ferrer-Miralles, N., Mangues, R., Villaverde, A., 2015. Towards protein-based viral mimetics for cancer therapies. Trends Biotechnol. 33, 253–258. https://doi.org/10.1016/j.tibtech.2015.02.007.

Unzueta, U., Serna, N., Sánchez-García, L., Roldán, M., Sánchez-Chardi, A., Mangues, R., Villaverde, A., Vázquez, E., 2017. Engineering multifunctional protein nanoparticles by in vitro disassembling and reassembling of heterologous building blocks. Nanotechnology 28, 505102. https://doi.org/10.1088/1361-6528/aa963e.

Vázquez, E., Villaverde, A., 2010. Engineering building blocks for self-assembling protein nanoparticles. Microb. Cell Factories 9 (2–5). https://doi.org/10.1186/1475-2859-9-101.

Verma, D., Gulati, N., Kaul, S., Mukherjee, S., Nagaich, U., 2018. Protein based nanostructures for drug delivery. J. Pharm. 2018, 1–18. https://doi.org/10.1155/2018/9285854.

Vlasova, I.I., Kapralov, A.A., Michael, Z.P., Burkert, S.C., Shurin, M.R., Star, A., Shvedova, A.A., Kagan, V.E., 2016. Enzymatic oxidative biodegradation of nanoparticles: mechanisms, significance and applications. Toxicol. Appl. Pharmacol. 299, 58–69. https://doi.org/10.1016/j.taap.2016.01.002.

Walvekar, P., Gannimani, R., Govender, T., 2019. Combination drug therapy via nanocarriers against infectious diseases. Eur. J. Pharm. Sci. 127, 121–141. https://doi.org/10.1016/j.ejps.2018.10.017.

Wang, J., Chen, X.Y., Zhao, Y., Yang, Y., Wang, W., Wu, C., Yang, B., Zhang, Z., Zhang, L., Liu, Y., Du, X., Li, W., Qiu, L., Jiang, P., Mou, X.Z., Li, Y.Q., 2019a. pH-switchable antimicrobial nanofiber networks of hydrogel eradicate biofilm and rescue stalled healing in chronic wounds. ACS Nano 13, 11686–11697. https://doi.org/10.1021/acsnano.9b05608.

Wang, S., Liu, X., Wang, Y., Xu, D., Liang, C., Guo, J., Ma, X., 2019b. Biocompatibility of artificial micro/nanomotors for use in biomedicine. Nanoscale 11, 14099–14112. https://doi.org/10.1039/c9nr03393a.

Wang, Jiajun, Song, J., Yang, Z., He, S., Yang, Y., Feng, X., Dou, X., Shan, A., 2019c. Antimicrobial peptides with high proteolytic resistance for combating gram-negative bacteria. J. Med. Chem. 62, 2286–2304. https://doi.org/10.1021/acs.jmedchem.8b01348.

Wang, Z., Liu, X., Teng, Da, Mao, R., Hao, Y., Yang, N., Wang, Xiao, Li, Z., Wang, Xiumin, Wang, J., 2020. Development of chimeric peptides to facilitate the neutralisation of lipopolysaccharides during bactericidal targeting of multidrug-resistant *Escherichia coli*. Commun. Biol. 3, 41. https://doi.org/10.1038/s42003-020-0761-3.

Wanmakok, M., Orrapin, S., Intorasoot, A., Intorasoot, S., 2018. Expression in Escherichia coli of novel recombinant hybrid antimicrobial peptide AL32-P113 with enhanced antimicrobial activity in vitro. Gene 671, 1–9. https://doi.org/10.1016/j.gene.2018.05.106.

Wei, G., Su, Z., Reynolds, N.P., Arosio, P., Hamley, I.W., Gazit, E., Mezzenga, R., 2017. Self-assembling peptide and protein amyloids: from structure to tailored function in nanotechnology. Chem. Soc. Rev. 46, 4661–4708. https://doi.org/10.1039/c6cs00542j.

Wei, X., Wu, R., Zhang, L., Ahmad, B., Si, D., Zhang, R., 2018. Expression, purification, and characterization of a novel hybrid peptide with potent antibacterial activity. Molecules 23, 1491. https://doi.org/10.3390/molecules23061491.

Wilson, N., 2018. Nanoparticles: environmental problems or problem solvers? Bioscience 68, 241–246. https://doi.org/10.1093/biosci/biy015.

World Health Organization, 2019. Antibacterial Agents in Clinical Development: An Analysis of the Antibacterial Clinical Development Pipeline. (Licence: CC BY-NC-SA 3.0 IGO).

Xiong, M., Bao, Y., Xu, X., Wang, H., Han, Z., Wang, Z., Liu, Y., Huang, S., Song, Z., Chen, J., Peek, R.M., Yin, L., Chen, L.F., Cheng, J., 2017. Selective killing of Helicobacter pylori with pH-responsive helix–coil conformation transitionable antimicrobial polypeptides. Proc. Natl. Acad. Sci. U. S. A. 114, 12675–12680. https://doi.org/10.1073/pnas.1710408114.

Xu, D., Chen, W., Tobin-Miyaji, Y.J., Sturge, C.R., Yang, S., Elmore, B., Singh, A., Pybus, C., Greenberg, D.E., Sellati, T.J., Qiang, W., Dong, H., 2018. Fabrication and microscopic and spectroscopic characterization of cytocompatible self-assembling antimicrobial nanofibers. ACS Infect. Dis. 4, 1327–1335. https://doi.org/10.1021/acsinfecdis.8b00069.

Xu, L., Shao, C., Li, G., Shan, A., Chou, S., Wang, J., Ma, Q., Dong, N., 2020. Conversion of broad-spectrum antimicrobial peptides into species-specific antimicrobials capable of precisely targeting pathogenic bacteria. Sci. Rep. 10, 1–9. https://doi.org/10.1038/s41598-020-58014-6.

Yang, Y., Wu, D., Wang, C., Shan, A., Bi, C., Li, Y., Gan, W., 2020. Hybridization with insect cecropin a (1–8) improve the stability and selectivity of naturally occurring peptides. Int. J. Mol. Sci. 21, 1470. https://doi.org/10.3390/ijms21041470.

Yuan, P., Ding, X., Yang, Y.Y., Xu, Q.H., 2018. Metal nanoparticles for diagnosis and therapy of bacterial infection. Adv. Healthc. Mater. 7, 1701392. https://doi.org/10.1002/adhm.201701392.

Zhang, S., 2017. Discovery and design of self-assembling peptides. Interface Focus 7, 20170028. https://doi.org/10.1098/rsfs.2017.0028.

Zhang, J. an, Liu, J., Wu, H. jin, Xu, Y., Si, C. cheng, Zhou, B. rong, Luo, D., 2019. The effects of antimicrobial peptides and hyaluronic acid compound mask on wound healing after ablative fractional carbon dioxide laser resurfacing. J. Cosmet. Laser Ther. 21, 217–224. https://doi.org/10.1080/14764172.2018.1516886.

Zhao, Y., Zhang, M., Qiu, S., Wang, J., Peng, J., Zhao, P., Zhu, R., Wang, H., Li, Y., Wang, K., Yan, W., Wang, R., 2016. Antimicrobial activity and stability of the d-amino acid substituted derivatives of antimicrobial peptide polybia-MPI. AMB Express 6, 122. https://doi.org/10.1186/s13568-016-0295-8.

Zhao, G., Chandrudu, S., Skwarczynski, M., Toth, I., 2017. The application of self-assembled nanostructures in peptide-based subunit vaccine development. Eur. Polym. J. 93, 670–681. https://doi.org/10.1016/j.eurpolymj.2017.02.014.

13

Hereafter the following papers have been placed in the annex section as they are involved in the PhD thesis and are mentioned during the discussion:

- **Annex 1:**
  Selecting subpopulations of high-quality protein conformers among conformational mixtures of recombinant bovine MMP-9 solubilized from inclusion bodies

- **Annex 2:**
  Potential of MMP-9 based nanoparticles at optimizing the cow dry period: pulling apart the effects of MMP-9 and nanoparticles

- **Annex 3:**
  Developing protein–antitumoral drug nanoconjugates as bifunctional antimicrobial agents

DISCUSSION

The emergence of bacterial drug resistance to conventional antibiotics is an alarming situation that threatens us all. This worrying scenario has forced the implementation of measures such us preventive actions (improved hygiene practices, safe food preparation and education, among others) or antibiotic stewardship (choose the right antibiotic and administer it only when necessary) to reduce antimicrobial usage in all areas in which these therapeutics are commonly used, including human and animal medicine and food-producing animal industry [1]. All these measures are intended to diminish the appearance and spread of drug resistance among bacteria, but when it comes to combat against drug or multidrug resistant bacteria, alternatives to traditional antibiotics are urgently needed. In this context, different strategies have been proposed as promising alternatives to antibiotics, including the use of cytokines and AMPs [89,112], two elements that have been the subject of the present research.

As with many drugs in development, cytokines and AMPs are subjected to several disadvantages that must be addressed prior to their possible biomedical application. In particular, low stability is a common drawback associated to these type of amino acid compounds. In this context, the vehicularization of these proteins or peptides into superior complexes have been proposed as an alternative to overcome this limitation [125]. Using recombinant technologies, these specific antibacterial alternatives can easily be produced, like other proteins, using different expression systems. It is precisely during recombinant expression when the newly synthetized proteins may be assembled into different oligomeric arrangements, leading to the formation of different proteins formats. The formation of this superior structures may be modulated by a direct rational design over the recombinant protein gene, such as the incorporation of certain peptides into the protein structure to generate building blocks for spontaneous self-assembling (soluble nanoparticles), or to obtain prone-to-aggregate proteins in form of insoluble aggregates (IBs). Therefore, different protein formats with a diverse set of properties can be generated, which can be exploited to deal with this public health threat.

Since the discovery of protein functionality in bacterial IBs, a great variety of studies have treated to take profit of the different advantages offered by this protein format [258,262]. In the recombinant protein production field, it was strongly stablished that proteins with high solubility corresponded with those with the best conformational quality and consequently the only suitable cell fraction for bioactivity purposes. However, the existence of insoluble protein byproducts displaying comparable functionality to the soluble version, supposed a radical change in the rules of the game and the creation of a new paradigm in the protein production field [270,271]. In this context, the presence of biological functionality in IBs indicated the existence

of active protein conformers inside these protein clusters [240], and therefore, a readily available alternative source of functional protein other than the soluble one [255]. Thus, the direct use of IBs [272] or its use as source for the isolation of soluble protein using solubilization methods [257] has opened a wide range of biotechnological and biomedical applications.

In this thesis, several strategies have been analyzed to compare the efficacy of higher-order structures of recombinant proteins, including soluble protein nanoparticles and IBs, with the performance of their soluble counterparts with the aim to develop therapeutic alternatives to antibiotics.

Enhancing protein aggregation by interspecific interaction of aggregation-prone peptides

The goal of recombinant protein production is to yield high amounts of a specific protein. As a result, the expression host is often forced to produce proteins above the physiological capacity of the cells. Proteins that do not require extensive folding assistance may adopt proper conformational structures, rendering abundant amounts of highly soluble protein species [273]. In these cases, aggregated protein represents only a low percentage of the total protein production. This behavior can be observed with highly soluble proteins such as the recombinant bovine interferon gamma (rBoIFN-γ) (**study 2, figure 1 b (bottom)**) and GFP (**study 1, figure 2 c**), where the percentage of aggregation is below 20 % in both cases. In other instances, the expressed protein may require further folding assistance, however, the overload of the protein expression machinery may impede an optimal folding capacity, leading to protein aggregation. In these cases, protein aggregation is driven by the intermolecular interactions between the exposed hydrophobic patches found in the different unfolded/misfolded protein conformers [274]. These proteins are considered as prone-to-aggregate proteins and the percentage of aggregation tend to be high (**figure 14 a**). Matrix metalloproteinase-9 (MMP-9) is an example of this behavior which accumulates mainly as IBs during recombinant expression in prokaryotic hosts (**annex 1**). In other instances, proteins tend to be distributed in both soluble and insoluble fractions. Therefore, these proteins cannot be classified in the previous categories, but may show preference for a certain fraction, as can be observed in the case of the near-infrared fluorescent protein (iRFP) which can be considered as partially soluble (**study 1, figure 1 c**). In any case, for most of the recombinant proteins, experimental conditions may lead to a partition of the produced protein between the soluble and insoluble cell fractions.

For some specific applications, IBs could be preferred over its soluble counterpart. For that reason different strategies have been developed in order to increase the protein yield present in the insoluble fraction [246]. One of the strategies used for the promotion of protein aggregation is the addition of prone-to-aggregate polypeptide tags to the protein of interest [250,252,275]. The fusion of these elements to the main polypeptide chain promotes protein aggregation by increasing the intermolecular interactions among protein units. However, contrary to prone-to-aggregate proteins, where the same polypeptide chain is responsible of either, aggregation and functionality, the intermolecular interactions are mainly promoted by the aggregation tag, while it is thought that the influence of the scaffold protein on this process is limited. In this sense, aggregation capacity and functionality are physically separated, forming a dual component [276].
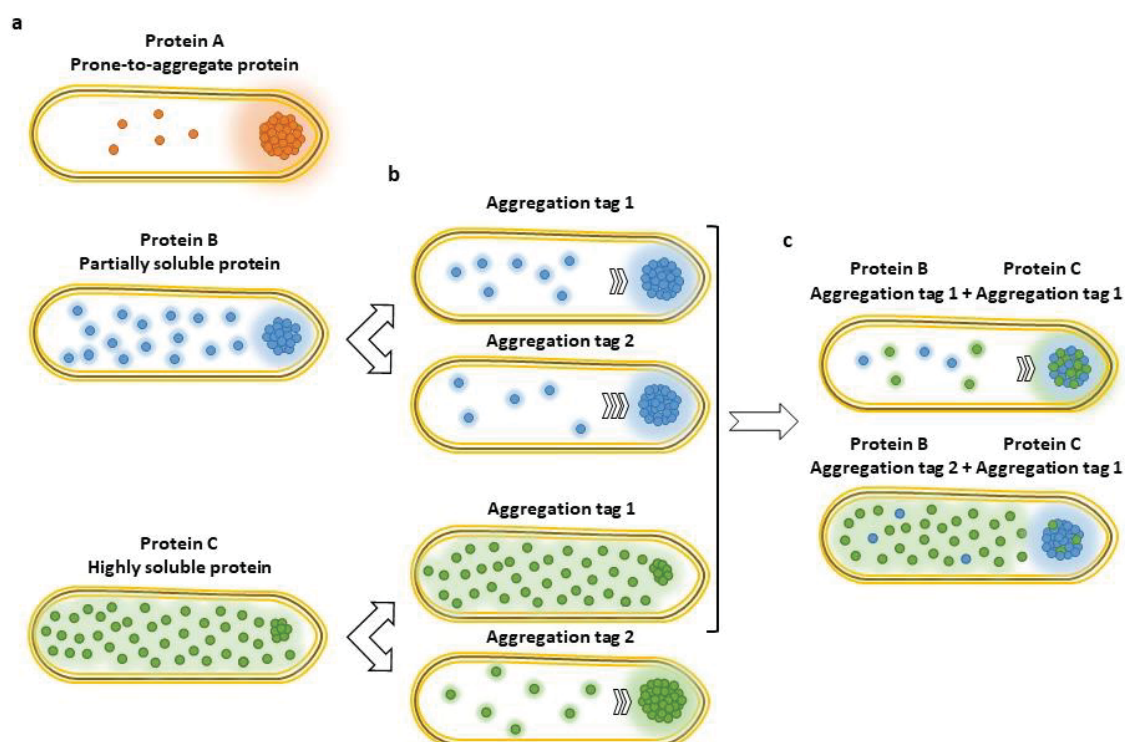
Figure 14. Visual representation of aggregation tag addition in different proteins and its influence on aggregation and coaggregation. **a.** Depending on the scaffold protein properties, aggregation tags can be considered as "strong" or "weak". **b.** Aggregation tag 1 is strong enough to promote aggregation of protein B. However, aggregation tendency of protein C is not promoted by the addition of the same tag. In this case, aggregation propensity is defined by the scaffold protein. Aggregation tag 2 is strong enough to promote aggregation of both, proteins B and C, surpassing the influence of the scaffold protein. **c.** Specificity during aggregation promotes protein coaggregation. When two different proteins bearing the same aggregation tag are coexpressed, the one with the major aggregation propensity is able to lead the most soluble one to the insoluble fraction. On the other hand, the presence of different aggregation tags does not promote coaggregation to the same extent.

In this work, several tags have been employed to promote the aggregation of proteins with high solubility. In **study 2**, three aggregation-prone peptides (APPs), L6K2, CYOB and HALRU, were fused to the same immunomodulatory protein (rBoIFN-γ) and their aggregation capabilities were compared. In all cases, as expected, protein solubility was reduced and significant differences were observed in terms of aggregation propensity among the different constructs (**study 2, figure 1 b (bottom)**). This is not surprising, as aggregation tags have a variable efficiency to promote protein aggregation. Depending on certain characteristics, such as the amino acid composition or peptide length of the APPs, the intermolecular forces that can be stablished among the different proteins may differ, resulting in distinct aggregation levels (**figure 14 b**). Moreover, when diverse scaffold proteins are fused to the same APP, the aggregation propensity may also differ. The fusion of the short self-assembling peptide L6K2 to rBoIFN-γ

reduced protein solubility by almost 70 % (**study 2, figure 1 b (bottom)**). On the other hand, the same APP fused to two different fluorescent proteins, GFP and iRFP, led to 10 and 30 % reduction of the protein solubility, respectively (**study 1, figures 1 c and 2 c**). These data suggest that the aggregation propensity of APPs on these type of fusion protein designs do not work independently of the scaffold protein, and therefore, the overall aggregation propensity should consider both components (**figure 14 a and b**).

In this sense, certain physicochemical characteristics of the scaffold protein, such as solubility, may counteract protein aggregation. In this case, proteins would require the addition of strong aggregation tags, i.e., tags with the ability to surpass the counteracting effects on aggregation propensity of the accompanying protein. On the other hand, the aggregation of proteins that normally tend to be equally distributed in both cellular fractions would be easily enhanced with the use of less strong aggregation tags. For example, the L6K2 APP is not strong enough to enhance the aggregation performance of the highly soluble GFP, nevertheless, the addition of the VP1 protein domain dramatically enhance its aggregation propensity (**study 1, figure 2 c**). In different circumstances, L6K2 improves the aggregation profile of iRFP, a protein with low solubility (**study 1, figures 1 c**). However, the increase was not as pronounced as the one observed in the case of VP1GFP.

On this basis, one of the factors that could be employed in order to measure the "aggregation potency" of aggregation tags would be the length of the amino acid sequence, as extracted from the data obtained in **study 1**. The use of L6K2 variants where the number of amino acids were rationally increased, showed a gradual improvement on aggregation propensity of GFP (**study 1, figure 2 c and 2 d**). However, this assumption cannot be regarded as an absolute truth, since the effect of small APPs on distinct scaffolds give rise to significantly different results in terms of aggregation. This can be observed with the comparison of the aggregation propensity of rBoIFN-γ L6K2 (**study 2, figure 1 b (bottom)**), GFPL6K2 (**study 1, figure 2 c**) and iRFPL6K2 (**study 1, figures 1 c**). For that reason, other parameters such as the self-assembling ability, the type of intermolecular interactions and the influence of the scaffold protein should be taken into consideration when designing this type of fusion proteins.

Regardless of the aggregation capabilities, the mechanism by which these aggregation tags act appears to be highly specific [237]. As previously mentioned, the addition of the L6K2 on GFP had no significant impact on aggregation, remaining in its soluble format (**study 1, figure 2 d**). However, the simultaneous expression of GFPL6K2 and iRFPL6K2 enhance the aggregation

tendency of GFPL6K2 (**study 1, figures 4 a**). These results indicate that the protein with the highest aggregation propensity, in this case iRFPL6K2, lead the accompanying soluble protein (GFPL6K2) to the insoluble cell fraction. Nevertheless, it is not clear the influence of the APP in this process, and make us wonder whether its presence is necessary or not to promote coaggregation. Indeed, scaffold contribution on the coaggregation process cannot be ruled out, because as mentioned before, both elements, aggregation tag and scaffold protein influence the overall aggregation tendency. But when the influence of the scaffold is kept out of the equation, the importance of the aggregation tag is revealed. When two very similar proteins (GFP and BFP) are fused to completely different aggregation tags (L6K2 and VP1, respectively), the fusion protein with the major aggregation tendency (VP1BFP) is not able to promote the coaggregation of GFPL6K2 (**study 1, figures 5a**). These data suggest that the mechanism by which aggregation tags interact to promote aggregation is highly specific (**figure 14 c**) and supports previous findings where similar results were observed [237].

In this sense, when using aggregation tags, the influence of the scaffold protein should be considered, because as it has been demonstrated, their different properties play a role on the overall aggregation tendency. Furthermore, some characteristics of the scaffold protein such as solubility defines the aggregation potency of these tags, although in some cases peptide length can be associated with higher aggregation tendency. Last but not least, aggregation propensity appears to be dictated by specific interaction among highly similar proteins sequences, highlighting the importance of these aggregation tags during aggregation processes.

Influence of pull-down aggregation tags on recombinant protein expression levels and functionality

The incorporation of APPs into the main polypeptide chain of certain proteins may have unexpected effects apart from the promotion of aggregation propensity. Compared to the unmodified protein, in **study 1 and 2** we have observed that both expression levels and functionality were affected. In the first case, the reduction in total protein yields might be a consequence of different factors including the length of the peptide. Shorter APPs, as for example L6K2, had almost no negative impact in protein yields, independently of the partner protein with which was fused to. On the other hand, longer peptides significantly affected protein yields (**study 1, figure 2 b and study 2, table S1**).

In **study 2**, it was described the use of different APPs to promote the aggregation of the bovine version of IFN-γ (rBoIFN-γ) (**study 2, figure 1 a**). In all cases, protein aggregation was promoted at the expense of final protein yields, and this decrease was especially pronounced in the case of larger peptides. HALRU and CYOB, approximately two and five times longer than L6K2, respectively, reduced protein yields by almost 50 % when compared to L6K2 (**study 2, table S1**). However, when HALRU and CYOB are compared, no significant differences are observed, indicating that other factors rather than peptide length are affecting protein expression. Many studies have identified sequence features that influence protein synthesis efficiency, as for example, the presence of mRNA structural elements that may hinder translation initiation by blocking ribosome binding sites [277] or the effect of certain amino acid sequences in the first five codons [278]. However, these studies have focused on the region close to the N-terminal, and in our case, in most of the recombinant protein designs generated, peptide addition have been made at the C-terminal position (**study 1, figure 2 a and study 2, figure 1 a**). Considering this, recent studies have highlighted the importance of this region in protein synthesis efficiency, demonstrating that the identity of the last amino acids has a strong influence on the protein expression levels [279].

In **study 1**, the highly soluble GFP was biosynthetically fused to different versions of the APP L6K2 (**study 1, figure 2 a**). These variants differed in length, being two and three times longer than the original L6K2, and consisted on the reiterated repetition of the leucine and lysine amino acids at different positions (**study 1, table 1**). These longer versions had a significant impact on protein aggregation, but at the same time reduced protein yields accordingly (**study 1, figure 2 b**). In such circumstances, and in addition to the already presented, other factor may be

influencing this differential expression levels. The presence of repetitive sequences of the same amino acid (leucine) may lead to tRNA^{LEU} depletion, which severely impairs synthesis by slowing down translation efficiency [280]. This effect can be especially observed if we compare the expression levels of two L6K2 derivatives, (L6K2)x2 and L12K4 (**study 1, figure 2 b**). In the first case, several lysines interrupt the consecutive arrangement of leucines, while in the second case, lysines are located at the N-terminus, leaving a complete sequence of 12 leucines without interruption (**study 1, table 1**). In (L6K2)x2, the "lysine bridge" between both leucine sequences may reduce the tRNA^{LEU} overuse and give an extra time to recharge tRNAs with new amino acids, improving the translation efficiency, and finally increasing the protein expression levels [281].

Moreover, another reason for the observed reduction in total protein yields may be due to the similarity between L6K2 and its derivatives with AMPs. The presence of an α-helix structure, a net positive charge and a defined anphipaticity are properties commonly associated to AMPs [282], which are also present to some extent in these specific APPs. This pernicious effect was confirmed when the antibacterial activity of the GFPL6K2 and GFP-(L6K2)x2 was evaluated, showing a dose-dependent effect on different bacterial strains, including *E. coli*, which was the host for the recombinant production of both proteins (**study 1, figure 3**). In this framework, AMPs are typically generated by chemical synthesis, and its recombinant production inside bacterial hosts tend to be avoided due to their inherent toxicity and sensitivity to proteases. To surpass those problems, AMPs tend to be fused to other partner proteins and subsequently released by chemical or enzymatic cleavage [283,284]. However, when tested, fusion proteins containing those AMPs still retained certain antibacterial activity [285,286], demonstrating that fusion to carrier proteins only partially masked AMPs toxicity. On this basis, reduced protein yields may be a consequence of the toxic effects performed by these APPs and their inherent similitudes to AMPs. Protein toxicity interfere with the survival of *E. coli* cells and cause significant defects in bacteria growth that dramatically decrease expression capabilities [287].

Apart from the expression levels, the addition of APPs into the protein structure has an important impact on protein functionality. Compared to rBoIFN-γ IBs, the presence of L6K2, CYOB and HALRU had a completely different outcome in terms of functionality. Whereas L6K2 potentiated the effect of this insoluble format, CYOB and HALRU showed the opposite behavior, significantly reducing the bioactivity of rBoIFN-γ (**study 2, figure 3 b**). Considering that IFN-γ functionality is defined by its ability to interact with its specific receptor, a proper conformation is of outmost importance. CYOB and HALRU may in some way impede the adoption of a proper conformation or directly block such interaction. However, the L6K2 case is more complex,

because its addition not only did not affect functionality, but significantly increased it (**study 2, figure 3 b and 3 d**). In this sense, the L6K2 incorporation into the rBoIFN-γ protein may preserve a better conformational quality of the soluble protein entrapped inside IBs or may positively influence the interaction with its receptor.

Additionally, conformational quality and functionality of proteins forming IBs are not the only factors that may be influencing the effectivity of these protein aggregates. The ability of these IBs to release these conformational variants under physiological conditions could be another limiting factor. The presence of different aggregation tags on rBoIFN-γ lead to the formation of IBs with dissimilar releasing efficiencies (**study 2, table S1**). However, a wider release is not always linked to a higher activity. Despite the releasing efficiency of rBoIFN-γ L6K2 IBs was much lower than that of rBoIFN-γ IBs, its bioactivity was higher (**study 2, figure 3 b**). Thus, it is possible to conclude that in our case the functional and conformational quality of the released content has a major impact on IBs bioactivity.

In summary, the addition of APPs either in N- or C- terminus may result in unpredictable outcomes in terms of protein production yields and functionality. Protein expression levels will depend on different factors, such as tRNA abundance, mRNA secondary structure, amino acid composition and protein toxicity. These effects can arise independently or in combination. On the other hand, the ability to maintain a proper conformational quality inside these insoluble protein formats appears to have a global impact on protein functionality. In this sense, the capacity to modulate the IBs formation by increasing the content and quality of the protein entrapped inside its inner structure seems to be of great importance for the direct use of this format as a source of soluble protein. This approach has been studied in great depth in **annex 1**, where the physicochemical characteristics and biological activity of different conformational protein species solubilized and purified from MMP9 IBs were analyzed in order to select the best-fitted protein populations.

Analyzing the conformational diversity and conformational quality of recombinant protein obtained in prokaryotic expression systems

Solubility is generally taken as the prime criterion for determining the quality of recombinant proteins. However, in contrast to what was formerly believed, the soluble fraction involves a spectrum of protein conformational variants (inactive, misfolded, soluble aggregates) with dissimilar functionalities [288]. Therefore, solubility is not a useful indicator of recombinant protein quality and cannot guarantee an adequate biological function [289].

Under physiological conditions, proteins expressed in its original host would have available all the adaptative and evolutionary mechanism to reach a specific conformational state compatible with an optimal functionality. However, the production of proteins of interest in heterologous expression hosts sometimes results in unpredictable outcomes, as for example, no or low expression levels, loss of functionality, proteolysis, aggregation or even toxicity.

Despite the above-mentioned limitations, one of the main advantages in the field of recombinant protein production is the availability of different expression systems including bacteria, yeast, filamentous fungi, unicellular algae, mammalian cell lines, and insect cell lines, among others. Depending on protein characteristics, certain production platforms may fit better than others. Furthermore, even similar expression systems may show different impact on the conformational quality and functionality of the expressed protein. In this work, two different prokaryotic expression systems have been employed. In **study 2**, the *L. lactis* codon-optimized bovine IFN-γ gene was expressed in both, *ClearColi* and *L. lactis*. In terms of soluble protein production yields, similar outcomes were obtained in both expression systems, being the total yield obtained in *L. lactis* slightly superior (**study 2, table S1**). On the other hand, when it comes to functionality, the rBoIFN-γ obtained from *ClearColi* displayed greater activity than that produced in *L. lactis* (**study 2, figure 3 a**). In the first case, the higher production yields observed in *L. lactis* may be a consequence of the codon optimization, which ultimately impacts the translational efficiency and gene expression levels [290]. Moreover, differences in bioactivity may be in part due to differences in the folding efficiency during the production process, leading to the formation of proteins with better conformational quality in *E. coli* [291].

In **annex 1**, a similar approach was followed. In this case *ClearColi* and *L. lactis* were used as microbial cell factories for the recombinant expression of the *L. lactis* codon-optimized bovine MMP-9. However, unlike the previous case, the expressed protein was mainly forming IBs, and

a mild solubilization process was required in order to obtain the soluble form from these protein aggregates. Differences in terms of protein activity derived from the different conformers obtained after IB solubilization and purification procedures will be discussed further below. However, previous to purification, during the recombinant protein production, a marked difference concerning cell growth was observed during culturing. In *ClearColi*, cell growth was compromised after the induction and until the end of the production as can be seen by the OD600/550, indicating certain toxic effect displayed by MMP-9 (**annex 1, Table S1**). On the other hand, cell growth on *L. lactis* proceeded normally during expression (**annex 1, Table S1**). In this sense, different studies have reported that inefficient translation may result in the generation of cryptic protein products with unanticipated functional effects or toxicity associated to altered protein variants [281,292], which could explain the results observed in *ClearColi.*

In this context, at best, proteins that are recombinantly expressed in prokaryotic expression systems may adopt native three-dimensional structures. However, in most cases, the existence of non-native conformational states is a common phenomenon [293]. At this point it is important to underline that several studies have demonstrated that proteins under conformational states distinct from fully folded structures are able to maintain biological functions [294–296]. One example is the existence of natively unfolded or intrinsically disordered proteins, which lack stable tertiary structure under physiological conditions. The presence of non-structured regions on these proteins leads to the existence of different conformational patters that can be associated with distinct functionality levels [297,298].

Thus, the recombinant expression of a specific protein may involve a heterogenous diversity of protein conformers [288]. Those that are stable enough would remain in the soluble fraction, while the most unstable would aggregate with other prone-to-aggregate conformational versions. However, considering that IBs also contain a wide range of soluble conformations, the insoluble protein fraction would represent the vast majority of this conformational diversity [299]. This is in accordance with results observed in **study 2**, where the polydispersity index (PI) of proteins released form IBs was higher than that of the soluble versions **(study 2, figure 4)**. Furthermore, purification techniques, such as affinity chromatography may restrict even more protein diversity in the soluble fraction by selecting specific subpopulations of protein conformers. In the case of His-tagged proteins, this selection would be based on the different ability of conformers to efficiently bind to the Ni^{2+} in the resin. Those conformers with a not properly exposed polyhistidine tag will not coordinate with the metal or will be weakly bound, eluting with the first fractions. In **annex 1**, MMP-9 protein was firstly solubilized from IBs and

subsequently purified by immobilized metal affinity chromatography (IMAC). The eluting pattern resulted in four different peaks, independently of the used bacterial expression system (**annex 1, figure 1 b**). This specific pattern suggests the existence of a spectrum of protein conformers with variable ability to interact and coordinate to the Ni^{2+} of the resin. However, it is important to bear in mind that although the conformational diversity may be higher in IBs, this observation is not limited to the protein released from these aggregates, since similar patters can also be observed with certain proteins coming from the soluble fraction (unpublished results).
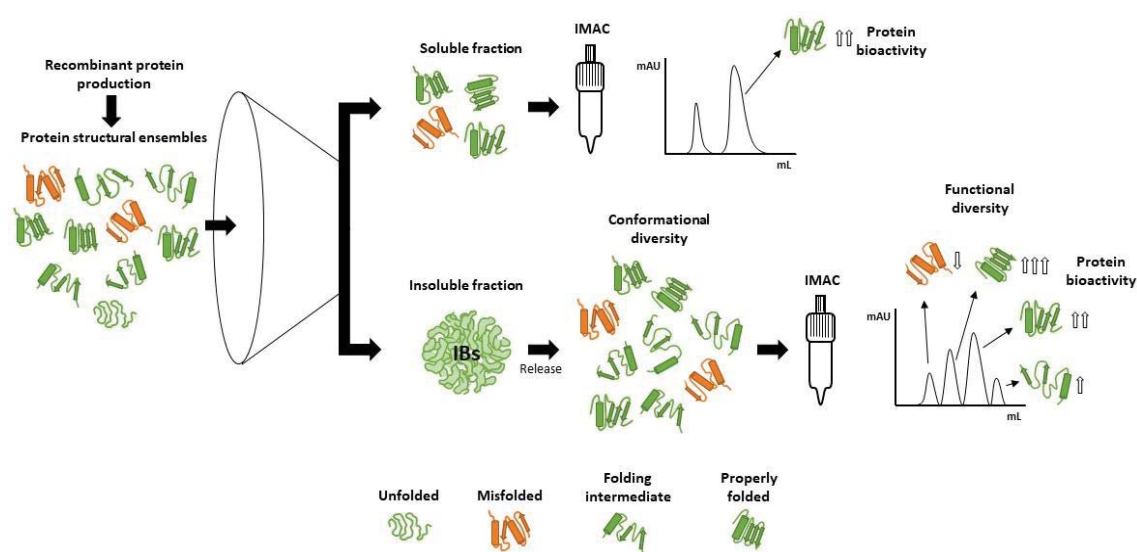
Figure 15. Schematic overview of functional and conformational diversity in both, soluble and insoluble fraction. Unlike the soluble fraction, the insoluble fraction harbors most of the structural and functional diversity. In some cases, immobilized metal affinity chromatography (IMAC) techniques select specific subpopulations of protein conformers based on their different ability to interact and coordinate to the Ni^{2+} of the resin.

In terms of functionality, protein conformational diversity is associated with dissimilar bioactivities [288]. After analyzing the protein conformers contained in the four MMP-9 protein peaks separately, it was concluded that peak 2 contained the most structured and functional protein conformers, and this is the case in both *ClearColi* and *L. lactis* (**annex 1, figure 2 b**). Initially, MMP-9 IBs contained a representative fraction of protein conformers generated during recombinant expression, after solubilization, some of these structural diverse proteins were released from IBs, and subsequently, specific populations were selected based on the ability of the released conformers to interact and coordinate to the Ni^{2+} during affinity chromatography procedures. However, the binding ability cannot be correlated with better conformational quality or functionality. Another example of such conformational diversity can be inferred from

study 2. In this case, rBoIFN-γ was produced in *L. lactis* in two different formats, IBs and soluble state (purified by his-tag affinity chromatography). When the specific activities were compared, the IBs showed greater functionality than the purified protein from the soluble fraction (**study 2, figure 3 a and b**). This effect was attributed to the partial and sustained release of the rBoIFN-γ from IBs. When equimolar concentrations of rBoIFN-γ produced in *L. lactis* and released from IBs or purified from the soluble fraction are compared, a significant difference in terms of bioactivity is observed (**study 2, figure 3 d**). In this case, the eluted protein conformers that have been selected from the soluble fraction by affinity chromatography techniques did not show an optimal functionality. On the other hand, proteins released from IBs present greater variety of protein conformers and may include protein species compatible with a better conformational quality and functionality (**figure 15**). This situation may explain the differences observed with regard to protein bioactivity. In this context, solubility and conformational quality are not necessarily coincident parameters [300].

Evaluating the immunoprotective effect of IFN-γ designs in different protein formats in a murine model of mammary gland infections

The immunoprophylactic use of IFN-γ to enhance bovine immune responses and to reduce or prevent intramammary infections in bovine mammary glands has been fairly investigated [301,302]. Its main functions are based on increasing neutrophil migration to the mammary gland and enhancing their bactericidal activity through phagocytosis and intracellular killing [303,304]. Alternatively, IFN-γ may also enhance the proliferation and differentiation of T cells and B cells during adaptive immune responses [122]. *In vitro* assays do not always correlate with *in vivo* efficacies inside the mammary gland [305], since aspects such as the complex milk environment influenced their activity. Therefore, an *in vivo* approach is necessary to evaluate the real performance of the different protein formats developed in this thesis. In **study 3**, the bactericidal effect associated to IFN-γ via immunostimulation has been evaluated in a murine model of mastitis [306]. Two different formats were assessed in parallel, soluble and IBs. Based on previous results, the addition of an aggregation tag to promote the formation of IFN-γ IBs was not justified. In spite of the good results obtained with the L6K2 APP and the highly soluble nature of rBoIFN-γ, the overproduction of this protein without any aggregation tag leads to the formation of properly formed IBs with excellent releasing efficiencies and an acceptable bioactivity (**study 2, figure 1 b, figure 2 a, figure 3 b and table S1**). These results were reproduced in the case of the murine version of IFN-γ (**study 3, figure 1 c and figure 5**). Furthermore, *in vitro* activity assays showed a lesser effect of the purified soluble version in comparison with the commercial mouse IFN-γ (**study 3, figure 3 b**) just as observed in the case of the rBoIFN-γ (**study 2, figure 3 d**).

With regard to *in vivo* administration, IBs made of IFN-γ reduced the bacterial burden in the mammary glands at the same level, or even higher, than the soluble counterpart (**study 3, figure 6 a and b**). This is in accordance with other publications that have previously demonstrated the *in vivo* therapeutic effects of proteins forming part of IBs [264,272] and in some cases even surpassing the effects of the soluble version [307]. However, the additive effects provided by the IB format should not be ruled out. In **annex 2**, it was demonstrated that the immunostimulatory effects provided by MMP-9 IBs in the bovine mammary gland were mainly due to the IB format instead of the inherent properties of the embedded protein. In this case, there was no difference between the performance of inactive or active MMP-9 IBs in the recruitment of immune cells (**annex 2, figure 3**). In this context, apart from the recombinantly produced protein, IBs also contain undetermined amounts of other bacterial components such as DNA, RNA, LPS,

146

peptidoglycan and lipids. The combination of all of them in an organized and well-defined stable structure may be responsible of the immunostimulant properties [308]. However, other studies involving the use of a different murine model (air-pouch model) demonstrated that the inflammatory response triggered by MMP-9 IBs was mainly due to the degradative capability of the embedded protein and not because of the inflammatory response attributed to the IB format itself [265]. In other cases, when IBs are made of immunostimulant proteins such as cytokines, a higher protection against bacterial infection *in vivo* is conferred in comparison to other non-immune relevant proteins [263]. In the context of the mouse mammary gland, the IB format seems not to confer this immunostimulant protective effect, since there are no significant differences when the IB format for GFP and IFN-γ are compared with their corresponding soluble versions (**study 3, figure 6 a and b**). Therefore, the immunoprotective effect against bacterial infection is predominantly due to the presence of IFN-γ, independently of the protein format.

One of the main drawbacks associated with cytokines is their low stability and short half-life, needing to be administered at high doses to achieve their therapeutic effects [309]. In this context, IBs may provide an stable environment where functionally active cytokines can be protected from degradation and sustainably release over time [262]. However, the differences observed with both formats, do not support the superiority of the IBs over the soluble format in this specific case (**study 3, figure 6 a and b**). This could be due to the high rates of protein release showed by IFN-γ IBs (**study 3, figure 1 c**), being the released protein rapidly exposed to the same environmental conditions than its soluble counterpart.

Especially interesting is the case of GWH1-IFN-γ where the addition of the GWH1 AMP [107] at the N-terminus did not only affect the expression levels but truncated the *in vitro* functionality of IFN-γ (**study 3, figure 3 b)**. As previously mentioned, peptide addition in either N or C terminus may influence protein expression. In the case of the N-terminus, some studies have pointed that the first codons are important for an efficient protein expression [310,311]. However, since GWH1 is an AMP, and as have been suggested in a previous section, the inherent antibacterial properties of these small peptides may be responsible of the reduced protein yields. Indeed, a dramatic reduction in protein productivity (> 90 %) was observed after the N-terminal incorporation of this small peptide into the IFN-γ and GFP sequences (**study 3, Table S1**). Regarding the functionality, as discussed in **study 2**, the N-terminus region of mouse IFN-γ plays an important role in receptor binding, therefore the addition of this AMP at this specific location may prevent such interaction [312]. However, *in vitro* results are not reproduced during *in vivo*

assays, where the effect on bacterial loads of GWH1-IFN-γ in both formats was comparable to the one observed for IFN-γ (**study 3, figure 6 a and b**). In this regard, the *in vivo* performance is the result of many parameters that do not always correlate with the *in vitro* behavior of proteins [307].

In summary, independently of the protein format, the recombinantly produced murine version of IFN-γ developed an immunoprotective effect on the mammary gland after administration. However, the IB format did not significantly improve the stability of this protein and a negative effect in terms of protein productivity and *in vitro* functionality was observed in those protein designs that included the GWH1 AMP.

Exploring AMP-containing protein nanoparticles as efficient anti-infective agents

The use of fusion partners to produce AMPs was initially used as a method for the recombinant production in bacterial host of these small peptides [313,314]. It is thought that the fusion protein protect the peptide from proteolytic degradation and block the peptide´s antimicrobial activity towards the bacterial host [315]. However, in some cases, the antimicrobial activity is not completely masked and results in the generation of a fusion protein with inherent antimicrobial properties that may have deleterious effects on the producing cell [285,286].

Furthermore, following a rational design based on the fusion of a cationic peptide (AMP) to a C-terminal his-tagged scaffold protein [223], it is possible to self-assemble these type of fusion proteins into larger soluble nanoparticles [111]. This last approach is of special importance to increase the stability and also to provide a format that may increase the antimicrobial performance of the isolated protein forms.

This work is the first to present the importance of this architectonic arrangement to enable and efficient antibacterial response. When the antibacterial activity of the monomeric form of GWH1-GFP was evaluated, a pronounced difference was observed in comparison with the multimeric format (**study 3, figure 2 d**). As discussed in **study 3**, we hypothesize that the self-assembling in multimeric complexes affords a high local concentration of monomeric units, reducing the critical concentration (threshold concentration) to achieve an antimicrobial effect. In this context, the monomeric form of these fusion proteins requires higher concentrations in order to display their activity. Another observation that further support the potential of the multimeric format is the antimicrobial performance showed by GWH1-IFN-γ. This fusion protein, despite following the previously described modular design [316], was unable to self-assemble into protein nanoparticles, showing a similar size to that observed for the unmodified IFN-γ (**study 3, figure 1 d**). The inability to reach a multimeric format had an impact on the antibacterial activity, displaying an identical performance to that observed for the unassembled version of GWH1-GFP (**study 3, compare GWH1-IFN-γ in figure 2 a with GWH1-GFP $_{PNPs}$ + 0.2 % N-lauroylsarcosine in figure 2 d**). On the other hand, GWH1-GFP IBs had a significantly lower effect on bacterial burden than the soluble multimeric format, which was the most effective (**study 3, figure 6 a and b**). This difference may be explained mainly by the fact that part of the released protein was found in a monomeric form (**study 3, figure 1 e**), and in addition it was released in small quantities (**study 3, figure 1 c**).

The ability to self-assemble into these multimeric complexes is not exclusively observed in the case of GWH1, as other cationic AMPs (PaDBS1R1) [317] have demonstrated the ability to promote self-assembling using as scaffold the his-tagged GFP, forming nanoparticles with a very coincident size when comparing both constructs (**annex 3, figure 1 c and 1 d**). Furthermore, the *in silico* modeling of GWH1-GFP shed some light on the architectonic structure of these multimeric complexes, indicating that dimers appear to be the primary building blocks in a model comprising twelve exposed copies of GWH1 on the nanoparticle surface (**annex 3, figure 1 e and 1 d**).

The multimeric arrangement necessarily carries a significantly higher density of charged residues which may contribute to a more effective electrostatic interactions with the negatively charged components on bacterial membranes. In some cases, it has been described a selective antimicrobial activity towards gram-negative bacteria through the interaction with specific structural elements such as LPS [318]. Although this possibility cannot be ruled out in the case of GWH1-GFP, the dissimilar antimicrobial performance of this multimeric protein against two gram-negative bacteria, *E. coli* (**study 3, figure 2 a**) and *P. aeruginosa* (**annex 3, figure 4 a**) indicates that if it occurred, it would not have a decisive influence on antimicrobial activity.

As have been described for other AMP-containing nanocomposites, after electrostatic interactions with bacterial membrane components, these multimeric assemblies are able to translocate across the cell envelope into the cytoplasm causing membrane perturbations [319] or disrupting the whole cell membrane and cell wall [320]. In the case of GWH1-GFP, the cell wall disruption was a dose-dependent effect observed in *S. aureus* (**annex 3, figure 7 a**). However, this effect was less obvious in the case of *E. coli* [111]. Based on this, we speculate that GWH1-GFP, at the tested concentrations, translocate bacterial membranes by causing membrane perturbation in gram-negative bacteria (*E. coli and P. aeruginosa*) and membrane disruption and pore formation in gram-positive bacteria (*S. aureus*) (**figure 16**). This is supported by experimental data presented in **annex 3**, in this study 2'-deoxy-5-fluorouridine pentamer (5-FdU) was chemically conjugated to GWH1-GFP protein oligomers and its antibacterial efficacy evaluated against *P. aeruginosa* and *S. aureus*. 5-FdU is a potent antimetabolite that displays its antibacterial effects by inhibiting thymidylate synthetase and impairing DNA synthesis [321], therefore, it needs to be internalized into the bacterial cell. In the case of *S. aureus*, this small molecule easily diffuses through the bacterial membrane reaching its internal target and displaying a deleterious effect (**annex 3, figures 4 a and 5 a**). In contrast, in *P. aeruginosa* the complex gram-negative membrane structure [322] may impede the free 5-FdU internalization

150

(**annex 3, figures 4 b and 5 a**). Membrane disruption and pore formation are mechanisms that facilitate the entry of other molecules [320], if it was the case in *P. aeruginosa*, the combination of GWH1-GFP oligomers and the free 5-FdU would result in low bacterial viabilities. However this behavior is not observed (**annex 3, figures 4 b and 5 a)**, suggesting that translocation across the bacterial membrane occur without causing significant perturbation [319].
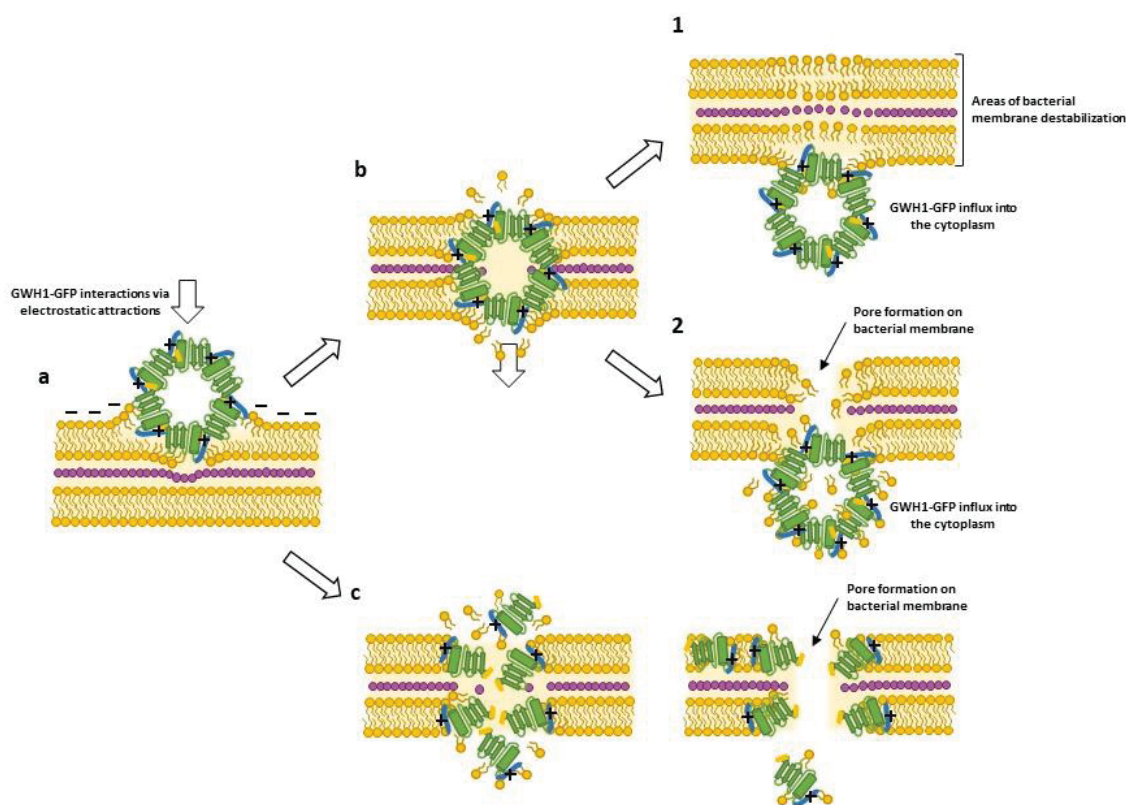
Figure 16. Hypothetical models of how GWH1-GFP nanoparticles display their antibacterial effects. **a**. GWH1-GFP initially binds via electrostatic interactions with negatively charged membrane components. **b**. The nanoparticles traverse the cell envelope causing membrane perturbations, but avoiding pore formation (**1**). In this case, cell lysis can be achieved by either, upregulated ion movement, induction of the apoptotic-like death pathway or targeting internal targets. The nanoparticles traverse the cell envelope causing membrane disruption and pore formation (**2**). **c**. When the nanoparticles are embedded in the bacterial cell membrane, the aqueous environment is replaced by the phospholipid bilayer environment, then the nanoparticles may disassemble and the building blocks continue disrupting the bacterial membrane by creating pores.

Altogether, the self-assembling arrangement offers a significant advantage over the isolated monomeric forms. The presence of higher densities of charged residues and increased local concentration of monomeric units are factors that may contribute to the more effective killing of bacteria. However, the mechanism of action is not completely clear and appear to differ from one bacterium to another. In this sense, antimicrobial agents may have more than one mode of action [323]. Apart from membrane destabilization/disruption, the presence of internal

targets [324,325] or the existence of programmed cell death mechanisms under stressful conditions such as membrane disruption [326] have been also described. Additionally, presented evidence make us suggest the ability of these GWH1-GFP oligomers to translocate across the bacterial membrane with or without cell wall disruption. This feature is potentiated when this multimeric arrangement is associated through conjugation with drugs that act on intracellular targets, as for example, 5-FdU.

Ultimately, this multimeric format tackle with several of the main disadvantages associated with the therapeutic application of AMPs. Hemolytic activity and cytotoxicity against eukaryotic cells are features typically associated to these small peptides. Nevertheless, the AMPs (GWH1 and PaD) included within these multimeric complexes in form of fusogenic building blocks do not produce hemolysis in exposed human erythrocytes (**annex 3, figure 7 b**) or cytotoxicity over mammalian cells (**annex 3, figure 7 c**). Other disadvantages are protease susceptibility and rapid renal filtration. In this context, peptide fusion to carrier proteins is proposed as a method to prevent the peptide proteolytic degradation [315]. On the other hand, nanoparticle formation increases the molecular size to such an extent that renal excretion is minimized, enhancing the bioavailability [226]. All these characteristics highlights the potential use and benefits of this nanoscale protein materials for the therapeutic treatment of bacterial-based infectious diseases.
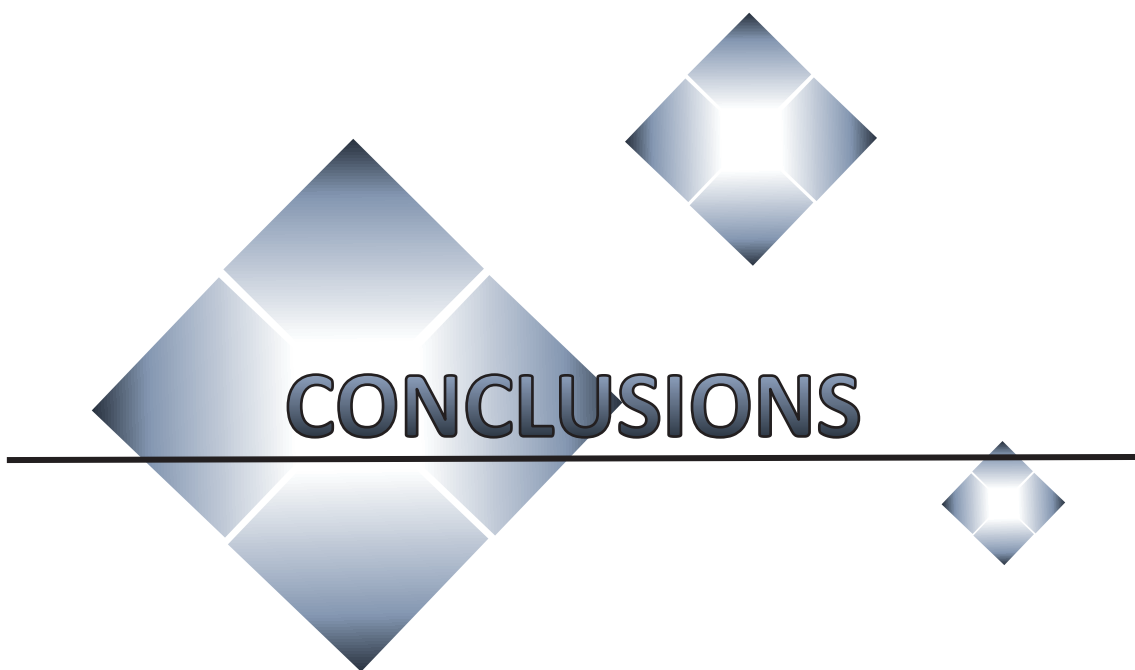
CONCLUSIONS

Due to the public health threat that the emergence of AMR represents, the development of novel alternatives to tackle with this global problem are of outmost importance. In this context, protein-based compounds such as cytokines and AMPs have been proposed as some of these promising options. Therefore, strategies intended to improve their stability and effectivity such as the use of different protein formats are highly desired (i.e. IBs and protein nanoparticles).

1. The aggregation propensity of a specific protein is determined by their inherent physicochemical properties. The incorporation of aggregation tags, such as L6K2 derivatives, influence this process in a variable degree. Therefore, in such fusion protein designs, the influence of both components (i.e. the protein and the fused APP) on the overall aggregation tendency must be considered.

2. As it has been shown in previous studies, aggregation propensity appears to be dictated by specific interactions among highly similar protein sequences. In this context, a common aggregation tag in structurally distinct scaffold proteins promote protein coaggregation, highlighting the importance of these elements during aggregation processes. The results validated the ability of APPs to generate hybrid protein aggregates with potential synergic activities in microbial cell factories.

3. The incorporation of APPs to the main polypeptide chain of proteins may have unexpected effects in terms of protein expression levels. In the case of L6K2 derivatives, reduced protein yields may be a consequence of the toxic effects performed by these APPs due to their inherent similitudes to AMPs.

4. Apart from improving aggregation propensity, the addition of APPs into the protein structure of rBoIFN-γ had an important impact on protein functionality which correlated with compactability of protein conformations. Whereas L6K2 potentiated the biological activity of the recombinant protein accumulated in IBs, CYOB and HALRU showed the opposite behavior, significantly reducing the bioactivity of rBoIFN-γ.

5. Certain purification techniques such as IMAC are able to select specific subpopulations of protein conformers based on their different ability to efficiently bind to the Ni^{2+} in the resin. This was demonstrated with the MMP-9 protein solubilized from IBs obtained from two prokaryotic expression systems, *ClearColi* and *L. lactis*.

6. The conformational diversity leads to the existence of different protein species with variable conformational quality and therefore dissimilar functionality (or biological activity). In the purification procedure of MMP-9 from IBs of two prokaryotic expression systems (*ClearColi* and *L. lactis*), four MMP-9 protein subpopulations were detected. Physicochemical characterization of the isolated subpopulations revealed the relationship between conformational quality and biological activity.

7. The self-assembled arrangement of recombinant proteins offers a significant advantage over the isolated soluble monomeric protein forms. When comparing the monomeric form of GWH1-GFP with the multimeric format (protein nanoparticles), a pronounced difference in terms of *in vitro* antibacterial activity was observed, being the latter more effective.

8. In the case of the murine version of IFN-γ, the addition of the GWH1 AMP at the N-terminus not only negatively affected the expression levels, but also truncated the *in vitro* functionality. Furthermore, GWH1-IFN-γ was unable to self-assemble into protein nanoparticles, showing a similar size to that observed for the unmodified IFN-γ.

9. The recombinantly produced IFN-γ showed an immunoprotective effect on the mammary gland after administration in a murine model of mastitis. This effect was comparable to the one observed for GWH1-IFN-γ. In addition, the IB format did not significantly improve the biological performance of any of these proteins even though protein release from IBs was favored.

10. In its soluble form, GWH1-GFP self-assembling nanoparticles were the most effective in reducing bacterial loads in *E. coli* infected mammary glands. On the other hand, protein release from this IB format was reduced and had a significantly lower effect on bacterial burden.

11. The performance of GWH1-GFP protein nanoparticles in the mastitis mouse model was superior for *E. coli* challenged animals than for *S. aureus* challenged animals, as previously described in *in vitro* antibacterial assays.

12. Depending on the bacteria, GWH1-GFP oligomers seem to translocate across the bacterial membrane with or without cell wall disruption. In this context, the conjugation with drugs

that act on intracellular targets such as 5-FdU potentiates the antimicrobial activity of this multimeric arrangement.

ANNEXES

ANNEX 1

Selecting subpopulations of high-quality protein conformers among conformational mixtures of recombinant bovine MMP-9 solubilized from inclusion bodies

Jose Vicente Carratalá, Laia Gifre-Renom, Ramon Roca-Pinilla, Antonio Villaverde, Anna Arís, Elena Garcia-Fruitós, Julieta María Sánchez and Neus Ferrer-Miralles

(Referenced manuscript)

Article

Selecting Subpopulations of High-Quality Protein Conformers among Conformational Mixtures of Recombinant Bovine MMP-9 Solubilized from Inclusion Bodies

Jose Vicente Carratalá [1,2,3], Laia Gifre-Renom [4], Ramon Roca-Pinilla [4], Antonio Villaverde [1,2,3], Anna Arís [4], Elena Garcia-Fruitós [4], Julieta María Sánchez [1,2,*,†] and Neus Ferrer-Miralles [1,2,3,*]

[1] Institute for Biotechnology and Biomedicine, Autonomous University of Barcelona, Bellaterra, 08193 Barcelona, Spain; josevicente.carratala@uab.cat (J.V.C.); Antoni.villaverde@uab.cat (A.V.)

[2] Department of Genetics and Microbiology, Autonomous University of Barcelona, Bellaterra, 08193 Barcelona, Spain

[3] Bioengineering, Biomaterials and Nanomedicine Networking Biomedical Research Centre (CIBER-BBN), Autonomous University of Barcelona, Bellaterra, 08193 Barcelona, Spain

[4] Department of Ruminant Production, Institute of Agrifood Research and Technology (IRTA), Caldes de Montbui, 08140 Barcelona, Spain; laiagifrerenom@gmail.com (L.G.-R.); ramon.rocap@gmail.com (R.R.-P.); anna.aris@irta.cat (A.A.); elena.garcia@irta.cat (E.G.-F.)

* Correspondence: jsanchezqa@gmail.com (J.M.S.); neus.ferrer@uab.cat (N.F.-M.)

† Permanent Address: Institute of Biological and Technological Research (IIByT), National Council for Scientific and Technical Research (CONICET), National University of Cordoba (UNC), Institute of Food Science and Technology (ICTA-FCEFyN-UNC), X5016GCN Cordoba, Argentina.

Abstract: A detailed workflow to analyze the physicochemical characteristics of mammalian matrix metalloproteinase (MMP-9) protein species obtained from protein aggregates (inclusion bodies—IBs) was followed. MMP-9 was recombinantly produced in the prokaryotic microbial cell factories *Clearcoli* (an engineered form of *Escherichia coli*) and *Lactococcus lactis*, mainly forming part of IBs and partially recovered under non-denaturing conditions. After the purification by affinity chromatography of solubilized MMP-9, four protein peaks were obtained. However, so far, the different conformational protein species forming part of IBs have not been isolated and characterized. Therefore, with the aim to link the physicochemical characteristics of the isolated peaks with their biological activity, we set up a methodological approach that included dynamic light scattering (DLS), circular dichroism (CD), and spectrofluorometric analysis confirming the separation of subpopulations of conformers with specific characteristics. In protein purification procedures, the detailed analysis of the individual physicochemical properties and the biological activity of protein peaks separated by chromatographic techniques is a reliable source of information to select the best-fitted protein populations.

Keywords: inclusion bodies; affinity chromatography; dynamic light scattering; the center of spectral mass; circular dichroism; protein conformers

1. Introduction

Recombinant proteins are obtained from a wide collection of microbial expression systems [1,2]. However, in some instances, the recombinant protein ends up accumulated in the insoluble cell fraction [3,4]. These protein aggregates or nanoclusters (NCs), known as inclusion bodies (IBs) in prokaryotic expression systems, are complex structures stabilized by protein–protein cross β-sheet interactions forming a protease-resistant scaffold, which coexist with internalized native and native-like conformers of the protein of interest [5–7]. The complete denaturation of the aggregates and the subsequent refolding of the released protein species has been a widely used protocol for the isolation of soluble proteins using IBs as the protein source [8,9]. However, this approach often results in variable efficiency in the recovery of correctly folded proteins and, the biological activity may be highly compromised [10]. In the last decades, the detection of biological activity in these protein

NCs fueled the development of alternative soluble protein purification procedures from IBs using non-denaturing conditions [11,12]. Taking into account the porous nature of these aggregates, the native and native-like species of the protein of interest may be separated from the scaffold structure by controlled release of soluble conformers through incubation with buffers containing mild detergents at low concentrations [13]. The resulting protein solution, enriched with the protein of interest in a soluble format, can be then easily separated from the aggregated remnants of IBs by centrifugation [11,13,14]. In addition, it might contain a wide range of folding intermediates with a dissimilar specific activity. In order to demonstrate the presence of this spectrum of protein species in the protein aggregates and with the aim to select protein subpopulations with the best conformational quality, we selected matrix metalloproteinase 9 (MMP-9) as a paradigm of difficult-to-produce eukaryotic protein in prokaryotic expression systems [15]. Matrix metalloproteinases (MMPs) constitute a family of zinc-dependent enzymes involved in the degradation and remodeling of the extracellular matrix. In addition, MMP-9 seems to play important roles in tissue reorganization in physiological processes, including embryogenesis, neovascularization and in the course of the restructuring of synaptic connections [16,17].

In this study, two endotoxin-free prokaryotic expression systems, *Clearcoli*® BL21(DE3) and *Lactococcus lactis* were transformed with an expression vector containing a His-tagged version of the bovine MMP-9 gene to compare for the ability of the corresponding protein folding machinery to cope with the product of the overexpressed gene. MMP-9 was produced mostly in the form of IBs in both expression systems, and mild detergent treatment was performed to release entrapped protein, as reported [18]. The results showed that in both cases, four different peaks were obtained after affinity chromatography analysis indicating the presence of several subpopulations of conformers with variable ability to interact and coordinate to the Ni^{2+} of the resin. The specific activity of the resulting protein peaks appeared to be related to higher helical content in the structure. In addition, the results linked the presence of more compact conformations to higher thermal stability. We expect that this type of analysis will be useful for understanding the conformational complexity of IB proteins and selecting the best-fitted population of native-like containing conformers from a complex mixture of protein species released from IBs under non-denaturing conditions.

2. Results and Discussion

2.1. Protein Production of Soluble MMP-9 in IBs

Mammalian MMP-9 is an aggregation-prone protein when recombinantly produced in prokaryotic expression systems, such as *E. coli and L. lactis*, being necessary to purify the soluble version from IBs [19]. Thus, the soluble form of prone-to-aggregate proteins, such as MMP-9, can only be obtained from bacterial IBs by using denaturing or non-denaturing procedures [11,13,20–23]. Recovering protein species in an active state by refolding protocols from denatured proteins is time-consuming and results in variable performance efficiency. For these reasons and based on the discovery of bioactive protein conformations as an important IB component, the application of non-denaturing solubilization protocols has become a promising alternative [12,13,21]. However, the heterogeneous nature of the protein forms released from IBs has not been studied. Herein, we have analyzed the different active conformers derived from the protein pool obtained after solubilizing MMP-9 protein from IBs of two generally recognized as safe (GRAS) microorganisms (*Clearcoli* and *L. lactis*). In both cases, the protein was primarily detected in the insoluble cell fraction as expected (data not shown). In the case of *Clearcoli*, the expression of the recombinant gene had a clear negative effect on the overall fitness of the cultures since the final OD_{550} of the cultures remained at the same level or slightly higher than the initial pre-induction values (Appendix A, Table S1).

### 2.2. Solubilization of Recombinant MMP-9 from IBs

Solubilization of MMP-9 from IBs of *L. lactis* and *Clearcoli* is shown in Figure 1a. Despite the release of the recombinant protein during the processing of the IB samples (see lanes Pellet (the content of IBs after resolubilization), SN1 (soluble cell fraction), SN2 (first washing of IBs), and SN3 (second washing of IBs)), a significant amount of the protein was detected in the soluble fraction in SN4 (solubilized proteins from IBs) after incubation with solubilization buffer (containing 0.2% N-lauroylsarcosine) of both *L. lactis* and *Clearcoli* IBs. During the solubilization step, the anionic detergent interacts with MMP-9 through its hydrophobic tail. Detergents might form micelles when achieving the critical micelle concentration (CMC), inducing the denaturation of the protein. However, the CMC of N-lauroylsarcosine is 14.6 mmol/L (ref Bagheri 2019), which was not reached in the tested conditions at 6.8 mmol/L (0.2%). Some protein bands of an apparent molecular weight similar to MMP-9 were detected in the SN2, SN3 and Pellet samples in *Clearcoli*. However, in Western blot analysis, those protein bands were not identified as MMP-9. Although the efficiency of protein solubilization from IBs was variable [13] in the expression systems evaluated here, a substantial proportion of MMP-9 protein in IBs was released, allowing further purification.

2.3. Purification of Recombinant MMP-9 by Affinity Chromatography

Affinity chromatography of the solubilized MMP-9 from *L. lactis* and *Clearcoli* generated four protein peaks containing MMP-9 (Figure 1b). The identity of MMP-9 was observed in each of the protein peaks (Figure 1a, lower panels). It has been described that recombinant MMP-9 forms mixtures of monomers with higher oligomeric species [24], and positive protein bands of high molecular weight were observed at least in the protein samples purified from *L. lactis*, indicative of the presence of oligomers. The low total amount of purified protein from *Clearcoli* was not enough to reveal the presence of oligomers under the tested experimental conditions. The presence of different protein peaks in the pool of solubilized protein indicates the coexistence of several protein conformers with dissimilar affinities for the Ni^{2+}-loaded resin. The variable affinity of the protein forms for the columns may be due to local conformational changes of the His-tag or to the presence of protein conformers with dissimilar occupancy of the seven Zn^{2+}-binding sites in the protein (UniProt P52176; Figure S2). The empty binding sites may interact with the coordinated Ni^{2+} displayed on the resin [25]. On the other hand, we have detected more than one elution peak in IMAC chromatography by using similar IB solubilization protocols in other families of proteins apart from metalloproteinases, suggesting that the presence of active folding intermediates in the solubilization mixture from IBs is not exclusive for metal-containing proteins (Figure S3). However, we cannot rule out the possibility that in the case of MMP-9, the distinct level of occupancy of the metal-binding sites may affect the distribution of conformational populations. In addition, we can consider the possibility that each protein peak was stabilized by a unique interaction with the detergent. In any case, irrespectively of the final yield of protein recovery in each of the peaks (compare the peak height for the two expression systems and the final yield in Figures 1b and 2a, respectively), a multi-peak elution profile was obtained for both expression systems (Figure 1b). However, the purity between the equally numbered protein peaks was not homogeneous. In fact, peak 1 obtained from *Clearcoli* included a great proportion of contaminant proteins and was discarded for further analysis (Figure 1a). Another case to mention was peak 3 of *Clearcoli* (62.5% purity), which was still included in protein characterization experiments as the contaminant protein bands were also detected in protein peak 2 of *Clearcoli*, considering then a similar interference between protein samples. In addition, equivalent peaks from each expression system eluted at different imidazole concentrations (Figure 1b insets), indicating that they may correspond to distinguishable protein conformational populations between both expression systems [26]. Several attempts were made to purify the low quantity of recombinant protein accumulated in the soluble cell fraction to obtain a quality

control reference. However, this protein version was difficult to purify and had a great tendency to aggregate under the tested experimental conditions.
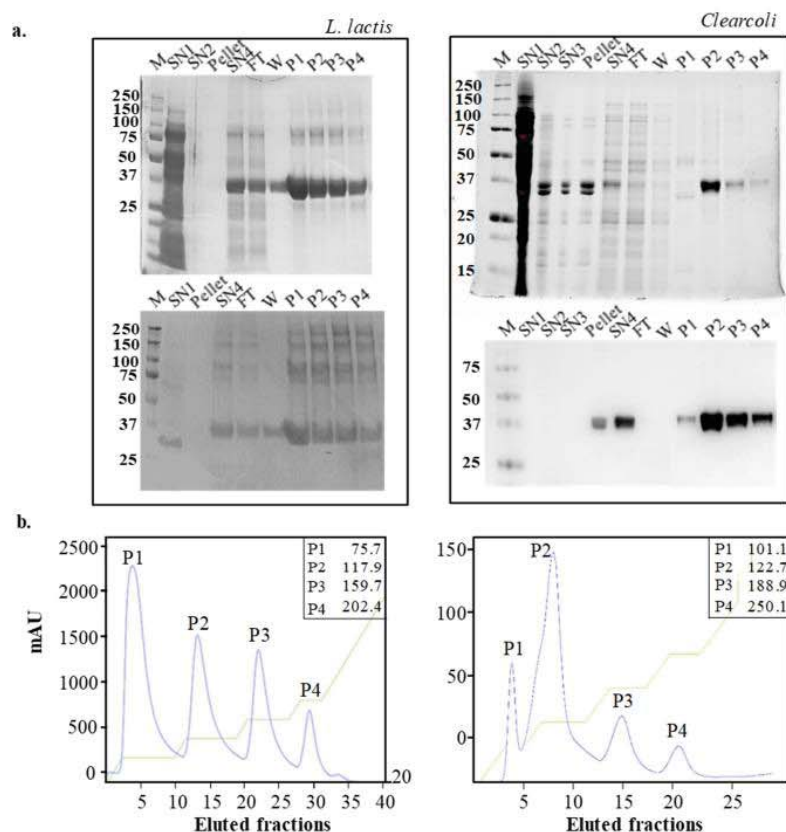
Figure 1. Detection of protein bands from inclusion bodies (IBs) produced in *L. lactis* (left) and *Clearcoli* (right) obtained during solubilization procedure. For each expression system, SDS–PAGE (above) and Western blot analyses (below) are shown (**a**). Immobilized metal affinity chromatography (IMAC) chromatograms for purifications of solubilized MMP-9 samples produced by *L. lactis* (left) and *Clearcoli* (right). Blue lines depict the absorbance signal (mAU) along the elution process and green lines the elution buffer (EB) gradient progress. The corresponding concentration of imidazole (mmol/L) is indicated for each eluted peak in the inset (**b**). SN1: soluble cell fraction of the cell lysate; SN2: soluble protein content after the first wash of the insoluble cell fraction; SN3: soluble protein content after second wash; pellet: pellet after solubilization of IBs with N-lauroylsarcosine; SN4: proteins solubilized from IBs after N-lauroylsarcosine treatment; FT: Flow-through; W: wash; P1-P4: protein peaks. M: molecular weight marker in kDa.

2.4. Activity of the MMP-9 Protein Peaks of L. Lactis and Clearcoli Obtained from IBs

The highest activity of *L. lactis* protein peaks corresponded to peak 1, although no significant differences were detected between peaks 1 and 2. Moreover, significant differences were obtained between peaks 1 and peaks 3 and 4 ($p = 0.0002$) (Figure 2b). On the other hand, *Clearcoli* protein peak 2 was the only one showing activity in this expression system ($p = 0.0002$). In any case, the activity of each of the *L. lactis* protein peaks was significantly higher than that of any of the protein peaks obtained from *Clearcoli*. This observation supports the potential of this expression system as a promising alternative to *E. coli* for the production of recombinant proteins [27]. These results clearly stressed that the selection of this prokaryotic expression system has a clear impact on the final quality of the produced recombinant protein.

a.

L. lactis	Yield (mg/L) mean ± se	Purity (%) mean ± se	*Clearcoli*	Yield (mg/L) mean ± se	Purity (%) mean ± se
Peak 1	6 ± 1.2	97.4 ± 1.2	Peak 1	0.049 ± 0.002	< 50
Peak 2	3.1 ± 0.5	97.9 ± 1.2	Peak 2	0.177 ± 0.007	94.4 ± 4.2
Peak 3	1.1 ± 0.5	98.2 ± 1.0	Peak 3	0.054 ± 0.001	62.6 ± 22.6
Peak 4	0.2 ± 0.1	97.3 ± 1.6	Peak 4	0.023[a]	79.6 ± 5.0

b.
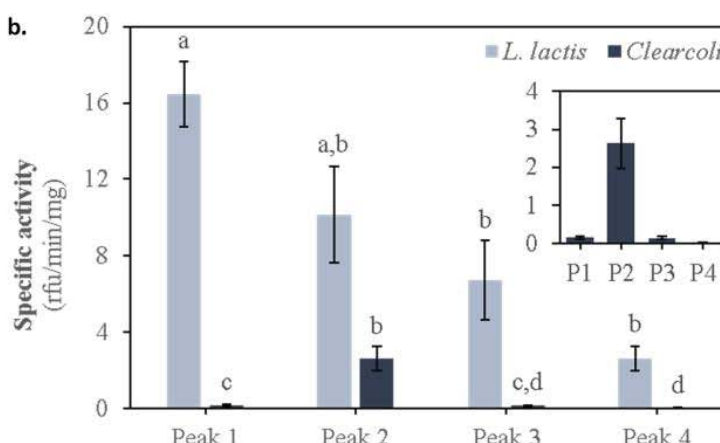
Figure 2. Table summarizing the yields for each peak, as mg of protein per peak per culture L (mg/L), and their purity in % for each expression system. [a] Peak 4 of *Clearcoli* was purified in enough amount to be quantified only once out of the 3 separate production experiments performed. Therefore, no SEM is shown (**a**). Specific activity for the MMP-9 in each peak solubilized from IBs produced by *L. lactis* and *Clearcoli*. Relative fluorescence units (rfu) refer to the fluorescence emitted by dye-quenched gelatin along its degradation kinetics due to MMP-9 activity. Specific activity is expressed as rfu per minute per MMP-9 mg (rfu/min/mg). Means and standard error of the mean (SEM) are depicted for each MMP-9 peak ($n = 4$). Different letters (a to d) depict differences between protein peaks ($p = 0.002$) (**b**).

2.5. Physicochemical MMP-9 Properties

In the biopharmaceutical industry, the biophysical characterization of therapeutic proteins follows a rigorous and standardized process [28]. In addition, some specific physicochemical methods are being established in protein structure studies [29]. However, in many research laboratories, access to specialized equipment and trained personnel is not common. In this case, the detection of more than one positive protein peak during the purification process is not evaluated under the parameters of conformational quality. In that sense, we selected some available methodological approaches to analyze the putative correlation between protein conformational quality and biological activity in the different protein peaks obtained during the purification process of MMP-9.

Interestingly, we detected a correlation between the affinity of the protein subpopulations towards the Ni^{2+} (i.e., higher peak number in Figure 1b) and the size of the protein species revealed by DLS (Figure 3a,b and Table 1), that is irrespective of the bacterial strain.
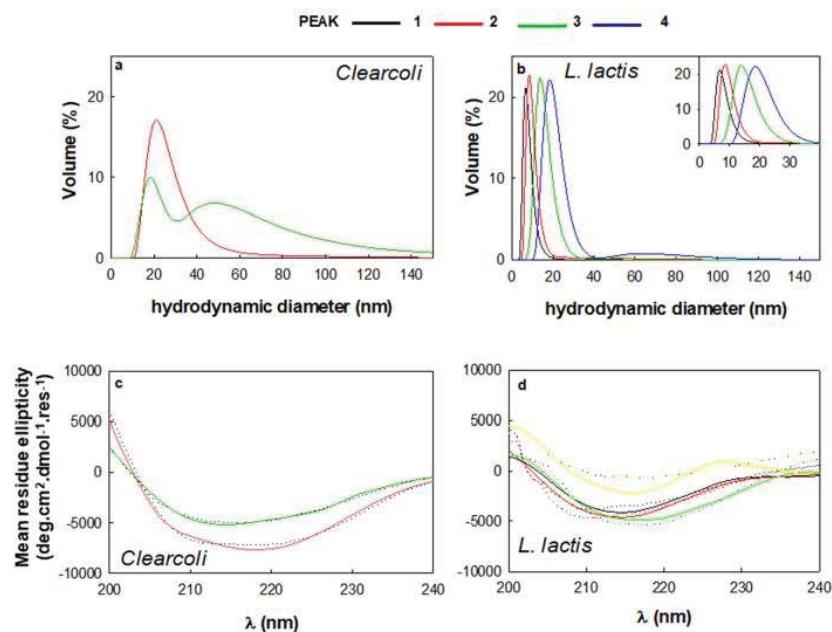
Figure 3. Volume weighted distribution determined by dynamic light scattering (DLS) of MMP-9 peaks from, *Clearcoli* (**a**) and *L. lactis* (**b**). Far UV-circular dichroism (CD) spectra of MMP-9 peaks from *Clearcoli* (**c**) and *L. lactis* (**d**). Experimental spectra (dotted lines) and fitted spectra (solid lines). (See Materials and Methods Section 3.8).

Table 1. DLS, CSM and unfolding temperature of isolated elution protein peaks obtained from *L. lactis* and *Clearcoli* IBs after solubilization. Values represent mean and SEM. Not determined (n.d.). Polydispersity index (pdi).

	Peak 1	Peak 2	Peak 3	Peak 4
Hydrodynamic diameter (nm)				
Clearcoli	n.d.	21 ± 9 (pdi = 0.6)	$18.2^{1} \pm 5.3$ (pdi = 0.47)	n.d.
L. lactis	6.5 ± 2.1 (pdi = 0.7)	8.04 ± 3.2 (pdi = 0.5)	15.7 ± 4.1 (pdi = 0.7)	18.2 ± 4.1 (pdi = 0.7)
Center of spectral mass (CSM, nm)				
Clearcoli	n.d.	357 ± 0.5	361 ± 9	n.d.
L. lactis	354.82 ± 0.1	354.89 ± 0.07	354.75 ± 0.2	354.92 ± 0.3
Unfolding temperature (Tm, °C)				
Clearcoli	n.d.	69.54 ± 8.2	n.d.	n.d.
L. lactis	60.6 ± 1.1	54.8 ± 0.7	52.4 ± 3.3	56.4 ± 2.5

[1] This value corresponds to the smaller peak shown in Figure 3. The second peak (around 50 nm) displayed a very broad size distribution.

In *L. lactis*, the protein size moves from 6–8 nm to approximately 20 nm or more, suggesting an oligomerization event. In fact, according to the Wilkins equation [30], the hydrodynamic diameter of recombinant protein MMP-9 in native corresponds to 5.2 nm, which is close to the size detected for peak 1 in *L. lactis* (Table 1). However, the enzyme functionality was also detected in samples of slightly higher hydrodynamic diameter (as peak 2 from *L. lactis*). On the other hand, the hydrodynamic diameter calculated with the same equation for the unfolded protein is 12.4 nm. Surprisingly, protein samples with similar hydrodynamic diameters displayed enzymatic activity (protein peaks 3 and 4 of *L. lactis* and peak 2 of *Clearcoli*). Therefore, the higher dimensions of protein peaks

could be explained by the presence of higher proportions of disordered structures (Table 2) rather than a full unfolding process, at least in the case of protein peaks 3 and 4 of *L. lactis*. In addition, as the size of the protein increases, the presence of alpha structure seems to fade away (Figure 3d, Table 2), suggesting a link between oligomerization and the secondary structure of the protein. In this context, MMP-9 from peaks 1 and 2 for *L. lactis* and peak 2 for *Clearcoli* exhibited a higher percentage of α-helix structure (a particularly noticeable minimum at around 208 nm (*L. lactis*) or at 210 and 222 nm (*Clearcoli*) that tends to disappear in peaks 3 and 4 (Table 2). Moreover, MMP-9 from peak 3 (*Clearcoli*), which contains more than one peak in the DLS analysis, revealed a β-sheet protein spectrum, as an incipient minimum around 216 nm was observed (Figure 3a and Table 2). Such protein conformational change concomitant with the oligomerization process has been previously described during the controlled protein assembly as regular size protein nanoparticles [31]. However, it cannot be ruled out that the increase in the size of the proteins might be due to the presence of disordered structures (Table 2).

Table 2. Secondary structure contents of the MMP-9 protein obtained by deconvoluting far-UV CD spectra.

	Peak 1	Peak 2	Peak 3	Peak 4
		Clearcoli		
Alpha helix	n.d.	0.242	0.132	n.d.
Beta sheet	n.d.	0.273	0.336	n.d.
Turns	n.d.	0.217	0.213	n.d.
Disordered	n.d.	0.266	0.319	n.d.
NRMSD	n.d.	0.095	0.057	n.d.
		L. lactis		
Alpha helix	0.091	0.125	0.06	0.039
Beta sheet	0.389	0.377	0.349	0.409
Turns	0.197	0.198	0.197	0.196
Disordered	0.323	0.3	0.394	0.356
NRMSD	0.491	0.411	0.176	0.498

NRMSD: normalized root means square deviation.

Another important parameter for the enzymatic activity of MMP-9 is the presence of metal ions. Therefore, in order to assess the Zn^{2+} occupancy in the protein conformers present in the protein peaks, inductively coupled plasma mass spectrometry (ICP-MS) was performed (Appendix A and Figure S4) as previously described [32]. Overall, the Zn^{2+} occupancy in all protein samples was below the expected molar ratio for this recombinant protein with 7 putative binding sites (Figure S2A). Surprisingly, the amount of Zn^{2+} was much lower for the protein samples obtained in *L. lactis* (Figure S4A), which corresponds to the expression system where the maximum specific activity of MMP-9 was achieved (*L. lactis* protein peak 1 and 2, see Figure 2b). In addition, in *Clearcoli*, protein peak 2, which displayed the highest specific activity (Figure 2b), contained the lowest amount of Zn^{2+} (Figure S4A). Even though the presence of metal ions is relevant for the biological activity of enzymes, in controlled experimental conditions, it has been described a negative impact on the specific activity relative to the metal ion concentration [33]. In the results presented here, most of the protein samples presented less than 7 Zn^{2+} ions per protein molecule, except for protein peak 3 from *Clearcoli* (Figure S4A). Moreover, data obtained for Ni^{2+} showed a similar trend, detecting much more signal in *Clearcoli* than in *L. lactis*, and with a concomitant increase in the amount of this cation while increasing the number of the protein peak (Figure S4B). However, when the total amount of metal ions was calculated, a clear proportional relationship between cation levels and protein peak number was observed (Figure S4C,D). One possible explanation of the detection of enzymatic activity on protein peaks with low content of metal cations would be the direct relationship between the presence of metal ions and the oligomerization state of protein samples [34,35]. In fact,

DLS results indicated an increase in size for protein peaks with lower enzymatic activity (Figure 3).

Another structural parameter, namely CSM, was obtained from the intrinsic fluorescence (IF) spectra. This value is related to the tertiary structure of the protein, and its increase indicates the hydration of the whole structure that, in many cases, accompanies protein unfolding. Figure 4 and Table 1 show the CSM values from each protein peak and from both bacterial hosts. Neither the supramolecular structure (DLS) nor the secondary structure (CD) allowed us to appreciate the differences between the peak-corresponding proteins produced in each expression system. However, at 25 °C, CSM values from *L. lactis* were around 354 nm with modest variability, while the ones from *Clearcoli* exhibit higher CSM values (Table 1 and Figure 4), which was probably related to the loss of the tertiary structure. Moreover, it is important to highlight the high variability in the CSM values observed when MMP-9 was obtained from *Clearcoli*.
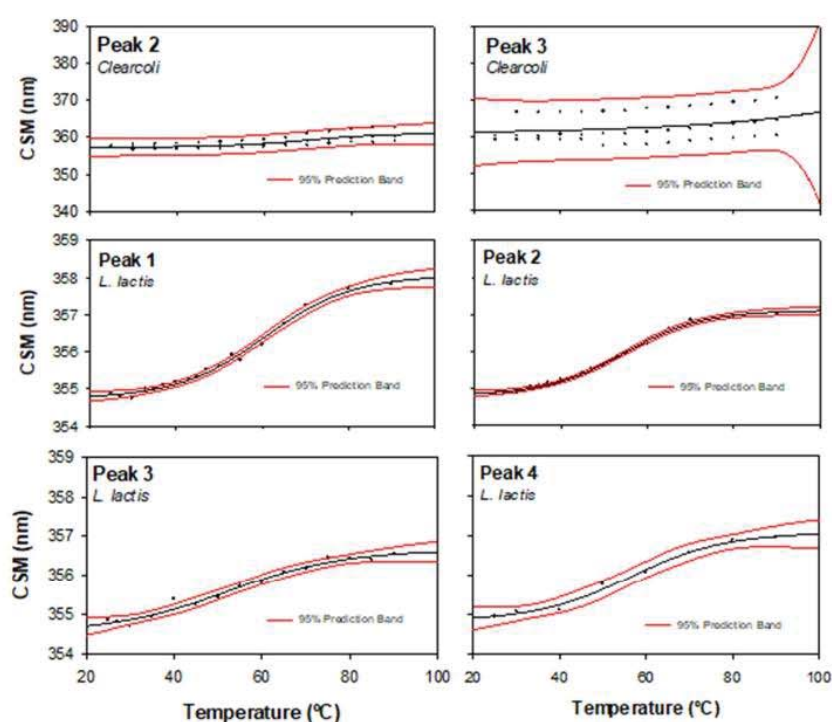
Figure 4. Center of spectral mass of the tryptophan fluorescence spectrum (CSM) versus temperature of each MMP-9 peak (indicated in the plot). The solid line indicated the nonlinear regression to a sigmoidal model; red lines indicated 95% of the prediction interval.

In Figure 4, we show the CSM thermal profile of each MMP-9 peak (raw data exemplified in Supplementary Material Figure S4) and the statistical estimation of the Tm values recorded in Table 1. As we discuss below, the highest structure-function quality and, at the same time, lower variability on the estimation were observed in samples from peak 2. In the case of *Clearcoli*, the sample from peak 2 was the only one that showed reliable data.

In biophysical terms, the native state of proteins is described as that of minimum energy with a limited number of conformational structures (or low conformational entropy) [36]. However, in many cases, the unfolded to native form transition occurs by a multistep folding process with the generation of conformation intermediates [37,38]. In this sense, the structure variability detected in different positive MMP-9 protein peaks after IB solubilization is in accordance with the presence of folding intermediates entrapped in the IBs irrespectively of the expression system. In addition, after the detailed physicochemical analysis of the individual protein peaks, we can conclude that the second protein peak

contained the protein in its best conformational state and presents the lowest variability regardless of the bacterial producing system. According to this analysis, the MMP-9 protein species from peak 2 produced in *L. lactis* contained the most structured and functional protein conformers.

3. Materials and Methods

3.1. Bacteria Strains and Plasmids

The *Lactococcus lactis* subsp. *cremoris* NZ9000 mutant ($clpP^-$, $htrA^-$, Em^R) strain, provided by INRA (France; patent n. EP1141337B1) was transformed with a pNZ8148 plasmid with chloramphenicol resistance gene (Cm^R) (MoBiTech GmbH, Goettingen, Germany) previously cloned with the DNA insert encoding for a bovine MMP-9 fragment (Phe107-Pro449, NCBI, NM_174744.2) [15].

The same DNA fragment encoding for the bovine Phe107-Pro449 MMP-9 was cloned (*Nco*I/*Hind*III restriction sites) into a pETDuet plasmid (Novagen, Madison, WI, USA) bearing the ampicillin resistance gene (Am^R) and transformed in *Clearcoli*® BL21(DE3) (Lucigen, Middleton, WI, USA) by electroporation (Appendix A).

The DNA fragment in both expression vectors was C-terminally fused to a 6His-tag and codon-optimized for *L. lactis* (GeneArt, Thermo Fisher, Waltham, MA, USA; Figure S1) [15].

3.2. Bacteria Strains and Plasmids

Batch cultures of *L. lactis* were grown at 30 °C in static cultures with M17 broth containing 0.5% glucose, 5 µg/mL chloramphenicol (Cm) and 2.5 µg/mL erythromycin (Em). Inductions of re-inoculated cultures were done with 12.5 ng/mL nisin at 0.4–0.6 OD_{600} for 3 h to get the recombinant protein expression.

Batch cultures of *Clearcoli* were grown at 37 °C in a shaker at 250 rpm with lysogeny broth (LB; 10 g/L tryptone, 5 g/L yeast extract, 10 g/L NaCl) and 100 µg/mL ampicillin. Inductions of re-inoculated cultures were done at 1 mmol/L IPTG when cell suspensions reached 0.6–0.8 OD_{550}. The cultures were then incubated at 30 °C and 250 rpm for 3 h (for protein production). Bacteria were harvested by centrifugation at $6000 \times g$ for 30 min at 4 °C.

3.3. Protein Purification

Soluble MMP-9 was obtained by protein solubilization from IBs as described [11]. For each solubilization process, five samples were generated: SN1 (i.e., supernatant 1, soluble cell fraction of the lysate), SN2 and SN3 from washes of the insoluble cell fraction after cell lysis, SN4 and the cell pellet obtained after solubilization with mild detergent incubation. The MMP-9 protein contained in SN4 was purified by affinity chromatography in an ÄKTA Pure fast protein liquid chromatography (FPLC) system (GE Healthcare, Chicago IL, USA) (Appendix A).

3.4. Protein Detection, Yield and Purity

The different protein fractions collected after the purification process were analyzed by SDS–PAGE and Western blot analyses. Briefly, a small aliquot of each fraction was independently mixed (1:1) with Lemmli buffer. Then, the different samples were boiled at 90 °C for 10 min and subsequently charged in a polyacrylamide gel. Samples containing aggregated protein (pellets) were boiled for 40 min. The electrophoresis was run in a buffer containing 0.1% of sodium dodecyl sulfate (SDS).

Positive protein bands were detected by Western blot. The conditions used were anti-his-tag monoclonal primary antibody (Santa Cruz Biotechnologies, Inc., Santa Cruz Biotechnologies, Inc., Dallas, TX, USA; scv-57598) used at 1:1000 dilution, and 6xhis monoclonal antibody (Takara Bio Inc., Kusatsu, Japan; 631212) used at 1:6000 dilution for *L. lactis* and *Clearcoli*, respectively, and goat anti-mouse secondary antibody at 1:5000 dilution

(Bio-Rad Laboratories Inc., Hercules, CA, USA; 170–6516). The images were acquired with the ChemiDoc™ touch imaging system (Bio-Rad Laboratories Inc., Hercules, CA, USA).

Soluble MMP-9 in each peak was quantified by NanoDrop (Thermo Fisher Scientific, Waltham, MA, USA) using the MMP-9 parameters (ε: 70,080 mol/L^{-1} cm^{-1}; ProtParam-ExPASy) and yield for each peak was obtained. The purity of MMP-9 peaks was analyzed by Coomassie blue or TGX (Bio-Rad Laboratories Inc., Hercules, CA, USA) staining using ImageLab software version 6.1.0 (Bio-Rad Laboratories Inc., Hercules, CA, USA). Briefly, measurements of the volume of the protein bands in each lane were considered as 100% of the protein content in the sample, and the volume of the protein band corresponding to MMP-9 was used to calculate the percentage it represents in the total protein bands in the lane.

3.5. MMP-9 Activity Determination by DQgelatinTM Degradation Kinetics

MMP-9 activity for each eluted peak from both *L. lactis* and *Clearcoli*® BL21(DE3) productions was quantified by dye-quenched gelatin (DQgelatin™, Thermo Fisher Scientific, Waltham, MA, USA) degradation kinetics (Appendix A). Specific activity for MMP-9 peaks was extracted for each sample by obtaining the initial velocity from the kinetics data (relative fluorescence units per minute, rfu/min) and correcting it by the MMP-9 mg in the wells (rfu/min/mg).

3.6. Dynamic Light Scattering (DLS)s

The volume size distribution of MMP-9 from each chromatographic peak was determined at 0.15 mg/mL in 20 mmol/L Tris-HCl pH 8 and 5% glycerol by DLS at 633 nm (Zetasizer Nano ZS, Malvern Instruments Limited, Malvern, UK). Samples were maintained at 25 °C. According to the Stokes–Einstein equation, the DLS algorithm calculates the hydrodynamic radius or hydrodynamic diameter from the diffusion coefficient of the particles [39].

3.7. Determination of Intrinsic Fluorescence

Fluorescence spectra were recorded in a Cary Eclipse spectrofluorometer (Agilent Technologies, Mulgrave, Australia). A quartz cell with 10 mm path length and a thermostated holder was used. The excitation and emission slits were set at 5 nm. Excitation wavelength (λ_{ex}) was set at 295 nm. Emission spectra (λ_{em}) were acquired within a range from 310 to 450 nm. The protein concentration was around 0.2 mg/mL in 20 mmol/L Tris-HCl pH 8 and 5% glycerol. Spectrum from each peak and of each bacterial strain was performed in triplicate. In order to evaluate the conformational difference between the proteins of each peak, we decided to calculate the center of spectral mass (CSM) for comparisons. CSM is a weighted average of the fluorescence spectrum peak. In addition, it is related to solvent exposure of the Trp. The maximum red-shift in the CSM of the tryptophan is compatible with a large solvent [20,40,41] and consequently a highly unfolded conformation.

The CSM was calculated for each of the fluorescence emission spectrum [42] according to Equation (1), where I_i is the fluorescence intensity measure at the wavelength λ_i.

$$\lambda = \frac{\sum \lambda_i I_i}{\sum I_i} \tag{1}$$

We also performed thermal unfolding analyses by measuring Trp fluorescence as a function of the temperature. For this approach, the heating rate was set at 1 °C/min.

3.8. Circular Dichroism (CD)

Measurements were made with a Jasco J-715 spectropolarimeter (JASCO, Oklahoma City, OK, USA) with a thermostated device by a Peltier system spectropolarimeter using a 1 mm path length quartz cell. Each spectrum was an average of six scans. The protein concentration was around 0.1–0.2 mg/mL in 20 mmol/L Tris-HCl pH 8 and 5% glycerol. Scan speed was set at 50 nm/min with a 1 s response time, and measurements were

carried out in the 200–240 nm region. Each final spectrum was obtained from two or three replicas. The ellipticity values were transformed in "mean residue ellipticity" as previously described [31]. The relative secondary structure contents of the protein from each peak was obtained by deconvoluting its far-UV CD spectrum by using the CONTIN-LL algorithm [43,44] run on the DichroWeb server [45].

3.9. Statistical Analysis

Data for the determination of MMP-9 activity by DQgelatin™ degradation kinetics were analyzed using a mixed-effects model, using SAS 9.4 (SAS Institute Inc., Cary, NC, USA). Replicates (n = 12 for peaks 2 and 3 obtained in *Clearcoli*; n = 9 for all peaks in *L. lactis*, and for peak 1 in *Clearcoli*; n = 4 for peak 4 in *Clearcoli*) were included as a random effect; strain, peak and their interaction were included as fixed effects. Differences between multiple means were further established using Tukey's test. Data were previously transformed to a natural logarithm to achieve a normal distribution when needed. Results are expressed as means and standard error of nontransformed data.

The values of melting temperature (Tm) were determined by fitting the experimental data from the CSM versus temperature plot to a sigmoidal equation of four parameters by a computer-aided nonlinear regression analysis by the least-squares method.

In order to evaluate the variability of CSM values within the thermal profile, we showed the 95% prediction interval. This region illustrates the standard deviation of experimental data with respect to the estimated value.

4. Conclusions

Many recombinant proteins used for biopharmaceutical and industrial purposes are obtained from IBs. Despite the development of different protocols for the recovery of functional proteins from these aggregates, there is an unmet need for analytical methods to evaluate the conformational and functional status of the proteins released from IBs. In this study, the physicochemical analysis of MMP-9 protein peaks rescued from IBs of two endotoxin-free prokaryotic expression systems revealed the presence of different pools of protein conformers with specific structural characteristics. The oligomeric status of these protein forms, together with the content in alpha helices and the corresponding thermal stability, had an impact on the specific activity of the protein pools. This type of analysis can provide comprehensive views of the conformational heterogeneous nature of the folding intermediates released from IBs as well as allow for the rational selection of the best-fitted populations of protein forms.

Appendix A

Appendix A.1. Bacterial Strains and Plasmids

Electroporation of *Clearcoli* was performed using Gene Pulser from Bio-Rad fitted with 2500 V, 200 Ω and 25 μF in a pre-cooled 2 cm electroporation cuvette. Then, the samples were supplemented with 900 μL of LB medium and incubated for two h at 37 °C. After this, 100 μL of the incubated mixture was plated and incubated overnight at 37 °C.

Appendix A.2. Protein Purification

Briefly, for *L. lactis*, each 500 mL of the bacterial pellet was suspended in 30 mL PBS containing protease inhibitors (EDTA-free Complete cocktail, Roche, Basel, Switzerland) and was subjected to 4 rounds of cell disruption by French Press at 1500 psi. After cell disruption, lysozyme was added to a final concentration of 0.05 mg/mL and lysates were incubated at 37 °C for 2 h and 250 rpm before washes. In the case of *Clearcoli*, cell pellets were resuspended in 20 mmol/L Tris-HCl pH 8 at 60 mL/g dry weight containing protease inhibitors (EDTA-free Complete cocktail, Roche) and were subjected to 3 rounds of cell disruption by French Press at 1200 psi. Cell lysates were centrifuged at $15,000 \times g$ for 30 min at 4 °C obtaining supernatant 1 (SN1) and pellet. Pellets were washed twice in Milli-Q water and centrifuged at $10,000 \times g$ for 30 min at 4 °C (generating samples SN2 in the first wash and SN3 in the second). All supernatants and pellets were stored at −80 °C and saved for further quality control analysis. Pellets were suspended in solubilization buffer (40 mmol/L Tris pH 8 with 0.2% N-lauroylsarcosine) at a ratio of 40 mL per g of pellet and were incubated in agitation (roller mixer) for 40 h (*L. lactis*) and 24 h (*Clearcoli*) at RT. The protein solution was centrifuged at $15,000 \times g$ and at 4 °C for 45 min, and the supernatant (SN4) containing the solubilized MMP-9 was filtered and purified by immobilized metal affinity chromatography (IMAC) using 1 mL-HiTrap chelating columns (GE Healthcare) in an ÄKTA purifier FPLC system (GE Healthcare). Binding and elution buffers both contained 0.2% N-lauroylsarcosine as well as 20 mmol/L Tris pH 8 and 500 mmol/L NaCl. In addition, binding and elution buffers were prepared with 20 mmol/L and 500 mmol/L imidazole or 10 mmol/L and 500 mmol/L imidazole for *L. lactis* and *Clearcoli*, respectively. The MMP-9 peaks were split by holding the elution buffer gradient at each increase in the absorbance signal in the chromatogram. The eluted peaks were dialyzed separately O/N against 20 mmol/L Tris-HCl pH 8 and 5% glycerol at 4 °C with gentle agitation,

centrifuged at 15,000× *g* for 15 min at 4 °C to remove possible precipitated protein and quantified. Aliquots were stored at −80 °C.

Appendix A.3. MMP-9 Activity Determination by DQgelatinTM Degradation Kinetics

Briefly, for all MMP-9 peaks, 1 μg MMP-9 was plated in a transparent flat-bottom black 96-well plate in triplicate, at a final volume of 150 μL in assay buffer (5 mmol/L CaCl₂, 50 mmol/L Tris pH 7.6, 150 mmol/L NaCl, 0.01% Tween20). Immediately after adding 0.25 μg of DQgelatin™ per well, the plate was bottom-read every two minutes for 2 h in a fluorescence microplate reader (Victor III multilabel counter, PerkinElmer) at 495/515 nm (excitation/emission wavelengths).

Appendix A.4. Inductively Coupled Plasma-Mass Spectrometry (ICP-MS) Analysis

Zn^{2+} and Ni^{2+} metal ions present in MMP-9 protein samples were analyzed on an ICP-MS Agilent 7500ce instrument (Santa Clara, CA, USA). Briefly, 100 μL of MMP-9 protein samples in 20 mmol/L Tris-HCl pH 8 and 5% glycerol were dispensed into individual polypropylene tubes in technical duplicates. Protein samples were incubated with 100 μL of HNO_3 at 80 °C for 30 min. The digested solutions were diluted up to a final volume of 2 mL with deionized water. The samples were analyzed by conventional ICP-MS for the detection of the metal elements Zn^{2+} and Ni^{2+}. Sample analysis and operation of the ICP-MS were done according to CCiTUB (www.ccit.ub.edu) in-house standard operating procedures.

References

1. Ferrer-Miralles, N.; Villaverde, A. Bacterial cell factories for recombinant protein production; expanding the catalogue. *Microb. Cell Fact.* **2013**, *12*. [CrossRef]
2. Sanchez-Garcia, L.; Martín, L.; Mangues, R.; Ferrer-Miralles, N.; Vázquez, E.; Villaverde, A. Recombinant pharmaceuticals from microbial cells: A 2015 update. *Microb. Cell Fact.* **2016**, *15*. [CrossRef]
3. Villaverde, A.; Corchero, J.L.; Seras-Franzoso, J.; Garcia-Fruitos, E. Functional protein aggregates: Just the tip of the iceberg. *Nanomedicine* **2015**, *10*, 2881–2891. [CrossRef] [PubMed]
4. De Marco, A.; Ferrer-Miralles, N.; Garcia-Fruitós, E.; Mitraki, A.; Peternel, S.; Rinas, U.; Trujillo-Roldán, M.A.; Valdez-Cruz, N.A.; Vázquez, E.; Villaverde, A. Bacterial inclusion bodies are industrially exploitable amyloids. *FEMS Microbiol. Rev.* **2019**, *43*. [CrossRef]
5. Singh, S.M.; Panda, A.K. Solubilization and refolding of bacterial inclusion body proteins. *J. Biosci. Bioeng.* **2005**, *99*, 303–310. [CrossRef]
6. Upadhyay, A.K.; Murmu, A.; Singh, A.; Panda, A.K. Kinetics of inclusion body formation and its correlation with the characteristics of protein aggregates in *Escherichia coli*. *PLoS ONE* **2012**, *7*, e33951. [CrossRef]
7. Elia, F.; Cantini, F.; Chiti, F.; Dobson, C.M.; Bemporad, F. Direct Conversion of an Enzyme from Native-like to Amyloid-like Aggregates within Inclusion Bodies. *Biophys. J.* **2017**, *112*, 2540–2551. [CrossRef] [PubMed]
8. Singh, A.; Upadhyay, V.; Panda, A.K. Solubilization and refolding of inclusion body proteins. *Methods Mol. Biol.* **2015**, *1258*, 283–291. [CrossRef] [PubMed]
9. Palmer, I.; Wingfield, P.T. Preparation and extraction of insoluble (inclusion-body) proteins from *Escherichia coli*. *Curr. Protoc. Protein Sci.* **2012**, *70*. [CrossRef] [PubMed]
10. Wang, Y.; van Oosterwijk, N.; Ali, A.M.; Adawy, A.; Anindya, A.L.; Domling, A.S.S.; Groves, M.R. A Systematic Protein Refolding Screen Method using the DGR Approach Reveals that Time and Secondary TSA are Essential Variables. *Sci. Rep.* **2017**, *7*, 9355. [CrossRef] [PubMed]
11. Gifre-Renom, L.; Cano-Garrido, O.; Fàbregas, F.; Roca-Pinilla, R.; Seras-Franzoso, J.; Ferrer-Miralles, N.; Villaverde, A.; Bach, À.; Devant, M.; Arís, A.; et al. A new approach to obtain pure and active proteins from *Lactococcus lactis* protein aggregates. *Sci. Rep.* **2018**, *8*. [CrossRef] [PubMed]
12. Singh, A.; Upadhyay, V.; Upadhyay, A.K.; Singh, S.M.; Panda, A.K. Protein recovery from inclusion bodies of *Escherichia coli* using mild solubilization process. *Microb. Cell Fact.* **2015**, *14*, 41. [CrossRef]
13. Peternel, S.; Grdadolnik, J.; Gaberc-Porekar, V.; Komel, R. Engineering inclusion bodies for non denaturing extraction of functional proteins. *Microb. Cell Fact.* **2008**, *7*, 34. [CrossRef]
14. Seras-Franzoso, J.; Peternel, S.; Cano-Garrido, O.; Villaverde, A.; Garcia-Fruitos, E. Bacterial inclusion body purification. *Methods Mol. Biol.* **2015**, *1258*, 293–305. [PubMed]
15. Cano-Garrido, O.; Sánchez-Chardi, A.; Parés, S.; Giró, I.; Tatkiewicz, W.I.; Ferrer-Miralles, N.; Ratera, I.; Natalello, A.; Cubarsi, R.; Veciana, J.; et al. Functional protein-based nanomaterial produced in microorganisms recognized as safe: A new platform for biotechnology. *Acta Biomater.* **2016**, *43*, 230–239. [CrossRef] [PubMed]

16. Bonnans, C.; Chou, J.; Werb, Z. Remodelling the extracellular matrix in development and disease. *Nat. Rev. Mol. Cell Biol.* **2014**, *15*, 786–801. [CrossRef]
17. Page-McCaw, A.; Ewald, A.J.; Werb, Z. Matrix metalloproteinases and the regulation of tissue remodelling. *Nat. Rev. Mol. Cell Biol.* **2007**, *8*, 221–233. [CrossRef] [PubMed]
18. Gifre-Renom, L.; Ugarte-Berzal, E.; Martens, E.; Boon, L.; Cano-Garrido, O.; Martínez-Núñez, E.; Luque, T.; Roca-Pinilla, R.; Conchillo-Solé, Ò.; Ferrer-Miralles, N.; et al. Recombinant protein-based nanoparticles: Elucidating their inflammatory effects in vivo and their potential as a new therapeutic format. *Pharmaceutics* **2020**, *12*, 450. [CrossRef]
19. Mohseni, S.; Moghadam, T.T.; Dabirmanesh, B.; Khajeh, K. Expression, purification, refolding and in vitro recovery of active full length recombinant human gelatinase MMP-9 in *Escherichia coli*. *Protein Expr. Purif.* **2016**, *126*, 42–48. [CrossRef]
20. Mohana-Borges, R.; Silva, J.L.; Ruiz-Sanz, J.; de Prat-Gay, G. Folding of a pressure-denatured model protein. *Proc. Natl. Acad. Sci. USA* **1999**, *96*, 7888–7893. [CrossRef] [PubMed]
21. Peternel, S.; Komel, R. Isolation of biologically active nanomaterial (inclusion bodies) from bacterial cells. *Microb. Cell Fact.* **2010**, *9*, 66. [CrossRef]
22. Padhiar, A.A.; Chanda, W.; Joseph, T.P.; Guo, X.; Liu, M.; Sha, L.; Batool, S.; Gao, Y.; Zhang, W.; Huang, M.; et al. Comparative study to develop a single method for retrieving wide class of recombinant proteins from classical inclusion bodies. *Appl. Microbiol. Biotechnol.* **2018**, *102*, 2363–2377. [CrossRef]
23. Yamaguchi, H.; Miyazaki, M. Refolding techniques for recovering biologically active recombinant proteins from inclusion bodies. *Biomolecules* **2014**, *4*, 235–251. [CrossRef]
24. Rosenblum, G.; Van den Steen, P.E.; Cohen, S.R.; Grossmann, J.G.; Frenkel, J.; Sertchook, R.; Slack, N.; Strange, R.W.; Opdenakker, G.; Sagi, I. Insights into the structure and domain flexibility of full-length pro-matrix metalloproteinase-9/gelatinase B. *Structure* **2007**, *15*, 1227–1236. [CrossRef] [PubMed]
25. Vorackova, I.; Suchanova, S.; Ulbrich, P.; Diehl, W.E.; Ruml, T. Purification of proteins containing zinc finger domains using immobilized metal ion affinity chromatography. *Protein Expr. Purif.* **2011**, *79*, 88–95. [CrossRef] [PubMed]
26. Neznansky, A.; Opatowsky, Y. Expression, purification and crystallization of the phosphate-binding PstS protein from *Pseudomonas aeruginosa*. *Acta Crystallogr. F Struct. Biol. Commun.* **2014**, *70*, 906–910. [CrossRef] [PubMed]
27. Cano-Garrido, O.; Rueda, F.L.; Sanchez-Garcia, L.; Ruiz-Avila, L.; Bosser, R.; Villaverde, A.; Garcia-Fruitos, E. Expanding the recombinant protein quality in *Lactococcus lactis*. *Microb. Cell Fact.* **2014**, *13*, 167. [CrossRef] [PubMed]
28. Berkowitz, S.A.; Engen, J.R.; Mazzeo, J.R.; Jones, G.B. Analytical tools for characterizing biopharmaceuticals and the implications for biosimilars. *Nat. Rev. Drug Discov.* **2012**, *11*, 527–540. [CrossRef]
29. Sahin, E.; Roberts, C.J. Size-exclusion chromatography with multi-angle light scattering for elucidating protein aggregation mechanisms. *Methods Mol. Biol.* **2012**, *899*, 403–423. [CrossRef]
30. Wilkins, D.K.; Grimshaw, S.B.; Receveur, V.; Dobson, C.M.; Jones, J.A.; Smith, L.J. Hydrodynamic radii of native and denatured proteins measured by pulse field gradient NMR techniques. *Biochemistry* **1999**, *38*, 16424–16431. [CrossRef]
31. Sanchez, J.M.; Sanchez-Garcia, L.; Pesarrodona, M.; Serna, N.; Sanchez-Chardi, A.; Unzueta, U.; Mangues, R.; Vazquez, E.; Villaverde, A. Conformational Conversion during Controlled Oligomerization into Nonamylogenic Protein Nanoparticles. *Biomacromolecules* **2018**, *19*, 3788–3797. [CrossRef]
32. Houston, S.; Hof, R.; Francescutti, T.; Hawkes, A.; Boulanger, M.J.; Cameron, C.E. Bifunctional role of the *Treponema pallidum* extracellular matrix binding adhesin Tp0751. *Infect. Immun.* **2011**, *79*, 1386–1398. [CrossRef]
33. Bujacz, G.; Alexandratos, J.; Wlodawer, A.; Merkel, G.; Andrake, M.; Katz, R.A.; Skalka, A.M. Binding of different divalent cations to the active site of avian sarcoma virus integrase and their effects on enzymatic activity. *J. Biol. Chem.* **1997**, *272*, 18161–18168. [CrossRef] [PubMed]
34. Batoulis, H.; Schmidt, T.H.; Weber, P.; Schloetel, J.-G.; Kandt, C.; Lang, T. Concentration Dependent Ion-Protein Interaction Patterns Underlying Protein Oligomerization Behaviours. *Sci. Rep.* **2016**, *6*, 24131. [CrossRef]
35. Salgado, E.N.; Lewis, R.A.; Mossin, S.; Rheingold, A.L.; Tezcan, F.A. Control of protein oligomerization symmetry by metal coordination: C_2 and C_3 symmetrical assemblies through Cu^{II} and Ni^{II} coordination. *Inorg. Chem.* **2009**, *48*, 2726–2728. [CrossRef] [PubMed]
36. Malhotra, P.; Udgaonkar, J.B. How cooperative are protein folding and unfolding transitions? *Protein Sci.* **2016**, *25*, 1924–1941. [CrossRef] [PubMed]
37. Otosu, T.; Ishii, K.; Tahara, T. Microsecond protein dynamics observed at the single-molecule level. *Nat. Commun.* **2015**, *6*, 7685. [CrossRef]
38. Teschke, C.M.; Parent, K.N. "Let the phage do the work": Using the phage P22 coat protein structures as a framework to understand its folding and assembly mutants. *Virology* **2010**, *401*, 119–130. [CrossRef]
39. Stetefeld, J.; McKenna, S.A.; Patel, T.R. Dynamic light scattering: A practical guide and applications in biomedical sciences. *Biophys. Rev.* **2016**, *8*, 409–427. [CrossRef]
40. Li, T.M.; Hook, J.W., III; Drickamer, H.G.; Weber, G. Plurality of pressure-denatured forms in chymotrypsinogen and lysozyme. *Biochemistry* **1976**, *15*, 5571–5580. [CrossRef] [PubMed]
41. Ruan, K.; Weber, G. Hysteresis and conformational drift of pressure-dissociated glyceraldephosphate dehydrogenase. *Biochemistry* **1989**, *28*, 2144–2153. [CrossRef] [PubMed]

42. Lakowicz, J.R.; Kusba, J.; Wiczk, W.; Gryczynski, I.; Szmacinski, H.; Johnson, M.L. Resolution of the conformational distribution and dynamics of a flexible molecule using frequency-domain fluorometry. *Biophys. Chem* **1991**, *39*, 79–84. [CrossRef]

43. Sreerama, N.; Woody, R.W. Estimation of Protein Secondary Structure from Circular Dichroism Spectra: Comparison of CONTIN, SELCON, and CDSSTR Methods with an Expanded Reference Set. *Anal. Biochem.* **2000**, *287*, 252–260. [CrossRef]

44. Provencher, S.W.; Glöckner, J. Estimation of globular protein secondary structure from circular dichroism. *Biochemistry* **1981**, *20*, 33–37. [CrossRef]

45. Whitmore, L.; Wallace, B.A. Protein secondary structure analyses from circular dichroism spectroscopy: Methods and reference databases. *Biopolymers* **2008**, *89*, 392–400. [CrossRef] [PubMed]

46. Chou, H.T.; Kuo, T.Y.; Chiang, J.C.; Pei, M.J.; Yang, W.T.; Yu, H.C.; Lin, S.B.; Chen, W.J. Design and synthesis of cationic antimicrobial peptides with improved activity and selectivity against *Vibrio* spp. *Int. J. Antimicrob. Agents* **2008**, *32*, 130–138. [CrossRef] [PubMed]

47. Giacalone, M.J.; Gentile, A.M.; Lovitt, B.T.; Berkley, N.L.; Gunderson, C.W.; Surber, M.W. Toxic protein expression in *Escherichia coli* using a rhamnose-based tightly regulated and tunable promoter system. *Biotechniques* **2006**, *40*, 355–364. [CrossRef] [PubMed]

Supplementary material by Carratalá et al.

Title: Selecting subpopulations of high-quality protein conformers among conformational mixtures of recombinant bovine MMP-9 solubilized from inclusion bodies.

Authors: Jose Vicente Carratalá[1,2,3], Laia Gifre-Renom[4], Ramon Roca[4], Julieta Sanchez[1,2,5], Antonio Villaverde[1,2,3], Anna Aris[4], Elena Garcia-Fruitós[4], Neus Ferrer-Miralles[1,2,3]

[1]Institute for Biotechnology and Biomedicine, Autonomous University of Barcelona, Bellaterra, Barcelona, Spain

[2]Department of Genetics and Microbiology, Autonomous University of Barcelona, Bellaterra, Barcelona, Spain

[3]Bioengineering, Biomaterials and Nanomedicine Networking Biomedical Research Centre (CIBER-BBN), Bellaterra, Barcelona, Spain

[4]Department of Ruminant Production, Institute of Agrifood Research and Technology (IRTA), Caldes de Montbui, Barcelona, Spain

[5]Permanent address: National University of Cordoba, Faculty of Exact, Physical and Natural Sciences, ICTA and Chemistry Department, CONICET Institute of Biological and Technological Research (IIByT) Cordoba Argentina

*Corresponding author. E-mail address: neus.ferrer@uab.cat (N. Ferrer-Miralles).

Materials and Methods

Bacteria strains and plasmids

Electroporation of *Clearcoli* was performed using Gene Pulser from Bio-rad fitted with 2500V, 200 Ω and 25 μF in a pre-cooled 2 cm electroporation cuvette. Following, samples were supplemented with 900 μL of LB medium and incubated for 2 h at 37 °C. After that, 100 μL of the incubated mixture was plated and incubated overnight at 37 °C.

Protein purification

Briefly, for *L. lactis*, each 500 mL of bacterial pellet was suspended in 30 mL PBS containing protease inhibitors (EDTA-free Complete cocktail, Roche) and was subjected to 4 rounds of cell disruption by French Press at 1,500 psi. After cell disruption, lysozyme was added to a final concentration of 0.05 mg/mL and lysates were incubated at 37 °C for 2 h and 250 rpm before washes. In the case of *Clearcoli*, cell pellets were resuspended in 20 mmol/L Tris-HCl pH 8 at 60 mL/g dry weight containing protease inhibitors (EDTA-free Complete cocktail, Roche) and were subjected to 3 rounds of cell disruption by French Press at 1,200 psi. Cell lysates were centrifuged at 15,000 x *g* for 30 min at 4 °C obtaining supernatant 1 (SN1) and pellet. Pellets were washed twice in Milli-Q water and centrifuged at 10,000 x *g* for 30 min at 4 °C (generating samples SN2 in the first wash and SN3 in the second). All supernatants

and pellets were stored at -80 °C and saved for further quality control analysis. Pellets were suspended in solubilization buffer (40 mmol/L Tris pH 8 with 0.2 % N-Lauroylsarcosine) at a ratio of 40 ml per g of pellet and were incubated in agitation (roller mixer) for 40 h (*L. lactis*) and 24 h (*Clearcoli*) at RT. The protein solution was centrifuged at 15,000 x *g* and at 4 °C for 45 min and the supernatant (SN4) containing the solubilized MMP-9 was filtered and purified by Immobilized Metal Affinity Chromatography (IMAC) using 1 mL-HiTrap Chelating columns (GE Healthcare) in an ÄKTA purifier FPLC system (GE Healthcare). Binding and elution buffers both contained 0.2 % N-Lauroylsarcosine as well as 20 mmol/L Tris pH 8 and 500 mmol/L NaCl. In addition, binding and elution buffers were prepared with 20 mmol/L and 500 mmol/L imidazole or 10 mmol/L and 500 mmol/L imidazole for *L. lactis* and *Clearcoli* respectively. The MMP-9 peaks were split by holding the elution buffer gradient at each increase in the absorbance signal in the chromatogram. The eluted peaks were dialyzed separately O/N against 20 mmol/L Tris-HCl pH 8 and 5 % glycerol at 4 °C with gentle agitation, centrifuged at 15,000 x *g* for 15 min at 4 °C to remove possible precipitated protein and quantified. Aliquots were stored at -80 °C.

MMP-9 activity determination by DQgelatin^{TM} degradation kinetics

Briefly, for all MMP-9 peaks 1 μg MMP-9 was plated in a transparent flat-bottom black 96-well plate in triplicate, at a final volume of 150 μl in assay buffer (5 mmol/L $CaCl_2$, 50 mmol/L Tris pH 7.6, 150 mmol/L NaCl, 0.01 % Tween20). Immediately after adding 0.25 μg of DQgelatin^{TM} per well, the plate was bottom-read every two minutes for 2 h

in a fluorescence microplate reader (Victor III multilabel counter, Perkin-Elmer) at 495/515 nm (excitation/emission wavelengths).

**Inductively coupled plasma-mass spectrometry (ICP-MS) analysis.**

Zn^{2+} and Ni^{2+} metal ions present in MMP-9 protein samples were analyzed on an ICP-MS Agilent 7500ce instrument (Santa Clara, CA, USA). Briefly, 100 µl of MMP-9 protein samples in 20 mmol/L Tris-HCl pH 8 and 5 % glycerol were dispensed into individual polypropylene tubes in technical duplicates. Protein samples were incubated with 100 µl of HNO_3 at 80 °C for 30 min. The digested solutions were diluted up to a final volume of 2 mL with deionized water. The samples were analyzed by conventional ICP-MS for the detection of the metal elements Zn^{2+} and Ni^{2+}. Sample analysis and operation of the ICP-MS were done according to CCiTUB (www.ccit.ub.edu) in-house standard operating procedures.

Atgg**ca**tttcaaacttttgaaggagaacttaaatggcatcatcataatattacttattggattcaaaattattcagaagatttacctcg

tgctgttattgatgatgcttttgcacgtgcttttgcattgtggagtgctgttactccattaacatttactagagtttatggacctgaagc

agatattgttattcaatttggtgttcgtgaacatggagatggttatccatttgatggaaaaaatggtttgcttgctcatgcatttccacc

tggaaaaggtattcaaggagatgctcattttgatgatgaagaattatggtcacttggaaaaggtgttgttattccaacttattttgga

aatgctaaaggtgctgcatgtcattttccatttacatttgaaggacgttcatattctgcatgtacaactgatggtagaagtgatgatat

gttgtggtgttcaacaactgctgattatgatgcagatcgtcaatttggattttgtccttctgaaagactttatactcaagatggaaatg

ctgatggtaaaccatgtgtttttccttttacatttcaaggtcgtacttatagtgcttgtacatcagatggacgttctgatggttatagat

ggtgtgctacaactgcaaattatgatcaagataaattgtatggttttttgtccaacacgtgttgatgctacagttactggaggtaatgc

tgcaggagaactttgtgtttttccatttacatttttaggaaaagaatattcagcttgtacacgtgaaggaagaaatgatggtcatttat

ggtgtgcaacaacttctaattttgataaagataaaaaatggggattttgtccagatcaaggttatagtttgtttttagttgctgcacat

gaatttggacatgctcttggttttggatcatacttctgttccagaagcattgatgtatcctatgtatcgttttacagaagaacatcctctt

catagagatgatgttcaaggtattcaacatttgtatggaccaagaccagaacctaaacatcatcatcatcatcattaa

Figure S1. *L. lactis* codon optimized DNA encoding sequence of the cloned Bovine MMP-9 fragment. In the DNA sequence design the nucleotides CA following *Nco*I restriction site were added to restore the reading frame. Gene sequence was codon optimized for the *L. lactis* expression host as indicated (Geneart).

184

MAFQTFEGEL·KWHHHNITYW·IQNYSEDLPR·AVIDDAFARA·FALWSAVTPL·
TFTRVYGPEA·DIVIQFGVRE·HGDGYPFDGK·NGLLAHAFPP·GKGIQGDAHF·
DDEELWSLGK·GVVIPTYFGN·AKGAACHFPF·TFEGRSYSAC·TTDGRSDDML·
WCSTTADYDA·DRQFGFCPSE·RLYTQDGNAD·GKPCVFPFTF·QGRTYSACTS·
DGRSDGYRWC·ATTANYDQDK·LYGFCPTRVD·ATVTGGNAAG·ELCVFPFTFL·
GKEYSACTRE·GRNDGHLWCA·TTSNFDKDKK·WGFCPDQGYS·LFLVAAHEFG·
HALGLDHTSV·PEALMYPMYR·FTEEHPLHRD·DVQGIQHLYG·PRPEP**KHHHH**·

HH

Figure S2. Amino acid sequence of the recombinant Bovine MMP-9 protein from Phe107 to Pro449 (NCBI, NM_174744.2). An Ala residue was added to the original sequence to restore the reading frame (marked in bold). Recombinant MMP-9 gene was C-terminally fused to a His-tag for detection and quantification by western blot analysis. A Lys residue was included at the N-terminus of the tag for putative elimination of the tag by exopeptidases (marked in bold). Structural Zn^{2+}-binding sites are displayed in yellow and Zn^{2+}-binding sites in the active site are displayed in green (UniProt P52176). Trp residues are marked in light grey. MW: 39.60 kDa.

a
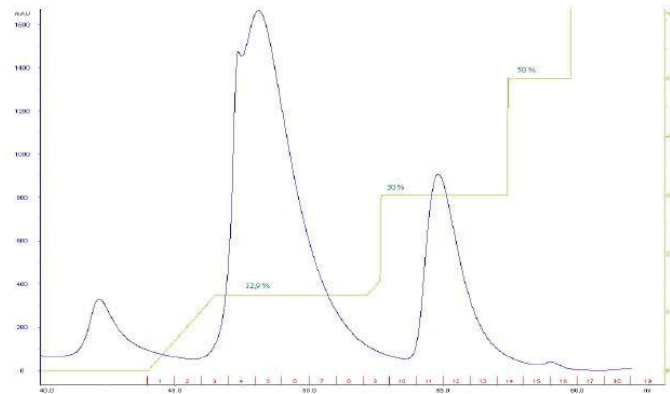
b
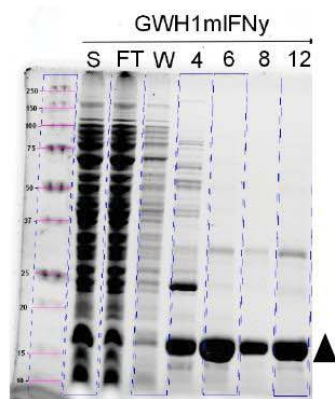
c
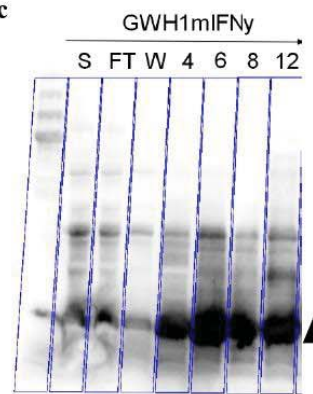
Figure S3. Purification of GW-H1-IFNγ in *E. coli* BL21(DE3) by IMAC. IMAC chromatogram of solubilized GW-H1-IFNγ from IBs. Blue line depicts the absorbance signal (mAU) along the elution process and green line the elution buffer (EB) gradient progress. The corresponding percentage of imidazole (%) is indicated above the green line for each eluted peak (Buffer A: 10 mmol/L imidazole; Buffer B: 500 mmol/L imidazole) (**a**). TGX SDS-PAGE (**b**) and western blot analysis of the purification procedure (**c**). S: proteins solubilized from IBs after N-Lauroylsarcosine incubation; FT: Flow through; W: wash; 4-12: protein fractions. Protein GW-H1-IFNg is a fusion

between an antimicrobial peptide (GW-H1, [46]) and the mouse IFNγ (UniprotKB P01580).
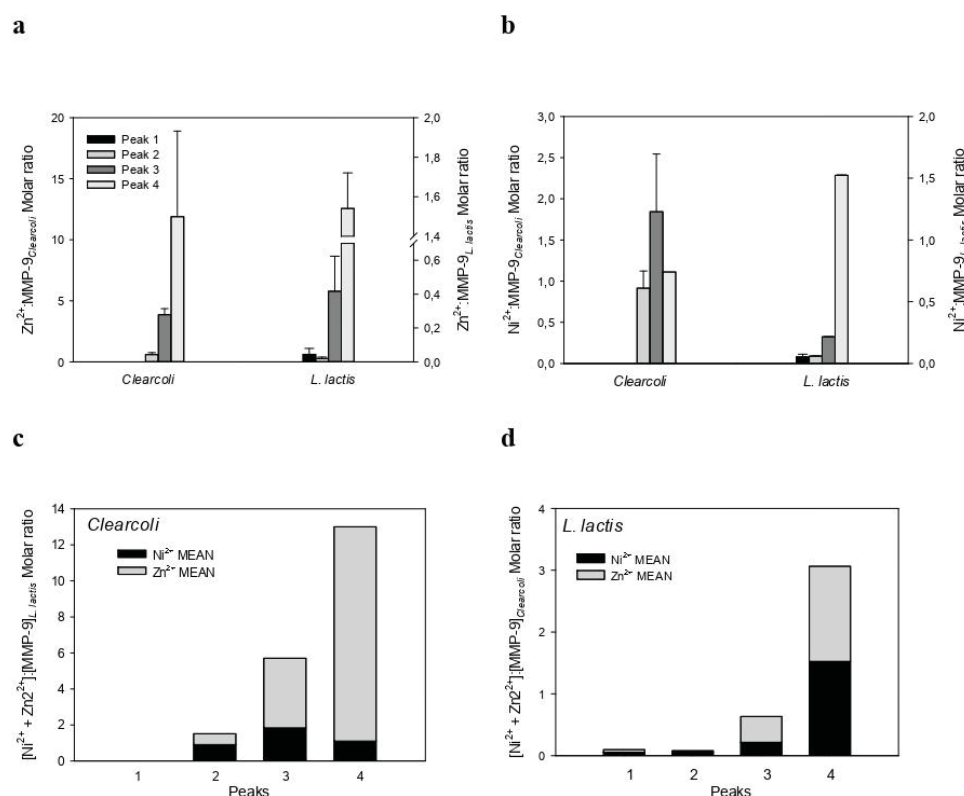
Fig. S4. ICP-MS quantification of metal ions (Zn^{2+} and Ni^{2+}) in purified recombinant MMP-9 protein samples. Molar ratio of Zn^{2+} in protein peaks obtained in *Clearcoli* and *L. lactis* (**a**). Molar ratio of Ni^{2+} in protein peaks obtained in *Clearcoli* and *L. lactis* (**b**). Molar ratio of Ni^{2+} + Zn^{2+} in protein peaks obtained in *Clearcoli* (**c**). Molar ratio of Ni^{2+} + Zn^{2+} in protein peaks obtained in *L. lactis* (**d**). Bars represent mean ± standard error of the mean (**a** and **b**) and mean (**c** and **d**). Protein peak 1 of *Clearcoli* was discarded as the protein purity was < 50 % (see Fig. 2a).

Table S1. Impact on bacterial culture growth of MMP-9 gene expression in *L. lactis* and *Clearcoli*

Host	Code	OD600/550 Pre-inoculum	OD600/550 pre-induction	OD600/550 post-induction	Induction time	Comments
L. lactis	1 (1.5 L)	3.020	0.49 ± 0.024	3.08 ± 0.02	3h 40m	15.9 mg/L (Solubilitzed O/N, 4 °C)
	2 (2.5 L)	3.015 ± 0.075	0.468 ± 0.015	2.715 ± 0.035	3 h	7.8 mg/L (Solub. 40 h RT)
	3 (2 L)	3.010	0.476 ± 0.0005	3 ± 0.1	3h 10m	9.6 mg/L (Solubilitzed. 40 h RT) **Fractioning error, repeated IMAC for Peak 1**
	4 (2 L)				3 h	8.1 mg/L (Solubilitzed. 40 h RT)
Clearcoli	1 (3 L)	1.975 ± 0.365	0.540 ± 0.007	0.594 ± 0.006	3 h	**Protein samples precipitated after dialysis against 20 mM Tris-HCl pH 8.00 + 5 % glycerol**
	2 (3 L)	1.455 ± 0.145	0.77 ± 0.005	2.786 ± 0.100	18 h	Protein yield was low. **Probable cause: loss of the plasmid**
	3 (3 x 2.4 L)	2.090 ± 0.113	0.568 ± 0.008	0.967 ± 0.078	4 h	0.287 ± 0.011 (mg/L)

As observed in Table S1, expression of MMP-9 gene had a negative effect on *Clearcoli* culture growth. After induction, the growth of the culture stopped (purification 1; Code 1). In addition, longer induction times (purification 2; Code 2) resulted only in tiny amounts of purified recombinant protein despite the higher OD_{550} postinduction measure, suggesting a positive pressure selection of newly appearing plasmid-free cells over the plasmid-bearing initial cell population. It has been widely described that gene expression needs to be tightly regulated for toxic proteins which is not the case of the leaky expression in T7 polymerase system [47].

References

46.   Chou, H.T.; Kuo, T.Y.; Chiang, J.C.; Pei, M.J.; Yang, W.T.; Yu, H.C.; Lin, S.B.; Chen, W.J. Design and synthesis of cationic antimicrobial peptides with improved activity and selectivity against *Vibrio* spp. *Int. J. Antimicrob. Agents* **2008**, *32*, 130–138.

47.   Giacalone, M.J.; Gentile, A.M.; Lovitt, B.T.; Berkley, N.L.; Gunderson, C.W.; Surber, M.W. Toxic protein expression in *Escherichia coli* using a rhamnose-based tightly regulated and tunable promoter system. *Biotechniques* **2006**, *40*, 355–364.

ANNEX 2

Potential of MMP-9 based nanoparticles at optimizing the cow dry period: pulling apart the effects of MMP-9 and nanoparticles

L. Gifre-Renom, J. V. Carratalá, S. Parés, L. Sánchez-García, N. Ferrer-Miralles,
A. Villaverde, A. Bach, Elena Garcia-Fruitós and Anna Arís

Scientific Reports, 10, 11299, 2020

(Referenced manuscript)

SCIENTIFIC REPORTS
natureresearch

Check for updates

OPEN # Potential of MMP-9 based nanoparticles at optimizing the cow dry period: pulling apart the effects of MMP-9 and nanoparticles

L. Gifre-Renom[1], J. V. Carratalá[2], S. Parés[1], L. Sánchez-García[2], N. Ferrer-Miralles[2,3,4], A. Villaverde[2,3,4], A. Bach[1,5], Elena Garcia-Fruitós[1]✉ & Anna Arís[1]✉

The cow dry period is a non-milking interval where the mammary gland involutes and regenerates to guarantee an optimal milk production in the subsequent lactation. Important bottlenecks such as the high risk of intramammary infections complicate the process. Antibiotics have been routinely used as a preventive treatment but the concerns about potential antibiotic resistance open a new scenario in which alternative strategies have to be developed. Matrix metalloproteinase-9 (MMP-9) is an enzyme able to degrade the extracellular matrix, triggering the involution and immune function of cow mammary gland. We have studied the infusion into the mammary gland of MMP-9 inclusion bodies as protein-based nanoparticles, demonstrating that 1.2 mg of MMP-9 enhanced the involution and immune function of the cow mammary gland. However, the comparison of the effects triggered by the administration of an active and an inactive form of MMP-9 led to conclude that the response observed in the bovine mammary gland was mainly due to the protein format but not to the biological activity of the MMP-9 embedded in the inclusion body. This study provides relevant information on the future use of protein inclusion bodies in cow mammary gland and the role of MMP-9 at dry-off.

The dry period is crucial to optimize milk production in dairy cattle[1]. During this period, the mammary gland regresses and, after that, it proliferates and differentiates to allow optimal milk production in the subsequent lactation. However, the presence of galactopoietic hormones due to a concomitant pregnancy does not facilitate the beginning of involution and delays the activation of the immune system, which orchestrates all this process[2]. Moreover, the high amount of milk accumulated in the mammary gland at dry-off exert high intra-mammary pressure and may lead to milk leakage, which in turn maintains the teat canal opened and full of nutrients, increasing the risk of a pathogen invasion[3]. When activated, the immune system recruits macrophages and neutrophils, which could fight against a possible infection[4]. Yet their phagocytic activity against pathogens is diminished at dry-off, as phagocytes are engaged at engulfing milk fat, cell debris, and other compounds derived from milk and accumulated in the mammary gland[4]. To reduce the risk of mastitis, antibiotics are infused routinely into the mammary gland at dry-off. However, the preventive use of antibiotics has raised concerns about the emergence of antibiotic resistances. In this context, there is a need to find new strategies to boost the immune system of the mammary gland and its involution at dry-off.

Recently, new strategies based on the use of matrix metalloproteinase-9 (MMP-9) have been studied mainly to modulate infiltration of immune cells and involution at dry-off. Matrix metalloproteinase-9 is a tissue-remodelling enzyme that degrades the extracellular matrix (ECM) and, in the mammary gland, is physiologically released by mammary epithelial cells and neutrophils entering into the tissue during the involution process[5,6]. It has been previously demonstrated that the proteolytic degradation of the ECM is a key factor during the loss of differentiation of mammary epithelial cells and the induction of apoptosis and involution[7]. Hence, in a

[1]Department of Ruminant Production, Institut de Recerca i Tecnologia Agroalimentàries (IRTA), 08140, Caldes de Montbui, Spain. [2]Institut de Biotecnologia i de Biomedicina, Universitat Autònoma de Barcelona, 08193, Cerdanyola del Vallès, Spain. [3]Departament de Genètica i de Microbiologia, Universitat Autònoma de Barcelona, 08193, Cerdanyola del Vallès, Spain. [4]CIBER de Bioingeniería, Biomateriales y Nanomedicina (CIBER-BBN), 08193, Cerdanyola del Vallès, Spain. [5]Institució Catalana de Recerca i Estudis Avançats (ICREA), Barcelona, Spain. ✉e-mail: elena.garcia@irta.cat; anna.aris@irta.cat
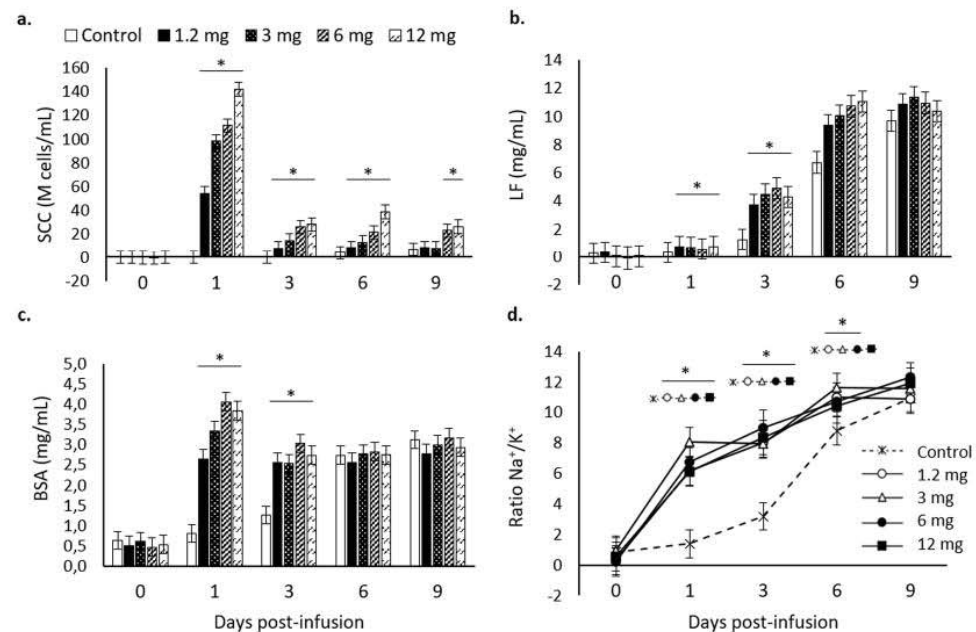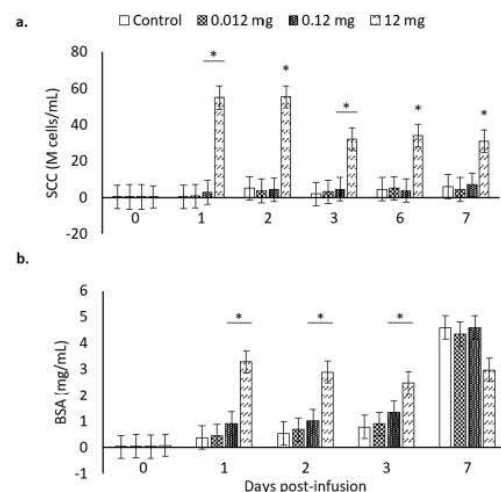
Figure 1. Mammary gland involution markers analysed from mammary gland secretions for the tested doses (0 –control–, 1.2, 3, 6, and 12 mg) of inclusion bodies containing matrix metalloproteinase-9 along 0, 1, 3, 6, and 9 d post-infusion. Non-transformed means and SEM (error bars) are represented while P-values were obtained from transformed data, when necessary. Asterisks depict significant differences between treatments and the control group within time. (**a**) Somatic cell counts (SCC) are expressed in million (10^6) cells per mL (M cells/ml); $P < 0.0001$. (**b**) Lactoferrin (LF); $P < 0.0001$. (**c**) Bovine serum albumin (BSA); $P < 0.0001$. (**d**) Na^+/K^+ ratio; $P < 0.0001$. For differences between different treatments within each time point, see Table S1 in the Supplementary Material.

previous work we hypothesized that exogenous administration of a recombinant MMP-9 (rMMP-9), which was not sensible to tissue inhibitors of metalloproteinases 1 and 3 (TIMP1 and TIMP3), could represent a strategy to accelerate tissue involution at dry-off. The administration of rMMP-9 into the mammary gland at dry-off was tested[8] using two recombinant protein formats: a soluble form, and a nanoparticulated format, also known as inclusion body (IB). Inclusion bodies are protein-based nanoparticles of few hundred nanometers formed during recombinant protein production processes[9] showing a clear biomedical potential[10]. Parés *et al.* (2017) reported an increase in the local immune response and mammary involution when administering rMMP-9 as an IB at dry-off in dairy cows, whereas the administration of rMMP-9 in a soluble form only increased the endogenous MMPs without affecting general parameters of immune stimulation and mammary involution markers[8]. These findings encouraged us to elucidate whether the observed effects of rMMP-9 IBs in the bovine mammary gland were due to a different performance of rMMP-9 embedded in the nanoparticles compared with a soluble form, or due to the effect of the nanoparticle or IB format itself. For this, we have determined *in vivo*, first, the lowest dose of rMMP-9 IBs that boost innate immunity and mammary involution, and second, whether this was due to the nanoparticle format or to the inherent properties of the rMMP-9 comprised in these IBs[11]. Through the comparison of the effects triggered by the administration of an inactive form of rMMP-9 IB at dry-off with its active counterpart, the real potential of rMMP-9 IBs during the cow dry period has been distinguished.

Results and Discussion

Determining the minimal inflammatory dose of rMMP-9 nanoparticles. The greatest tested dose (12 mg) of MMP-9 IBs at dry-off was previously reported by Parés *et al.* (2017) as a potent immunostimulator of the bovine mammary gland[8]. Herein, in Exp. 1, three lower doses were evaluated along with the 12-mg dose. All used doses enhanced the recruitment of immune cells into mammary gland (namely SCC) up to 6 d post dry-off (Fig. 1a). At day 9, the myeloid cells recruited in the controls started to rise but were still below those obtained with the 12- and 6-mg doses (Fig. 1a). Lactoferrin synthesis, whose rise is also associated with an augmented immune activity[12], increased at day 1 after dry-off until day 3 in all the tested doses (Fig. 1b). The involution markers BSA and Na^+/K^+, whose increase reflects the disruption of tight junction and the mixture of blood components in milk secretion[13], followed similar patterns as lactoferrin with a marked increase at day 1 after infusions (Fig. 1c,d). For all doses tested in Exp. 1 there was a shift in the levels of the analysed parameters at day 1 and these values were kept above controls until day 3 or day 6 for BSA and Na^+/K^+, respectively (Fig. 1c,d). Importantly, this experiment replicated the results observed by Parés *et al.* (2017)[8], consolidating the potential of rMMP-9 IBs

Figure 2. Mammary gland involution markers analysed from mammary gland secretions for the tested doses (0 –control–, 0.012, 0.12, and 12 mg) of inclusion bodies containing matrix metalloproteinase-9 along 0, 1, 2, 3, 6, and 7 d post-infusion. Non-transformed means and SEM (error bars) are represented while *P*-values were obtained from transformed data, when necessary. Asterisks depict significant differences between treatments and the control group within time. (**a**) Somatic cell counts (SCC) are expressed in million (10^6) cells per mL (M cells/ml); $P < 0.0001$. (**b**) Bovine serum albumin (BSA); $P < 0.0001$. For differences between different treatments within each time point, see Table S2 in the Supplementary Material.

to locally stimulate the recruitment of immune cells in the mammary gland at dry-off and to accelerate the onset of involution biomarkers after 24 h of infusions.

Since all the tested doses in Exp. 1 (Fig. 1) induced similar effects during the week following dry-off, either regarding the immune stimulation or involution parameters, Exp. 2 was conducted to test lower doses of rMMP-9 IBs (Fig. 2). In this case, there was a lack of effect of low doses only observing a slight increase over control quarters with 0.12 mg (Fig. 2). Given that the minimum amount of rMMP-9 IBs eliciting a clear immunostimulating effect in the mammary gland was 1.2 mg (Fig. 2), this dose was chosen to further analyse the effects of rMMP-9 in Exp. 3.

Differentiation of rMMP-9 and IB format effects. Aiming to determine whether the detected immune response triggered in the mammary gland by rMMP-9 IBs[8] (Fig. 1) was only due to the nanoparticle format or whether the activity of the MMP-9 embedded in such nanoparticles was also relevant, as observed in mice[14], an Exp. 3 was conducted. We compared the performance between rMMP-9 nanoparticles and the mutant and inactive rMMP-9 counterpart at the established dose of 1.2 mg in bovine mammary gland. Surprisingly, there was no difference between the performance of inactive or active rMMP-9 nanoparticles in the recruitment of immune cells, neither in the general (i.e., WBC) nor in mononuclear or polymorphonuclear cells, being these levels much greater than in control quarters for both treatments (Fig. 3). As expected, the main recruited cells were neutrophils (determined as PMNCs, Fig. 3d), as they are the first immune cell to arrive to the inflammatory site, and in agreement with the behaviour previously observed in mice after the administration of rMMP-9 IBs[14]. However, in the mouse model, the inactive rMMP-9 nanoparticles only induced a slightly and transitory inflammatory effect, whereas the active form had a clear and sustained effect over time[14]. Thus, the performance of mutMMP-9 nanoparticles was different in the mouse intra-dermis model compared with the bovine mammary gland.

When other immune or involution parameters of bovine mammary gland were assessed, only in very few instances the active rMMP-9 nanoparticles had a slightly different performance compared to the inactive rMMP-9 form. Concretely, BSA levels were greater at days 1 and 6 in quarters treated with active rMMP-9 nanoparticles (Fig. 4a), suggesting that MMP-9 had some activity behind the unspecific format effects. Also, Na^+/K^+ ratio increased at day 6 and this was sustained at day 9 (Fig. 4d). This indicates that the splitting time-point for both specific and unspecific effects of rMMP-9 IBs in bovine mammary gland at dry-off may occur later on, compared with the murine model[14]. However, during the analysed time in Exp. 3, and as observed for cellular recruitment, there were no rMMP-9-specific effects in lactoferrin nor in endogenous MMP-9 levels (Fig. 4b,c). Thus, these results confirm that the obtained effects in the bovine mammary gland were mainly due to the format (i.e., IB) but not due to the activity of the protein embedded in these nanoparticles. Again, this was an unexpected outcome because, in mice, the effect of MMP-9 could be clearly differentiated already at day 1 after injections from the inflammatory consequences of the nanoparticle format[14]. The question now is what is causing such different effects between the two animal models? Divergence in the MMP-9 nanoparticle effects observed in mice model and in bovine mammary gland could be explained by important differences between the two *in vivo* models. On one hand, the mice model was knock-out for endogenous MMP-9, favouring a clear split between the MMP-9-specific effect from the format-linked unspecific effect. Nonetheless, in bovine, mammary gland endogenous
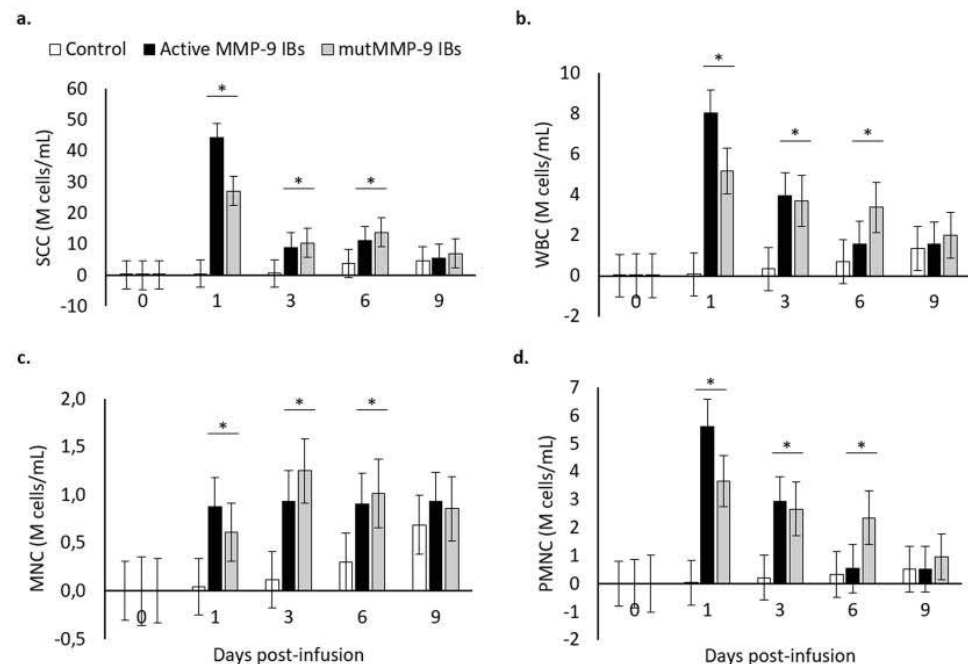
Figure 3. Mammary gland cell populations analysed from mammary gland secretions for the 1.2 mg dose of inclusion bodies containing active (MMP-9 IBs) or inactive (mutMMP-9 IBs) matrix metalloproteinase-9 and control, along 0, 1, 3, 6, and 9 days-post infusion. All cell measurements are expressed in million (10^6) cells per mL (M cells/ml). Non-transformed means and SEM (error bars) are represented while P-values were obtained from transformed data, when necessary. Asterisks depict significant differences between treatments and the control group within time. (**a**) Somatic cell counts (SCC); $P < 0.0001$. (**b**) White blood cells (WBC); $P < 0.0001$. a^t $P = 0.053$. (**c**) Mononuclear cells (MNC); $P < 0.0001$. (**d**) Polymorphonuclear cells (PMNC); $P < 0.0001$. For differences between different treatments within each time point, see Table S3 in the Supplementary Material.

MMP-9 seems not to have an important role at dry-off[8]. On the other hand, lactating and involuting mammary glands are very immune-active and responsive organs that, in fact, have been compared with strong mucosal immune programs[15]. This agrees with our results indicating that while in mice the nanoparticle unspecific effect was limited to 24 h, in the dairy cow mammary gland this was extended for a minimum of 9 d (except for Na$^+$/K$^+$ ratio, differenced at day 6, and the short specific effect in BSA). In this context, the same stimulus could trigger a greater inflammatory effect in cows than in rodents. Moreover, it has been demonstrated that soluble rMMP-9 does not exert any effect on immune and involution parameters at the beginning of bovine dry period[8]. This finding indicates that the protein embedded in the nanoparticles is not as relevant as in the mouse air pouches model, specifically designed to evaluate the MMP-9 activity and further infiltration of immune cells.

The effects of the IB format on the inflammation of a host were also previously studied by Torrealba *et al.* (2016a)[16]. They have demonstrated that protein nanoparticles could induce inflammation in Zebrafish and act as an adjuvant[16], and this effect could be even increased through using nanoparticles composed by proteins with a relevant immune function, such as a cytokine[17]. Similar to results herein, Torrealba *et al.* (2016b) also described a dose-dependent effect when an unspecific protein like GFP was injected in Zebrafish, with a fast-induced immunostimulating effect[17]. This is in agreement with other studies performed previously with LPS[18,19], chitosan[20], *Panax ginseng* extracts[21,22], among others, in which a rapid immunostimulating effect is observed at dry-off.
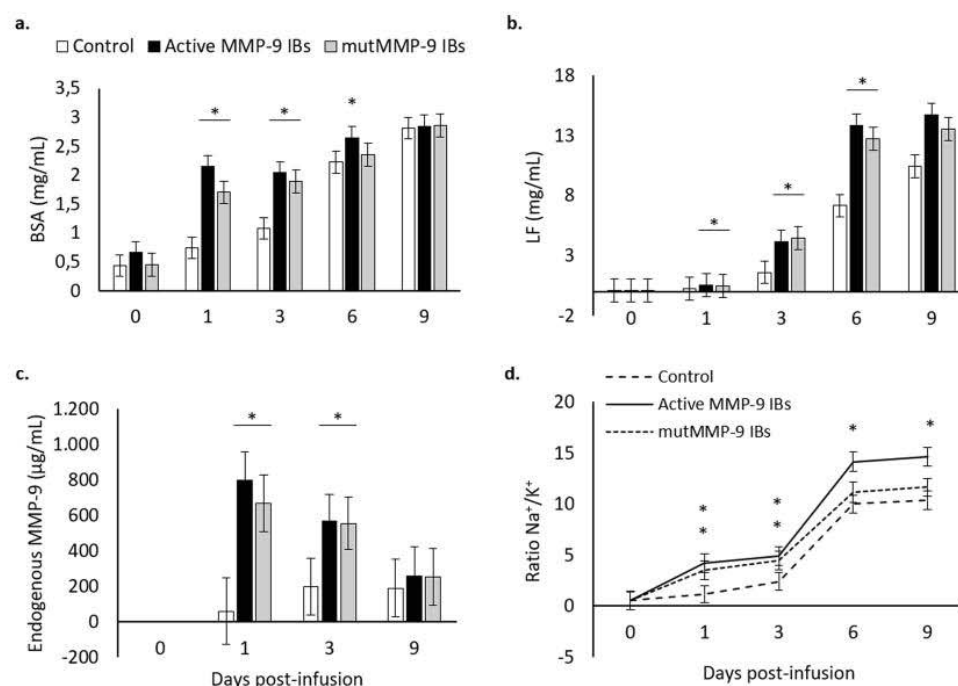
Conclusions

Protein nanoparticles or inclusion bodies trigger a clear immunostimulant effect in the bovine mammary gland at dry-off. Matrix metalloproteinase-9 protein forming such nanostructures exerts no relevant effect in the context of the bovine dry-off. Thus, protein nanoparticles could be considered as an appealing strategy at bovine dry-off to accelerate this process and enhance the immune protection although MMP-9 protein itself does not provide any extra value during the first week of the dry period.

Materials and Methods

Bacteria strains and plasmids.   *Lactococcus lactis* subsp. *cremoris* NZ9000 double mutant ClpP$^-$ HtrA$^-$ (*clpP-htrA*; Em^R) strain[23,24] (kindly provided by INRA (Jouy-en-Josas, France); patent n. EP1141337B1) was used to recombinantly produce the MMP-9 proteins. The genes encoding for an active bovine rMMP-9 fragment (Phe107 - Pro449, NCBI, NM_174744.2) and for the same rMMP-9 fragment with the E402Q single mutation[25,26], which makes it an inactive rMMP-9 proteoform, were cloned in pNZ8148 plasmid (Cm^R) and transformed into

Figure 4. Mammary gland involution markers analysed from mammary gland secretions for the 1.2 mg dose of inclusion bodies containing active (MMP-9 IBs) or inactive (mutMMP-9 IBs) matrix metalloproteinase-9 and control along 0, 1, 3, 6, and 9 d post-infusion. Non-transformed means and SEM (error bars) are represented while P-values were obtained from transformed data when necessary. Asterisks depict significant differences between treatments and the control group within time. (**a**) Bovine serum albumin (BSA); $P < 0.0001$. (**b**) Lactoferrin (LF); $P < 0.0001$. (**c**) Endogenous MMP-9 was analysed only for selected times: 0, 1, 3 and 9 d post-infusions; $P < 0.05$. (**d**) Na$^+$/K$^+$ ratio; $P < 0.0001$. For differences between different treatments within each time point, see Table S4 in the Supplementary Material.

competent *L. lactis clpP-htrA* cells. Both genes were fused to a His-tag in the C-terminal and were codon-optimised (Geneart) for *L. lactis*[11].

Protein Production in *L. lactis*. Both, active and inactive rMMP-9 were produced in *L. lactis*, which was grown under static conditions at 30 °C in M17 broth supplemented with 0.5% glucose, 5 µg/mL chloramphenicol and 2.5 µg/mL erythromycin. Cultures were re-inoculated to an initial OD$_{600nm}$ of 0.05 and protein expression was induced with 12.5 ng/mL nisin when the OD$_{600nm}$ reached values between 0.4 and 0.6. The recombinant proteins were produced along 3 h and bacteria were recovered by centrifugation at 6,000 x g for 30 min at 4 °C and stored at −80 °C until use.

Purification of IBs. Pellets from 50 mL culture were suspended in 30 mL PBS, frozen/thawed at −80 °C and disrupted with 3 French press (Thermo FA-078A) rounds at 1,500 psi, ice-coated, and with protease inhibitors (cOmplete protease inhibitor cocktail EDTA-free, Roche). After that a previously established purification protocol was applied as described[27]. Samples were tested for sterility by plating an aliquot in agar-M17 plates with 0.5% glucose and incubating them overnight at 30 °C. Aliquots of rMMP-9 IBs and mutant inactive rMMP-9 IBs were tested for purity through SDS-PAGE electrophoresis and Coomassie blue staining (75.7% purity obtained for MMP-9 IBs and 70.3% for mutMMP-9 IBs), and were quantified by interpolation with the bands obtained by a solubilized rMMP-9 as the standard[28], using ImageJ software (version 1.46r, U. S. National Institutes of Health, Bethesda, Maryland, USA). The activity of the MMP-9 IBs and the inactivity of the mutMMP-9 IBs, were validated *in vitro* both by zymography and DQgelatin (data not shown).

Protein infusions in cow mammary glands. Thirty-three multiparous pregnant Holstein cows in their second gestation, after 274 to 379 days in lactation and between 215 and 225 days of gestation, producing from 25.5 to 43.7 kg of milk per day during the last week before dry-off, and with <200,000 somatic cell counts (SCC)/mL in milk at dry-off per cow, were selected in this study. Cows were dried abruptly without any previous dietary nor milking routine intervention.

Experiments were performed in accordance with relevant guidelines and regulations under the evaluation and permission of the Ethical Committee of IRTA, protocol number 9705.

Three experiments were performed (Exp. 1, Exp. 2, and Exp. 3); 2 experiments aimed at optimizing the minimum effective protein dose to trigger an immune reaction in the mammary gland at dry off (Exp. 1 and Exp. 2), and the third aimed at dissecting the effects triggered either by the protein activity or by the protein format (Exp. 3).

Udder quarter was used as an independent experimental unit and these were randomly allocated to treatments considering cows a random effect. A total of 46, 44 and 30 quarters used for Exp. 1, Exp. 2 and Exp. 3, respectively (2 animals were discarded due to mastitis and abortion, one for each Exp. 1 and Exp. 2). After the last milking before dry-off and just before protein infusions, 10 mL of mammary gland secretions (MGS) were collected from all quarters as a day 0 sampling.

In the first experiment (Exp. 1), a range of different doses of rMMP-9 IBs were infused into 10 quarters per treatment (due to mastitis, 1 quarter per treatment was discarded, except for control) through the teat canal using sterile blunt tip cannulas immediately after MGS collection at day 0. Namely, 1.2, 3, 6, and 12 mg of rMMP-9 IBs suspended in 10 mL saline solution were infused, and 10 mL saline solution infusions was used as negative controls. Following infusions, all quarters were treated with broad-spectrum antibiotics (Mamyzin secado, Boehringer Ingelheim) following common production practices. At days 1, 3, 6, and 9 after protein infusions, 10 mL of MGS were collected from each quarter. After the last sampling, all glands were sealed with teat sealant. All MGS were analysed fresh for SCC (n = 9 observations) as described below, and aliquots were stored at $-80\,°C$ until these were analysed for bovine serum albumin (BSA; n = 9), lactoferrin (LF; n = 8) and Na$^+$/K$^+$ (n = 9) levels.

The second experiment (Exp. 2) aimed at testing lower doses of rMMP-9. After collecting MGS at day 0, doses of 0.012, 0.12, and 12 mg of MMP-9 IBs and 10 mL of saline solution were infused into 11 quarters for each dose, and all of them were treated with antibiotics as described for Exp. 1. At days 1, 2, 3, 6, and 7 after infusions, MGS were obtained from each quarter and after the last collection, teat sealant was applied. The MGS were analysed fresh for SCC (n = 11), and BSA was analysed from aliquots after preservation at $-80\,°C$ (n = 11).

In the third experiment (Exp. 3), the minimum effective dose determined from Exp. 1 and Exp. 2 was used to compare the effects of the active and the inactive rMMP-9 IBs on the mammary gland at dry-off. Thus, rMMP-9 IBs and inactive rMMP-9 IBs (**mutMMP-9** IBs) at selected dose, and 10 mL of saline solution were infused into 10 quarters per treatment and then quarters were treated with antibiotics following previously detailed steps in Exp. 1. At days 1, 3, 6, and 9, after protein infusions, MGS were obtained and analysed fresh for SCC (n = 10) and for immune cell populations (n = 10), and aliquots were stored at $-80\,°C$ until analysed for BSA (n = 10), LF (n = 8), Na$^+$/K$^+$ (n = 10) and endogenous MMP-9 (n = 6).

Mammary secretion analyses. *Somatic cell counts.* Half mL of each MGS was mixed with half mL Dulbecco's phosphate-buffered saline (DPBS; GIBCO), inverted several times and centrifuged at 1,000 x g for 2 min at RT. Fat, located on top of the sample mixture, was removed by gently swirling a cotton swab around the top of the centrifuge tube. The supernatants were discarded without touching the cell pellets, and these were suspended in 1 mL DPBS and centrifuged again. Cells were washed twice, repeating the previous steps and were suspended in 0.5 mL DPBS. Cell suspensions were counted using a Scepter 2.0 Handheld Automated Cell Counter (Merck Millipore, Billerica, MA). Cells were diluted when appropriate to obtain a best resolution in the Scepter histograms, and particle counts with diameters below 6 μm were discarded for all samples.

Immune cell populations. After SCC, cell suspensions were stored overnight at 4 °C, and sent to the Veterinary Clinic Haematology Service at the Autonomous University of Barcelona (UAB, Barcelona, Spain) for the analyses of immune cell populations. Using a XN-1000 analyser (Sysmex), white blood cells (WBC), polymorphonuclear cells (PMNC) and mononuclear cells (MNC) were differentiated and counted following morphological measurements by flow cytometry, selecting the body fluid mode.

Bovine serum albumin quantification. Bovine Serum Albumin (BSA) in MGS was quantified as described elsewhere[29]. One mL of each MGS was centrifuged at 1,000 x g for 10 min at RT and fat was removed with a swab as detailed in the section for SCC determination. A commercial BSA was used as the standard curve and an eight-point serial dilution curve from 60 mg/mL was prepared. Two hundred μL of each supernatant were mixed in 450 μL dH$_2$0 and 450 μL of Bromocresol Green working solution (consisting in three parts succinic acid at pH 4 and a part of bromocresol green sodium salt dissolved in 5 mM NaOH, and 0.8% Brij L23). The solutions for all samples and standards were centrifuged at 1,900 x g for 10 min at RT and 150 μL of each supernatant were plated by duplicate in flat bottom transparent 96-well plates and were read at 640 nm. Concentration of BSA in MGSs was interpolated to the 4-parametric standard curve.

Lactoferrin quantification. Whole MGS were analysed for lactoferrin concentrations using a bovine lactoferrin ELISA quantitation set (Bethyl Laboratories Inc., Montgomery, TX, USA). A commercial bovine lactoferrin calibrator was used as the standard curve, ranging from 500 to 7.8 ng/ml. After coating the plates with 0.01 mg/mL anti-bovine lactoferrin, followed by a blocking step as indicated in the manufacturer protocol, samples diluted at 1/10,000 or 1/100,000 and standards were plated per duplicate and incubated for 1 h at RT. After several washes, HRP conjugated anti-bovine lactoferrin detection antibody was added at a final concentration of 0.01 μg/mL and incubated for 1 h at RT. Following several washes, 3,3′,5,5′-Tetramethylbenzidine (TMB) substrate solution was added and reaction was stopped after 15 min with 0.18 M H$_2$SO$_4$. Plates were read at 450 nm and lactoferrin concentrations were interpolated from the 4-parametric standard curve.

Sodium and potassium quantification. All samples were analysed for Na$^+$ and K$^+$ concentrations at the Chemical Analysis Service at the UAB. An aliquot of 0.1 g of MGSs was diluted in Triton X-100 0.1% (v/v). Clotted samples

198

were previously digested in HNO_3 concentrate in a Ultrawave microwave digestion system (Milestone). Na^+ and K^+ levels were determined by inductively coupled plasma-Optical emission spectrometry (ICP-OES; Optima 4300DV, Perkin-Elmer, Waltham, MA, USA).

Endogenous MMP-9 zymography. Skimmed MGS were quantified for endogenous MMP-9 activity through zymography analysis. Solubilized MMP-9[28] was used to prepare an eight-point standard curve ranging from 400 to 25 ng. Sample supernatants were diluted 1/10 and diluted samples and standards were loaded with non-denaturing loading buffer into 10% SDS-PAGE gels containing 1% porcine gelatine. Electrophoresis was run at constant 50 mA and gels were washed twice in 2.5% Triton X-100, once in distilled water, and were incubated in static overnight at 37 °C in developing buffer containing 50 mM Tris pH 7.5, 200 mM NaCl and 10 mM $CaCl_2$. Afterwards, Coomassie Blue staining was used to dye the gels for 2 h at RT and these were distained in a methanol-acetic solution. Degradation bands were analysed using ImageJ software and MMP-9 activity quantification was interpolated from the solubilized MMP-9 standard curve.

Statistical analyses. A total of 46, 44, and 30 quarters were used in Exp. 1, Exp. 2 and Exp. 3, respectively. Quarters were randomly allocated to treatments, considering cows a random effect. For immune cell populations, outliers considered as 2-times standard deviation were discarded. Variables were log-transformed in Exp. 1, Exp. 2 and Exp. 3, or root-transformed for Na^+/K^+ in Exp. 1, to normalize data when necessary. Data were analysed using a fixed-effects model using SAS 9.4 (SAS Inst. Inc., Cary, NC). Time, dose and the interaction between time and dose were included the model, with quarters nested within cows and cows as random effects. Time was included as a repeated measure and for each analysed variable, quarters within cows (the error term) was subjected to 2 variance-covariance structures: compound symmetry and autoregressive order 1. The covariance structure that yielded the smallest Schwarz's Bayesian information criterion was considered the most desirable analysis. Means and standard deviations represented in graphs correspond to non-transformed or back-transformed data, while *P*-values and asterisks correspond to the output from transformed data when required. Additional information on the differences among treatments within each time point can be found in the Supplementary Material.

References

1. Bachman, K. C. & Schairer, M. L. Invited review: Bovine studies on optimal lengths of dry periods. *J. Dairy Sci.* **86**, 3027–3037 (2003).
2. Pezeshki, A. *et al.* An integrated view on how the management of the dry period length of lactating cows could affect mammary biology and defence. *J. Anim. Physiol. Anim. Nutr. (Berl).* **94**, 7–30 (2010).
3. Gott, P. N., Rajala-Schultz, P. J., Schuenemann, G. M., Proudfoot, K. L. & Hogan, J. S. Intramammary infections and milk leakage following gradual or abrupt cessation of milking. *J. Dairy Sci.* **99**, 4005–4017 (2016).
4. Burvenich, C. *et al.* Cumulative physiological events influence the inflammatory response of the bovine udder to Escherichia coli infections during the transition period. *J. Dairy Sci.* **90**, E39–E54 (2007).
5. Yu, T. C. *et al.* Involvement of TNF-α and MAPK pathway in the intramammary MMP-9 release via degranulation of cow neutrophils during acute mammary gland involution. *Vet. Immunol. Immunopathol.* **147**, 161–169 (2012).
6. Chen, Q. *et al.* TGF-β1 Induces EMT in Bovine Mammary Epithelial Cells Through the TGFβ1/Smad Signaling Pathway. *Cell. Physiol. Biochem.* **43**, 82–93 (2017).
7. Boudreau, N., Sympson, C. J., Werb, Z. & Bissell, M. J. Suppression of ICE and Apoptosis in Mammary Epithelial Cells by Extracellular Matrix. *Science.* **267**, 891–893 (1995).
8. Parés, S. *et al.* Facilitating mammary involution at dry-off by intra-mammary infusion of Matrix Metalloproteinase-9. *Strategies for the optimization of cow dry period (Thesis)* (2017).
9. Rinas, U. *et al.* Bacterial Inclusion Bodies: Discovering Their Better Half. *Trends Biochem. Sci.* **42**, 726–737 (2017).
10. Seras-Franzoso, J. *et al.* Integrating mechanical and biological control of cell proliferation through bioinspired multieffector materials. *Nanomedicine* **10**, 873–891 (2015).
11. Cano-Garrido, O. *et al.* Functional protein-based nanomaterial produced in GRAS microorganism: A new platform for biotechnology. *Acta Biomater.* **43**, 230–239 (2016).
12. Shimazaki, K. & Kawai, K. Advances in lactoferrin research concerning bovine mastitis. *Biochem. Cell Biol.* **95**, 69–75 (2017).
13. Shamay, A., Shapiro, F., Leitner, G. & Silanikove, N. Infusions of casein hydrolyzates into the mammary gland disrupt tight junction integrity and induce involution in cows. *J. Dairy Sci.* **86**, 1250–1258 (2003).
14. Gifre-Renom, L. *et al.* Recombinant Protein-Based Nanoparticles: Elucidating their Inflammatory Effects In Vivo and their Potential as a New Therapeutic Format. *Pharmaceutics.* **12**, 450 (2020).
15. Betts, C. B. *et al.* Mucosal Immunity in the Female Murine Mammary Gland. *J. Immunol.* **201**, 734–746 (2018).
16. Torrealba, D. *et al.* Complex particulate biomaterials as immunostimulant-delivery platforms. *PLoS One* **11**, 1–17 (2016).
17. Torrealba, D. *et al.* Nanostructured recombinant cytokines: A highly stable alternative to short-lived prophylactics. *Biomaterials* **107**, 102–114 (2016).
18. Oliver, S. & Smith, K. L. Bovine Mammary Involution Following Intramammary Infusion of Colchicine and Endotoxin at Drying Off. *J. Dairy Sci.* **65**, 801–813 (1982).
19. Dallard, B. E. *et al.* The effect of a single intramammary infusion of a biological response modifier in cows at drying off. *Vet. Res. Commun.* **34**, 519–532 (2010).
20. Lanctôt, S. *et al.* Effect of intramammary infusion of chitosan hydrogels at drying-off on bovine mammary gland involution. *J. Dairy Sci.* **100**, 2269–2281 (2017).
21. Baravalle, C. *et al.* Proinflammatory cytokines and CD14 expression in mammary tissue of cows following intramammary inoculation of Panax ginseng at drying off. *Vet. Immunol. Immunopathol.* **144**, 52–60 (2011).
22. Baravalle, C. *et al.* Intramammary infusion of Panax ginseng extract in bovine mammary gland at cessation of milking induces changes in the expression of toll-like receptors, MyD88 and NF-kB during early involution. *Res. Vet. Sci.* **100**, 52–60 (2015).
23. Cortes-Perez, N. G. *et al.* Construction and characterization of a Lactococcus lactis strain deficient in intracellular ClpP and extracellular HtrA proteases. *Microbiology* **152**, 2611–2618 (2006).
24. Poquet, I. *et al.* HtrA is the unique surface housekeeping protease in Lactococcus lactis and is required for natural protein processing. *Mol. Microbiol.* **35**, 1042–1051 (2000).

7

199

25. Rowsell, S. *et al.* Crystal Structure of Human MMP9 in Complex with a Reverse Hydroxamate Inhibitor. *J. Mol. Biol.* **319**, 173–181 (2002).
26. Roderfeld, M. *et al.* Inhibition of hepatic fibrogenesis by matrix metalloproteinase-9 mutants in mice. *FASEB J.* **20**, 444–454 (2006).
27. Cano-Garrido, O. *et al.* Supramolecular organization of protein-releasing functional amyloids solved in bacterial inclusion bodies. *Acta Biomater.* **9**, 6134–6142 (2013).
28. Gifre-Renom, L. *et al.* A new approach to obtain pure and active proteins from Lactococcus lactis protein aggregates. *Sci. Rep.* **8**, 1–10 (2018).
29. Ponchon, B., Lacasse, P., Silanikove, N., Ollier, S. & Zhao, X. Effects of intramammary infusions of casein hydrolysate, ethylene glycol-bis(β-aminoethyl ether)-N,N,N',N'-tetraacetic acid, and lactose at drying-off on mammary gland involution. *J. Dairy Sci.* **97**, 779–788 (2014).

Acknowledgements

Author contributions

L.G.-R., J.V.C., S.P., and L.S.-G. performed the experiments and prepared the final data and figures. A.A. and E.G.-F. conceived the experiments and supervised the work. L.G.-R., A.A., and E.G.-F. wrote the manuscript text with contributions from the other authors. N.F.M., A.V., and A.B. outlined the structure and reviewed the manuscript. All authors took part in the analysis of the data and approved the final version of the manuscript.

Competing interests

The authors declare no competing interests.

Additional information

Supplementary information is available for this paper at https://doi.org/10.1038/s41598-020-67176-2.

Correspondence and requests for materials should be addressed to E.G.-F. or A.A.

Reprints and permissions information is available at www.nature.com/reprints.

Publisher's note Springer Nature remains neutral with regard to jurisdictional claims in published maps and institutional affiliations.

ANNEX 3

Developing protein-antitumoral drug nanoconjugates as bifunctional antimicrobial agents

Naroa Serna, Jose Vicente Carratalá, Eloi Parladé, Alejandro Sánchez-Chardi, Anna Aviñó, Ugutz Unzueta, Ramón Mangues, Ramón Eritja, Neus Ferrer-Miralles, Esther Vazquez, and Antonio Villaverde

(Referenced manuscript)

Developing Protein−Antitumoral Drug Nanoconjugates as Bifunctional Antimicrobial Agents

Naroa Serna, Jose Vicente Carratalá, Eloi Parladé, Alejandro Sánchez-Chardi, Anna Aviñó, Ugutz Unzueta, Ramón Mangues, Ramón Eritja, Neus Ferrer-Miralles, Esther Vazquez,* and Antonio Villaverde*

Cite This: https://dx.doi.org/10.1021/acsami.0c18317

Read Online

ACCESS | Metrics & More | Article Recommendations

ABSTRACT: A novel concept about bifunctional antimicrobial drugs, based on self-assembling protein nanoparticles, has been evaluated here over two biofilm-forming pathogens, namely *Pseudomonas aeruginosa* and *Staphylococcus aureus*. Two structurally different antimicrobial peptides (GWH1 and PaDBS1R1) were engineered to form regular nanoparticles of around 35 nm, to which the small molecular weight drug Floxuridine was covalently conjugated. Both the assembled peptides and the chemical, a conventional cytotoxic drug used in oncotherapy, showed potent antimicrobial activities that were enhanced by the combination of both molecules in single pharmacological entities. Therefore, the resulting prototypes show promises as innovative nanomedicines, being potential alternatives to conventional antibiotics. The biological performance and easy fabrication of these materials fully support the design of protein-based hybrid constructs for combined molecular therapies, expected to have broad applicability beyond antimicrobial medicines. In addition, the approach taken here validates the functional exploration and repurposing of antitumoral drugs, which at low concentrations perform well as unexpected biofilm-inhibiting agents.

KEYWORDS: protein materials, nanoparticles, hybrid materials, self-assembling, antimicrobial drugs
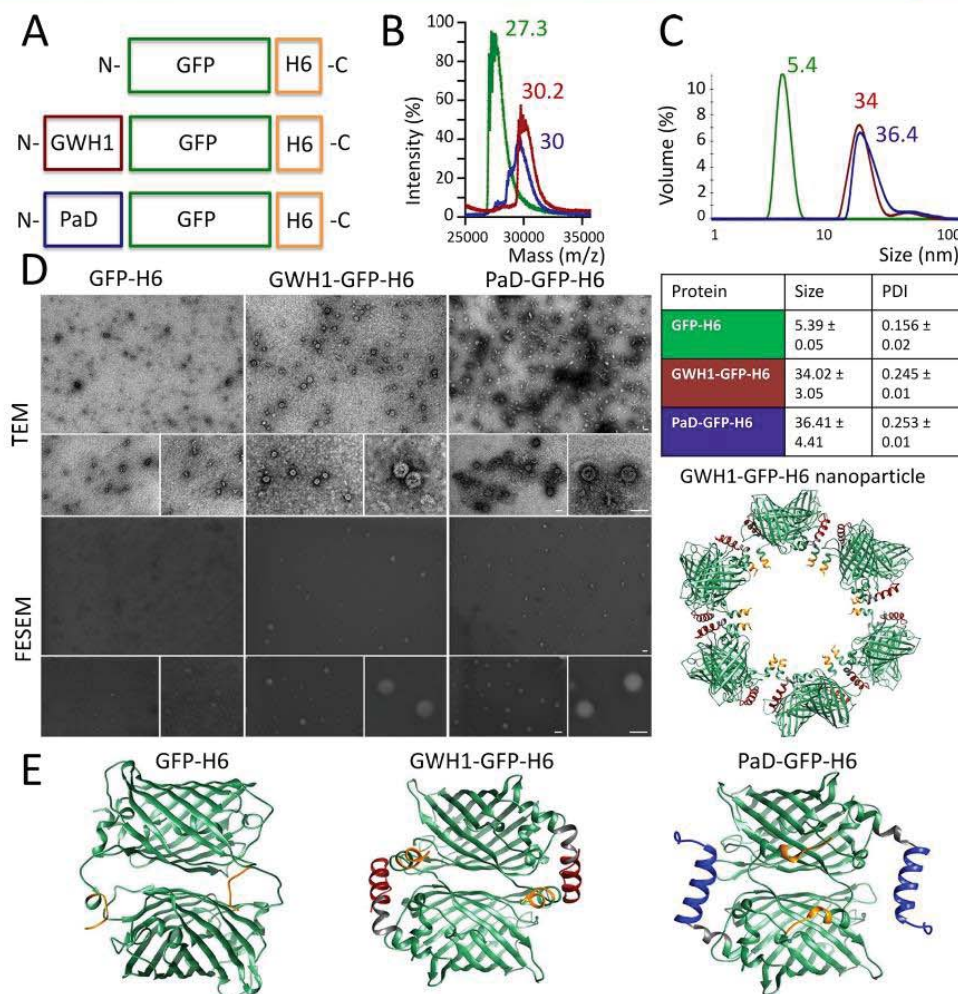
1. INTRODUCTION

Overuse of antibiotics during almost a century has selected antimicrobial resistant (AMR) strains of pathogenic bacteria, thus generating an unexpected health challenge of dramatically increasing dimensions.[1] Because, generically, antibiotics are progressively becoming less effective, antimicrobial peptides (AMPs), namely short protein stretches with diverse mechanisms of action over bacteria,[2,3] have emerged as a promising alternative.[4−7] However, it is difficult to envisage them as the ultimate clinical alternative to conventional antibiotics. Indeed, their antimicrobial activities require the administration of high doses due to low peptide stability and rapid renal filtration, which result in severe side toxicities over mammalian cells and organs.[8−10] In this context, nanotechnology represents a promising approach to improve pharmacokinetic profiles and to increase the local concentration of AMPs.[11] On the other hand, the therapeutic combination of antimicrobial agents with a different mechanism of action is expected to maximize effectiveness and to limit the selection of resistant mutants. Then, the combined use of AMPs at sublethal doses with unconventional antibiotics appears as a promising strategy to exploit in full the antimicrobial potential of AMPs.[12,13] Low concentrations of AMPs still show a remarkable biological

impact on bacteria,[13,14] inhibiting biofilm formation,[15] binding exotoxins,[16] affecting quorum sensing,[17] or restricting the secretion of virulence factors,[18] among others. At such low doses, AMPs should prevent the development of resistances[19] and allow synergistic activities with coadministered drugs.[7] In this sense, unconventional antibiotics such as 5-fluorouracil (FU), a small molecular weight drug used for decades in the systemic chemotherapy for colorectal cancer,[20] have been observed as potential antimicrobial drugs but mostly employed to disinfect surfaces and medical instruments such as venous catheters.[21] If conveniently formulated and targeted, they might be usable *in vivo* for this purpose at doses much lower than those in which they are administered as cytotoxic drugs in oncology.[22,23] Such a possibility is supported by few and side observations in studies usually not conceived to confirm those

Figure 1. Production and characterization of protein-only antimicrobial nanoparticles. (A) Modular organization of antimicrobial fusion proteins. The antimicrobial peptides GWH1 and PaD were fused to the green fluorescent protein (GFP), which acts as a scaffold. A hexahistidine tag (H6) was fused for cation-coordinated protein oligomerization and for purification purposes. (B) MALDI-TOF mass spectrometry analysis of purified recombinant GWH1-GFP-H6, PaD-GFP-H6, and GFP-H6 proteins, showing the expected molecular weights (in kDa). (C) Hydrodynamic size distribution plots (top) of GWH1-GFP-H6 and PaD-GFP-H6 nanoparticles and of the dimeric GFP-H6. (bottom) Polydispersion index (PDI). Data are represented as mean ± standard error of the mean (SEM). (D) Representative high-resolution images of electron microscopy (TEM and FESEM, left) of GFP-H6 monomers and GWH1-GFP-H6 and PaD-GFP-H6 nanoparticles. Bar size: 40 nm. At right, *in silico* representation of a GWH1-GFP-H6 nanoparticle. (E) Predicted three-dimensional structure of dimeric GWH1-GFP-H6 and PaD-GFP-H6 building blocks and of GFP-H6.

suspected antimicrobial activities.[24] Therefore, it would be highly convenient to perform systematic analyses to allow considering the repurposing of this drug (and possibly others) once presented in convenient administration formats, like the above-mentioned low-dose treatment combined with AMPs. The almost five decades of experience in the clinics of FU and Floxuridine (2′-deoxy-5-fluorouridine, FdU)[20] would be supportive of such a new application, while the innovative combination of chemical and biological agents in single pharmacological hybrid entities is expected to offer new and synergistic ways of action.[12,13]

In this context, we have recently developed procedures to chemically conjugate, in a functional form, FdU oligomers (and other small molecular weight chemicals with antitumoral activity[25]) and engineered self-assembling proteins (resulting

in regular nanoparticles)[26] for administration as cell-targeted anticancer nanomedicines.[27] In these studies, FdU oligomers acted as prodrugs, which release the active FdU monophosphate by degradation by nucleases,[28] and the protein acted as a nanoscale cell-targeted drug vehicle, as it contained a tumor-homing peptide.[27] On the other hand, but from a related context, we have also developed a generic self-assembling protein platform that has allowed generating AMP-containing protein-only nanoparticles[29] (among other type of therapeutic protein-only nanoparticles[30−34]) that are fully functional against a diversity of bacterial species.[35,36] Therefore, we wondered whether we would be able to design nanoconjugates based on self-assembling, engineered protein nanoparticles that enable the multivalent display of fused AMPs and that enclose a set of conjugated oligomeric FdU molecules for simultaneous delivery

in the form of chemically hybrid, bifunctional antimicrobial nanomedicines. A nanostructured format is expected to increase drug stability and prevent renal filtration,[37−39] while the hybrid concept in the design of nanomedicine-oriented nanoparticles would generically offer new routes for drug discovery based on multivalence and a selected stoichiometry of the drug nano-conjugates.

2. MATERIALS AND METHODS

2.1. Protein Design, Production, and Purification. The two modular constructs GWH1-GFP-H6 and PaD-GFP-H6 (Figure 1A) were designed in-house, and gene synthesis was performed by GeneArt (ThermoFisher). The control GFP-H6 was described elsewhere.[40] Both genetic fusions were subcloned in the plasmid pET22b and further transformed by heat shock (42 °C for 45 s) in chemically competent *Escherichia coli* BL21 (DE3) cells (Novagen). Ampicillin-resistant transformed cells were incubated at 37 °C until they reached OD_{550} = 0.5−0.7. Then, protein production was performed at 20 °C overnight after the addition of isopropyl β-D-1-thiogalactopyranoside (IPTG) at a final concentration of 100 μmol/L. Bacterial cells were harvested (5000 g for 15 min at 4 °C) and stored at −80 °C until use.

For protein purification, cell pellets were thawed and resuspended in a wash buffer (20 mmol/L Tris-HCl, 500 mmol/L NaCl, 10 mmol/L imidazole, pH 8.0) supplemented with the protease inhibitor Complete EDTA-free (Roche). Bacterial cell lysis was performed in a French Press (Thermo FA-078A) at 1200 psi, and the soluble fraction was separated after centrifugation (45 min, 15000 g at 4 °C). Recombinant proteins were purified in an Äkta Pure FPLC system (GE Healthcare) by immobilized metal affinity chromatography (IMAC). After selective binding to a HisTrap HP 1 mL column (GE Healthcare), proteins were eluted by a linear gradient of elution buffer (20 mmol/L Tris-HCl, 500 mmol/L NaCl, and 500 mmol/L imidazole, pH 8.0). The eluted protein fractions were dialyzed against sodium bicarbonate salt buffer (166 mml/L NaCO₃H and 333 mmol/L NaCl, pH 8.0). The final protein concentration was determined by the Bradford assay. Protein integrity was determined by MALDI-TOF mass spectrometry.

2.2. Characterization of Nanoparticles. The volume size distribution and Z-potential of nanoparticles were determined in a Zetasizer Nano ZS (Malvern Instruments Limited) by dynamic light scattering (DLS) and electrophoretic light scattering (ELS), respectively, at 633 nm. Protein samples were applied at 1 mg/mL in sodium bicarbonate salt buffer. Measurements were performed in triplicate, and the average size and zeta potential were expressed as mean ± standard error. Ultrastructural morphometry of monomers (GFP-H6) and nanoparticles (GWH1-GFP-H6 and PaD-GFP-H6) at a nearly native state was assessed with two high-resolution electron microscopy (EM) techniques. Drops of 5 μL of samples resuspended in its buffer were deposited in silicon wafers (Ted Pella Inc.) for 2 min, air-dried, and immediately observed without coating in a field emission scanning electron microscope (FESEM) Merlin (Zeiss) operating at 1 kV and equipped with a high-resolution in-lens secondary electron detector. Representative images of general fields and nanostructures details were collected at three magnifications (100000×, 250000×, and 450000×). For negative staining, drops of 5 μL of the same samples were deposited for 1 min in 200 mesh copper grids coated with carbon, contrasted with uranyl acetate 2% (Polysciences Inc.) for 1 min, air-dried, and observed with a transmission electron microscope (TEM) JEM-1400 (Jeol Ltd.) operating at 120 kV and equipped with a Gatan Orius SC200 CCD camera (Gatan Inc.). Representative images of general fields and nanostructures details were collected at three magnifications (10000×, 45000×, and 100000×).

2.3. Oligo-FdU Conjugation. GWH1-GFP-H6 nanoparticles were covalently linked to oligo 5-fluoro-2′-deoxyuridine (oligo-FdU or 5FdU) molecules through external protein lysine−amines in a two-step reaction using a bifunctional linker.[26] First, thiol-functionalized 5FdU molecules were separated from protecting DTT though NAP-10 shepadex gravity columns (GE Healthcare). Then thiol-5FdU molecules were reacted with a 6-maleimidohexanoic acid N-hydroxy-succinimide ester bifunctional linker (EMCS) by the thiol−maleimide

reaction in a 1:1 molar ratio for 15 min at room temperature (RT). The resulting ester-functionalized 5FdU molecules were finally reacted with GWH1-GFP-H6 nanoparticles through external lysines by the ester−amine reaction in a 1:5 molar ratio O/N at RT. The product was subsequently dialyzed against sodium bicarbonate buffer to remove nonreacted 5FdU molecules. The quantity of conjugated 5FdU molecules was determined by FdU absorbance at 260 nm in a UV/vis light spectrophotometer using a molar extinction coefficient (ε: 43500 M^{-1} cm^{-1}).

2.4. *In Silico* Modeling and Visualization. The structure of both GWH1-GFP-H6 and PaD-GFP-H6 constructs was predicted by using the RosettaCM[41] high-resolution approach through the Robetta server.[42] Protein sequences were used as query, and no templates were provided. Parameters were set to 1000 sampling models, 1 register shift, and a probability of 0.1 of sampling fragments within template regions. The candidates with the highest confidence score and lowest estimate error were selected. UCSF Chimera[43] was used to assemble nanoparticles, join 5FdU molecules and represent the 3D structures of GWH1-GFP-H6 and GWH1-GFP-H6-FdU.

2.5. Bactericidal Activity Assay. The effect of the different antimicrobial nanoparticles was evaluated against *P. aeruginosa* ATCC-27853 and *S. aureus* ATCC-29737. To determine the minimum inhibitory concentration (MIC) of protein nanoparticles, a broth microdilution method was used. In 96-well plates, after a 2-fold serial dilution process of antimicrobial nanoparticles (in Mueller Hinton Broth Cation-adjusted medium, MHB-2, Sigma-Aldrich), each well contained a specific amount of the corresponding protein, ranging from 0.5 to 8 μmol/L in 50 μL. Then, 50 μL of MHB-2 medium containing 10^6 colony-forming units per mL (CFU/mL) of *P. aeruginosa* or *S. aureus* was inoculated in each well, and the plates were incubated without agitation at 37 °C for 18 h. The lowest concentration showing no bacterial growth (evaluated by visual inspection) was taken as the minimum inhibitory concentration (MIC). In addition to visual MIC evaluation, bacterial growth was measured by OD_{620}, and bacterial viability was determined by CFU counting. The number of CFU per mL was obtained by plating serial dilutions of the bacterial suspension. Each concentration sample was evaluated in quadruplicates.

2.6. Evaluation of Biofilm Formation. Quantification of the biofilm biomass in the broth microdilution plate was performed by crystal violet (CV) staining. For that, wells were washed three times with distilled water, fixed at 60 °C for 1 h, and stained for 15 min with 200 μL of CV solution at 0.1%. The stained biofilms were rinsed with distilled water, allowed to dry at 37 °C for 30 min, and then extracted with 200 mL of 30% acetic acid. The amount of biofilm was quantified by measuring the OD_{550} of CV using the multilabel plater reader VICTOR3 (PerkinElmer). Biofilm formation was normalized by cell growth and reported as relative biofilm formation. Each concentration was evaluated in quadruplicates.

2.7. Imaging of Antimicrobial Effects. Ultrastructural effects of GWH1-GFP-H6-FdU nanoconjugates were evaluated in *S. aureus* ATCC29737 cultures. Bacteria were incubated on coverglasses, alone (0 μmol/L) or exposed to two nanoconjugate concentrations (2 and 4 μmol/L) in 24-well plates and evaluated at 18 h. For FESEM, coverglasses were fixed in 2.5% (v/v) glutaraldehyde (Merck) in a 0.1 mol/L phosphate buffer (PB; Sigma-Aldrich) for 2 h at 4 °C, postfixed in 1% (w/v) osmium tetraoxide (TAAB) in PB for 2 h at 4 °C, then dehydrated in graded series of ethanol at RT, and dried with CO_2 in a Bal-Tec CPD030 critical-point dryer (Balzers). Samples were mounted in metal stubs and observed without coating in a FESEM Merlin (Zeiss) operating at 0.8 kV and equipped with a standard secondary electron detector. Representative images of general fields and bacterial cell details were collected at three magnifications (5000×, 45000×, and 100000×).

2.8. Cell Viability Assay. The potential cytotoxicity of GFP-H6, GWH1-GFP-H6, and Pad-GFP-H6 was explored with the Titer-GloLuminescent Cell Viability Assay (Promega). For that, HeLa ATCC−CCL-2 cells were maintained in Eagle's Minimum Essential Medium (Gibco) supplemented with 10% fetal bovine serum (Gibco) and incubated under a humidified atmosphere at 37 °C and 5% of CO_2. A total of 3500 cells/well were cultured in opaque-walled 96-well plates

C
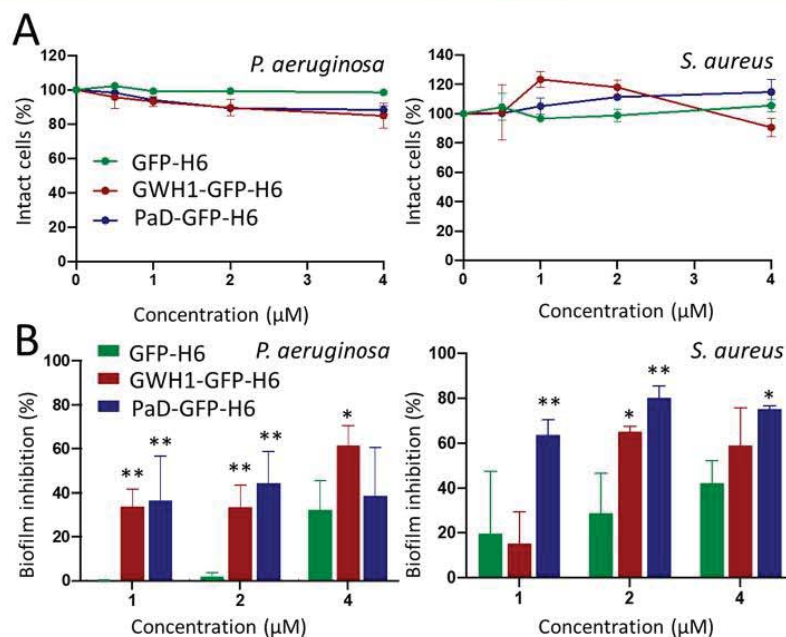
Figure 2. Antibacterial effects of protein-only nanoparticles at sublethal concentrations. (A) Variation of the cell integrity of *P. aeruginosa* and *S. aureus* cultures, measured by their optical density at 620 nm, upon incubation of nanoparticles in serial 2-fold dilutions (0.5, 1, 2, and 4 μmol/L) at 37 °C for 18 h. (B) Effect of nanoparticle concentration in the biofilm formation of bacterial cells on the surface of the microtiter wells. Significant differences between antimicrobial nanoparticles and the control GFP-H6 are indicated as *$p < 0.05$ and **$p < 0.01$.

for 24 h at 37 °C until reaching 70% confluence and then exposed to proteins at 8 μmol/L for 48 h. After incubation, a lysis solution was added according to the manufacturer's instructions. The resulting luminescent signal, proportional to the amount of ATP present in the sample, was measured in a conventional microplate reader VICTOR3 (PerkinElmer). The cell viability experiments were performed in triplicate.

2.9. Hemolysis Assay. Freshly drawn human erythrocytes were harvested by centrifugation for 5 min at 1500*g* and washed three times with PBS. Then, a 1% (v/v) cell suspension in PBS was added to 100 μL of 8 mol/L protein in a 96-well plate. PBS and 1% (v/v) Triton X-100 were also added to generate no hemolysis and full hemolysis controls, respectively. After incubation at 37 °C for 1 h, plates were centrifuged for 5 min at 1500*g*, and 100 μL of the supernatant was transferred to a new 96-well plate to measure the absorbance at 405 nm in a microplate reader VICTOR3 (PerkinElmer). Experiments were performed in duplicates.

2.10. Statistical Analysis. The quantitative data of the experiments were reported as mean $\pm$ standard error of the mean (SEM). Pairwise comparisons between groups were determined by unpaired *t* test using GraphPad Prism 8 software. Significant differences between groups were considered at $p < 0.05$, and relevant divergences were labeled as *$p < 0.05$ and **$p < 0.01$.

3. RESULTS AND DISCUSSION

To explore the feasibility of the proposed concept of bifunctional nanoconjugate materials, we selected the AMPs GWH1[44] and PaDBS1R1[45] (abbreviated here as PaD) to construct GFP-based, polyhistidine (H6)-tagged fusion proteins (namely GWH1-GFP-H6 and PaD-GFP-H6, Figure 1A), which were produced in *Escherichia coli* and purified by affinity chromatography (Figure 1B). These proteins, in contrast to the control GFP-H6, self-assembled as nanoparticles of 35 nm in size (Figure 1C, top), with a relatively low polydispersion index (Figure 1C, bottom) and with a very coincident size when

comparing both constructs. The cationic character of the *N*-terminal AMPs is necessary, combined with the *C*-terminal H6 tag, to form regular oligomers by a particular arrangement of electrostatic charges[46] and metal-H6 coordination.[47] Under microscopy observation, both GWH1-GFP-H6 and PaD-GFP-H6 particles adopted a toroid-like morphology (Figure 1D, left) with particle sizes compatible with those determined by DLS. In agreement with those observations, the *in silico* modeling of GWH1-GFP-H6 fully supported the cyclic architecture of such H6 tag-mediated oligomers (Figure 1D, right), as it was previously determined for related protein constructs.[48] In the present model, 12 copies of GWH1 (in red) were exposed to the nanoparticle surface while the H6 tails were condensed in the inner side.[47] Some PaD-GFP-H6 nanoparticles appeared as rod-shaped entities (Figure 1D, left) that might be resulting from the staking of several toroid entities. Similar stacking was previously observed in related protein constructs that mimic the assembly of plant viruses with helicoidal capsid symmetries.[49] GFP-H6 showed a hydrodynamic size (around 5 nm, Figure 1C) compatible with the dimeric form of GFP (modeled in Figure 1E). In agreement, no nanoparticles but building blocks were observed by electron microscopy when analyzing GFP-H6 (Figure 1D, left), again with sizes compatible with dimers. In fact, dimers appeared to be also the basic building blocks of GWH1-GFP-H6 and PaD-GFP-H6 nanoparticles (Figure 1E), which adopt a canonical architectonic pattern common in such a family of GFP-derived H6-assisted oligomers.[38,48]

The antimicrobial effect of these proteins, in such nano-structured form, was evaluated in two ESKAPE (ESKAPE is an acronym of six bacterial pathogens commonly carrying antimicrobial resistance genes[50,51]) pathogens, namely *Pseudomonas aeruginosa* and *Staphylococcus aureus*. As observed (Figure 2A), none of them affected the final biomass achieved by
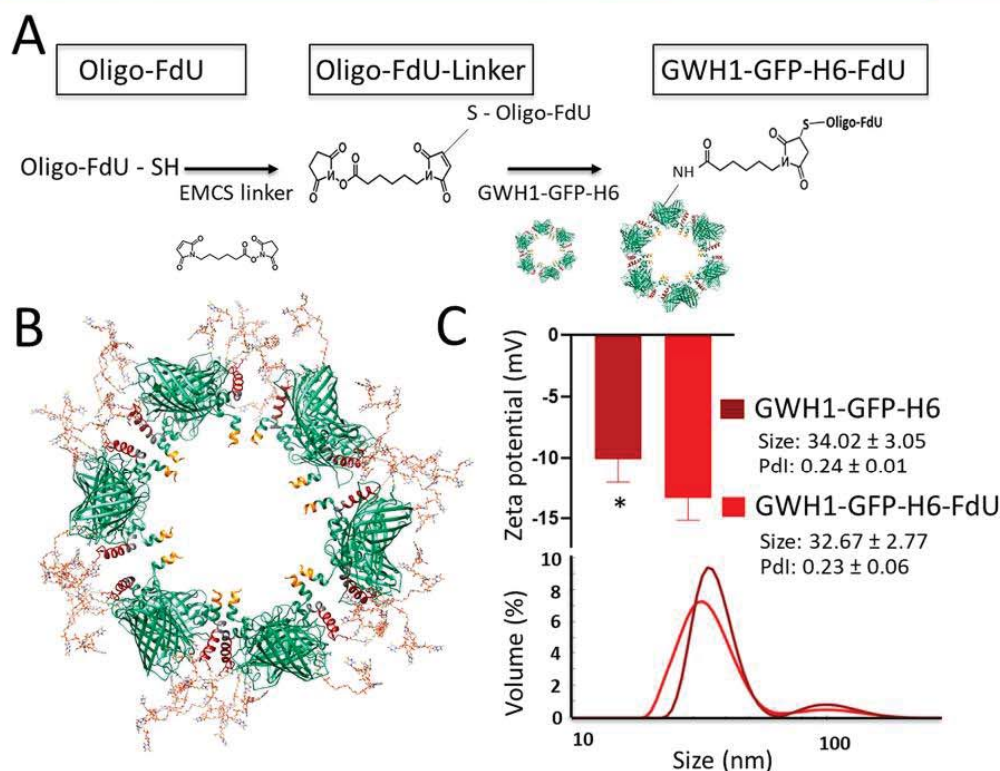
Figure 3. Generation and characterization of GWH1-GFP-H6-FdU nanoconjugates. (A) Details of the two-step chemical conjugation of oligo-FdU to GWH1-GFP-H6 nanoparticles through protein lysine−amines by a bifunctional EMCS linker. (B) Schematic representation of GWH1-GFP-H6-FdU nanoconjugates. Six GWH1 copies of dimeric GWH1-GFP-H6 (in red) are exposed to the nanoparticle surface while the H6 tails are condensed in the inner side (orange). Oligo-FdU molecules are solvent-exposed. (C) Volume size distribution and zeta potential of GWH1-GFP-H6-FdU nanoconjugates and native GWH1-GFP-H6 as determined by dynamic light scattering and electrophoretic light scattering, respectively. PdI indicates polydispersion index. Data are represented as mean ± standard error of the mean (SEM). Significant differences between relevant data are indicated as *$p < 0.05$.

conventional bacterial cultures after a batch growth for 18 h, indicative of no effect on bacterial cell integrity or culture growth. However, the same materials clearly inhibited biofilm formation in both species, with an effect that was more obvious at the lowest tested doses (Figure 2B). This fact revealed subinhibitory concentration effects of GWH1 and PaD. Because of such mild antimicrobial effect of both nanoparticles, we wondered whether this activity would be complemented by that from an unconventional antibiotic. For that, a FdU pentamer (5FdU) was chemically conjugated to the GWH1-GFP-H6 protein oligomers, as a selected study model, by an N-ε-malemidocaproyloxysuccinimide (EMCS) ester linker (Figure 3A). The coupling event resulted in stable nanoconjugates that carried four FdU pentamers per protein, for which a 3D representation was generated (Figure 3B) to illustrate the most likely positions in which the 5FdU molecules bind to solvent-exposed lysines. The conjugation with the oligo-FdU slightly modified both the surface charge of the nanoparticles and their hydrodynamic size (Figure 3C), although those modifications were not expected to alter the biological properties of the protein partner in the nanoconjugate.

At that point, these hybrid materials were tested by their antimicrobial effect. As observed, the presence of the FdU pentamer dramatically enhanced the antimicrobial capability of the nanoparticles (Figure 4). The MIC of GWH1-GFP-H6-FdU

was determined to be 4 μmol/L when tested over *S. aureus* and 8 μmol/L over *P. aeruginosa*, corresponding to the lowest concentration in which bacterial growth was not observed. Importantly, at MIC values, nanoconjugates clearly affected bacterial viability as determined by the number of colony forming units (CFU) (Figure 5). Indeed, the exposure of *S. aureus* and *P. aeruginosa* to the bifunctional nanoparticles resulted in a reduction, by 2 and 4 orders of magnitude, respectively, of the bacterial cell viability compared to untreated bacteria (Figure 5B). It must be noted that *P. aeruginosa* tolerates well (and grows in the presence of) 25−50 μmol/L of FdU, in agreement with previous data.[52] Interestingly, the antimicrobial effect shown by the nanoconjugate (MIC: 8 μmol/L) was significantly more potent than that of free FdU and also when compared to bacterial cultures treated with a mixture of unconjugated nanoparticles and 5FdU added at the same molar concentrations (Figures 4B and 5A). In the case of *S. aureus*, being already very sensitive to FdU (the described MIC values are around 0.3–3 μmol/L),[53] this effect was not so clearly observed. In fact, the antimicrobial effect shown by the free oligo-FdU, the nanoconjugate, and a mixture of both agents was very similar. Interestingly, GFP-H6-FdU did not affect bacterial growth and viability, since the conjugation of FdU might prevent its internalization and subsequent action. This fact suggests that in GWH1-GFP-H6-FdU nanoconjugates the antimicrobial
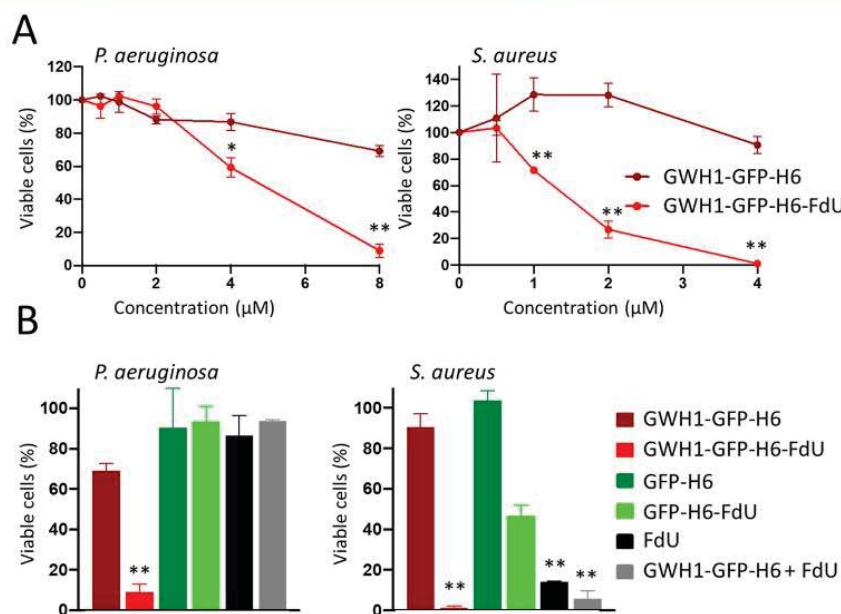
Figure 4. Impact of the GWH1-GFP-H6-FdU on bacterial integrity. (A) Bacterial integrity of *P. aeruginosa* and *S. aureus* measured by the optical density at 620 nm, after incubation of GWH1-GFP-H6 and GWH1-GFP-H6-FdU in serial 2-fold dilutions (from 0.5 to 8 μmol/L) at 37 °C for 18 h. Significant differences between relevant data are indicated as $*p < 0.05$ and $**p < 0.01$. (B) Comparative antimicrobial effect of GWH1-GFP-H6-FdU and control proteins at 8 μmol/L for *P. aeruginosa* and 4 μmol/L for *S. aureus*. Significant differences between proteins and GFP-H6-FdU are indicated as $*p < 0.05$ and $**p < 0.01$.

peptide GWH1 would be targeting the bacterial membrane and thus allowing the bifunctional drug performing its action. Finally, the formation of biofilms was efficiently inhibited by the nanoconjugates in both bacterial species as compared with the control GWH1-GFP-H6 nanoparticle (Figure 6A,B), mainly because of the subinhibitory effects of GWH1 which are efficiently conserved in the hybrid material. Even so, an enhancement in the biofilm inhibition was also observed in 5FdU-carrying nanoparticles, probably due to the antivirulence effects already described for this cytotoxic drug.[52,54] Interestingly, the pore formation activities generically associated with AMPs were confirmed for GWH1, that in the form of GWH1-GFP-H6-FdU nanoconjugates caused cell wall disruption in *S. aureus* cells (Figure 7A). The appearance of cell debris in the culture was compatible with such AMP activity, supported by the generically strong AMP amphiphilic character combining positive charges with hydrophobic amino acids. The positive segments of the peptide selectively bind the negatively charged microbial cell surfaces, which results in the breakdown of the transmembrane potential when the peptide concentration reaches a critical threshold, for GWH1 defined since 3 μmol/L and depending on the target bacterial species.[44,45] Such activity was then maintained in the GWH1-containing nanoconjugate, and it was fully selective over bacterial cell membranes, as it did not produce any hemolysis in exposed human erythrocytes (Figure 7B). Both GWH1- and PaD-based protein nanoparticles were also not hemolytic (Figure 7B) or cytotoxic over mammalian cells (Figure 7C), which fully confirmed the full and intrinsic biocompatibility and safety of nanoscale protein materials as components of hybrid therapeutic nanoconjugates.

4. CONCLUSIONS

Taken together, the results presented here demonstrate the feasibility of hybrid multifunctional materials at the nanoscale for a robust antimicrobial effect of their combined components. This approach would benefit from drug repurposing, as the unmet need for new antimicrobials has pushed to identify side activities of interest in conventional chemical drugs.[55−57] The proposed concept of chemically hybrid nanoscale materials in which proteins act at the same time as drugs and as drug carriers is supported by the self-assembling capabilities of such biomolecules, which allow the formation of supramolecular complexes under principles of synthetic biology.[30,58−63] If conveniently tailored by incorporating end-terminal polyhistidine tails, which will be coordinated with ions from the media,[64−67] the protein building blocks spontaneously self-organize in regular oligomers, resulting in the controlled formation of multivalent nanoparticles with the ability to exclusively bind interacting protein domains in complex media.[48] The generated data also stand out the use of hybrid materials as single-structure entities for an optimal antibacterial effect that in the prototypes developed here was promoted by a selective binding of the exposed AMPs to the bacterial outer membrane and the subsequent internalization of a chemical conjugated drug.
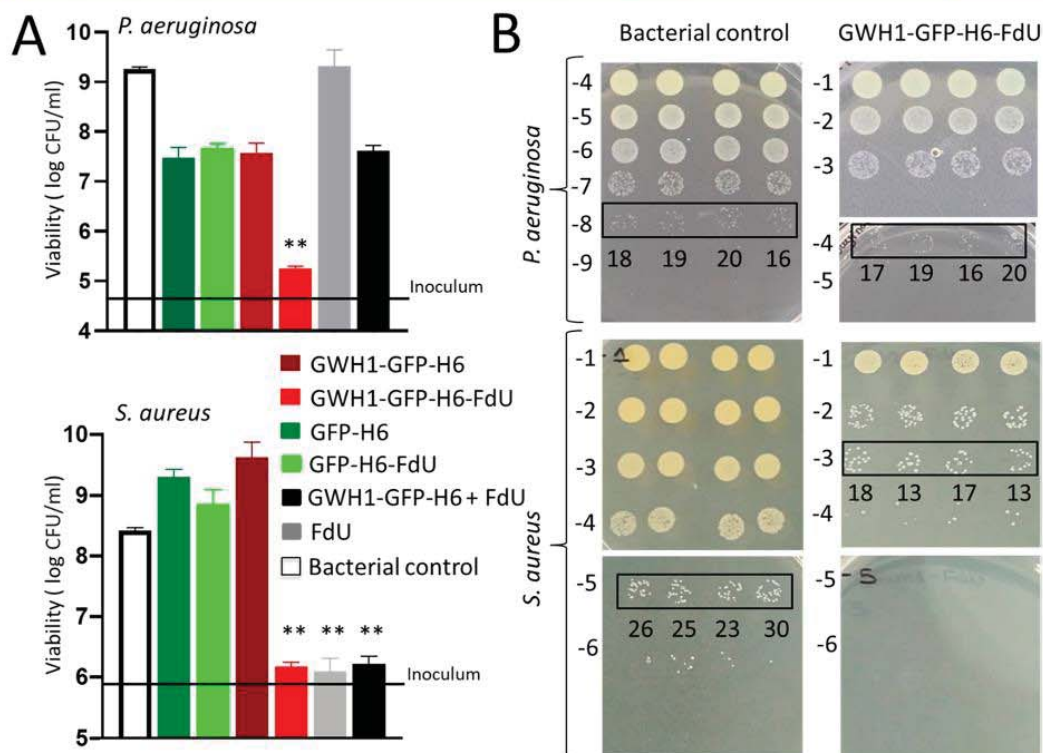
■ AUTHOR INFORMATION

Corresponding Authors

Esther Vazquez − *Institut de Biotecnologia i de Biomedicina and Departament de Genètica i de Microbiologia, Universitat Autònoma de Barcelona, 08193 Barcelona, Spain; CIBER de Bioingeniería, Biomateriales y Nanomedicina (CIBER-BBN),*

Figure 5. Effects of GWH1-GFP-H6-FdU on bacterial cell viability. (A) Number of colony forming units (log CFU/mL) of *P. aeruginosa* and *S. aureus* after treatment with antimicrobial nanoconjugate at 8 μmol/L for *P. aeruginosa* and 4 μmol/L for *S. aureus* for 18 h at 37 °C. (B) Representative bacterial plates of cell control and GWH1-GFP-H6-FdU at the serial dilutions between 10^1 and 10^8 showing statistically acceptable CFU counting in GWH1-GFP-H6-FdU at 10^4 dilution in the case of *P. aeruginosa* and at 10^3 dilution for *S. aureus*. Significant differences between values under treatment and without treatment are indicated as $**p < 0.01$.
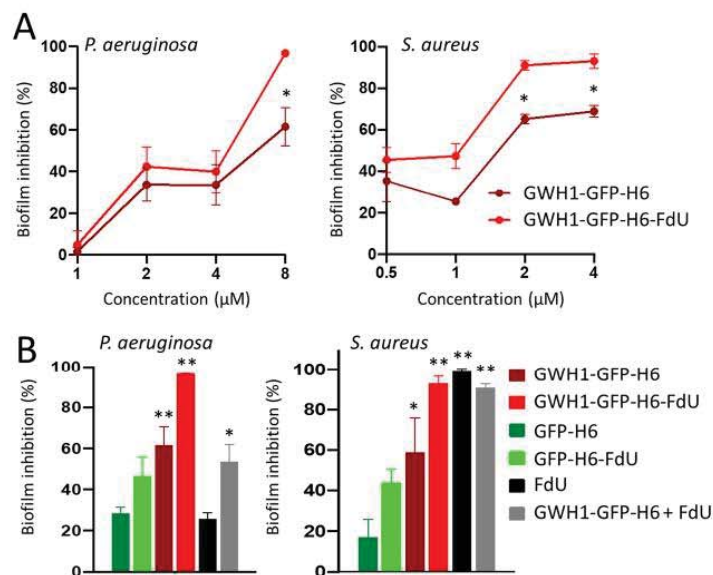
Figure 6. Inhibition of biofilm formation by GWH1-GFP-H6-FdU. (A) Effect of nanoconjugate concentration on biofilm formation. Significant differences between GWH1-GFP-H6-FdU and GWH1-GFP-H6 are indicated as $*p < 0.05$ and $**p < 0.01$. (B) Comparison of the effect on biofilm formation between GWH1-GFP-H6-FdU and control proteins at 8 μmol/L for *P. aeruginosa* and 4 μmol/L for *S. aureus*. Significant differences between proteins and GFP-H6 control are indicated as $*p < 0.05$ and $**p < 0.01$.

G
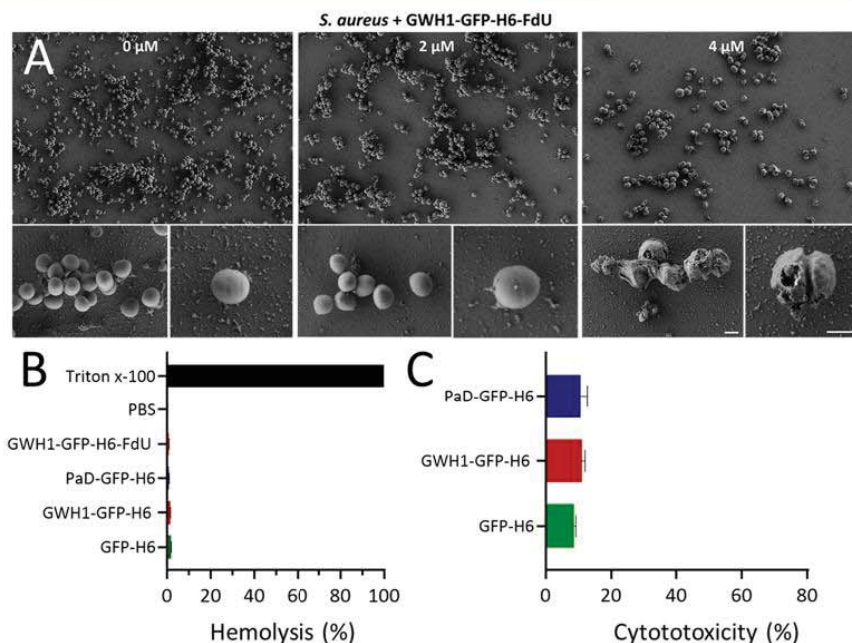
Figure 7. Physical impact of GWH1-GFP-H6-FdU and protein nanoparticles on bacterial and mammalian cells. (A) Representative high-resolution FESEM images of *S. aureus* cells nonexposed (0 μmol/L) and exposed to GWH1-GFP-H6-FdU nanoconjugates (at either 2 or 4 μmol/L) for 18 h. Bar size: 500 nm. (B) Absence of hemolytic activity associated with protein materials and nanoconjugates over human erythrocytes. (C) Absence of cytotoxicity in the presence of 8 μmol/L protein nanoparticles over cultured HeLa cells, recorded 48 h after exposure.

28029 Madrid, Spain; orcid.org/0000-0003-1052-0424;
Email: esther.vazquez@uab.es

Antonio Villaverde — *Institut de Biotecnologia i de Biomedicina and Departament de Genètica i de Microbiologia, Universitat Autònoma de Barcelona, 08193 Barcelona, Spain; CIBER de Bioingeniería, Biomateriales y Nanomedicina (CIBER-BBN), 28029 Madrid, Spain;* orcid.org/0000-0002-2615-4521;
Email: antoni.villaverde@uab.es

Authors

Naroa Serna — *Institut de Biotecnologia i de Biomedicina and Departament de Genètica i de Microbiologia, Universitat Autònoma de Barcelona, 08193 Barcelona, Spain; CIBER de Bioingeniería, Biomateriales y Nanomedicina (CIBER-BBN), 28029 Madrid, Spain*

Jose Vicente Carratalá — *Institut de Biotecnologia i de Biomedicina and Departament de Genètica i de Microbiologia, Universitat Autònoma de Barcelona, 08193 Barcelona, Spain; CIBER de Bioingeniería, Biomateriales y Nanomedicina (CIBER-BBN), 28029 Madrid, Spain*

Eloi Parladé — *Institut de Biotecnologia i de Biomedicina, Universitat Autònoma de Barcelona, 08193 Barcelona, Spain; CIBER de Bioingeniería, Biomateriales y Nanomedicina (CIBER-BBN), 28029 Madrid, Spain*

Alejandro Sánchez-Chardi — *Servei de Microscòpia, Universitat Autònoma de Barcelona, 08193 Barcelona, Spain; Departament de Biologia Evolutiva, Ecologia i Ciències Ambientals, Facultat de Biologia, Universitat de Barcelona, 08028 Barcelona, Spain*

Anna Aviñó — *CIBER de Bioingeniería, Biomateriales y Nanomedicina (CIBER-BBN), 28029 Madrid, Spain; Institute for Advanced Chemistry of Catalonia (IQAC), CSIC, 08034 Barcelona, Spain*

Ugutz Unzueta — *Departament de Genètica i de Microbiologia, Universitat Autònoma de Barcelona, 08193 Barcelona, Spain; CIBER de Bioingeniería, Biomateriales y Nanomedicina (CIBER-BBN), 28029 Madrid, Spain; Biomedical Research Institute Sant Pau (IIB Sant Pau), 08025 Barcelona, Spain;* orcid.org/0000-0001-5119-2266

Ramón Mangues — *CIBER de Bioingeniería, Biomateriales y Nanomedicina (CIBER-BBN), 28029 Madrid, Spain; Biomedical Research Institute Sant Pau (IIB Sant Pau), 08025 Barcelona, Spain*

Ramón Eritja — *CIBER de Bioingeniería, Biomateriales y Nanomedicina (CIBER-BBN), 28029 Madrid, Spain; Institute for Advanced Chemistry of Catalonia (IQAC), CSIC, 08034 Barcelona, Spain;* orcid.org/0000-0001-5383-9334

Neus Ferrer-Miralles — *Institut de Biotecnologia i de Biomedicina and Departament de Genètica i de Microbiologia, Universitat Autònoma de Barcelona, 08193 Barcelona, Spain; CIBER de Bioingeniería, Biomateriales y Nanomedicina (CIBER-BBN), 28029 Madrid, Spain;* orcid.org/0000-0003-2981-3913

Complete contact information is available at:
https://pubs.acs.org/10.1021/acsami.0c18317

Author Contributions

Funding

Notes

■ ACKNOWLEDGMENTS

■ ABBREVIATIONS

AMPs, antimicrobial peptides; CFU, colony-forming units; CV, crystal violet; DLS, dynamic light scattering; ELS, electrophoretic light scattering; FdU, Floxuridine; FU, 5-fluorouracil; GFP, green fluorescent protein; H6, hexahistidine; IMAC, immobilized metal affinity chromatography; IPTG, isopropyl β-D-1-thiogalactopyranoside; MIC, minimum inhibitory concentration; PdI, polydispersion index; FESEM, field emission scanning electron microscopy; TEM, transmission electron microscopy; SEM, standard error of the mean.

■ REFERENCES

(1) Niewiadomska, A. M.; Jayabalasingham, B.; Seidman, J. C.; Willem, L.; Grenfell, B.; Spiro, D.; Viboud, C. Population-Level Mathematical Modeling of Antimicrobial Resistance: A Systematic Review. *BMC Med.* **2019**, *17*, 81.

(2) Seo, M. D.; Won, H. S.; Kim, J. H.; Mishig-Ochir, T.; Lee, B. J. Antimicrobial Peptides for Therapeutic Applications: A Review. *Molecules* **2012**, *17*, 12276−86.

(3) Mahlapuu, M.; Hakansson, J.; Ringstad, L.; Bjorn, C. Antimicrobial Peptides: An Emerging Category of Therapeutic Agents. *Front. Cell. Infect. Microbiol.* **2016**, *6*, 194.

(4) Bhopale, G. M. Antimicrobial Peptides: A Promising Avenue for Human Healthcare. *Curr. Pharm. Biotechnol.* **2020**, *21*, 90−96.

(5) Wang, J.; Dou, X.; Song, J.; Lyu, Y.; Zhu, X.; Xu, L.; Li, W.; Shan, A. Antimicrobial Peptides: Promising Alternatives in the Post Feeding Antibiotic Era. *Med. Res. Rev.* **2019**, *39*, 831−859.

(6) Verderosa, A. D.; Totsika, M.; Fairfull-Smith, K. E. Bacterial Biofilm Eradication Agents: A Current Review. *Front. Chem.* **2019**, *7*, 824.

(7) Carratalá, J. V.; Serna, N.; Villaverde, A.; Vázquez, E.; Ferrer-Miralles, N. Nanostructured Antimicrobial Peptides: The Last Push Towards Clinics. *Biotechnol. Adv.* **2020**, *44*, 107603.

(8) Lei, J.; Sun, L.; Huang, S.; Zhu, C.; Li, P.; He, J.; Mackey, V.; Coy, D. H.; He, Q. The Antimicrobial Peptides and Their Potential Clinical Applications. *Am. J. Translational Res.* **2019**, *11*, 3919−3931.

(9) Mourtada, R.; Herce, H. D.; Yin, D. J.; Moroco, J. A.; Wales, T. E.; Engen, J. R.; Walensky, L. D. Design of Stapled Antimicrobial Peptides That Are Stable, Nontoxic and Kill Antibiotic-Resistant Bacteria in Mice. *Nat. Biotechnol.* **2019**, *37*, 1186−1197.

(10) Chen, C. H.; Lu, T. K. Development and Challenges of Antimicrobial Peptides for Therapeutic Applications. *Antibiotics (Basel, Switz.)* **2020**, *9*, 24.

(11) Teixeira, M. C.; Carbone, C.; Sousa, M. C.; Espina, M.; Garcia, M. L.; Sanchez-Lopez, E.; Souto, E. B. Nanomedicines for the Delivery of Antimicrobial Peptides (Amps). *Nanomaterials* **2020**, *10*, 560.

(12) Ruden, S.; Rieder, A.; Chis Ster, I.; Schwartz, T.; Mikut, R.; Hilpert, K. Synergy Pattern of Short Cationic Antimicrobial Peptides against Multidrug-Resistant *Pseudomonas aeruginosa*. *Front. Microbiol.* **2019**, *10*, 2740.

(13) Casciaro, B.; Cappiello, F.; Verrusio, W.; Cacciafesta, M.; Mangoni, M. L. Antimicrobial Peptides and Their Multiple Effects at Sub-Inhibitory Concentrations. *Curr. Top. Med. Chem.* **2020**, *20*, 1264−1273.

(14) Vasilchenko, A. S.; Rogozhin, E. A. Sub-Inhibitory Effects of Antimicrobial Peptides. *Front. Microbiol.* **2019**, *10*, 1160.

(15) Batoni, G.; Maisetta, G.; Esin, S. Antimicrobial Peptides and Their Interaction with Biofilms of Medically Relevant Bacteria. *Biochim. Biophys. Acta, Biomembr.* **2016**, *1858*, 1044−60.

(16) Zou, G.; de Leeuw, E. Neutralization of *Pseudomonas aeruginosa* Exotoxin a by Human Neutrophil Peptide 1. *Biochem. Biophys. Res. Commun.* **2018**, *501*, 454−457.

(17) Cummins, J.; Reen, F. J.; Baysse, C.; Mooij, M. J.; O'Gara, F. Subinhibitory Concentrations of the Cationic Antimicrobial Peptide Colistin Induce the Pseudomonas Quinolone Signal in Pseudomonas Aeruginosa. *Microbiology* **2009**, *155*, 2826−2837.

(18) Wang, Y.; Wang, X.; Jiang, W.; Wang, K.; Luo, J.; Li, W.; Zhou, X.; Zhang, L. Antimicrobial Peptide Gh12 Suppresses Cariogenic Virulence Factors of Streptococcus Mutans. *J. Oral Microbiol.* **2018**, *10*, 1442089.

(19) Duperthuy, M. Antimicrobial Peptides: Virulence and Resistance Modulation in Gram-Negative Bacteria. *Microorganisms* **2020**, *8*, 280.

(20) Lee, J. J.; Beumer, J. H.; Chu, E. Therapeutic Drug Monitoring of 5-Fluorouracil. *Cancer Chemother. Pharmacol.* **2016**, *78*, 447−64.

(21) Walz, J. M.; Avelar, R. L.; Longtine, K. J.; Carter, K. L.; Mermel, L. A.; Heard, S. O. Anti-Infective External Coating of Central Venous Catheters: A Randomized, Noninferiority Trial Comparing 5-Fluorouracil with Chlorhexidine/Silver Sulfadiazine in Preventing Catheter Colonization. *Crit. Care Med.* **2010**, *38*, 2095−102.

(22) Fang, X. J.; Jeyakkumar, P.; Avula, S. R.; Zhou, Q.; Zhou, C. H. Design, Synthesis and Biological Evaluation of 5-Fluorouracil-Derived Benzimidazoles as Novel Type of Potential Antimicrobial Agents. *Bioorg. Med. Chem. Lett.* **2016**, *26*, 2584−8.

(23) Campbell, O.; Gagnon, J.; Rubin, J. E. Antibacterial Activity of Chemotherapeutic Drugs against Escherichia Coli and Staphylococcus Pseudintermedius. *Lett. Appl. Microbiol.* **2019**, *69*, 353−357.

(24) Papanicolas, L. E.; Gordon, D. L.; Wesselingh, S. L.; Rogers, G. B. Not Just Antibiotics: Is Cancer Chemotherapy Driving Antimicrobial Resistance? *Trends Microbiol.* **2018**, *26*, 393−400.

(25) Pallares, V.; Unzueta, U.; Falgas, A.; Sanchez-Garcia, L.; Serna, N.; Gallardo, A.; Morris, G. A.; Alba-Castellon, L.; Alamo, P.; Sierra, J.;

Villaverde, A.; Vazquez, E.; Casanova, I.; Mangues, R. An Auristatin Nanoconjugate Targeting Cxcr4+ Leukemic Cells Blocks Acute Myeloid Leukemia Dissemination. *J. Hematol. Oncol.* **2020**, *13*, 36.

(26) Avino, A.; Unzueta, U.; Virtudes Cespedes, M.; Casanova, I.; Vazquez, E.; Villaverde, A.; Mangues, R.; Eritja, R. Efficient Bioactive Oligonucleotide-Protein Conjugation for Cell-Targeted Cancer Therapy. *ChemistryOpen* **2019**, *8*, 382−387.

(27) Cespedes, M. V.; Unzueta, U.; Avino, A.; Gallardo, A.; Alamo, P.; Sala, R.; Sanchez-Chardi, A.; Casanova, I.; Mangues, M. A.; Lopez-Pousa, A.; Eritja, R.; Villaverde, A.; Vazquez, E.; Mangues, R. Selective Depletion of Metastatic Stem Cells as Therapy for Human Colorectal Cancer. *EMBO Mol. Med.* **2018**, *10*, e8772.

(28) Gmeiner, W. H.; Sahasrabudhe, P.; Pon, R. T.; Sonntag, J.; Srinivasan, S.; Iversen, P. L. Preparation of Oligomeric 2′-Deoxy-5-Fluorouridylate of Defined Length and Backbone Composition: A Novel Pro-Drug Form of the Potent Anti-Cancer Drug 2′-Deoxy-5-Fluorouridylate. *Nucleosides Nucleotides* **1995**, *14*, 243−253.

(29) Serna, N.; Cespedes, M. V.; Sanchez-Garcia, L.; Unzueta, U.; Sala, R.; Sanchez-Chardi, A.; Cortes, F.; Ferrer-Miralles, N.; Mangues, R.; Vazquez, E.; Villaverde, A. Peptide-Based Nanostructured Materials with Intrinsic Proapoptotic Activities in Cxcr4+ Solid Tumors. *Adv. Funct. Mater.* **2017**, *27*, 1700919.

(30) Sanchez, J. M.; Lopez-Laguna, H.; Alamo, P.; Serna, N.; Sanchez-Chardi, A.; Nolan, V.; Cano-Garrido, O.; Casanova, I.; Unzueta, U.; Vazquez, E.; Mangues, R.; Villaverde, A. Artificial Inclusion Bodies for Clinical Development. *Advanced science* **2020**, *7*, 1902420.

(31) Serna, N.; Alamo, P.; Ramesh, P.; Vinokurova, D.; Sanchez-Garcia, L.; Unzueta, U.; Gallardo, A.; Cespedes, M. V.; Vazquez, E.; Villaverde, A.; Mangues, R.; Medema, J. P. Nanostructured Toxins for the Selective Destruction of Drug-Resistant Human Cxcr4(+) Colorectal Cancer Stem Cells. *J. Controlled Release* **2020**, *320*, 96−104.

(32) Falgas, A.; Pallares, V.; Serna, N.; Sanchez-Garcia, L.; Sierra, J.; Gallardo, A.; Alba-Castellon, L.; Alamo, P.; Unzueta, U.; Villaverde, A.; Vazquez, E.; Mangues, R.; Casanova, I. Selective Delivery of T22-Pe24-H6 to Cxcr4(+) Diffuse Large B-Cell Lymphoma Cells Leads to Wide Therapeutic Index in a Disseminated Mouse Model. *Theranostics* **2020**, *10*, 5169−5180.

(33) Sánchez-García, L.; Sala, R.; Serna, N.; Álamo, P.; Parladé, E.; Alba-Castellón, L.; Voltà-Durán, E.; Sánchez-Chardi, A.; Unzueta, U.; Vázquez, E.; Mangues, R.; Villaverde, A. A Refined Cocktailing of Pro-Apoptotic Nanoparticles Boosts Anti-Tumor Activity. *Acta Biomater.* **2020**, *113*, 584−596.

(34) Serna, N.; Cano-Garrido, O.; Sánchez-García, L.; Pesarrodona, M.; Unzueta, U.; Sánchez-Chardi, A.; Mangues, R.; Vázquez, E.; Villaverde, A. Engineering Protein Venoms as Self-Assembling Cxcr4-Targeted Cytotoxic Nanoparticles. *Part. Part. Syst. Charact.* **2020**, *37*, 2000040.

(35) Serna, N.; Sanchez-Garcia, L.; Sanchez-Chardi, A.; Unzueta, U.; Roldan, M.; Mangues, R.; Vazquez, E.; Villaverde, A. Protein-Only, Antimicrobial Peptide-Containing Recombinant Nanoparticles with Inherent Built-in Antibacterial Activity. *Acta Biomater.* **2017**, *60*, 256−263.

(36) Serna, N.; Sanchez, J. M.; Unzueta, U.; Sanchez-Garcia, L.; Sanchez-Chardi, A.; Mangues, R.; Vazquez, E.; Villaverde, A. Recruiting Potent Membrane Penetrability in Tumor Cell-Targeted Protein-Only Nanoparticles. *Nanotechnology* **2019**, *30*, 115101.

(37) Duncan, R.; Gaspar, R. Nanomedicine(s) under the Microscope. *Mol. Pharmaceutics* **2011**, *8*, 2101−41.

(38) Cespedes, M. V.; Unzueta, U.; Tatkiewicz, W.; Sanchez-Chardi, A.; Conchillo-Sole, O.; Alamo, P.; Xu, Z.; Casanova, I.; Corchero, J. L.; Pesarrodona, M.; Cedano, J.; Daura, X.; Ratera, I.; Veciana, J.; Ferrer-Miralles, N.; Vazquez, E.; Villaverde, A.; Mangues, R. In Vivo Architectonic Stability of Fully De Novo Designed Protein-Only Nanoparticles. *ACS Nano* **2014**, *8*, 4166−76.

(39) López-Laguna, H.; Sala, R.; Sánchez, J. M.; Álamo, P.; Unzueta, U.; Sánchez-Chardi, A.; Serna, N.; Sánchez-García, L.; Voltà-Durán, E.; Mangues, R.; Villaverde, A.; Vázquez, E. Nanostructure Empowers Active Tumor Targeting in Ligand-Based Molecular Delivery. *Part. Part. Syst. Charact.* **2019**, *36*, 1900304.

(40) Vazquez, E.; Roldan, M.; Diez-Gil, C.; Unzueta, U.; Domingo-Espin, J.; Cedano, J.; Conchillo, O.; Ratera, I.; Veciana, J.; Daura, X.; Ferrer-Miralles, N.; Villaverde, A. Protein Nanodisk Assembling and Intracellular Trafficking Powered by an Arginine-Rich (R9) Peptide. *Nanomedicine* **2010**, *5*, 259−68.

(41) Song, Y.; DiMaio, F.; Wang, R. Y.; Kim, D.; Miles, C.; Brunette, T.; Thompson, J.; Baker, D. High-Resolution Comparative Modeling with Rosettacm. *Structure* **2013**, *21*, 1735−42.

(42) Kim, D. E.; Chivian, D.; Baker, D. Protein Structure Prediction and Analysis Using the Robetta Server. *Nucleic Acids Res.* **2004**, *32*, W526−W531.

(43) Pettersen, E. F.; Goddard, T. D.; Huang, C. C.; Couch, G. S.; Greenblatt, D. M.; Meng, E. C.; Ferrin, T. E. Ucsf Chimera−a Visualization System for Exploratory Research and Analysis. *J. Comput. Chem.* **2004**, *25*, 1605−12.

(44) Chou, H. T.; Kuo, T. Y.; Chiang, J. C.; Pei, M. J.; Yang, W. T.; Yu, H. C.; Lin, S. B.; Chen, W. J. Design and Synthesis of Cationic Antimicrobial Peptides with Improved Activity and Selectivity against Vibrio Spp. *Int. J. Antimicrob. Agents* **2008**, *32*, 130−8.

(45) Irazazabal, L. N.; Porto, W. F.; Fensterseifer, I. C. M.; Alves, E. S. F.; Matos, C. O.; Menezes, A. C. S.; Felicio, M. R.; Goncalves, S.; Santos, N. C.; Ribeiro, S. M.; Humblot, V.; Liao, L. M.; Ladram, A.; Franco, O. L. Fast and Potent Bactericidal Membrane Lytic Activity of Padbs1r1, a Novel Cationic Antimicrobial Peptide. *Biochim. Biophys. Acta, Biomembr.* **2019**, *1861*, 178−190.

(46) Unzueta, U.; Ferrer-Miralles, N.; Cedano, J.; Zikung, X.; Pesarrodona, M.; Saccardo, P.; Garcia-Fruitos, E.; Domingo-Espin, J.; Kumar, P.; Gupta, K. C.; Mangues, R.; Villaverde, A.; Vazquez, E. Non-Amyloidogenic Peptide Tags for the Regulatable Self-Assembling of Protein-Only Nanoparticles. *Biomaterials* **2012**, *33*, 8714−22.

(47) Lopez-Laguna, H.; Unzueta, U.; Conchillo-Sole, O.; Sanchez-Chardi, A.; Pesarrodona, M.; Cano-Garrido, O.; Volta, E.; Sanchez-Garcia, L.; Serna, N.; Saccardo, P.; Mangues, R.; Villaverde, A.; Vazquez, E. Assembly of Histidine-Rich Protein Materials Controlled through Divalent Cations. *Acta Biomater.* **2019**, *83*, 257−264.

(48) Rueda, F.; Cespedes, M. V.; Conchillo-Sole, O.; Sanchez-Chardi, A.; Seras-Franzoso, J.; Cubarsi, R.; Gallardo, A.; Pesarrodona, M.; Ferrer-Miralles, N.; Daura, X.; Vazquez, E.; Garcia-Fruitos, E.; Mangues, R.; Unzueta, U.; Villaverde, A. Bottom-up Instructive Quality Control in the Biofabrication of Smart Protein Materials. *Adv. Mater.* **2015**, *27*, 7816−22.

(49) Unzueta, U.; Saccardo, P.; Domingo-Espin, J.; Cedano, J.; Conchillo-Sole, O.; Garcia-Fruitos, E.; Cespedes, M. V.; Corchero, J. L.; Daura, X.; Mangues, R.; Ferrer-Miralles, N.; Villaverde, A.; Vazquez, E. Sheltering DNA in Self-Organizing, Protein-Only Nano-Shells as Artificial Viruses for Gene Delivery. *Nanomedicine* **2014**, *10*, 535−41.

(50) Pendleton, J. N.; Gorman, S. P.; Gilmore, B. F. Clinical Relevance of the Eskape Pathogens. *Expert Rev. Anti-Infect. Ther.* **2013**, *11*, 297−308.

(51) Mulani, M. S.; Kamble, E. E.; Kumkar, S. N.; Tawre, M. S.; Pardesi, K. R. Emerging Strategies to Combat Eskape Pathogens in the Era of Antimicrobial Resistance: A Review. *Front. Microbiol.* **2019**, *10*, 539.

(52) Ueda, A.; Attila, C.; Whiteley, M.; Wood, T. K. Uracil Influences Quorum Sensing and Biofilm Formation in Pseudomonas Aeruginosa and Fluorouracil Is an Antagonist. *Microb. Biotechnol.* **2009**, *2*, 62−74.

(53) Lau, Q. Y.; Tan, Y. Y.; Goh, V. C.; Lee, D. J.; Ng, F. M.; Ong, E. H.; Hill, J.; Chia, C. S. An Fda-Drug Library Screen for Compounds with Bioactivities against Meticillin-Resistant Staphylococcus Aureus (Mrsa). *Antibiotics (Basel, Switz.)* **2015**, *4*, 424−34.

(54) Imperi, F.; Massai, F.; Facchini, M.; Frangipani, E.; Visaggio, D.; Leoni, L.; Bragonzi, A.; Visca, P. Repurposing the Antimycotic Drug Flucytosine for Suppression of *Pseudomonas aeruginosa* Pathogenicity. *Proc. Natl. Acad. Sci. U. S. A.* **2013**, *110*, 7458−7463.

(55) Farha, M. A.; Brown, E. D. Drug Repurposing for Antimicrobial Discovery. *Nature microbiology* **2019**, *4*, 565−577.

(56) Gajdacs, M.; Spengler, G. The Role of Drug Repurposing in the Development of Novel Antimicrobial Drugs: Non-Antibiotic Pharma-

cological Agents as Quorum Sensing-Inhibitors. *Antibiotics (Basel, Switz.)* **2019**, *8*, 270.

(57) Younis, W.; Thangamani, S.; Seleem, M. N. Repurposing Non-Antimicrobial Drugs and Clinical Molecules to Treat Bacterial Infections. *Curr. Pharm. Des.* **2015**, *21*, 4106−11.

(58) Hamley, I. W. Protein Assemblies: Nature-Inspired and Designed Nanostructures. *Biomacromolecules* **2019**, *20*, 1829−1848.

(59) Maniaci, B.; Lipper, C. H.; Anipindi, D. L.; Erlandsen, H.; Cole, J. L.; Stec, B.; Huxford, T.; Love, J. J. Design of High-Affinity Metal-Controlled Protein Dimers. *Biochemistry* **2019**, *58*, 2199−2207.

(60) Yang, M.; Song, W. J. Diverse Protein Assembly Driven by Metal and Chelating Amino Acids with Selectivity and Tunability. *Nat. Commun.* **2019**, *10*, 5545.

(61) Korpi, A.; Anaya-Plaza, E.; Valimaki, S.; Kostiainen, M. Highly Ordered Protein Cage Assemblies: A Toolkit for New Materials. *Wiley Interdiscip. Rev.: Nanomed. Nanobiotechnol.* **2020**, *12*, e1578.

(62) Ulijn, R. V.; Lampel, A. Order/Disorder in Protein and Peptide-Based Biomaterials. *Isr. J. Chem.* **2019**, DOI: 10.1002/ijch.201900051.

(63) Hansen, W. A.; Khare, S. D. Recent Progress in Designing Protein-Based Supramolecular Assemblies. *Curr. Opin. Struct. Biol.* **2020**, *63*, 106−114.

(64) Sánchez, J.; López-Laguna, H.; Álamo, P.; Serna, N.; Sánchez-Chardi, A.; Nolan, V.; Cano-Garrido, O.; Casanova, I.; Unzueta, U.; Vazquez, E.; Mangues, R.; Villaverde, A. Artificial Inclusion Bodies for Clinical Development. *Advanced science* **2020**, *7*, 1902420.

(65) López-Laguna, H.; Cubarsi, R.; Unzueta, U.; Mangues, R.; Vázquez, E.; Villaverde, A. Endosomal Escape of Protein Nanoparticles Engineered through Humanized Histidine-Rich Peptides. *Science China Materials* **2020**, *63*, 644−653.

(66) López-Laguna, H.; Sánchez-García, L.; Serna, N.; Voltà-Durán, E.; Sánchez, J. M.; Sánchez-Chardi, A.; Unzueta, U.; Łoś, M.; Villaverde, A.; Vázquez, E. Engineering Protein Nanoparticles out from Components of the Human Microbiome. *Small* **2020**, *16*, e2001885.

(67) López-Laguna, H.; Sánchez, J.; Unzueta, U.; Mangues, R.; Vázquez, E.; Villaverde, A. Divalent Cations: A Molecular Glue for Protein Materials. *Trends Biochem. Sci.* **2020**, *45*, 992−1003.
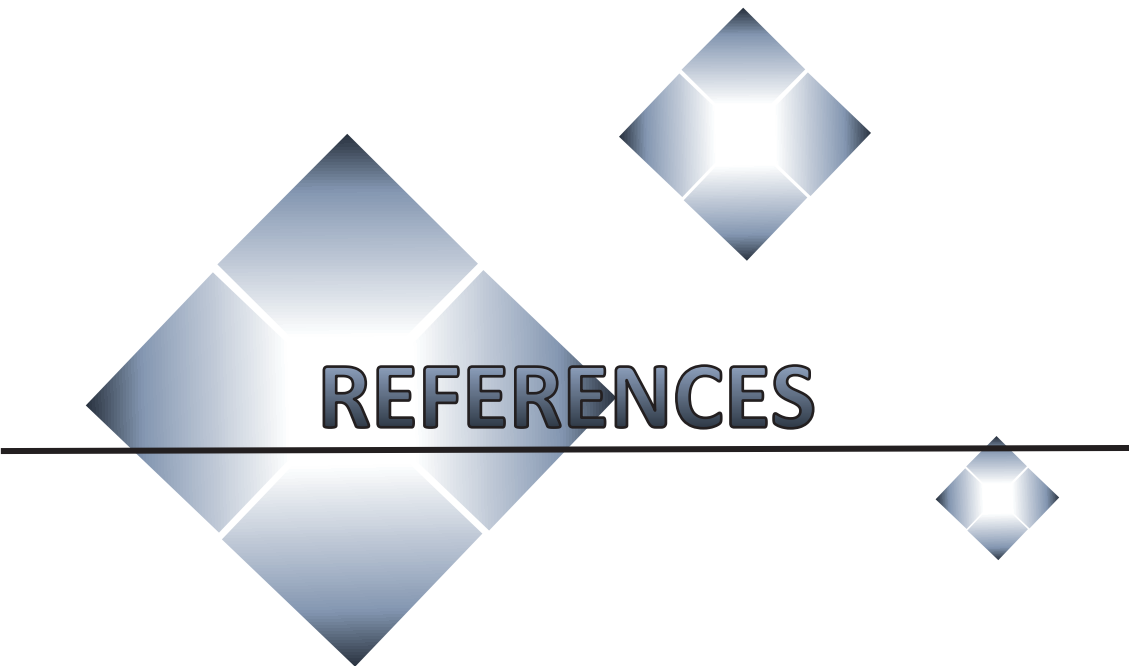
REFERENCES

1. Chokshi, A., Sifri, Z., Cennimo, D. & Horng, H. Global Contributors to Antibiotic Resistance. *J. Glob. Infect. Dis.* **11**, 36–42 (2019).

2. D'Souza, M. J., Li, R. C., Gannon, M. L. & Wentzien, D. E. 1997-2017 Leading Causes of Death Information Due to Diabetes, Neoplasms, and Diseases of the Circulatory System, Issues Cautionary Weight-Related Lesson to the US Population at Large. *IEEE Netw.* **2019**, 1–6 (2019).

3. Jasovský, D., Littmann, J., Zorzet, A. & Cars, O. Antimicrobial resistance-a threat to the world's sustainable development. *Ups. J. Med. Sci.* **121**, 159–164 (2016).

4. Swift, B. M. C. *et al.* Anthropogenic environmental drivers of antimicrobial resistance in wildlife. *Sci. Total Environ.* **649**, 12–20 (2019).

5. Sharma, C. *et al.* Antimicrobial resistance: Its surveillance, impact, and alternative management strategies in dairy animals. *Front. Vet. Sci.* **4**, 1–27 (2018).

6. Ganguly, N. K. *et al.* Rationalizing antibiotic use to limit antibiotic resistance in India. *Indian J. Med. Res.* **134**, 281–294 (2011).

7. Martinez, J. L. & Baquero, F. Mutation frequencies and antibiotic resistance. *Antimicrob. Agents Chemother.* **44**, 1771–1777 (2000).

8. Toprak, E. *et al.* Evolutionary paths to antibiotic resistance under dynamically sustained drug selection. *Nat. Genet.* **44**, 101–105 (2011).

9. Palmer, K. L., Kos, V. N. & Gilmore, M. S. Horizontal gene transfer and the genomics of enterococcal antibiotic resistance. *Curr. Opin. Microbiol.* **13**, 632–639 (2010).

10. Komp Lindgren, P., Karlsson, A. & Hughes, D. Mutation rate and evolution of fluoroquinolone resistance in Escherichia coli isolates from patients with urinary tract infections. *Antimicrob. Agents Chemother.* **47**, 3222–3232 (2003).

11. McManus, M. C. Mechanisms of bacterial resistance to antimicrobial agents. *Am. J. Heal. Pharm. AJHP Off. J. Am. Soc. Heal. Pharm.* **54**, 1420–1426 (1997).

12. Garcia, S. N., Osburn, B. I. & Cullor, J. S. A one health perspective on dairy production and dairy food safety. *One Heal.* **7**, 100086 (2019).

13. Higgins, H. M., Golding, S. E., Mouncey, J., Nanjiani, I. & Cook, A. J. C. Understanding veterinarians' prescribing decisions on antibiotic dry cow therapy. *J. Dairy Sci.* **100**, 2909–2916 (2017).

14. Ventola, C. L. The antibiotic resistance crisis: part 1: causes and threats. *P T* **40**, 277–283 (2015).

15. Mainous, A. G. 3rd, Everett, C. J., Post, R. E., Diaz, V. A. & Hueston, W. J. Availability of antibiotics for purchase without a prescription on the internet. *Ann. Fam. Med.* **7**, 431–435 (2009).

16. Aminov, R. I. A brief history of the antibiotic era: lessons learned and challenges for the future. *Front. Microbiol.* **1**, 134 (2010).

17. Bartlett, J. G., Gilbert, D. N. & Spellberg, B. Seven ways to preserve the miracle of antibiotics. *Clin. Infect. Dis. an Off. Publ. Infect. Dis. Soc. Am.* **56**, 1445–1450 (2013).

18. Gould, I. M. & Bal, A. M. New antibiotic agents in the pipeline and how they can help overcome microbial resistance. *Virulence* **4**, 185–191 (2013).

REFERENCES

19. Kimera, Z. I., Mshana, S. E., Rweyemamu, M. M., Mboera, L. E. G. & Matee, M. I. N. Antimicrobial use and resistance in food-producing animals and the environment: an African perspective. *Antimicrob. Resist. Infect. Control* **9**, 37 (2020).

20. Pokharel, S., Shrestha, P. & Adhikari, B. Antimicrobial use in food animals and human health: time to implement 'One Health' approach. *Antimicrobial resistance and infection control* vol. **9**, 181 (2020).

21. Ma, F., Xu, S., Tang, Z., Li, Z. & Zhang, L. Use of antimicrobials in food animals and impact of transmission of antimicrobial resistance on humans. *Biosaf. Heal.* **3**, 32–38 (2020).

22. European Medicines Agency. Sales of veterinary antimicrobial agents in 31 European countries in 2017: Trends from 2010-2017. *Ninth ESVAC Rep. - EMA/294674/2019* 106 (2019).

23. Laxminarayan, R. *et al.* Antibiotic resistance-the need for global solutions. *Lancet. Infect. Dis.* **13**, 1057–1098 (2013).

24. Smith, T. C. *et al.* Methicillin-resistant Staphylococcus aureus (MRSA) strain ST398 is present in midwestern U.S. swine and swine workers. *PLoS One* **4**, e4258 (2009).

25. Lazarus, B., Paterson, D. L., Mollinger, J. L. & Rogers, B. A. Do human extraintestinal Escherichia coli infections resistant to expanded-spectrum cephalosporins originate from food-producing animals? A systematic review. *Clin. Infect. Dis. an Off. Publ. Infect. Dis. Soc. Am.* **60**, 439–452 (2015).

26. Hummel, R., Tschäpe, H. & Witte, W. Spread of plasmid-mediated nourseothricin resistance due to antibiotic use in animal husbandry. *J. Basic Microbiol.* **26**, 461–466 (1986).

27. Collignon, P. C. *et al.* World Health Organization Ranking of Antimicrobials According to Their Importance in Human Medicine: A Critical Step for Developing Risk Management Strategies to Control Antimicrobial Resistance from Food Animal Production. *Clin. Infect. Dis.* **63**, 1087–1093 (2016).

28. Collignon, P., Powers, J. H., Chiller, T. M., Aidara-Kane, A. & Aarestrup, F. M. World Health Organization ranking of antimicrobials according to their importance in human medicine: A critical step for developing risk management strategies for the use of antimicrobials in food production animals. *Clin. Infect. Dis. an Off. Publ. Infect. Dis. Soc. Am.* **49**, 132–141 (2009).

29. Aarestrup, F. M., Wegener, H. C. & Collignon, P. Resistance in bacteria of the food chain: epidemiology and control strategies. *Expert Rev. Anti. Infect. Ther.* **6**, 733–750 (2008).

30. Cheng, A. C. *et al.* Control of fluoroquinolone resistance through successful regulation, Australia. *Emerg. Infect. Dis.* **18**, 1453–1460 (2012).

31. Dutil, L. *et al.* Ceftiofur resistance in Salmonella enterica serovar Heidelberg from chicken meat and humans, Canada. *Emerg. Infect. Dis.* **16**, 48–54 (2010).

32. Hutjens, M. F. Dairy Farm Management Systems: Dry-Lot Dairy Cow Breeds. *Reference Module in Food Science.* 52–58 (2016).

33. Bradley, A. J. & Green, M. J. The importance of the nonlactating period in the epidemiology of intramammary infection and strategies for prevention. *Vet. Clin. North Am. Food Anim. Pract.* **20**, 547–568 (2004).

34. He, W. *et al.* Prevalence, etiology, and economic impact of clinical mastitis on large dairy

farms in China. *Vet. Microbiol.* **242**, 108570 (2020).

35. Adkins, P. R. F. & Middleton, J. R. Methods for Diagnosing Mastitis. *Vet. Clin. North Am. - Food Anim. Pract.* **34**, 479–491 (2018).

36. Ruegg, P. L. Making Antibiotic Treatment Decisions for Clinical Mastitis. *Vet. Clin. North Am. - Food Anim. Pract.* **34**, 413–425 (2018).

37. Schabauer, A. *et al.* The relationship between clinical signs and microbiological species, spa type, and antimicrobial resistance in bovine mastitis cases in Austria. *Vet. Microbiol.* **227**, 52–60 (2018).

38. Gomes, F. & Henriques, M. Control of Bovine Mastitis: Old and Recent Therapeutic Approaches. *Curr. Microbiol.* **72**, 377–382 (2016).

39. Krömker, V. & Leimbach, S. Mastitis treatment—Reduction in antibiotic usage in dairy cows. *Reprod. Domest. Anim.* **52**, 21–29 (2017).

40. Ganda, E. K. *et al.* Longitudinal metagenomic profiling of bovine milk to assess the impact of intramammary treatment using a third-generation cephalosporin. *Sci. Rep.* **6**, 37565 (2016).

41. Vasquez, A. K., Nydam, D. V., Capel, M. B., Eicker, S. & Virkler, P. D. Clinical outcome comparison of immediate blanket treatment versus a delayed pathogen-based treatment protocol for clinical mastitis in a New York dairy herd. *J. Dairy Sci.* **100**, 2992–3003 (2017).

42. Ashraf, A. & Imran, M. Causes, types, etiological agents, prevalence, diagnosis, treatment, prevention, effects on human health and future aspects of bovine mastitis. *Anim. Heal. Res. Rev.* **21**, 36–49 (2020).

43. Scherpenzeel, C. G. M. *et al.* Effect of different scenarios for selective dry-cow therapy on udder health, antimicrobial usage, and economics. *J. Dairy Sci.* **99**, 3753–3764 (2016).

44. Mishra, R. P. N., Oviedo-Orta, E., Prachi, P., Rappuoli, R. & Bagnoli, F. Vaccines and antibiotic resistance. *Curr. Opin. Microbiol.* **15**, 596–602 (2012).

45. Rappuoli, R., Bloom, D. E. & Black, S. Deploy vaccines to fight superbugs. *Nature* **552**, 165–167 (2017).

46. Jansen, K. U. & Anderson, A. S. The role of vaccines in fighting antimicrobial resistance (AMR). *Hum. Vaccin. Immunother.* **14**, 2142–2149 (2018).

47. L., S. *et al.* Efficacy of a locally prepared bovine mastitis vaccine. *Benha Vet. Med. J.* **30**, 302–311 (2016).

48. Wilson, D. J. & González, R. N. Vaccination strategies for reducing clinical severity of coliform mastitis. *Vet. Clin. North Am. - Food Anim. Pract.* **19**, 187–197 (2003).

49. Landin, H., Mörk, M. J., Larsson, M. & Waller, K. P. Vaccination against Staphylococcus aureus mastitis in two Swedish dairy herds. *Acta Vet. Scand.* **57**, 81 (2015).

50. Freick, M. *et al.* Mastitis vaccination using a commercial polyvalent vaccine or a herd-specific Staphylococcus aureus vaccine. Results of a controlled field trial on a dairy farm. *Tierarztl. Prax. Ausg. G. Grosstiere. Nutztiere.* **44**, 219–229 (2016).

51. Ismail, Z. B. Mastitis vaccines in dairy cows: Recent developments and recommendations of application. *Vet. World* **10**, 1057–1062 (2017).

52. Imperial, I. C. V. J. & Ibana, J. A. Addressing the antibiotic resistance problem with probiotics: Reducing the risk of its double-edged sword effect. *Front. Microbiol.* **7**, 1–10 (2016).

53. Shang, Z., Chan, S. Y., Song, Q., Li, P. & Huang, W. The Strategies of Pathogen-Oriented Therapy on Circumventing Antimicrobial Resistance. *Research* **2020**, 1–32 (2020).

54. Saeidi, N. *et al.* Engineering microbes to sense and eradicate Pseudomonas aeruginosa, a human pathogen. *Mol. Syst. Biol.* **7**, 521 (2011).

55. Cheng, W. N. & Han, S. G. Bovine mastitis: risk factors, therapeutic strategies, and alternative treatments — A review. *Asian-Australasian J. Anim. Sci.* **33**, 1699–1713 (2020).

56. Pellegrino, M., Berardo, N., Giraudo, J., Nader-Macías, M. E. F. & Bogni, C. Bovine mastitis prevention: humoral and cellular response of dairy cows inoculated with lactic acid bacteria at the dry-off period. *Benef. Microbes* **8**, 589–596 (2017).

57. Berardo, N. *et al.* Intramammary inoculation with lactic acid bacteria at dry-off triggers an immunomodulatory response in dairy cows. *Benef. Microbes* **11**, 561–572 (2020).

58. Wallis, J. K., Krömker, V. & Paduch, J.-H. Biofilm Challenge: Lactic Acid Bacteria Isolated from Bovine Udders versus Staphylococci. *Foods* **8**, 79 (2019).

59. Mater, D. D. G., Langella, P., Corthier, G. & Flores, M.-J. A probiotic Lactobacillus strain can acquire vancomycin resistance during digestive transit in mice. *J. Mol. Microbiol. Biotechnol.* **14**, 123–127 (2008).

60. Liu, C., Zhang, Z-Y., Dong, K., Yuan, J-P. & Guo, X-K. Antibiotic Resistance of Probiotic Strains of Lactic Acid Bacteria Isolated from Marketed Foods and Drugs. *Biomed. Environ. Sci.* **22**, 401–412 (2009).

61. AlSheikh, H. M. Al *et al.* Plant-Based Phytochemicals as Possible Alternative to Antibiotics in Combating Bacterial Drug Resistance. *Antibiot.* **9**, 480 (2020).

62. Montironi, I. D., Cariddi, L. N. & Reinoso, E. B. Evaluation of the antimicrobial efficacy of Minthostachys verticillata essential oil and limonene against Streptococcus uberis strains isolated from bovine mastitis. *Rev. Argent. Microbiol.* **48**, 210–216 (2016).

63. Santana, H. F., Barbosa, A. A. T., Ferreira, S. O. & Mantovani, H. C. Bactericidal activity of ethanolic extracts of propolis against Staphylococcus aureus isolated from mastitic cows. *World J. Microbiol. Biotechnol.* **28**, 485–491 (2012).

64. Kher, M. N., Sheth, N. R. & Bhatt, V. D. In Vitro Antibacterial Evaluation of Terminalia chebula as an Alternative of Antibiotics against Bovine Subclinical Mastitis. *Anim. Biotechnol.* **30**, 151–158 (2019).

65. Federman, C., Joo, J., Almario, J. A., Salaheen, S. & Biswas, D. Citrus-derived oil inhibits Staphylococcus aureus growth and alters its interactions with bovine mammary cells. *J. Dairy Sci.* **99**, 3667–3674 (2016).

66. Zhu, H., Du, M., Fox, L. & Zhu, M. J. Bactericidal effects of Cinnamon cassia oil against bovine mastitis bacterial pathogens. *Food Control* **66**, 291–299 (2016).

67. Abboud, M., R, E. R., Jammal, B. & Sleiman, M. In Vitro and In Vivo Antimicrobial Activity of two Essential Oils Thymus Vulgaris and Lavandula Angustifolia against Bovine Staphylococcus and Streptococcus Mastitis Pathogen. *Middle East J. Agric. Res.* **04**, 975–983 (2015).

68. Abedon, S. T., Kuhl, S. J., Blasdel, B. G. & Kutter, E. M. Phage treatment of human infections. *Bacteriophage* **1**, 66–85 (2011).

69. Gravitz, L. Turning a new phage. *Nat. Med.* **18**, 1318–1320 (2012).

70. Wienhold, S.-M., Lienau, J. & Witzenrath, M. Towards Inhaled Phage Therapy in Western Europe. *Viruses* **11**, 295 (2019).

71. Hamza, A., Perveen, S., Abbas, Z. & Ur Rehman, S. The Lytic SA Phage Demonstrate Bactericidal Activity against Mastitis Causing Staphylococcus aureus. *Open Life Sci.* **11**, 39–45 (2016).

72. Iwano, H. *et al.* Bacteriophage ΦSA012 Has a Broad Host Range against Staphylococcus aureus and Effective Lytic Capacity in a Mouse Mastitis Model. *Biology (Basel).* **7**, 8 (2018).

73. da Silva Duarte, V. *et al.* Genomic analysis and immune response in a murine mastitis model of vB_EcoM-UFV13, a potential biocontrol agent for use in dairy cows. *Sci. Rep.* **8**, 6845 (2018).

74. Labrie, S. J., Samson, J. E. & Moineau, S. Bacteriophage resistance mechanisms. *Nat. Rev. Microbiol.* **8**, 317–327 (2010).

75. Gomes, F. & Henriques, M. Control of Bovine Mastitis: Old and Recent Therapeutic Approaches. *Curr. Microbiol.* **72**, 377–382 (2016).

76. O'Flaherty, S., Coffey, A., Meaney, W. J., Fitzgerald, G. F. & Ross, R. P. Inhibition of bacteriophage K proliferation on Staphylococcus aureus in raw bovine milk. *Lett. Appl. Microbiol.* **41**, 274–279 (2005).

77. McLean, S. K., Dunn, L. A. & Palombo, E. A. Phage inhibition of Escherichia coli in ultrahigh-temperature-treated and raw milk. *Foodborne Pathog. Dis.* **10**, 956–962 (2013).

78. Porter, J., Anderson, J., Carter, L., Donjacour, E. & Paros, M. In vitro evaluation of a novel bacteriophage cocktail as a preventative for bovine coliform mastitis. *J. Dairy Sci.* **99**, 2053–2062 (2016).

79. Tiwari, R. *et al.* Wonder world of phages: potential biocontrol agents safeguarding biosphere and health of animals and humans- current scenario and perspectives. *Pakistan J. Biol. Sci. PJBS* **17**, 316–328 (2014).

80. Schmelcher, M., Donovan, D. M. & Loessner, M. J. Bacteriophage endolysins as novel antimicrobials. *Future Microbiol.* **7**, 1147–1171 (2012).

81. Rios, A. C. *et al.* Alternatives to overcoming bacterial resistances: State-of-the-art. *Microbiol. Res.* **191**, 51–80 (2016).

82. Wu, H., Lu, H., Huang, J., Li, G. & Huang, Q. EnzyBase: a novel database for enzybiotic studies. *BMC Microbiol.* **12**, 54 (2012).

83. Ghose, C. & Euler, C. W. Gram-negative bacterial lysins. *Antibiotics* **9**, 1–13 (2020).

84. Briers, Y., Walmagh, M. & Lavigne, R. Use of bacteriophage endolysin EL188 and outer membrane permeabilizers against Pseudomonas aeruginosa. *J. Appl. Microbiol.* **110**, 778–785 (2011).

85. Yan, G. *et al.* External lysis of Escherichia coli by a bacteriophage endolysin modified with hydrophobic amino acids. *AMB Express* **9**, 106 (2019).

86. Vander Elst, N. *et al.* Characterization of the Bacteriophage-Derived Endolysins PlySs2 and PlySs9 with In Vitro Lytic Activity against Bovine Mastitis Streptococcus uberis. *Antibiot. (Basel, Switzerland)* **9**, 621 (2020).

87. Gutiérrez, D. *et al.* Phage Lytic Protein LysRODI Prevents Staphylococcal Mastitis in Mice. *Front. Microbiol.* **11**, 7 (2020).

88. Pachón-Ibáñez, M. E., Smani, Y., Pachón, J. & Sánchez-Céspedes, J. Perspectives for clinical use of engineered human host defense antimicrobial peptides. *FEMS Microbiol. Rev.* **41**, 323–342 (2017).

89. Wang, S., Zeng, X., Yang, Q. & Qiao, S. Antimicrobial Peptides as Potential Alternatives to Antibiotics in Food Animal Industry. *Int. J. Mol. Sci.* **17**, 603 (2016).

90. Kumar, P., Kizhakkedathu, J. N. & Straus, S. K. Antimicrobial peptides: Diversity, mechanism of action and strategies to improve the activity and biocompatibility in vivo. *Biomolecules* **8**, 4 (2018).

91. Le, C.-F., Fang, C.-M. & Sekaran, S. D. Intracellular Targeting Mechanisms by Antimicrobial Peptides. *Antimicrob. Agents Chemother.* **61**, e02340-16 (2017).

92. Zhang, L.-J. & Gallo, R. L. Antimicrobial peptides. *Curr. Biol.* **26**, R14-9 (2016).

93. Ibrahim, O. O. Classification of Antimicrobial Peptides Bacteriocins, and the Nature of Some Bacteriocins with Potential Applications in Food Safety and Bio-Pharmaceuticals. *EC Microbiology* **7**, 591–608 (2019).

94. Cascales, E. *et al.* Colicin biology. *Microbiol. Mol. Biol. Rev.* **71**, 158–229 (2007).

95. Duquesne, S., Petit, V., Peduzzi, J. & Rebuffat, S. Structural and functional diversity of microcins, gene-encoded antibacterial peptides from enterobacteria. *J. Mol. Microbiol. Biotechnol.* **13**, 200–209 (2007).

96. Alvarez-Sieiro, P., Montalbán-López, M., Mu, D. & Kuipers, O. P. Bacteriocins of lactic acid bacteria: extending the family. *Appl. Microbiol. Biotechnol.* **100**, 2939–2951 (2016).

97. Angelopoulou, A., Warda, A. K., Hill, C. & Ross, R. P. Non-antibiotic microbial solutions for bovine mastitis–live biotherapeutics, bacteriophage, and phage lysins. *Crit. Rev. Microbiol.* **45**, 564–580 (2019).

98. Wu, J., Hu, S. & Cao, L. Therapeutic effect of nisin Z on subclinical mastitis in lactating cows. *Antimicrob. Agents Chemother.* **51**, 3131–3135 (2007).

99. Gong, Z. *et al.* Identification and Rational Design of a Novel Antibacterial Peptide Dermaseptin-AC from the Skin Secretion of the Red-Eyed Tree Frog Agalychnis callidryas. *Antibiotics* **9**, 243 (2020).

100. Liu, Y. *et al.* Structure–activity relationship of an antimicrobial peptide, phylloseptin-PHa: Balance of hydrophobicity and charge determines the selectivity of bioactivities. *Drug Des. Devel. Ther.* **13**, 447–458 (2019).

101. Xu, L. *et al.* Conversion of Broad-Spectrum Antimicrobial Peptides into Species-Specific Antimicrobials Capable of Precisely Targeting Pathogenic Bacteria. *Sci. Rep.* **10**, 1–9 (2020).

102. Li, J. *et al.* Targeted and Intracellular Antibacterial Activity against S. agalactiae of the Chimeric Peptides Based on Pheromone and Cell-Penetrating Peptides. *ACS Appl. Mater. Interfaces* **12**, 44459–44474 (2020).

103. Rozek, A., Powers, J. P. S., Friedrich, C. L. & Hancock, R. E. W. Structure-Based Design of an Indolicidin Peptide Analogue with Increased Protease Stability. *Biochemistry* **42**, 14130–14138 (2003).

104. Oliva, R. *et al.* Exploring the role of unnatural amino acids in antimicrobial peptides. *Sci. Rep.* **8**, 1–16 (2018).

105. Zhao, Y. *et al.* Antimicrobial activity and stability of the d-amino acid substituted derivatives of antimicrobial peptide polybia-MPI. *AMB Express* **6**, 122 (2016).

106. Di, Y. P. *et al.* Enhanced therapeutic index of an antimicrobial peptide in mice by increasing safety and activity against multidrug-resistant bacteria. *Sci. Adv.* **6**, eaay6817 (2020).

107. Chou, H. *et al.* Design and synthesis of cationic antimicrobial peptides with improved activity and selectivity against Vibrio spp . **32**, 130–138 (2008).

108. Chen, Y.-L. S. *et al.* Novel cationic antimicrobial peptide GW-H1 induced caspase-dependent apoptosis of hepatocellular carcinoma cell lines. *Peptides* **36**, 257–265 (2012).

109. Pan, W.-R., Chen, Y.-L. S., Hsu, H.-C. & Chen, W.-J. Antimicrobial peptide GW-H1-induced apoptosis of human gastric cancer AGS cell line is enhanced by suppression of autophagy. *Mol. Cell. Biochem.* **400**, 77–86 (2015).

110. Serna, N. *et al.* Recruiting potent membrane penetrability in tumor cell-targeted protein-only nanoparticles. *Nanotechnology* **30**, 115101 (2019).

111. Serna, N. *et al.* Protein-only, antimicrobial peptide-containing recombinant nanoparticles with inherent built-in antibacterial activity. *Acta Biomater.* **60**, 256–263 (2017).

112. Netea, M. G., Kullberg, B.-J. & Van der Meer, J. W. M. Proinflammatory cytokines in the treatment of bacterial and fungal infections. *BioDrugs* **18**, 9–22 (2004).

113. Dalton, D. K. *et al.* Multiple defects of immune cell function in mice with disrupted interferon-gamma genes. *Science* **259**, 1739–1742 (1993).

114. Huang, S. *et al.* Immune response in mice that lack the interferon-gamma receptor. *Science* **259**, 1742–1745 (1993).

115. Buchmeier, N. A. & Schreiber, R. D. Requirement of endogenous interferon-gamma production for resolution of Listeria monocytogenes infection. *Proc. Natl. Acad. Sci. U. S. A.* **82**, 7404–7408 (1985).

116. Kamijo, R. *et al.* Mice that lack the interferon-gamma receptor have profoundly altered responses to infection with Bacillus Calmette-Guérin and subsequent challenge with lipopolysaccharide. *J. Exp. Med.* **178**, 1435–1440 (1993).

117. Kullberg, B. J., van 't Wout, J. W., Hoogstraten, C. & van Furth, R. Recombinant interferon-gamma enhances resistance to acute disseminated Candida albicans infection in mice. *J. Infect. Dis.* **168**, 436–443 (1993).

118. Coelho, C. & Casadevall, A. Cryptococcal therapies and drug targets: the old, the new and the promising. *Cell. Microbiol.* **18**, 792–799 (2016).

119. Seger, R. A. Modern management of chronic granulomatous disease. *Br. J. Haematol.* **140**, 255–266 (2008).

120. Hashemi, H. *et al.* Hyperimmunoglobulin E syndrome: Genetics, immunopathogenesis,

clinical findings, and treatment modalities. *J. Res. Med. Sci. Off. J. Isfahan Univ. Med. Sci.* **22**, 53 (2017).

121. Brodzki, P., Kostro, K., Krakowski, L. & Marczuk, J. Inflammatory cytokine and acute phase protein concentrations in the peripheral blood and uterine washings of cows with subclinical endometritis in the late postpartum period. *Vet. Res. Commun.* **39**, 143–149 (2015).

122. Sordillo, L. M. Mammary Gland Immunobiology and Resistance to Mastitis. *Vet. Clin. North Am. - Food Anim. Pract.* **34**, 507–523 (2018).

123. Daley, M. *et al.* Prevention and treatment of Staphylococcus aureus infections with recombinant cytokines. *Cytokine* **5**, 276–284 (1993).

124. Sordillo, L. M. & Babiuk, L. A. Controlling acute Escherichia coli mastitis during the periparturient period with recombinant bovine interferon gamma. *Vet. Microbiol.* **28**, 189–198 (1991).

125. Molineux, G. Pegylation: engineering improved biopharmaceuticals for oncology. *Pharmacotherapy* **23**, 3S-8S (2003).

126. Canning, P. *et al.* Efficacy and clinical safety of pegbovigrastim for preventing naturally occurring clinical mastitis in periparturient primiparous and multiparous cows on US commercial dairies. *J. Dairy Sci.* **100**, 6504–6515 (2017).

127. Wang, M., Zhang, Y. & Zhu, J. Anti-Staphylococcus aureus single-chain variable region fragments provide protection against mastitis in mice. *Appl. Microbiol. Biotechnol.* **100**, 2153–2162 (2016).

128. Wang, M., Wang, T., Guan, Y., Wang, F. & Zhu, J. The preparation and therapeutic roles of scFv-Fc antibody against Staphylococcus aureus infection to control bovine mastitis. *Appl. Microbiol. Biotechnol.* **103**, 1703–1712 (2019).

129. Machado, V. S. *et al.* Effect of an injectable trace mineral supplement containing selenium, copper, zinc, and manganese on the health and production of lactating Holstein cows. *Vet. J.* **197**, 451–456 (2013).

130. Kang, S. J., Cho, Y. Il, Kim, K. H. & Cho, E. S. Proteomic Analysis to Elucidate the Antibacterial Action of Silver Ions Against Bovine Mastitis Pathogens. *Biol. Trace Elem. Res.* **171**, 101–106 (2016).

131. Reyes-Jara, A., Cordero, N., Aguirre, J., Troncoso, M. & Figueroa, G. Antibacterial Effect of Copper on Microorganisms Isolated from Bovine Mastitis. *Front. Microbiol.* **7**, 626 (2016).

132. Moreira, L. H. *et al.* Use of photodynamic therapy in the treatment of bovine subclinical mastitis. *Photodiagnosis Photodyn. Ther.* **21**, 246–251 (2018).

133. Felipe, V. *et al.* Chitosan disrupts biofilm formation and promotes biofilm eradication in Staphylococcus species isolated from bovine mastitis. *Int. J. Biol. Macromol.* **126**, 60–67 (2019).

134. Lanctôt, S. *et al.* Effect of intramammary infusion of chitosan hydrogels at drying-off on bovine mammary gland involution. *J. Dairy Sci.* **100**, 2269–2281 (2017).

135. Overton, T. W. Recombinant protein production in bacterial hosts. *Drug Discov. Today* **19**, 590–601 (2014).

136. Chen, R. Bacterial expression systems for recombinant protein production: E. coli and beyond. *Biotechnol. Adv.* **30**, 1102–1107 (2012).

137. Andersson, L. *et al.* Large-scale synthesis of peptides. *Biopolymers* **55**, 227–250 (2000).

138. Nilsson, B. L., Soellner, M. B. & Raines, R. T. Chemical synthesis of proteins. *Annu. Rev. Biophys. Biomol. Struct.* **34**, 91–118 (2005).

139. Ongey, E. L. & Neubauer, P. Lanthipeptides: chemical synthesis versus in vivo biosynthesis as tools for pharmaceutical production. *Microb. Cell Fact.* **15**, 97 (2016).

140. Li, Y. Recombinant production of antimicrobial peptides in Escherichia coli: A review. *Protein Expr. Purif.* **80**, 260–267 (2011).

141. Ingham, A. B. & Moore, R. J. Recombinant production of antimicrobial peptides in heterologous microbial systems. *Biotechnol. Appl. Biochem.* **47**, 1–9 (2007).

142. Cao, J. *et al.* Yeast-Based Synthetic Biology Platform for Antimicrobial Peptide Production. *ACS Synth. Biol.* **7**, 896–902 (2018).

143. Khalilzadeh, R. *et al.* Process development for production of recombinant human interferon-gamma expressed in Escherichia coli. *J. Ind. Microbiol. Biotechnol.* **31**, 63–69 (2004).

144. Khalilzadeh, R. *et al.* Process development for production of human granulocyte-colony stimulating factor by high cell density cultivation of recombinant Escherichia coli. *J. Ind. Microbiol. Biotechnol.* **35**, 1643–1650 (2008).

145. Razaghi, A., Owens, L. & Heimann, K. Review of the recombinant human interferon gamma as an immunotherapeutic: Impacts of production platforms and glycosylation. *J. Biotechnol.* **240**, 48–60 (2016).

146. Nausch, H. *et al.* Recombinant production of human interleukin 6 in Escherichia coli. *PLoS One* **8**, e54933 (2013).

147. Demain, A. L. & Vaishnav, P. Production of recombinant proteins by microbes and higher organisms. *Biotechnol. Adv.* **27**, 297–306 (2009).

148. Sanchez-Garcia, L. *et al.* Recombinant pharmaceuticals from microbial cells: A 2015 update. *Microb. Cell Fact.* **15**, 1–7 (2016).

149. Rosano, G. L. & Ceccarelli, E. A. Recombinant protein expression in Escherichia coli: Advances and challenges. *Front. Microbiol.* **5**, 1–17 (2014).

150. Rosano, G. L., Morales, E. S. & Ceccarelli, E. A. New tools for recombinant protein production in Escherichia coli: A 5-year update. *Protein Sci.* **28**, 1412–1422 (2019).

151. Blattner, F. R. *et al.* The complete genome sequence of Escherichia coli K-12. *Science* **277**, 1453–1462 (1997).

152. Sezonov, G., Joseleau-Petit, D. & D'Ari, R. Escherichia coli physiology in Luria-Bertani broth. *J. Bacteriol.* **189**, 8746–8749 (2007).

153. Shiloach, J. & Fass, R. Growing E. coli to high cell density--a historical perspective on method development. *Biotechnol. Adv.* **23**, 345–357 (2005).

154. Li, J., Jaitzig, J., Lu, P., Süssmuth, R. D. & Neubauer, P. Scale-up bioprocess development for production of the antibiotic valinomycin in Escherichia coli based on consistent fed-batch cultivations. *Microb. Cell Fact.* **14**, 83 (2015).

155. Kesik-Brodacka, M. Progress in biopharmaceutical development. *Biotechnol. Appl. Biochem.* **65**, 306–322 (2018).

156. Hayat, S. M. G., Farahani, N., Golichenari, B. & Sahebkar, A. H. Recombinant Protein Expression in Escherichia coli (E.coli): What We Need to Know. *Curr. Pharm. Des.* **24**, (2018).

157. Orrapin, S. & Intorasoot, S. Recombinant expression of novel protegrin-1 dimer and LL-37-linker-histatin-5 hybrid peptide mediated biotin carboxyl carrier protein fusion partner. *Protein Expr. Purif.* **93**, 46–53 (2014).

158. Aleinein, R. A., Hamoud, R., Schäfer, H. & Wink, M. Molecular cloning and expression of ranalexin, a bioactive antimicrobial peptide from Rana catesbeiana in Escherichia coli and assessments of its biological activities. *Appl. Microbiol. Biotechnol.* **97**, 3535–3543 (2013).

159. Xia, L., Zhang, F., Liu, Z., Ma, J. & Yang, J. Expression and characterization of cecropinXJ, a bioactive antimicrobial peptide from Bombyx mori (Bombycidae, Lepidoptera) in Escherichia coli. *Exp. Ther. Med.* **5**, 1745–1751 (2013).

160. Luan, C. *et al.* Recombinant expression of antimicrobial peptides using a novel self-cleaving aggregation tag in Escherichia coli. *Can. J. Microbiol.* **60**, 113–120 (2014).

161. Babaeipour, V., Khanchezar, S., Mofid, M. R. & Pesaran Hagi Abbas, M. Efficient process development of recombinant human granulocyte colony-stimulating factor (rh-GCSF) production in Escherichia coli. *Iran. Biomed. J.* **19**, 102–110 (2015).

162. Babaeipour, V., Shojaosadati, S. A. & Maghsoudi, N. Maximizing Production of Human Interferon-γ in HCDC of Recombinant E. coli. *Iran. J. Pharm. Res. IJPR* **12**, 563–572 (2013).

163. Mamat, U. *et al.* Endotoxin-free protein production—ClearColi™ technology. *Nat. Methods* **10**, 916–916 (2013).

164. García-Fruitós, E. Lactic acid bacteria: A promising alternative for recombinant protein production. *Microb. Cell Fact.* **11**, 22–24 (2012).

165. Maeshima, N. & Fernandez, R. C. Recognition of lipid A variants by the TLR4-MD-2 receptor complex. *Front. Cell. Infect. Microbiol.* **3**, 3 (2013).

166. Morello, E. *et al.* Lactococcus lactis, an efficient cell factory for recombinant protein production and secretion. *J. Mol. Microbiol. Biotechnol.* **14**, 48–58 (2007).

167. Jørgensen, C. M., Vrang, A. & Madsen, S. M. Recombinant protein expression in Lactococcus lactis using the P170 expression system. *FEMS Microbiol. Lett.* **351**, 170–178 (2014).

168. Peng, C. *et al.* Factors influencing recombinant protein secretion efficiency in gram-positive bacteria: Signal peptide and beyond. *Front. Bioeng. Biotechnol.* **7**, 1–9 (2019).

169. Freudl, R. Signal peptides for recombinant protein secretion in bacterial expression systems. *Microb. Cell Fact.* **17**, 52 (2018).

170. Anné, J., Economou, A. & Bernaerts, K. Protein Secretion in Gram-Positive Bacteria: From Multiple Pathways to Biotechnology. *Curr. Top. Microbiol. Immunol.* **404**, 267–308 (2017).

171. Lee, M. J. & Kim, P. Recombinant Protein Expression System in Corynebacterium glutamicum and Its Application. *Front. Microbiol.* **9**, 2523 (2018).

172. Sun, M. *et al.* Enhanced production of recombinant proteins in Corynebacterium glutamicum by constructing a bicistronic gene expression system. *Microb. Cell Fact.* **19**, 113 (2020).

173. Song, A. A. L., In, L. L. A., Lim, S. H. E. & Rahim, R. A. A review on Lactococcus lactis: From food to factory. *Microb. Cell Fact.* **16**, 1–15 (2017).

174. Sriraman, K. & Jayaraman, G. HtrA is essential for efficient secretion of recombinant proteins by Lactococcus lactis. *Appl. Environ. Microbiol.* **74**, 7442–7446 (2008).

175. Poquet, I. *et al.* HtrA is the unique surface housekeeping protease in Lactococcus lactis and is required for natural protein processing. *Mol. Microbiol.* **35**, 1042–1051 (2000).

176. Kuipers, O. P., Beerthuyzen, M. M., de Ruyter, P. G., Luesink, E. J. & de Vos, W. M. Autoregulation of nisin biosynthesis in Lactococcus lactis by signal transduction. *J. Biol. Chem.* **270**, 27299–27304 (1995).

177. MoBiTec. NICE. Expression System for Lactococcus lactis. 34 (2015).

178. Mierau, I. & Kleerebezem, M. 10 years of the nisin-controlled gene expression system (NICE) in Lactococcus lactis. *Appl. Microbiol. Biotechnol.* **68**, 705–717 (2005).

179. Xu, C. *et al.* Biosynthesis of Polysaccharides-Capped Selenium Nanoparticles Using Lactococcus lactis NZ9000 and Their Antioxidant and Anti-inflammatory Activities. *Front. Microbiol.* **10**, 1632 (2019).

180. Bermúdez-Humarán, L. G. *et al.* Intranasal immunization with recombinant Lactococcus lactis secreting murine interleukin-12 enhances antigen-specific Th1 cytokine production. *Infect. Immun.* **71**, 1887–1896 (2003).

181. Bermúdez-Humarán, L. G. *et al.* Serine protease inhibitors protect better than IL-10 and TGF-β anti-inflammatory cytokines against mouse colitis when delivered by recombinant lactococci. *Microb. Cell Fact.* **14**, 26 (2015).

182. Liu, S., Li, Y., Deng, B. & Xu, Z. Recombinant Lactococcus lactis expressing porcine insulin-like growth factor I ameliorates DSS-induced colitis in mice. *BMC Biotechnol.* **16**, 25 (2016).

183. Mus-Veteau, I. Membrane proteins production for structural analysis. *Membr. Proteins Prod. Struct. Anal.* 1–425 (2014).

184. Gifre-Renom, L. *et al.* A new approach to obtain pure and active proteins from Lactococcus lactis protein aggregates. *Sci. Rep.* **8**, 13917 (2018).

185. Villatoro-Hernandez, J. *et al.* Secretion of biologically active interferon-gamma inducible protein-10 (IP-10) by Lactococcus lactis. *Microb. Cell Fact.* **7**, 22 (2008).

186. Feizollahzadeh, S. *et al.* Expression of biologically active murine interleukin-18 in Lactococcus lactis. *FEMS Microbiol. Lett.* **363**, fnw234 (2016).

187. Cortes-Perez, N. G., da Costa Medina, L. F., Lefèvre, F., Langella, P. & Bermúdez-Humarán, L. G. Production of biologically active CXC chemokines by Lactococcus lactis: evaluation of its potential as a novel mucosal vaccine adjuvant. *Vaccine* **26**, 5778–5783 (2008).

188. Bermúdez-Humarán, L. G., Cortes-Perez, N. G., L'Haridon, R. & Langella, P. Production of biological active murine IFN-γ by recombinant Lactococcus lactis. *FEMS Microbiol. Lett.* **280**, 144–149 (2008).

189. Volzing, K., Borrero, J., Sadowsky, M. J. & Kaznessis, Y. N. Antimicrobial peptides targeting

Gram-negative pathogens, produced and delivered by lactic acid bacteria. *ACS Synth. Biol.* **2**, 643–650 (2013).

190. Tanhaeian, A., Mirzaii, M., Pirkhezranian, Z. & Sekhavati, M. H. Generation of an engineered food-grade Lactococcus lactis strain for production of an antimicrobial peptide: in vitro and in silico evaluation. *BMC Biotechnol.* **20**, 19 (2020).

191. Tanhaieian, A., Sekhavati, M. H., Ahmadi, F. S. & Mamarabadi, M. Heterologous expression of a broad-spectrum chimeric antimicrobial peptide in Lactococcus lactis: Its safety and molecular modeling evaluation. *Microb. Pathog.* **125**, 51–59 (2018).

192. Choi, J. H. & Lee, S. Y. Secretory and extracellular production of recombinant proteins using Escherichia coli. *Appl. Microbiol. Biotechnol.* **64**, 625–635 (2004).

193. Horga, L. G. *et al.* Tuning recombinant protein expression to match secretion capacity. *Microb. Cell Fact.* **17**, 199 (2018).

194. Derouazi, M. *et al.* High-yield production of secreted active proteins by the Pseudomonas aeruginosa type III secretion system. *Appl. Environ. Microbiol.* **74**, 3601–3604 (2008).

195. Gustafsson, C., Govindarajan, S. & Minshull, J. Codon bias and heterologous protein expression. *Trends Biotechnol.* **22**, 346–353 (2004).

196. Burgess-Brown, N. A. *et al.* Codon optimization can improve expression of human genes in Escherichia coli: A multi-gene study. *Protein Expr. Purif.* **59**, 94–102 (2008).

197. Komar, A. A. Unraveling co-translational protein folding: Concepts and methods. *Methods* **137**, 71–81 (2018).

198. Liu, Y. A code within the genetic code: codon usage regulates co-translational protein folding. *Cell Commun. Signal.* **18**, 145 (2020).

199. Yu, C.-H. *et al.* Codon Usage Influences the Local Rate of Translation Elongation to Regulate Co-translational Protein Folding. *Mol. Cell* **59**, 744–754 (2015).

200. Cortazzo, P. *et al.* Silent mutations affect in vivo protein folding in Escherichia coli. *Biochem. Biophys. Res. Commun.* **293**, 537–541 (2002).

201. Anfinsen, C. B. & Scheraga, H. A. Experimental and theoretical aspects of protein folding. *Adv. Protein Chem.* **29**, 205–300 (1975).

202. Adamcik, J. & Mezzenga, R. Amyloid Polymorphism in the Protein Folding and Aggregation Energy Landscape. *Angew. Chem. Int. Ed. Engl.* **57**, 8370–8382 (2018).

203. Schramm, F. D., Schroeder, K. & Jonas, K. Protein aggregation in bacteria. *FEMS Microbiol. Rev.* **44**, 54–72 (2019).

204. Mogk, A., Bukau, B. & Kampinga, H. H. Cellular Handling of Protein Aggregates by Disaggregation Machines. *Mol. Cell* **69**, 214–226 (2018).

205. Carrió, M. M. & Villaverde, A. Protein aggregation as bacterial inclusion bodies is reversible. *FEBS Lett.* **489**, 29–33 (2001).

206. Kolaj, O., Spada, S., Robin, S. & Wall, J. G. Use of folding modulators to improve heterologous protein production in Escherichia coli. *Microb. Cell Fact.* **8**, 9 (2009).

207. de Marco, A., Deuerling, E., Mogk, A., Tomoyasu, T. & Bukau, B. Chaperone-based procedure to increase yields of soluble recombinant proteins produced in E. coli. *BMC Biotechnol.* **7**, 32 (2007).

208. Martínez-Alonso, M., García-Fruitós, E., Ferrer-Miralles, N., Rinas, U. & Villaverde, A. Side effects of chaperone gene co-expression in recombinant protein production. *Microb. Cell Fact.* **9**, 64 (2010).

209. Vera, A., González-Montalbán, N., Arís, A. & Villaverde, A. The conformational quality of insoluble recombinant proteins is enhanced at low growth temperatures. *Biotechnol. Bioeng.* **96**, 1101–1106 (2007).

210. Schellman, J. A. Temperature, stability, and the hydrophobic interaction. *Biophys. J.* **73**, 2960–2964 (1997).

211. Li, Y. Self-cleaving fusion tags for recombinant protein production. *Biotechnol. Lett.* **33**, 869–881 (2011).

212. Kuo, W.-H. K. & Chase, H. A. Exploiting the interactions between poly-histidine fusion tags and immobilized metal ions. *Biotechnol. Lett.* **33**, 1075–1084 (2011).

213. Santalices, I., Gonella, A., Torres, D. & Alonso, M. J. Advances on the formulation of proteins using nanotechnologies. *J. Drug Deliv. Sci. Technol.* **42**, 155–180 (2017).

214. Verma, D., Gulati, N., Kaul, S., Mukherjee, S. & Nagaich, U. Protein Based Nanostructures for Drug Delivery. *J. Pharm.* **2018**, 1–18 (2018).

215. Gou, Y. *et al.* Bio-Inspired Protein-Based Nanoformulations for Cancer Theranostics. *Front. Pharmacol.* **9**, 421 (2018).

216. McManus, J. J., Charbonneau, P., Zaccarelli, E. & Asherie, N. The physics of protein self-assembly. *Curr. Opin. Colloid Interface Sci.* **22**, 73–79 (2016).

217. Hagan, M. F. Modeling Viral Capsid Assembly. *Adv. Chem. Phys.* **155**, 1–68 (2014).

218. Stella, S., Falconi, M., Lammi, M., Gualerzi, C. O. & Pon, C. L. Environmental Control of the In vivo Oligomerization of Nucleoid Protein H-NS. *J. Mol. Biol.* **355**, 169–174 (2006).

219. Eaton, W. A. & Hofrichter, J. Sickle Cell Hemoglobin Polymerization. *Adv. Protein Chem.* **40**, 63–279 (1990).

220. Knowles, T. P. J., Vendruscolo, M. & Dobson, C. M. The amyloid state and its association with protein misfolding diseases. *Nat. Rev. Mol. Cell Biol.* **15**, 384–396 (2014).

221. Kushnir, N., Streatfield, S. J. & Yusibov, V. Virus-like particles as a highly efficient vaccine platform: diversity of targets and production systems and advances in clinical development. *Vaccine* **31**, 58–83 (2012).

222. Rohovie, M. J., Nagasawa, M. & Swartz, J. R. Virus-like particles: Next-generation nanoparticles for targeted therapeutic delivery. *Bioeng. Transl. Med.* **2**, 43–57 (2017).

223. Unzueta, U. *et al.* Sheltering DNA in self-organizing, protein-only nano-shells as artificial viruses for gene delivery. *Nanomedicine* **10**, 535–541 (2014).

224. Unzueta, U. *et al.* Non-amyloidogenic peptide tags for the regulatable self-assembling of protein-only nanoparticles. *Biomaterials* **33**, 8714–8722 (2012).

225. Unzueta, U. *et al.* Intracellular CXCR4$^+$ cell targeting with T22-empowered protein-only nanoparticles. *Int. J. Nanomedicine* **7**, 4533–4544 (2012).

226. Céspedes, M. V. *et al.* In vivo architectonic stability of fully de novo designed protein-only nanoparticles. *ACS Nano* **8**, 4166–4176 (2014).

227. López-Laguna, H. *et al.* Assembly of histidine-rich protein materials controlled through divalent cations. *Acta Biomater.* **83**, 257–264 (2019).

228. Sánchez-García, L. *et al.* Self-assembling toxin-based nanoparticles as self-delivered antitumoral drugs. *J. Control. Release* **274**, 81–92 (2018).

229. Williams, D. C., Van Frank, R. M., Muth, W. L. & Burnett, J. P. Cytoplasmic inclusion bodies in Escherichia coli producing biosynthetic human insulin proteins. *Science* **215**, 687–689 (1982).

230. Chrunyk, B. A., Evans, J., Lillquist, J., Young, P. & Wetzel, R. Inclusion body formation and protein stability in sequence variants of interleukin-1 beta. *J. Biol. Chem.* **268**, 18053–18061 (1993).

231. Jürgen, B. *et al.* Quality control of inclusion bodies in Escherichia coli. *Microb. Cell Fact.* **9**, 41 (2010).

232. Carrió, M. M., Cubarsi, R. & Villaverde, A. Fine architecture of bacterial inclusion bodies. *FEBS Lett.* **471**, 7–11 (2000).

233. Gupta, A., Lloyd-Price, J., Neeli-Venkata, R., Oliveira, S. M. D. & Ribeiro, A. S. In vivo kinetics of segregation and polar retention of MS2-GFP-RNA complexes in Escherichia coli. *Biophys. J.* **106**, 1928–1937 (2014).

234. Winkler, J. *et al.* Quantitative and spatio-temporal features of protein aggregation in Escherichia coli and consequences on protein quality control and cellular ageing. *EMBO J.* **29**, 910–923 (2010).

235. Proenca, A. M., Rang, C. U., Qiu, A., Shi, C. & Chao, L. Cell aging preserves cellular immortality in the presence of lethal levels of damage. *PLoS Biol.* **17**, e3000266 (2019).

236. de Groot, N. S., Sabate, R. & Ventura, S. Amyloids in bacterial inclusion bodies. *Trends Biochem. Sci.* **34**, 408–416 (2009).

237. Morell, M. *et al.* Inclusion bodies: specificity in their aggregation process and amyloid-like structure. *Biochim. Biophys. Acta* **1783**, 1815–1825 (2008).

238. Wang, L., Maji, S. K., Sawaya, M. R., Eisenberg, D. & Riek, R. Bacterial inclusion bodies contain amyloid-like structure. *PLoS Biol.* **6**, e195 (2008).

239. Cano-Garrido, O. *et al.* Supramolecular organization of protein-releasing functional amyloids solved in bacterial inclusion bodies. *Acta Biomater.* **9**, 6134–6142 (2013).

240. García-Fruitós, E. *et al.* Aggregation as bacterial inclusion bodies does not imply inactivation of enzymes and fluorescent proteins. *Microb. Cell Fact.* **4**, 27 (2005).

241. Rinas, U., Hoffmann, F., Betiku, E., Estapé, D. & Marten, S. Inclusion body anatomy and functioning of chaperone-mediated in vivo inclusion body disassembly during high-level recombinant protein production in Escherichia coli. *J. Biotechnol.* **127**, 244–257 (2007).

242. King, J., Haase-Pettingell, C., Robinson, A. S., Speed, M. & Mitraki, A. Thermolabile folding intermediates: inclusion body precursors and chaperonin substrates. *FASEB J. Off. Publ. Fed. Am. Soc. Exp. Biol.* **10**, 57–66 (1996).

243. Fink, A. L. Protein aggregation: folding aggregates, inclusion bodies and amyloid. *Fold. Des.* **3**, R9-23 (1998).

244. Speed, M. A., Wang, D. I. & King, J. Specific aggregation of partially folded polypeptide chains: the molecular basis of inclusion body composition. *Nat. Biotechnol.* **14**, 1283–

232

1287 (1996).

245. Rajan, R. S., Illing, M. E., Bence, N. F. & Kopito, R. R. Specificity in intracellular protein aggregation and inclusion body formation. *Proc. Natl. Acad. Sci. U. S. A.* **98**, 13060–13065 (2001).

246. De Marco, A. *et al.* Bacterial inclusion bodies are industrially exploitable amyloids. *FEMS Microbiol. Rev.* **43**, 53–72 (2019).

247. Arié, J.-P., Miot, M., Sassoon, N. & Betton, J.-M. Formation of active inclusion bodies in the periplasm of Escherichia coli. *Mol. Microbiol.* **62**, 427–437 (2006).

248. Nahalka, J. & Nidetzky, B. Fusion to a pull-down domain: a novel approach of producing Trigonopsis variabilisD-amino acid oxidase as insoluble enzyme aggregates. *Biotechnol. Bioeng.* **97**, 454–461 (2007).

249. Lin, Z., Zhou, B., Wu, W., Xing, L. & Zhao, Q. Self-assembling amphipathic alpha-helical peptides induce the formation of active protein aggregates in vivo. *Faraday Discuss.* **166**, 243–256 (2013).

250. Wang, X., Zhou, B., Hu, W., Zhao, Q. & Lin, Z. Formation of active inclusion bodies induced by hydrophobic self-assembling peptide GFIL8. *Microb. Cell Fact.* **14**, 88 (2015).

251. Wu, W., Xing, L., Zhou, B. & Lin, Z. Active protein aggregates induced by terminally attached self-assembling peptide ELK16 in Escherichia coli. *Microb. Cell Fact.* **10**, 9 (2011).

252. Zhou, B., Xing, L., Wu, W., Zhang, X.-E. & Lin, Z. Small surfactant-like peptides can drive soluble proteins into active aggregates. *Microb. Cell Fact.* **11**, 10 (2012).

253. Ramón, A., Señorale-Pose, M. & Marín, M. Inclusion bodies: Not that bad... *Front. Microbiol.* **5**, 2010–2015 (2014).

254. Villaverde, A., Corchero, J. L., Seras-Franzoso, J. & Garcia-Fruitós, E. Functional protein aggregates: Just the tip of the iceberg. *Nanomedicine* **10**, 2881–2891 (2015).

255. Jevsevar, S. *et al.* Production of nonclassical inclusion bodies from which correctly folded protein can be extracted. *Biotechnol. Prog.* **21**, 632–639 (2005).

256. de Groot, N. S. & Ventura, S. Effect of temperature on protein quality in bacterial inclusion bodies. *FEBS Lett.* **580**, 6471–6476 (2006).

257. Peternel, S., Grdadolnik, J., Gaberc-Porekar, V. & Komel, R. Engineering inclusion bodies for non denaturing extraction of functional proteins. *Microb. Cell Fact.* **7**, 34 (2008).

258. Hrabárová, E., Achbergerová, L. & Nahálka, J. Insoluble protein applications: the use of bacterial inclusion bodies as biocatalysts. *Methods Mol. Biol.* **1258**, 411–422 (2015).

259. Rueda, F. *et al.* Production of functional inclusion bodies in endotoxin-free Escherichia coli. *Appl. Microbiol. Biotechnol.* **98**, 9229–9238 (2014).

260. Cano-Garrido, O. *et al.* Functional protein-based nanomaterial produced in microorganisms recognized as safe: A new platform for biotechnology. *Acta Biomater.* **43**, 230–239 (2016).

261. Maji, S. K. *et al.* Functional amyloids as natural storage of peptide hormones in pituitary secretory granules. *Science* **325**, 328–332 (2009).

262. Vázquez, E. *et al.* Functional inclusion bodies produced in bacteria as naturally occurring

nanopills for advanced cell therapies. *Adv. Mater.* **24**, 1742–1747 (2012).

263. Torrealba, D. *et al.* Nanostructured recombinant cytokines: A highly stable alternative to short-lived prophylactics. *Biomaterials* **107**, 102–114 (2016).

264. Pesarrodona, M. *et al.* Targeting Antitumoral Proteins to Breast Cancer by Local Administration of Functional Inclusion Bodies. *Adv. Sci.* **6**, 1900849 (2019).

265. Gifre-Renom, L. *et al.* Recombinant Protein-Based Nanoparticles: Elucidating their Inflammatory Effects In Vivo and their Potential as a New Therapeutic Format. *Pharmaceutics* **12**, 450 (2020).

266. Seras-Franzoso, J. *et al.* A nanostructured bacterial bioscaffold for the sustained bottom-up delivery of protein drugs. *Nanomedicine (Lond).* **8**, 1587–1599 (2013).

267. Villaverde, A. *et al.* Packaging protein drugs as bacterial inclusion bodies for therapeutic applications. *Microb. Cell Fact.* **11**, 76 (2012).

268. Singh, A., Upadhyay, V., Upadhyay, A. K., Singh, S. M. & Panda, A. K. Protein recovery from inclusion bodies of Escherichia coli using mild solubilization process. *Microb. Cell Fact.* **14**, 1–10 (2015).

269. Upadhyay, V., Singh, A., Jha, D., Singh, A. & Panda, A. K. Recovery of bioactive protein from bacterial inclusion bodies using trifluoroethanol as solubilization agent. *Microb. Cell Fact.* **15**, 100 (2016).

270. Rinas, U. *et al.* Bacterial Inclusion Bodies: Discovering Their Better Half. *Trends Biochem. Sci.* **42**, 726–737 (2017).

271. González-Montalbán, N., García-Fruitós, E. & Villaverde, A. Recombinant protein solubility - does more mean better? *Nature biotechnology* **25**, 718–720 (2007).

272. Unzueta, U. *et al.* Release of targeted protein nanoparticles from functional bacterial amyloids: A death star-like approach. *J. Control. Release* **279**, 29–39 (2018).

273. Peternel, Š. & Komel, R. Active protein aggregates produced in Escherichia coli. *Int. J. Mol. Sci.* **12**, 8275–8287 (2011).

274. Zbilut, J. P. *et al.* Protein aggregation/folding: the role of deterministic singularities of sequence hydrophobicity as determined by nonlinear signal analysis of acylphosphatase and Abeta(1-40). *Biophys. J.* **85**, 3544–3557 (2003).

275. Jong, W. S. P. *et al.* Application of an E. coli signal sequence as a versatile inclusion body tag. *Microb. Cell Fact.* **16**, 50 (2017).

276. Yang, X., Pistolozzi, M. & Lin, Z. New trends in aggregating tags for therapeutic protein purification. *Biotechnol. Lett.* **40**, 745–753 (2018).

277. Martin-Farmer, J. & Janssen, G. R. A downstream CA repeat sequence increases translation from leadered and unleadered mRNA in Escherichia coli. *Mol. Microbiol.* **31**, 1025–1038 (1999).

278. Verma, M. *et al.* A short translational ramp determines the efficiency of protein synthesis. *Nat. Commun.* **10**, 5774 (2019).

279. Weber, M. *et al.* Impact of C-terminal amino acid composition on protein expression in bacteria. *Mol. Syst. Biol.* **16**, e9208 (2020).

280. Tuller, T. *et al.* An evolutionarily conserved mechanism for controlling the efficiency of

protein translation. *Cell* **141**, 344–354 (2010).

281. Boël, G. *et al.* Codon influence on protein expression in E. coli correlates with mRNA levels. *Nature* **529**, 358–363 (2016).

282. Lei, J. *et al.* The antimicrobial peptides and their potential clinical applications. *Am. J. Transl. Res.* **11**, 3919–3931 (2019).

283. Cheng, K. T. *et al.* High level expression and purification of the clinically active antimicrobial peptide P-113 in Escherichia coli. *Molecules* **23**, 800 (2018).

284. Li, Y. Production of human antimicrobial peptide LL-37 in Escherichia coli using a thioredoxin–SUMO dual fusion system. *Protein Expr. Purif.* **87**, 72–78 (2013).

285. Yu, H., Li, H., Gao, D., Gao, C. & Qi, Q. Secretory production of antimicrobial peptides in Escherichia coli using the catalytic domain of a cellulase as fusion partner. *J. Biotechnol.* **214**, 77–82 (2015).

286. Sun, B., Wibowo, D., Sainsbury, F. & Zhao, C. X. Design and production of a novel antimicrobial fusion protein in Escherichia coli. *Appl. Microbiol. Biotechnol.* **102**, 8763–8772 (2018).

287. Saïda, F., Uzan, M., Odaert, B. & Bontems, F. Expression of highly toxic genes in E. coli: special strategies and genetic tools. *Curr. Protein Pept. Sci.* **7**, 47–56 (2006).

288. Martínez-Alonso, M., González-Montalbán, N., García-Fruitós, E. & Villaverde, A. The Functional quality of soluble recombinant polypeptides produced in Escherichia coli is defined by a wide conformational spectrum. *Appl. Environ. Microbiol.* **74**, 7431–7433 (2008).

289. Kwon, S. Bin *et al.* Quality Screening of Incorrectly Folded Soluble Aggregates from Functional Recombinant Proteins. *Int. J. Mol. Sci.* **20**, 907 (2019).

290. Mauro, V. P. Codon Optimization in the Production of Recombinant Biotherapeutics: Potential Risks and Considerations. *BioDrugs* **32**, 69–81 (2018).

291. Marini, G. *et al.* Experimental design approach in recombinant protein expression: determining medium composition and induction conditions for expression of pneumolysin from Streptococcus pneumoniae in Escherichia coli and preliminary purification process. *BMC Biotechnol.* **14**, 1 (2014).

292. Mauro, V. P. & Chappell, S. A. A critical analysis of codon optimization in human therapeutics. *Trends Mol. Med.* **20**, 604–613 (2014).

293. Stirling, P. C., Lundin, V. F. & Leroux, M. R. Getting a grip on non-native proteins. *EMBO Rep.* **4**, 565–570 (2003).

294. Bemporad, F. *et al.* Biological function in a non-native partially folded state of a protein. *EMBO J.* **27**, 1525–1535 (2008).

295. Fink, A. L. Natively unfolded proteins. *Curr. Opin. Struct. Biol.* **15**, 35–41 (2005).

296. Nishikawa, K. Natively unfolded proteins: An overview. *Biophysics (Oxf).* **5**, 53–58 (2009).

297. Palopoli, N. *et al.* Intrinsically Disordered Protein Ensembles Shape Evolutionary Rates Revealing Conformational Patterns. *J. Mol. Biol.* **433**, 166751 (2021).

298. Zea, D. J. *et al.* Disorder transitions and conformational diversity cooperatively modulate biological function in proteins. *Protein Sci.* **25**, 1138–1146 (2016).

299. Cano-Garrido, O. *et al.* Supramolecular organization of protein-releasing functional amyloids solved in bacterial inclusion bodies. *Acta Biomater.* **9**, 6134–6142 (2013).

300. Martínez-Alonso, M., García-Fruitós, E. & Villaverde, A. Yield, solubility and conformational quality of soluble proteins are not simultaneously favored in recombinant Escherichia coli. *Biotechnol. Bioeng.* **101**, 1353–1358 (2008).

301. Pighetti, G. M. & Sordillo, L. M. Specific immune responses of dairy cattle after primary inoculation with recombinant bovine interferon-gamma as an adjuvant when vaccinating against mastitis. *Am. J. Vet. Res.* **57**, 819–824 (1996).

302. Sordillo, L. M. & Babiuk, L. A. Modulation of bovine mammary neutrophil function during the periparturient period following in vitro exposure to recombinant bovine interferon gamma. *Vet. Immunol. Immunopathol.* **27**, 393–402 (1991).

303. Riollet, C., Rainard, P. & Poutrel, B. Cells and cytokines in inflammatory secretions of bovine mammary gland. *Adv. Exp. Med. Biol.* **480**, 247–258 (2000).

304. WEDLOCK, D. N. *et al.* Effects of yeast expressed recombinant interleukin-2 and interferon-γ on physiological changes in bovine mammary glands and on bactericidal activity of neutrophils. *J. Dairy Res.* **67**, 189–197 (2000).

305. Demon, D. *et al.* The intramammary efficacy of first generation cephalosporins against Staphylococcus aureus mastitis in mice. *Vet. Microbiol.* **160**, 141–150 (2012).

306. Brouillette, E. & Malouin, F. The pathogenesis and control of Staphylococcus aureus-induced mastitis: study models in the mouse. *Microbes Infect.* **7**, 560–568 (2005).

307. Gifre-Renom, L. *et al.* The Biological Potential Hidden in Inclusion Bodies. *Pharmaceutics* **12**, 157 (2020).

308. Torrealba, D. *et al.* Complex Particulate Biomaterials as Immunostimulant-Delivery Platforms. *PLoS One* **11**, e0164073 (2016).

309. Kontermann, R. E. Strategies for extended serum half-life of protein therapeutics. *Curr. Opin. Biotechnol.* **22**, 868–876 (2011).

310. Goodman, D. B., Church, G. M. & Kosuri, S. Causes and effects of N-terminal codon bias in bacterial genes. *Science* **342**, 475–479 (2013).

311. Voges, D., Watzele, M., Nemetz, C., Wizemann, S. & Buchberger, B. Analyzing and enhancing mRNA translational efficiency in an Escherichia coli in vitro expression system. *Biochem. Biophys. Res. Commun.* **318**, 601–614 (2004).

312. Magazine, H. I. *et al.* Use of synthetic peptides to identify an N-terminal epitope on mouse γ interferon that may be involved in function. *Proc. Natl. Acad. Sci. U. S. A.* **85**, 1237–1241 (1988).

313. Meiyalaghan, S. *et al.* Expression and purification of the antimicrobial peptide GSL1 in bacteria for raising antibodies. *BMC Res. Notes* **7**, 15–17 (2014).

314. Soundrarajan, N. *et al.* Green fluorescent protein as a scaffold for high efficiency production of functional bacteriotoxic proteins in Escherichia coli. *Sci. Rep.* **6**, 1–10 (2016).

315. Li, Y. Carrier proteins for fusion expression of antimicrobial peptides in Escherichia coli. *Biotechnol. Appl. Biochem.* **54**, 1–9 (2009).

316. Serna, N. *et al.* Rational engineering of single-chain polypeptides into protein-only, BBB-

targeted nanoparticles. *Nanomedicine Nanotechnology, Biol. Med.* **12**, 1241–1251 (2016).

317. Irazazabal, L. N. *et al.* Fast and potent bactericidal membrane lytic activity of PaDBS1R1, a novel cationic antimicrobial peptide. *Biochim. Biophys. acta. Biomembr.* **1861**, 178–190 (2019).

318. Sun, Y. & Shang, D. Inhibitory Effects of Antimicrobial Peptides on Lipopolysaccharide-Induced Inflammation. *Mediators Inflamm.* **2015**, 167572 (2015).

319. Lam, S. J. *et al.* Combating multidrug-resistant Gram-negative bacteria with structurally nanoengineered antimicrobial peptide polymers. *Nat. Microbiol.* **1**, 16162 (2016).

320. Lei, R. *et al.* Self-Assembling Myristoylated Human α-Defensin 5 as a Next-Generation Nanobiotics Potentiates Therapeutic Efficacy in Bacterial Infection. *ACS Nano* **12**, 5284–5296 (2018).

321. Attenello, F., Raza, S. M., Dimeco, F. & Olivi, A. Chemotherapy for brain tumors with polymer drug delivery. *Handb Clin Neurol.* **104**, 339–353 (2012).

322. Jones, S. Permeability rules for antibiotic design. *Nat. Biotechnol.* **35**, 639 (2017).

323. Morones-Ramirez, J. R., Winkler, J. A., Spina, C. S. & Collins, J. J. Silver enhances antibiotic activity against gram-negative bacteria. *Sci. Transl. Med.* **5**, 190ra81 (2013).

324. Hancock, R. E. W. & Sahl, H. G. Antimicrobial and host-defense peptides as new anti-infective therapeutic strategies. *Nat. Biotechnol.* **24**, 1551–1557 (2006).

325. Henriques, S. T., Melo, M. N. & Castanho, M. A. R. B. Cell-penetrating peptides and antimicrobial peptides: how different are they? *Biochem. J.* **399**, 1–7 (2006).

326. Erental, A., Sharon, I. & Engelberg-Kulka, H. Two programmed cell death systems in Escherichia coli: an apoptotic-like death is inhibited by the mazEF-mediated death pathway. *PLoS Biol.* **10**, e1001281 (2012).

Departament de genètica i microbiologia

Facultat de biociències